Year : 2021

Analysis of the heat sensing and signaling pathway in A. thaliana

Bourgine Baptiste

Bourgine Baptiste, 2021, Analysis of the heat sensing and signaling pathway in A. thaliana

Originally published at : Thesis, University of Lausanne

Posted at the University of Lausanne Open Archive http://serval.unil.ch
Document URN : urn:nbn:ch:serval-BIB_92F3212CBE027

UNIL | Université de Lausanne
Faculté de biologie
et de médecine

Département de Biologie Moléculaire Végétale (DBMV)

Analysis of the heat sensing and signaling pathway in *A. thaliana*

Thèse de doctorat sciences de la vie (PhD)

présentée à la

Faculté de biologie et de médecine
de l'Université de Lausanne

par

Baptiste Bourgine

Master, Université de Rouen, France

Jury

Prof. Ian Sanders, Président
Prof. Pierre Goloubinoff, Directeur de thèse
Dr. Anthony Guihur, Co-directeur
Prof. Etienne Bucher, expert
Prof. David Macherel, expert

Lausanne 2021

UNIL | Université de Lausanne
Faculté de biologie et de médecine

Département de Biologie Moléculaire Végétale (DBMV)

Analysis of the heat sensing and signaling pathway in *A. thaliana*

Thèse de doctorat sciences de la vie (PhD)

présentée à la

Faculté de biologie et de médecine
de l'Université de Lausanne

par

Baptiste Bourgine

Master, Université de Rouen, France

Jury

Prof. Ian Sanders, Président
Prof. Pierre Goloubinoff, Directeur de thèse
Dr. Anthony Guihur, Co-directeur
Prof. Etienne Bucher, expert
Prof. David Macherel, expert

Lausanne 2021

UNIL | Université de Lausanne
Faculté de biologie
et de médecine

Ecole Doctorale
Doctorat ès sciences de la vie

Imprimatur

Vu le rapport présenté par le jury d'examen, composé de

Président·e	Monsieur	Prof.	Ian	**Sanders**
Directeur·trice de thèse	Monsieur	Prof.	Pierre	**Goloubinoff**
Co-directeur·trice	Monsieur	Dr	Anthony	**Guihur**
Expert·e·s	Monsieur	Prof.	Etienne	**Bucher**
	Monsieur	Prof.	David	**Marcherel**

le Conseil de Faculté autorise l'impression de la thèse de

Monsieur Baptiste Bourgine

Master, Université de Rouen, France

intitulée

Analysis of the heat sensing and signaling pathway in *A. thaliana*

Date de l'examen : 18 février 2021

Date d'émission de l'imprimatur : Lausanne, le 12 avril 2021

pour le Doyen
de la Faculté de biologie et de médecine

Prof. Niko GELDNER
Directeur de l'Ecole Doctorale

Table of content

Acknowledgments

I would like to thank the jury members of my Ph.D. thesis, Dr. Prof. Etienne Bucher, Dr. Prof. David Macherel, Dr. Prof. Ian Sanders, Dr. Prof. Pierre Goloubinoff, and Dr. Anthony Guihur for their devoting time to my Ph.D. thesis, correction, and advice.

All my gratitude to my mentor, Dr. Prof. Pierre Goloubinoff, for having given me the opportunity to perform my thesis in his laboratory (and nice hiking!). Thanks for your precious time and supervision over these 5 years that allowed me to evolve scientifically. Thanks equally for the corrections to this manuscript.

Many thanks to Dr. Anthony Guihur for his strong and very good supervising. You taught me the ways of scientific thinking, plant techniques, and science. You allowed me to judge and criticize in the right way with arguments and making me a better scientist. Many thanks for your availability, advices, and scientific discussion at all times.

Especial thanks to Dr. Elia Stahl, Dr. Kay Gully, Dr. Robertas Ursache, Dr. Raphaël Groux, and Dr. Prof. Paul-Emile Bourgine for their advice and correction on this manuscript. Special thanks to the Ph.D. Alexandra Waskow for proofreading the review. I would like to express all my gratitude to my previous and actual laboratory members John Perrin, Dr. Bruno Fauvet, Dr. Satyam Tiwari, Ph.D. Mathieu Rebeaud, Tatiana Fomekong, Dr. Flavia Canellas, Dr. Tam Xuan Lam for scientific discussion, support, and critical advice.

Thanks to all the members of our Department of Plant Molecular Biology (DBMV) for advice, technical assistance, friendship, kindness, and for the great atmosphere (and parties!) over these amazing years. I want to thank Blaise Tissot for the management of plants in the greenhouse. Equally to Debora Zoia and Laurence Cienciala for the administrative work at the secretary office and for enjoyable long conversations.

Deep thanks to my girlfriend Evangéline Lhermenier, for your incredible patience, support and love for helping me in the middle of the hard moments. Many thanks to my family living far away from me. I hope to see you more than twice a year.

Abbreviations

ABA = Abscisic Acid

APX1 = Ascorbate Peroxidase 1

ARP6 = Actin Related Protein 6

AT = Acquired Thermotolerance

BA = Benzyl Alcohol

BRI1 = BRASSINOSTEROID INSENSITIVE 1

CaM = Calmodulin

cAMP = Cyclic Adenosine Monophosphate

CaMBD = Calmodulin Binding Domain

CBK3 = Calmodulin Binding Protein Kinase 3

CIHSP = CHEMICAL INDUCTION HEAT SHOCK PROTEIN

CMLs = Calmodulin-like proteins

CNBD = Cyclic Nucleotide Binding Domain

CNGC = Cyclic Nucleotide Gated Channel

DAO1 = D-Amino Acid Oxidase 1

DREBE2A = Dehydration Responsive Element Binding Protein 2A

EMS = Ethyl Methyl Sulfonate

FGS = Forward Genetic Screen

FLG22 = FLAGELLIN 22

GPAT6 = Glycerol-3-Phosphate SN-2-Acyltransferase 6

HIBAT = HEAT INDUCIBLE BIOLUMINESCENCE AND TOXICITY

HS = Heat Stress

HSBP1 = Heat Shock Binding Protein 1

HSE = Heat Shock Element

HSF = Heat Shock Transcription Factor

HSR = Heat Shock Response

HSP = Heat Shock Protein

HSBP1 = Heat Shock Binding Protein 1

L5 = Light 5

MAPK6 = Mitogen activated Protein Kinase 6

miRNAs = microRNAs small interfering RNAs

nLUC = Nano-Luciferase

PMCA = The plasma Membrane Ca^{2+} ATPase

RFP = Red Fluorescent Protein

ROS = Reactive Oxygen Species

Rubisco = Ribulose 1,5-bisphosphate carboxylase

SES1 = Sensitive to Salt 1

siRNAs = small interfering RNAs

SNPs = Single Nucleotide Polymorphisms

TAGs = Triacylglycerols

TE = Transposable Element

VOZ1 = VASCULAR PLANT ONE-ZINC-FINGER 1

WGDS = Whole Genome DNA Sequencing

W5 = N-(6-Aminohexyl)-1-naphtalensulfonamide

W7 = N-(6Aminohexyl)-5-chloro-1-naphtalenesulfonamide hydrochloride

List of figures and tables

Chapter 1: General introduction

Chapter 2: Generation and characterization of an *A. thaliana* transgenic line for a forward genetic screen.

Chapter 3: A forward genetic screen in *A. thaliana* to search for new genes involved in plant heat sensing and signaling pathway.

Chapter 4: **Investigation of a possible epigenetic program to reversibly repress the heat shock response in *A. thaliana*.**

Chapter 5: A forward genetic screen in *A. thaliana* to search for repressors of the heat shock response at low temperatures.

Chapter 6: **Generation of *cam1* and *cam5* Arabidopsis mutants by CRISPR methodology and T-DNA insertion lines.**

Abstract

Sessile land plants cannot escape to noxious heat shock (HS) occurring usually at midday until late in the afternoon during heat waves events. To survive, they need to perceive mild temperature variations in order to prime molecular defenses. Among them, heat shock proteins (HSPs), whose expression is strongly repressed at a low temperature, become overexpressed during HS. HSPs can reduce damages such as misfolding, protein aggregation and participate in the stabilization of membranes leading to the acquired thermotolerance (AT) in plants. In the plasma membrane, cells express cyclic nucleotide-gated channels (CNGC) that act as thermosensors and drive a conditional entry of external Ca^{2+} within the cytosol. This results in an unclear signal that activates heat shock transcription factor 1 and causes the accumulation of HSPs. In the context of global warming, it is important to clarify which are all the heat sensors and the signaling pathways ultimately triggering the proper expression of protective HSPs for the onset of AT.

The aim of this thesis was to search for components involved in the repression at low temperatures and the activation at high temperatures of the accumulation of HSPs in the model plant *A. thaliana*. A new transgenic line called HIBAT was generated as a reporter to analyze the heat shock response (HSR) *in vivo*. It contains a fusion protein made of a bioluminescent nano-luciferase and a conditionally toxic negative marker, called D-amino acid oxidase. This chimeric protein was strictly under the control of a heat-inducible promoter from small HSPs. The reporter line served in a forward genetic screen in an attempt to identify genes whose mutations would render plants defective in their ability to sense and/or to transduce HS signals. Under HS, seven isolated candidates were apparently unable to accumulate the fusion protein leading to be resistant in the presence of D-valine, did not produce light, and ultimately showed a reduced HSPs accumulation. Some of them were not respecting an expected segregation at the M3 and F2 generation but were submitted to the whole genome sequencing. Yet, too many single nucleotide polymorphisms (SNPs) were found which did not allow to clearly identify genes responsible for heat sensing and signaling. Moreover, most offspring candidates were able to accumulate the same amount of the fusion reporter and HSPs compared to the parental line under HS. 24-fold more non-mutagenized HIBAT lines were found to survive at several iterative HS and in the presence of D-valine compared to plants growing with the additional inhibitor of DNA methylation, called zebularine. Few survivors were found to

recover the expression of the fusion protein and HSPs following a single HS treatment, 2 weeks later the end of HS cycles. This result indicated that the loss of heat sensing has resulted from reversible epigenetic DNA methylation. Additionally, we found a strong indication that plants might be able to establish such a program under iterative HS which would have transiently and being reversible the expression of one, if not all, heat-induced proteins which might become deleterious when excessively expressed.

The fifth chapter aims to screen mutants whose mutations affected the repressory machinery preventing the expression of HSPs at non-HS temperature by using the mutagenized HIBAT line but in the absence of D-valine and HS. One mutant was isolated that produced a higher amount of bioluminescence and HSPs at low (22°C) and mild (31°C) temperatures. The plant candidate was sequenced and a list of 232 putatively SNPs involved in the repression of HSPs remains to further refine by sequencing the F2 mutant to reduce the genetic background which is not related to the phenotype.

The sixth chapter addresses the role of calmodulin (CaM) 1 and CaM 5 in the HS signaling. Both CaMs were found to strongly interact specifically with the CNGC2 cytosolic domain in a yeast two-hybrid screen, suggesting they are involved in the heat shock signaling pathway. A double *cam1/cam5* mutant was generated by crossing T-DNA insertions lines and by using the CRISPR technology in *A. thaliana*. Their role in the HSR remains to be analyzed in the mutants which are expected to be defective to accumulate HSPs under HS.

The seventh chapter emphasizes the fact that a specific class of small HSPs is strongly repressed at low temperatures, and the HSR is not only involved in their accumulation but also in their derepression. This suggests that if small HSPs were unnecessary express at non-HS temperature, it would cause a deleterious effect in plants. Therefore, this question was addressed by designing an *A. thaliana* transgenic line in which the small HSP17.6a, normally strongly repressed at low temperature, can be conditionally accumulated under the control of a chemical. This line was generated but remains to be analyzed with regards to its ability to overproduced small HSPs at low temperatures and to address the expected deleterious effect.

In the context of global warming, this research aimed to be better elucidate how plants sense the temperature on time to accumulate appropriate molecular defenses leading to an otherwise deadly HS. Understanding this aspect is the first step to what is

controlling this phenomenon opening the possibility to eventually prepare crops plant to better respond to extreme temperatures in the future.

Résumé

Les plantes terrestres sessiles ne peuvent pas échapper à un choc thermique nocif (CT) qui se produit généralement à midi jusqu'à tard dans l'après-midi pendant des vagues de chaleur. Pour survivre, elles doivent être capables de percevoir les augmentations de température afin d'amorcer des défenses moléculaires appropriées. Parmi elles, les protéines de choc thermique (HSPs), dont l'expression est fortement réprimée à basse température, deviennent surexprimées au cours du CT. Elles peuvent réduire les dommages tels que le mauvais repliement, l'agrégation des protéines et participer à la stabilisation des membranes ce qui conduit les plantes à acquérir la thermotolérance. Dans la membrane plasmique, les cellules végétales contiennent des capteurs de chaleur appelés canaux cycliques nucléotidiques (CNGCs). Elles permettent une entrée d'ions Ca^{2+} dans le cytosol pendant un CT. Il en résulte un signal inconnu qui active néanmoins les facteurs de transcription HSFA1 ce qui déclenche l'accumulation de HSPs. Dans un contexte de réchauffement climatique, il reste à élucider tous les mécanismes de perception et de signalisation de la chaleur conduisant à accumuler les HSPs chez les plantes.

Le but de cette thèse visait à trouver de nouveaux partenaires impliqués dans la répression à basse et l'activation à haute température des HSPs dans la plante modèle *A. thaliana*. Une nouvelle lignée transgénique appelée HIBAT a été générée, en tant que rapporteur, afin d'analyser *in vivo* la réponse au choc thermique (RCT). Elle contient une protéine de fusion composée d'une nano-luciférase bioluminescente et d'un marqueur négatif conditionnellement toxique appelé D-amino acide oxydase. Cette protéine chimérique est strictement sous le contrôle d'un promoteur inductible par la chaleur provenant d'une petite HSP. La lignée HIBAT a servi dans un criblage génétique direct pour identifier les gènes dont les mutations rendraient les plantes défectueuses à détecter et/ou à transduire des signaux de CT. Après un CT, sept candidats isolés étaient apparemment incapables d'accumuler la protéine de fusion conduisant à être résistante en présence de D-valine, n'ont pas produit de lumière et ont finalement montré une accumulation réduite de HSPs. Certains d'entre eux ne suivaient la ségrégation attendue aux générations M3 et F2 mais ont été néanmoins soumis à l'ensemble du séquençage du génome. Pourtant, beaucoup de polymorphismes mono-nucléotidiques (PMN) ont été trouvés, ce qui n'a pas permis d'identifier les gènes responsables de la détection et de la signalisation de la chaleur. De plus, la plupart des descendants venant des candidats

isolés, étaient capables d'accumuler la même quantité de protéine de fusion et des HSPs par rapport à la lignée parentale sous CT. Il a été trouvé 24 fois plus de plantes HIBAT non mutagénisées survivants à plusieurs CT itératives et en présence de D-valine, par rapport aux plantes cultivées avec un inhibiteur de la méthylation de l'ADN, appelé zébularine. De plus, deux semaines après la fin des cycles CT, peu de survivants étaient capables d'exprimer la protéine de fusion et les HSPs après un seul CT. Ce résultat indiquait que la perte de détection de la chaleur résultait des méthylations réversibles sur l'ADN induit par un programme épigénétique établit par les plantes sous CT itérative. Ce programme pourrait donc réprimer de manière transitoire et réversible l'expression d'une, sinon toutes, des HSPs ce qui pourrait indiquer aussi que leur surexpression pourrait être délétère pour les plantes.

Le cinquième chapitre se focalise sur l'isolation de mutants dont les mutations affectaient le mécanisme de répression impliqué dans l'expression des HSPs à basse température en utilisant la lignée HIBAT mais en l'absence de D-valine et de CT. Un mutant a été isolé qui produisait à la fois une bioluminescence et des HSPs plus élevés à des températures basses (22°C) et moyennes (31°C). Il a été séquencé et en a résulté une liste de 232 PMN. Il reste à affiner davantage cette liste en séquençant le mutant à la génération F2 afin de réduire le bruit génétique n'étant pas lié au phénotype.

Le sixième chapitre aborde le rôle de la calmoduline (CaM) 1 et CaM 5 dans la signalisation du CT. Les deux CaMs se sont révélées à interagir spécifiquement avec le domaine cytosolique CNGC2 dans une expérience à deux hybrides de levure, ce qui suggère qu'elles sont impliquées dans la voie de signalisation du CT. Un double mutant *cam1/cam5* a été généré en croisant des lignées d'insertion d'ADN-T et un utilisant la technologie CRISPR chez *A. thaliana*. Leur rôle dans la RCT doit être analysé chez les mutants où l'on s'attend à ce qu'ils soient défectueux pour accumuler des HSPs sous CT.

Le septième chapitre souligne le fait qu'une classe spécifique des petits HSPs est fortement réprimée à basse température, et la RCT n'est pas seulement impliqué dans leur accumulation mais aussi dans leur dérépression. Cela suggère que si elles étaient exprimées à une température basse cela provoquerait un effet délétère chez les plantes. Par conséquent, nous avons abordé cette question en concevant une lignée transgénique *A. thaliana* dans laquelle HSP17.6a, normalement fortement réprimé à basse température, peut être accumulé de manière conditionnelle sous le contrôle d'un produit chimique.

Cette lignée a été générée mais elle reste à être analysée dans sa capacité à surproduire la HSP17.6a à basse température et en s’attendant à un effet délétère.

Dans un contexte de réchauffement climatique, mes recherches visaient à mieux comprendre comment les plantes ressentent la chaleur à temps en accumulant des défenses moléculaires appropriées pour empêcher un CT mortel. Comprendre cet aspect est la première étape pour contrôler ce phénomène, ouvrant la possibilité de préparer les plantes cultivées afin qu'elles répondent aux futures températures extrêmes.

Résumé grand public

Les plantes terrestres sessiles ne peuvent pas échapper à un choc thermique nocif qui se produit généralement à midi jusqu'à tard dans l'après-midi pendant des vagues de chaleur. Pour survivre, elles doivent être capables de percevoir des augmentations de température afin d'amorcer des défenses moléculaires appropriés. Parmi elles, les protéines de choc thermique sont exclusivement produites à haute et fortement réprimées à basse température. Elles sont considérées comme des molécules « policières ». Elles réduisent considérablement les dommages produits par la chaleur dans les cellules végétales et participent donc massivement à l'acquisition de la thermotolérance chez les plantes. Au niveau de la membrane plasmique des cellules végétales, des capteurs de chaleur permettent l'entrée de calcium pendant un stress thermique. Il en résulte un signal inconnu qui active néanmoins les protéines de choc thermique. Dans un contexte de réchauffement climatique, il reste à élucider les mécanismes établis par les plantes pour percevoir la chaleur en émettant un signal dans les cellules afin d'accumuler les protéines de choc thermique.

Les travaux de mon doctorat visaient donc à trouver de nouveaux partenaires impliqués dans la répression à basse et l'activation à haute température des protéines de choc thermique dans la plante modèle *A. thaliana*. Pour visualiser leurs réponses à la chaleur, nous avons généré une lignée transgénique appelée HIBAT. C'est seulement à haute température que la lignée HIBAT produit deux protéines : l'une émane de la lumière dite « bioluminescence » et l'autre se révèle toxique en présence d'une molécule appelée D-valine. L'ADN des plantes code en partie pour des composés impliqués dans l'activation des protéines de choc thermique mais ils n'ont pas tous été identifiés. Pour les trouver, nous avons donc modifié l'ADN de manière aléatoire de plusieurs plantes HIBAT. Nous avons sélectionné celles qui étaient capables de résister à la D-valine sous choc thermique, qui n'émettaient pas de bioluminescence et n'accumulaient pas de protéines de choc thermique. De manière surprenante, plusieurs de ces plantes ont perdu leurs caractéristiques au fil des générations, supposément dû aux traitements thermiques successifs nécessaires à leur sélection. Nous avons découvert que cela n'était pas dû à des mutations de l'ADN mais à des modifications du génome (épigénétique) qui se produisent transitoirement et réversiblement empêchant les protéines de choc thermique de s'accumuler. Nous avons conclu que les plantes pourraient inhiber en partie l'expression de certaines protéines induites par la chaleur car supposées trop coûteuses

et néfastes pour les cellules. Ce mécanisme chimique dit de « méthylation de l'ADN » se révèle alors récurent lors de plusieurs stress thermiques chez les plantes.

En parallèle, nous avons utilisé des lignées HIBAT à l'ADN modifié pour trouver, cette fois, de nouveaux partenaires impliqués dans la répression des protéines de choc thermique à basse température. Nous avons sélectionné une plante qui exprimait anormalement de la bioluminescence à basse (22°C) et à moyenne (31°C) température. Après une analyse de son ADN, nous avons obtenu une liste de plusieurs partenaires et il reste à déterminer lesquels sont réellement impliqués dans la répression de ces protéines.

Par ailleurs, la thèse vise à comprendre le rôle de deux molécules appelées calmoduline 1 et 5. Elles ont été identifiées pour interagir avec les capteurs de chaleur des cellules végétales et pourraient être impliquées dans la médiatisation du signal thermique. Nous avons créé une plante transgénique qui n'exprime pas ces deux calmodulines. Ainsi, l'absence d'accumulation de protéines de choc thermique dans cette plante indiquerait le rôle de ces deux molécules dans la signalisation de la chaleur.

Enfin, parmi toutes les protéines de choc thermique, la classe numéro 20 est la plus réprimée à basse température et la plus induite par la chaleur dans les plantes. Nous avons cherché à comprendre pourquoi un tel mécanisme de répression est établi à basse température. Par conséquent, une nouvelle lignée transgénique dans *A. thaliana* a été générée pour exprimer, uniquement sous induction chimique et à des températures basses, une protéine de choc thermique de classe 20. Il nous reste à analyser l'effet de sa surproduction en supposant qu'elle pourrait induire des effets délétères chez la plante.

Dans un contexte de réchauffement climatique inéluctable, notre recherche visait à mieux comprendre comment les plantes détectent les augmentations de température en établissant des défenses appropriées pour faire face à des stress thermiques extrêmes. En comprenant cet aspect, nous pourrions être en mesure de planter des cultures contrôlées et les préparées à survivre à des températures élevées.

Chapter 1: General introduction

I) Impact of heat stress on plants

I.1) Global warming

Plants colonized dry lands ~450 million years ago exposing them to high light, strong UV radiation, free oxygen, drought, and seasonal variations of ambient temperatures (1). As sessile organisms, land plants cannot evade exposure to extreme abiotic stresses. Among them, heat stress (HS) impact depends on the duration, severity, the number of iterative exposures and stresses combinations such as drought, light, salinity, and ozone (2). Within a day and in contrast to naturally temperate oceans, diurnal land temperatures can vary around 30°C in an arid environment. The desert legume *Retama raetam* resists temperature fluctuation starting at 18°C at 3 a.m and reaching a maximum of 42°C at 3 p.m (3). Thus, plant adaptation has resulted from new sensory and signaling systems to perceive and respond to periodic temperature increments.

Land plants are facing faster climate changing and predictions indicate that the mean temperature will increase by 2°C to 3°C by the end of the 21st century (Fig. 1a and b) (4,5). Each plant has evolved to grow and reproduce at the specific given optimal temperatures and a minor variation can lead to a significant impact on growth, reproduction, and development (6). The rise of global temperature on earth leads to higher heat waves frequency which becomes longer and intense impacting no adapted plants (7). The number of heat waves has 10 fold-times raised in the American region for the last fifty years (Fig. 1c) (7). Additionally, the increasing frequency of other stresses such as drought, wind, and flooding renders plants more vulnerable (8,9). The worldwide rate of production is then affected in which each degree-Celsius raise might lead to a reduction between 3% to 7% of wheat, rice, maize, and soybean (10). Since the human population depends on 90% of plants for their needs and predicted to reach around 8 to 10 billion individuals in 2050, a shortage of food is expected (11). Therefore, the heat stress response (HSR) and perception mechanisms have raised interest in order to understand how land plants can activate protection mechanisms to maintain cellular homeostasis when perceiving daily increments or long warming temperatures (12).

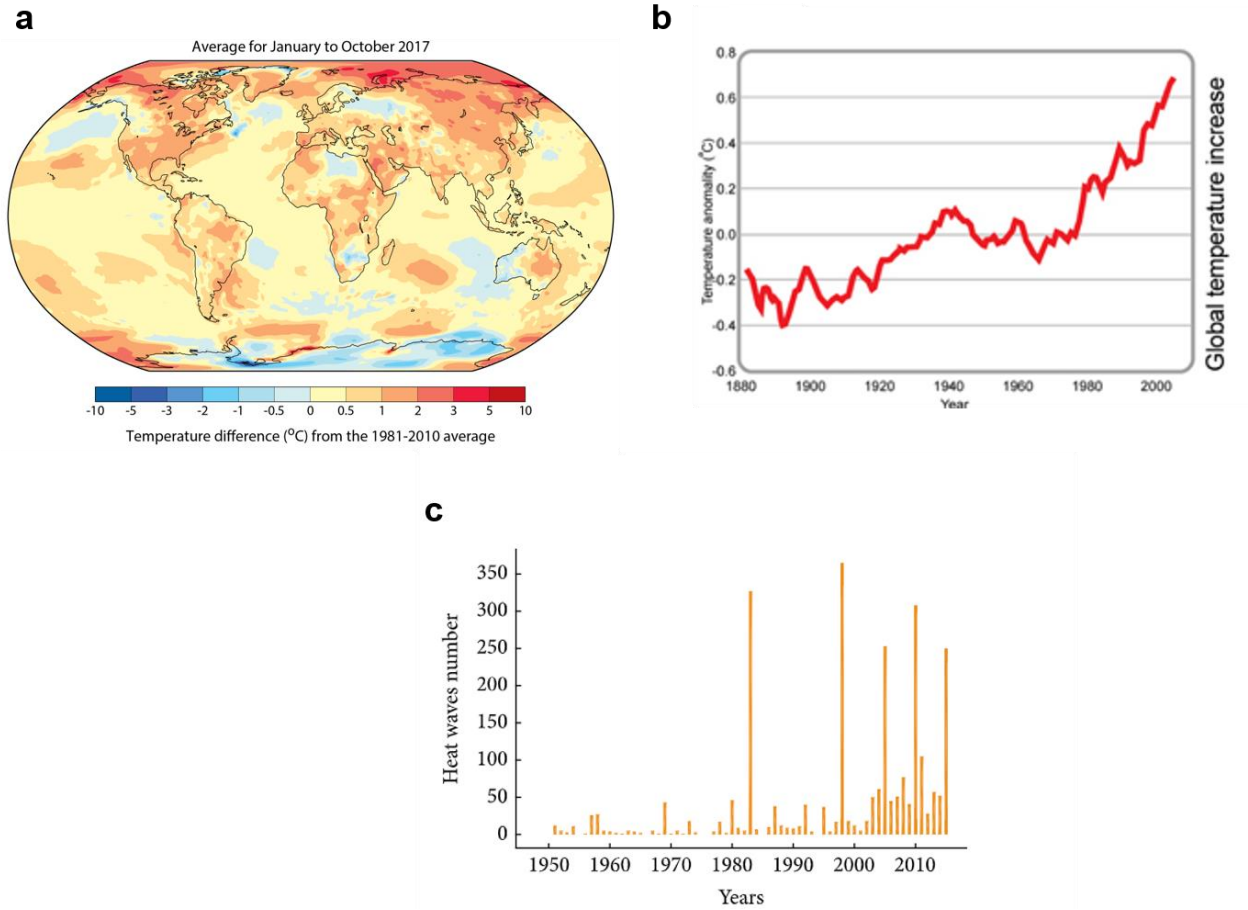

Figure 1: Global climate change. (**a**) Map of the average temperatures in the world from January to October 2017 (Source: World Meteorological Organization). Temperature's increment affects all parts of the world including oceans and ecosystems. (**b**) Global temperature increment from 1880 to 2013 in the world (Bita EC et al., 2013). (**c**) Annual heat waves number accumulated for the period 1948–2015 in intra America's region (from Angeles-Malaspina et al., 2018).

I.2) Heat conditions on plants

Arabidopsis thaliana is a model land plant that can be used to study the impact of temperatures since it grows quickly, produces many seeds, has a small genome (~114.5 Mb), and is genetically well characterized (13,14). Heat conditions in *A. thaliana* are classified into three categories; warm temperatures (22°C to 27°C), high temperatures (27°C to 30°C), and HS temperatures (37°C to 42°C) (15). Warming and high temperatures treatment may reduce growth and cause early flowering of heat acclimated plants (16). In contrast, HS happens when the rise of temperature is fast and beyond a threshold level inducing irreversible damages (17). In *A. thaliana*, transcriptomic analysis shows that warm (27°C) treatment accumulates less HSR transcripts than HS (37°C) conditions (ref 2, Fig. 2b).

I.3) Basal and acquired thermotolerance

Basal thermotolerance is when plants adapt to tolerate elevated temperatures within a range that do not necessitate heat acclimation. In contrast, the acquired thermotolerance (AT) is a plant adaptative capacity to survive a subsequent noxious HS when it is previously primed by a sublethal or warming temperature (12,18,19). *A. thaliana* seedlings prime at 36°C for 2 hours and then exposed to a noxious temperature of 45°C for 2 hours ultimately develop AT. The absence of heat prior exposure leads to death within 6 days (Fig. 2). In nature, HS priming can be achieved by plants on a daily basis, for example when the sun rises, resulting in the adjustment of mRNA, proteins, metabolism compounds, and lipids leading to their ability to survive to incoming noxious HS early in the afternoon (20–22). Yet, plants may not establish molecular defenses on time when excessively abrupt fluctuation of temperatures occurs. Noticeably, the synthesis of plant defenses during HS priming might have a cost on growth and reproduction. In *Elodea canadis* and soybean, primed leaves have a loss of chlorophyll and swollen chloroplast suggesting a negative impact on photosynthesis rate (23). Thus, HS priming can be a costly investment but conferring protective benefits, which is necessary for the onset of AT (Fig. 2) (Wasternack, 2017; Finka et al., 2012b).

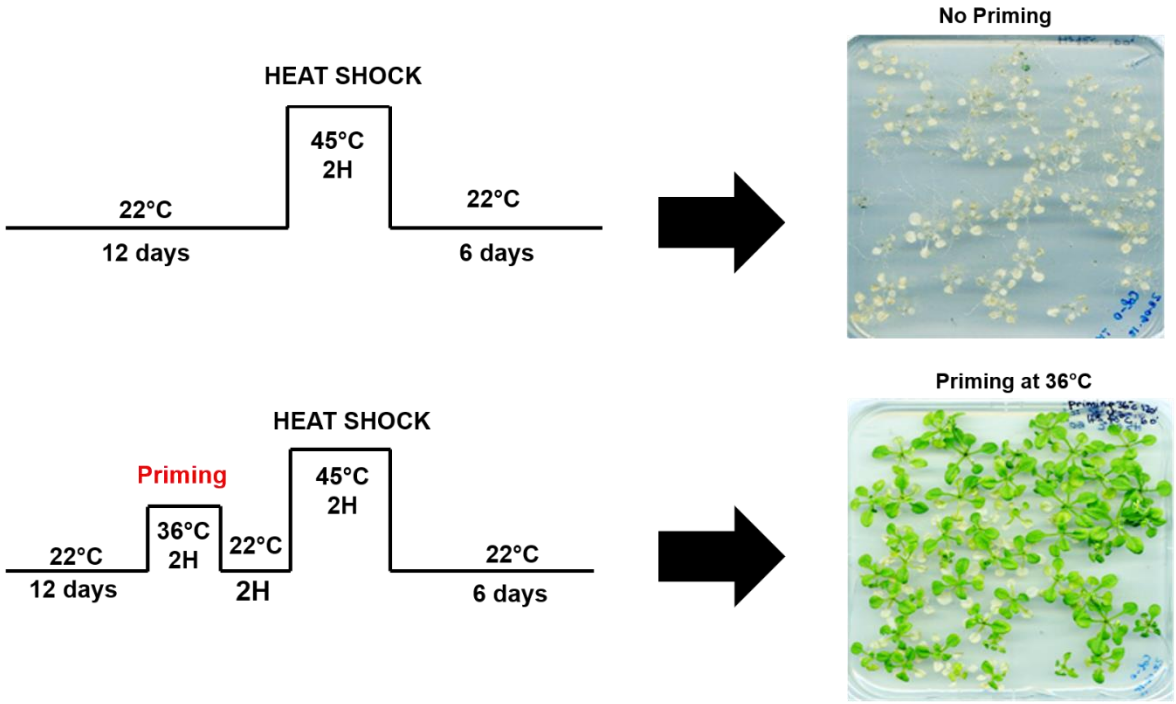

Figure 2: The Onset of acquired thermotolerance in *A. thaliana*. 12 days seedlings old were exposed to noxious heat for 2 hours at 45°C (Top) or with an additional pre-exposure of a heat priming at 36°C for 2 hours followed by 2 hours at 22°C of post-incubation (bottom). Within the next 6 following days, the direct noxious heat shock caused death, whereas the heat priming conferred AT to plants (unpublished data).

I.4) Effect of heat stress at the physiology, cellular and molecular levels

Physiology effects

All plant tissues are negatively impacted by elevated temperatures (Fig. 3a). In particular reproductive tissue where a few degrees increment can result in the partial loss of seed production (26). The fertilization processes are found impaired in pollen germination, meiosis in both male and female organs, and reduced pollen tube growth (27,28). Other physiological injuries can be observed such as scorching of stems and leaves, leaf abscission and senescence, shoot and root growth inhibition (29). The plant architecture is affected and may result in extended petiole and hypocotyls elongation which is similar to morphological responses occurring on shade avoidance (30,31). HS also disturbs stomata closures changing turgor pressure and altering the membrane integrity which decreases cell size and ultimately plant growth. Stomata regulate gas exchange, in particular CO_2 and oxygen, which its deregulation negatively impacts photosynthesis activity in maize and pearl millet (32,33). Additionally, HS decreases the rate of seed germination by altering their imbibition, and germinated seeds can show reduced radicle and plumule (34).

Cellular and molecular effects

Cell integrity and organization are dramatically damaged by prolonged elevated temperature. HS may induce high fluidization of membranes affecting both lipid bilayer properties and proteins embedded causing electrolyte leakage and acidification of the cytosol (35,36). The cytoskeleton is damaged by heat since microtubules and actin filaments, which play a major role in mechanical support and protein trafficking, can be destabilized affecting cell divisions (37,38). In chloroplast, components of the photosynthetic apparatus are particularly sensitive to high temperatures. In *Saccharum officinarum*, a net decrease in carbon assimilation was observed caused by a deregulation of photosystem II in the photosynthetic electron transfer and ATP synthesis (39,40). When the temperature is above 30°C in cotton and tobacco, the Calvin-Benson cycle which includes the ribulose 1,5-bisphosphate carboxylase (Rubisco) and Rubisco activase are negatively impacted resulting in carbon assimilation decrease (41–43).

Accumulation of reactive oxygen species (ROS) in the cell during HS can cause irreversible damages to proteins, DNA, and lipids (44,45) (Fig. 3b). Excessive ROS also mediate the onset of program cell death (46). In chloroplast, photosystem II generates oxidative singlet oxygen which disturbs photosynthesis reaction (39,40). Increment of H_2O_2 in mitochondria, produced by the respiratory electron transport chain, negatively affects

cell structure (47,48). Additionally, the damaged phospholipid cardiolipin which is located in the mitochondrial membrane, interacts with cytochrome C increasing the ROS content (35,49,50). HS would decrease the concentration of sugars required for glycolysis and tricarboxylic acid cycles impacting on ATP production (51).

Soluble proteins often harbor a hydrophobic core which may be affected at higher temperatures causing their aggregation. Hydrophobic exposed surfaces of proteins would increase their affinity for membranes affecting their integrity (52). Under HS, in mammalian cells, nascent unfolded proteins appear to be the most vulnerable to misfolding when the proteostasis becomes disrupt (53). In *Saccharomyces cerevisiae*, when the temperature is above 46°C, protein synthesis is dramatically inhibited (54). In *A. thaliana*, the translation (around 50%) is affected causing by a decrease of the association of mRNA to polysomes (55). The impact of HS on DNA can cause double-stranded breaks and can also affect the DNA repair mechanism (56). In *A. thaliana*, the damaged DNA binding proteins 1A and 2 are required for the DNA repair mechanism and confer thermotolerance and UV protection (57).

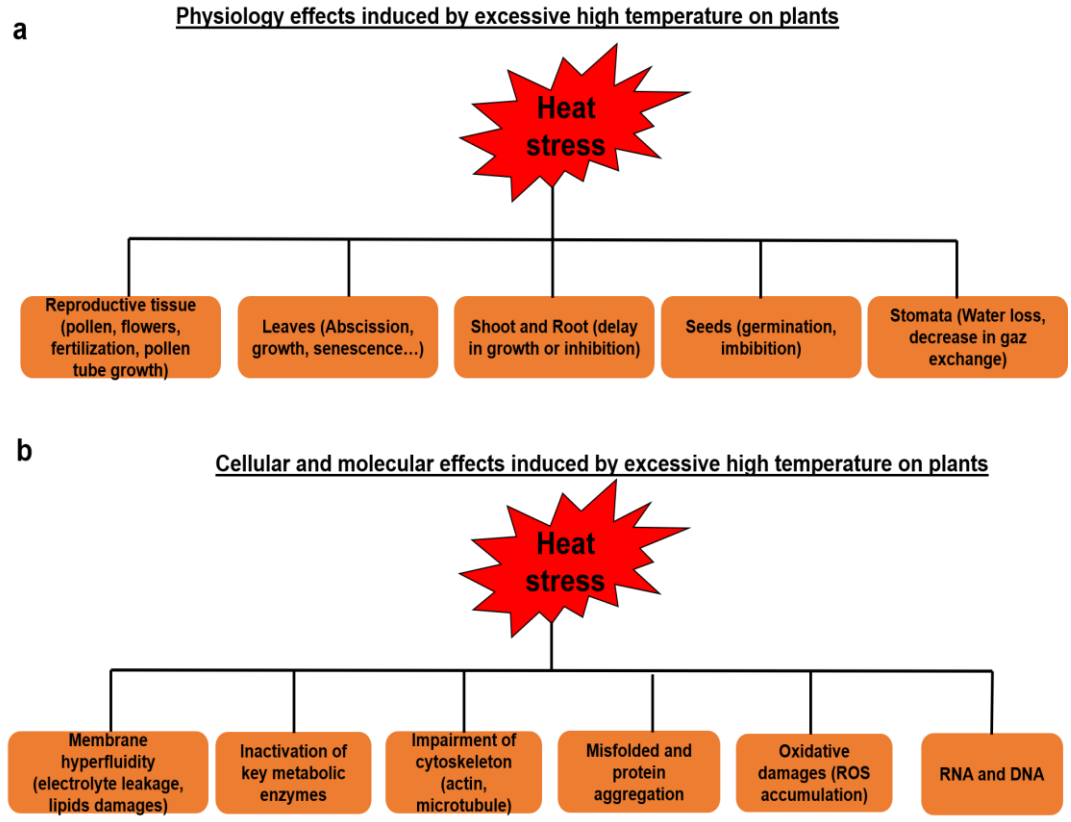

Figure 3: Major effects of extreme temperatures at the physiology, cellular and molecular levels in plants. (**a**) Main physiology damages induce by excessive-high temperature on plants. (**b**) Main cellular and molecular damages induce by excessive-high temperature in plants. Bracket indicates the negative impact.

II) The heat shock response

II.1) Accumulation of protective heat shock proteins

To counteract and prevent irreversible molecular damages under extreme HS, all organisms, including plants, accumulate heat shock proteins (HSPs). They are synthesized under mildly rising temperatures to minimize expected damage and establish AT (58,59). Under HS, both transcriptomic and proteomic studies indicate a reprogramming of gene expression which includes the large families of HSPs which confer AT (Qin et al., 2008; Xin et al., 2016; Mangelsen et al., 2011; Finka et al., 2011). Some of them, such as the ascorbate peroxidase I and II (APX) are important because they can decrease ROS content accumulated by heat (Koussevitzky et al., 2008; Panchuk et al., 2002). Others can belong to a sub-family called heat-induced molecular chaperones. Yet, a meta-analysis in *A. thaliana* and human shows that a protein which belongs to the chaperone family is 20 times more likely to be heat-inducible than proteins which are not chaperones (22). This result indicates that there is a strong correlation between the function of chaperones and AT.

The five major conserved families of HSP chaperones are the HSP100s, HSP90s, HSP70s, HSP60s, and HSP20s, some of which are constitutively expressed, whereas others are heat-inducible (65–67). HSP chaperones necessitate the energy of ATP hydrolysis to act upon misfolded proteins except for the HSP20 family. They can mediate cellular signaling, protein repair, prevent protein misfolding and participate in protein degradation. Under HS, their main role is to repair structurally damaged proteins, stabilize membranes, prevent protein misfolded and aggregation (68–71). HSP chaperones can persist for hours to several days in cells and are required for plants efficiency at establishing AT (72,73). Each family of heat-induced molecular chaperones has a unique molecular mechanism.

- HSP70

HSP70s are ubiquitous molecular chaperones that participate in a large array of cellular signalization, protein folding, and protein structure remodeling. HSP70s can unfold nascent protein to their final translocation, prevent the formation of misfolded protein, and can recruit HSP100 for protein disaggregation (71,74–76). HSP70s are assisted by co-chaperone HSP40 and the nucleotide exchange factor GrpE which increases the refolding rate of denatured protein (77). In unstressed plant, animal, and bacteria cells, HSP70s represent between 0.5 to 2% of the total protein mass (78). *A. thaliana* contains eighteen

predicted HSP70 proteins localized in the ER, chloroplast, mitochondria, and cytosol. Some of them are constitutively expressed whereas others are up-regulated by heat (79). The overexpression of the heat-inducible HSP70-1 improves thermotolerance whereas reducing expression of HSP70-1 appears lethal for plants (80). Members of HSP70 mediate resistance to other stresses such as cold where their proper accumulation is required for acclimation in grape leaves (81).

- HSP100

HSP100 mainly participates in protein disaggregation and degradation which require the cooperation with cognate HSP70 chaperone systems to maintain cellular proteostasis (82,83). *A. thaliana* encodes for 7 classes of HSP101 which can be constitutively expressed at low-temperature levels and highly accumulated under HS (84). In *A. thaliana*, *Hot1* HSP101 mutant shows to be more sensitive to HS as compared to WT, and HSP101 is likely required for basal thermotolerance and AT (85). Additionally, HSP101 might be necessary for the memory of heat acclimation (86). Besides their role during HS, several classes of HSP100s can perform housekeeping functions in plant growth and chloroplast development (84,87).

- HSP90

HSP90 soluble proteins represent 1 to 2% of the total protein mass of the cell and are associated with HSP70 system machinery (88,89). Roles of HSP90 are described in protein folding, signaling, and trafficking such as activation of protein kinases and hormone receptors (65,90). In *A. thaliana*, seven genes encoding HSP90s can be expressed in the cytosol, mitochondria, ER, and chloroplasts (91). The expression of HSP90s may confer resistance to several biotic and abiotic stresses such as heavy metal, oxidative and salt stresses, and pathogen infection (92). HSP90 is thought to prevent the activity of heat shock transcription factor 1 (HSF1) at low temperatures. Under HS, HSP90 might release HSF1 which becomes activated for the transcription and accumulation of HSPs (93–95). This observation was suggested since at low temperatures, optimal concentrations of HSP90 inhibitors such as radicicol caused the dissociation of HSF1 resulting in a mild activation of the HSR (96–98). HSP90 inhibitors can cause abnormal morphological phenotype in seedling by affecting organ growth supporting the role of HSP90s in plant development (99).

- HSP60

HSP60s is classified into two subfamilies (65). The first is localized in the mitochondria and chloroplast where HSP60 is assisted by the cochaperone HSP10 and mediates protein folding, disaggregation, and assist plastid proteins such as Rubisco (100,101). They are also involved in newly imported proteins to the chloroplast and can interact with synthesized mitochondrial proteins (102,103). The second is expressed in the cytosol mainly required for the assembly of actin and tubulin filament (104,105).

II.2) Small heat shock proteins (HSP20s)

HSP20s are the most inducible by heat, and a large majority are the most repressed at low temperatures in plants (67,106–108). They are composed of subunits between 12 to 43 kDa and contain an alpha-crystalline domain suggested to binds denatured proteins (Fig. 4a) (109–111). HSP20s also present a variable N- terminal domain and a short C-terminal sequence that would be responsible for their oligomerization (Fig. 4a). The *A. thaliana* genome encodes for nineteen HSP20s which are divided into six classes localized in the cytosol, nucleus, ER, chloroplast, peroxisome, and mitochondria (112,113). HSP20s can bind early unfolding substrate to prevent the aggregation of heat-labile protein in an ATP-independent manner (114,115). The small HSP IbpB in *E. coli* collaborate with HSP40, HSP60, and HSP70 chaperones complex and assist the refolding of proteins such as the malate dehydrogenase (115). Supporting these observations, sHSP18.1, and sHSP16.6 bind misfolded proteins and allow further refolding by HSP70 and HSP100 complexes in *Pisum sativum* and *Synechocystis sp.* (116). Under HS, HSP20s bind misfolded proteins and address them to HSP70 and HSP100 to be disaggregated and after refolded to their native state (Fig. 4b) (107,117–121). HSP20s may stabilize lipid bilayers and thereby protect the plasma membrane from high fluidity under excessive temperatures (118,122).

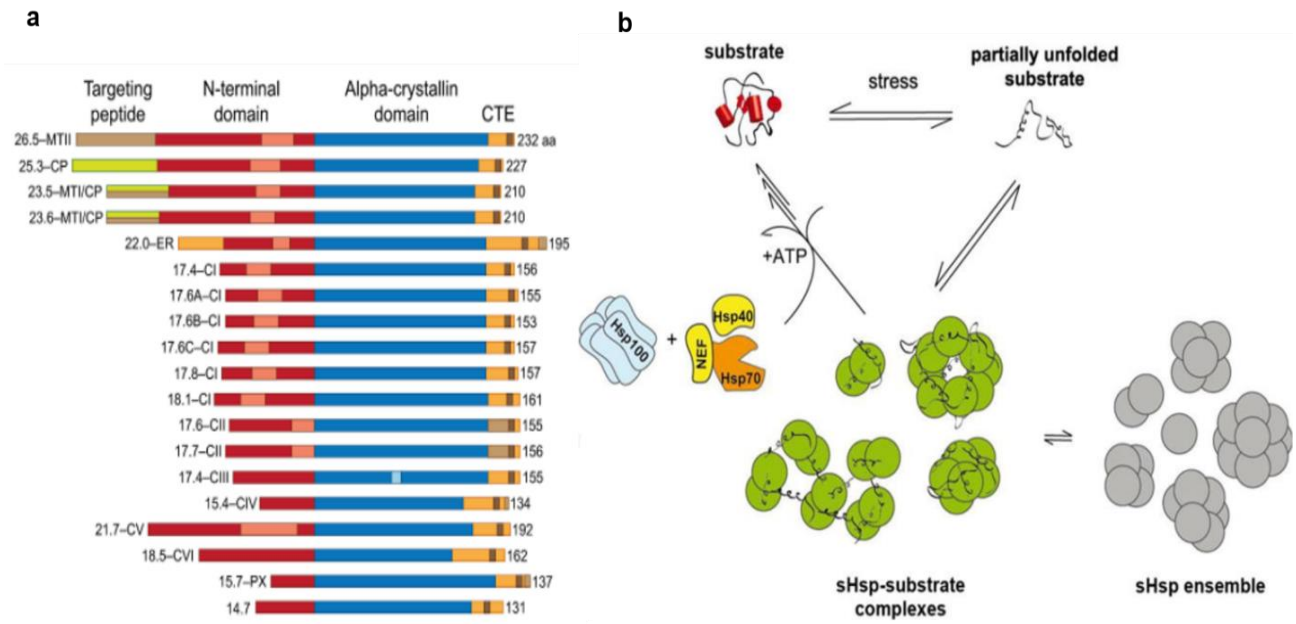

Figure 4: Illustration of small heat shock proteins in *A. thaliana* and their assistance to the refolding of denatured proteins. (**a**) Small heat shock proteins in *A. thaliana*. HSP20s have all in common an alpha-crystallin domain and their N-terminal may differ which indicates their localization in the cell. MT; mitochondrial, CP; chloroplastic; ER; endoplasmic reticulum; C; cytosolic class; and PX; peroxisome. Brown, green, and orange represent specific amino acid sequences for targeting peptides in mitochondria, chloroplast, and ER. Red represents the N-terminal domain in which embedded pink color are amino acids of the alpha helix. Blue is the alpha-crystallin domain and yellow is the C-terminal domain in which embedded brown color corresponds to specific motifs required for their oligomerization. The protein length for each HSP20s is indicated on the right of the C-terminal (CTE) (From Vierling et al., 2020). (**b**) Adapted model for the chaperone function of HSP20s. Under stress conditions such as HS, HSP20s can be assembled in a minimum to 12 oligomers and bind accumulated misfolded proteins to prevent their excessive denaturation. HSP20s work in an ATP-independent manner. The misfolded substrate can be next addressed to the HSP70/40, nucleotide exchange factor, and HSP100 machinery that will use the energy from ATP to refold misfolded protein to their native state protecting the homeostasis of the cell (from Haslbeck and Vierling, 2016).

The accumulation of HSP20s is required for basal thermotolerance and for the onset of AT. The lack of expression of HSP17.6II in *A. thaliana* causes a defective AT whereas the overexpression of LimHSP16.45, from *Lilium davidii*, rescues the phenotype (123). These results are supported with RNAi *A. thaliana* lines targeting six cytosolic class I or II of HSP20s presenting a reduced basal thermotolerance and AT. Overexpression lines of HSP20s restore and reduce the hypersensitivity phenotype (124). In wheat, the chloroplastic HSP26 is required for seed maturation, germination, and to develop tolerance to HS. Plants impaired in the expression of HSP26 are more sensitive when exposed to 39°C (Chauhan et al., 2012). Besides providing protection against HS,

HSP20s can confer resistance to salt, drought, and cold stresses (112,125–127). HSP20s may also be involved in plant growth processes such as somatic embryogenesis, pollen development, and seed germination (108,128,129).

Interestingly in several plant species, Western and Northern blots or transcriptomic and proteomic analysis show virtually a total absence of HSP20s at non-HS temperatures (25,67,130,131). In contrast, other HSP chaperones may have a high background of constitutive expression at low temperatures (67,73). This raises the question: why would plants so tightly prevent HSP20s expression at low temperatures? The complete repression at non-HS temperatures of HSP20s suggests that their constitutive expression would be problematic. To date, one study has reported the deleterious unnecessary expression of HSP20s. The overexpression of sHSP17 from *Agrostis stolonifera* in *A. thaliana* shows a reduction of leaf chlorophyll content and photosynthesis activity at both low and high temperatures. Additionally, the mutant line is hypersensitive to exogenous ABA and salinity during germination and post-germinative growth (132). Other related studies indicate that the overexpression of HSP molecular chaperones might be deleterious for plants. Although the overexpression of HSP70-1 improved the thermotolerance, it results in a dwarf phenotype (80). Furthermore, the overexpression of HSP90 in *A. thaliana* impairs the expression of a stress-responsive gene which reduces resistance to salt and drought stresses. Overexpression lines of HSP90.2, HSP90.5, or HSP90.7 show a lower germination rate and fresh weight tissues (133). Thus, plants have established a sophisticated mechanism to tightly regulate the proper expression of HSP chaperones, presumably because their unnecessary production at low temperatures could impose a cost on their fitness.

III) Heat sensing and signaling: from the plasma membrane to the activation of HSF1

III.1) The plasma membrane is the main heat sensors in plant

To properly establish molecular defenses, plant cells must sense a temperature increment and trigger a signal for the accumulation of defenses HSPs. The nucleus, ER, cytosol, mitochondria, and chloroplast may contain different heat sensors (97,134–140). Yet, the accumulation of HSPs strictly depends on the Ca^{2+} entry across the plasma membrane. Electrophysiology measurements in a recombinant reporter line in *P. patens* protoplasts, expressing the calcium-sensitive fluorescent protein aequorin, show a

maximal accumulation of cytosolic Ca^{2+} within the first 10 to 15 min following an abrupt rise of temperature from 24°C to 36°C (97). In *A. thaliana* protoplasts and evidence in *P. patens* indicate that preventing artificially the entry of periplasmic Ca^{2+} leads to a lack of HSP accumulation. A defective HSR is also observed in presence of ionomycin and thapsigargin, which are ionophores known to release Ca^{2+} from internal stores such as the ER (25,97). These results strongly indicate that the HSR strictly depends on the entry of periplasmic Ca^{2+} through the plasma membrane.

The plasma membrane can reach different degrees of fluidity depending on the temperature which delivers different degrees of message through the activation of heat-responsive calcium channels. Artificial membrane fluidizer such as benzyl alcohol (BA), increases membrane fluidity and triggers a mild HSR at non-HS temperatures in moss (141). In K562 mammalian cells, both BA and heptanol induce a downshift of the HSR at a low temperature, resulting in the overexpression of HSP70 (142). In contrast, dimethyl sulfoxide (DMSO) generally increases the rigidity of membranes. In *Chlamydomonas reinhardtii* and *Medicago sativa,* DMSO treatment negatively regulates the heat-induced HSP22E at mild HS (143,144). A high plasma membrane fluidity induces an HSR, whereas a rigidity decreases the response to HS which also depends on the lipid composition. Lipid desaturase expression can provide a balance between saturated and unsaturated lipids which ultimately affects the HSR (145). *P. patens* acclimated for one week at 32°C contained a higher saturated lipid content than when grown at 22°C. The acclimated moss exposed to a short HS at 35°C has reduced Ca^{2+} influx and HSP expression compared to the non-acclimated plant due to higher amounts of saturated lipids (146). A lipidome analysis in *A. thaliana* shows that saturated fatty acids in the plasma membrane increase when the growth temperature is shifted above 30°C for an extended amount of time (21,147). Thus, plants can actively modulate their saturated and unsaturated lipid content in their membrane to adapt to recurrent HS and warm temperature. This adaptation in lipid content makes the HSR dependent on the basal temperature of growth.

III.2) CNGCs located at the plasma membrane can act as thermosensors

The plasma membrane displays cyclic nucleotide-gated channels (CNGCs) which are tetrameric cation channels and contain six transmembrane domains (Fig. 5a). They are predicted to modulate Ca^{2+} entry in the apoplast and other ions such as K^+, Na^+, or Pb^+ in which their selectivity would depend on specific CNGCs (148). The cytosolic C-terminal of CNGCs harbors a cyclic nucleotide-binding domain (CNBD) and a calmodulin-

binding domain (CaMBD) in which a CaM-binding IQ (isoleucine-glutamine) motif is embedded. The cytosolic N-terminal may also contain a CaMBD which is not present for all CNGCs (149) (Fig. 5a). Both CNBD and CaMBD predict that cyclic nucleotide monophosphate and calmodulins (CaMs) regulate negatively or positively CNGC activity under environmental conditions (150). *A. thaliana* have twenty CNGCs families which can be assembled as homotetrameric or heterotetrameric complexes. These allow to form a large array of CNGCs sensors capable to respond to different environmental cues (Fig. 5a) (148,149). Phylogenetic analysis in *A. thaliana* reveals that AtCNGC2 and AtCNGC4 present the higher sequence identity among CNGC families suggesting common function in plant cells (Fig 5.b) (148). These two channels and their orthologs CNGCb and CNGCd in *P. patens,* act as a main primary heat sensor. Both mutants of *cngc2* and *cngcb* have a hyperthermosensitive phenotype resulting in a higher accumulation of HSPs at lower temperatures and indicate that their mutations deregulate the HSR (73,141). Before being discovered as heat sensors, *cngc2* and *cngc4* mutants are known as defense no death 1 and 2, and have been shown to mediate resistance against *Pseudomonas syringae* infection (151). Besides their roles under HS, CNGCs participate in other processes such as flowering transition, and root growth development (Tan et al., 2020). Other CNGCs may act as thermosensors in *A. thaliana* since *cngc6* knockout mutant accumulates significantly less transcript levels (around 30%) of sHSP18.2, sHSP25.3, and HSP70 at 37°C, compared to the wild type (150). Similarly, pollen of *cngc16* mutant shows an attenuated expression of several HSR response genes such as HSFA2 and HSFB1 which are required for the regulation of HSPs (153). Additionally, *cngc14* and *cngc16* mutants in rice display a lower survival rate and a higher H_2O_2 accumulation under HS compared to plant control. Furthermore, elevated HSP expression levels at low temperatures are observed in both mutants, similar to *cngc2* and *cngc4* mutants in *A. thaliana* (25,154). These observations comfort the role of specific CNGCs acting as the primary heat sensors in plants. Other calcium channels are described to respond to heat. In *A. thaliana* the lack of expression of synaptotagmin A decreases the accumulation of several HSP members family in response to heat (155). Glutamate receptor-like channels may participate in Ca^{2+} signaling since exogenous glutamate improves the basal thermotolerance in maize seedlings (156).

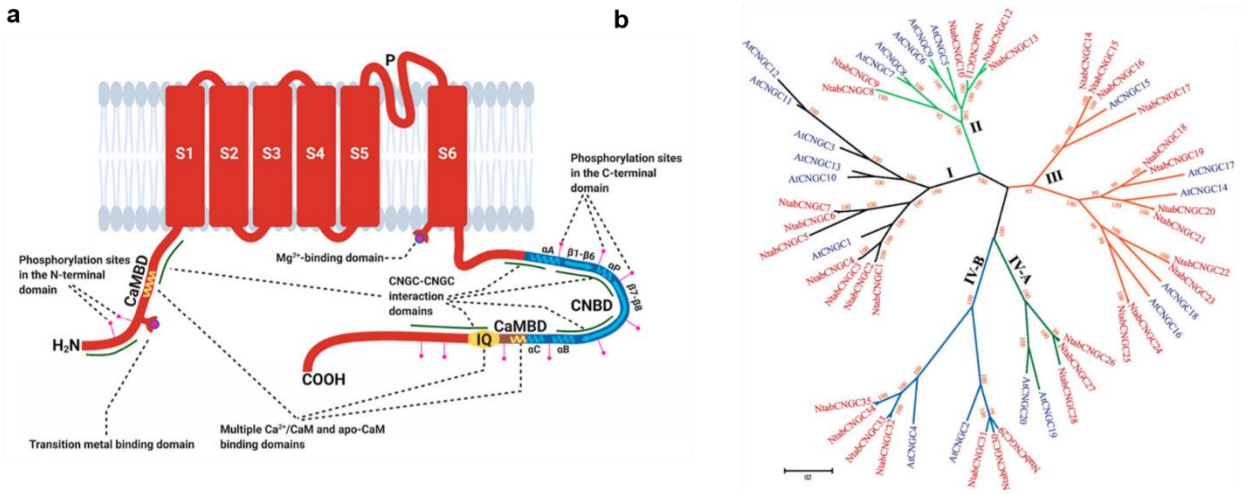

Figure 5: Cyclic nucleotide-gated channel subunit structure and their phylogenetic analysis in *A. thaliana*. (**a**) CNGC consists of six transmembrane domains (S1-S6) with a pore region between S5 and S6. The C-terminal cytosolic part may contain a CamBD and a CNBD. The N-terminal domain is also cytosolic and may present a CaMBD depending on the CNGC family. The CaMBD can have an IQ (isoleucine-glutamine) motif which can be bound by CaMs. An Mg^{2+} binding domain may be present downstream of the CNGC pore as well as a transition metal-binding domain in the N-terminus (from Jarratt-Barnham et al., 2021). (**b**) Phylogenetic tree protein analysis of the entire CNGC family in *A. thaliana* (blue) and *Nicotiana tabacum* (red). CNGC families are classified into 5 groups, respectively I (black branches), II (green branches), III (orange branches), IV-A (dark green branches), and IV-B (dark blue branches). We can notice that AtCNGC2 and AtCNGC4 are found to be sharing the highest protein sequence homology, being both thermosensors (from Jarratt-Barnham et al., 2021).

III.3) Components acting downstream to CNGCs and upstream of HSF1 activation

Once CNGCs are activated by increased temperatures and mediate the entry of periplasmic Ca^{2+} into the cytosol, the signaling molecules that ultimately activate HSF1s are unclear. Since CNGCs contain a CaMBD, CaMs may be involved in the heat signaling. *A. thaliana* encodes nine CAMs which the first seven are highly conserved and share close protein sequence homology up to 80% (see chapter 6). They are made of calcium-binding loops called E and F that each can bind two Ca^{2+} ions. CaMs are mainly located in the cytosol and can mediate several biotic and abiotic signaling pathways depending on the Ca^{2+} pattern (157–160). *A. thaliana* also contains fifty members of calmodulin-like proteins (CMLs) which are protein calcium sensors. They have between two to six predicted Ca^{2+}-binding EF hand motifs. CMLs are described to mediate stress perception and plant development (161,162). AtCaM2, AtCaM4, AtCaM6, AtCaM7 and AtCML8 are shown, through a yeast two-hybrid screen, to strongly interact with the C-terminal of several CNGCs family, including AtCNGC2 and AtCNGC4 (163). Interestingly, the

thermosensor AtCNGC6 can be negatively regulated by CaM2/3/5 and CaM7 under HS by interacting with the IQ motif and impacting Ca^{2+} entry (164). In *A. thaliana*, the *cam3* knockout mutant accumulates less AtHSP18.2, HSP25.3, and HSP83 transcripts at 37°C leading to a strong reduction of thermotolerance. The overexpression of AtCaM3 significantly restores the resistance against HS by increasing HSP expression (165). AtCaM3 activates several mediators of the heat shock signaling pathway such as mitogen-activated protein kinase 6 and calmodulin-binding protein kinase 3 (CBK3) (155,166). CBK3 can promote HSFA1 activation by phosphorylation triggering HSP transcription in *A. thaliana* (Fig. 7b) Under HS, the *cbk3* knockout line shows a lower expression of sHSP18.2 and sHSP25.3 resulting in a defective basal thermotolerance. The *cbk3* overexpression line accumulates higher levels of HSPs and rescues the hypersensitivity phenotype (167,168). In other plant species, several CaMs are identified to mediate the heat signal such as OsCaM1-1 isoform in rice, a close ortholog of AtCaM7, which mediates Ca^{2+} signals resulting in the accumulation of HSP (169). Similarly, CaM1-2 in wheat is accumulated earlier than HSP26 and HSP70 at 37°C suggesting to act upstream of the HSP gene transcription (170).

III.4) Heat shock transcription factors act as ultimate components of the heat shock signaling pathway

In plants, HSFs are classified into three groups (HSFA, HSFB, and HSFC). All HSFs have in common a DNA binding, oligomerization, and nuclear localization domains. Yet, they may differ upon the presence of an activator or an inhibitor region (Fig. 6) (171,172). Promoters of HSP genes have a conserved DNA motif called heat shock elements (HSE) which can be bound by HSFA leading to the transcription of HSPs (173,174). In contrast, HSFBs would act as antagonist repressors and compete for HSFAs at late HS by binding HSEs and thereby repressing the transcription of HSPs. HSFCs might have a similar function as HSFBs but their role is less understood and do not contain a repressor domain (175,176). In *A. thaliana*, twenty-one genes encode for HSFs and the class of HSFA1s contains four homologs (172). HSFA1a and HSFA1d are the main positive activators of the heat signaling pathway and regulate the expression of HSPs in *A. thaliana* and tomato. At 37°C, the *hsfa1a/b/d/e* mutant is confirmed to be ineffective at accumulating HSP transcripts such as HSP101, HSP90, HSA32, and HSP25.3, affecting the onset of AT (177,178). Under HS, HSFA2, HSFA3, HSFA7a, multiprotein bridging factor 1C, and dehydration-responsive element-binding protein 2A

(DREB2A), are activated by HSFA1, triggering HSP expression in *A. thaliana* (179–181). Additionally, the central role of HSF1s is not specific to the plant kingdom and is described as key components of the heat shock signaling in several organisms such as in *Candida albicans, S. cerevisiae*, and in humans (Anckar and Sistonen, 2011; Nicholls et al., 2009; Gallo et al., 1993). The role of HSFs is also mentioned regarding other environmental responses and plant growth such as oxidative, drought stresses, and seed germination (186).

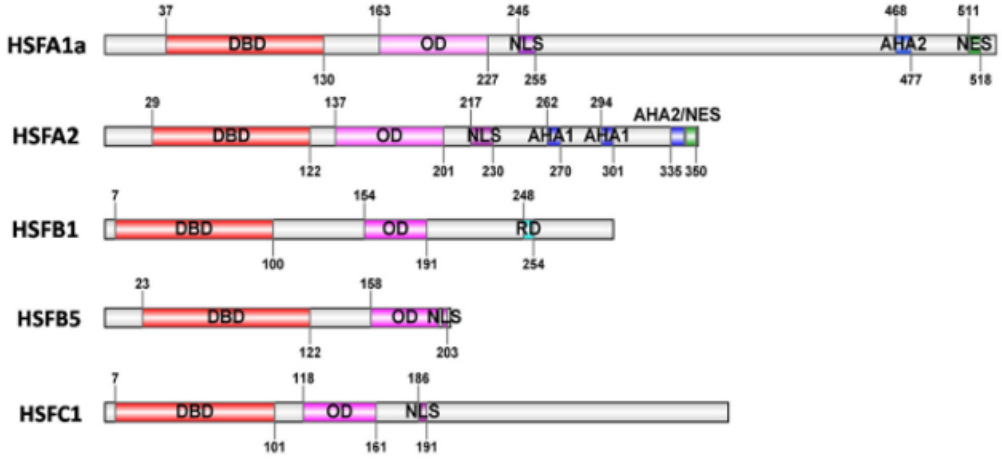

Figure 6: Structure of HSFAs, HSFBs and HSFCs in plants. All HSFs have in common a DNA binding (DBD), oligomerization (OD, and nuclear localization domains (NLS). Groups of HSFs may differ by the presence of an activator domain in HSFA (AHA) and a repressor domain in HSFB (RD). As mentioned in the text, the function of HSFCs remain unclear and do not contain an activator or repressor domain (from Guo et al., 2016).

At resting low temperatures, HSF1s are found to be hypophosphorylated in the cytosol and may bind to HSP90 and HSP70 which inhibit their activity (Fig. 7a) (95). Under HS, evidence suggests that the activation of HSF1s occurs when dissociated from HSP90 and HSP70 which are sequestrated by the increased levels of misfolded thermolabile protein in the cytosol and would serve as initial thermosensors (Fig. 7b) (187–190). Yet, when the Ca^{2+} entry through the plasma membrane is prevented during HS and thermolabile proteins although denatured, the HSR does not take place (97). Additionally, the bound HSF1 fraction should be reassessed. At rest, optimal concentrations of HSP90 inhibitors (geldanamycin and radicicol) cause the dissociation of HSF1 and activate a small HSR fraction (96–98). These observations indicate that even though all HSP90s are dissociated, a major fraction of HSF1s is not yet activated. Treatment with a saturated amount of HSP90 inhibitors triggers a minor HSR whereas a full-blown of the HSR can be

further obtained upon increase of temperatures. This result indicates that a major fraction of unexpressed HSF at low temperature is not dependent HSP90 binding (97). The majority of free HSF1s might be activated independently from an unknown signal which depends on the Ca^{2+} entry at the plasma membrane (Fig. 7a).

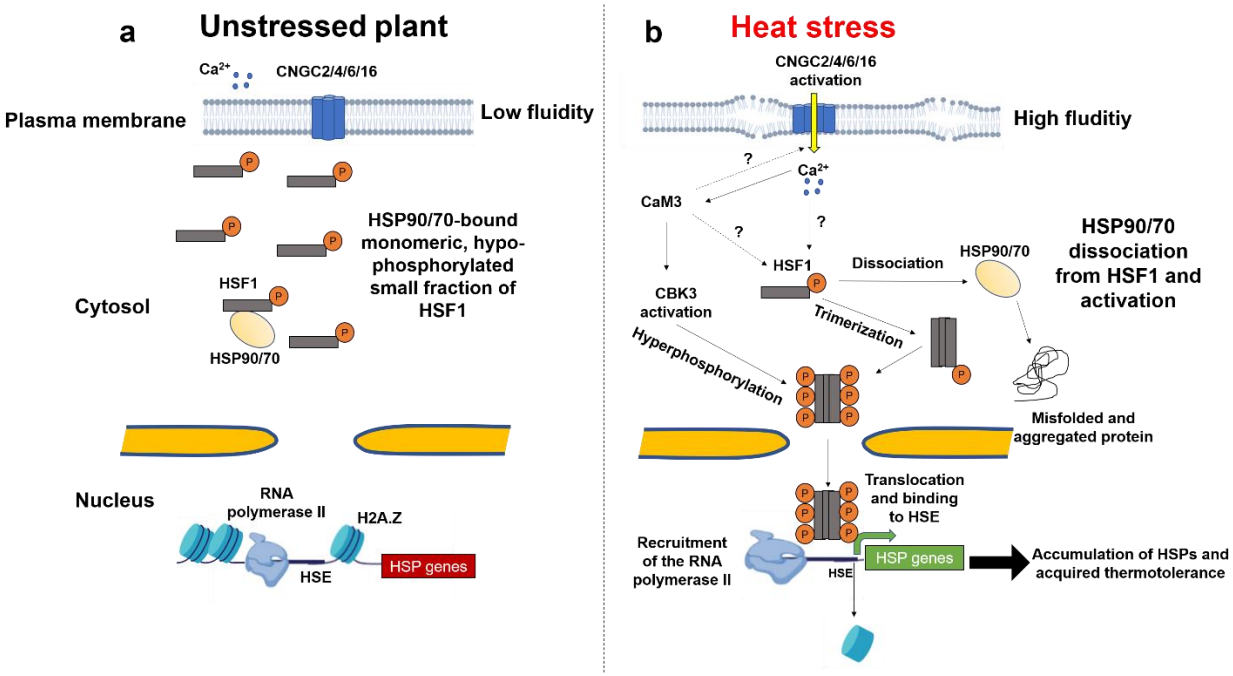

Figure 7: Heat perception by the plasma membrane and mechanisms leading to the onset of acquired thermotolerance in plants. (**a**) In unstressed plants, the rigidity of the plasma membrane avoids the activation of hypophosphorylated HSF1 which a small fraction seems to be bound to HSP90 and HSP70 complex in the cytosol. Histones wrap DNA and prevent the RNA polymerase to access HSP genes for active transcription. (**b**) The HS induces an increase in the fluidity of the plasma membrane resulting in the activation of the primary heat sensors AtCNGC2, AtCNGC4, AtCNGC6, and AtCNGC16. Transient periplasmic Ca^{2+} entry into the cytosol mediates an unknown signaling cascade that activates HSF1. Because HS is expected to denature heat-labile proteins in the cytosol, it is assumed to recruit HSP90 and HSP70 which are in part bound to HSF1. The dissociation of HSP90 and HSP70 is a key step that leads to the hyperphosphorylation of HSFA1, by CBK3, leading to their translocation into the nucleus. HSF1 can bind HSEs and might send a signal to the chromosome remodeling machinery to remove bound histones from HSP genes. RNA polymerase II is then recruited for the transcription of HSP genes ultimately leading to AT.

IV) Bound histones prevent the transcription of HSPs in unstressed plants

IV.1) Histones block RNA polymerase accessibility for the transcription of HSP genes

Expectedly, under HS, HSP genes which become actively transcribed need to be unwrapped from histones. A global rearrangement of the chromatin is observed following

HS such as in rice, rye seedlings, and *A. thaliana* where 45S rDNA and 5S rDNA loci become decondensed and transcribed (191–193). In *A. thaliana*, the actin-related protein 6 (ARP6) is an essential component of the chromatin remodeling complex required for H2A.Z incorporation (194). The *arp6* mutant shows a constitutive de-repression of HSP70 promoter resulting in HSP70 accumulation at mild and non-HS temperatures. HSP70 abnormal accumulation leads to defective phenotypes associated with warm temperatures such as accelerated growth, early flowering, and hypocotyl elongation (195,196). H2A.Z is also associated with many types of genes which are not obligatorily induced by heat such as genes responding to phosphate starvation or pathogen resistance (197–199). Therefore, the removal of H2A.Z from HSP genes cannot be considered as a specific mechanism allowing the activation of the HSR.

The signal that leads to the dissociation of the bound histone from HSP genes is not yet understood. Evidence in mammalian HEK293 cells shows that HSF1 may interact with the chromatin transcription complex following HS. It results in histone displacement which maintains the chromatin in an open state for the docking of RNA polymerase II and HSP70 transcription (Fujimoto et al., 2012). Yet, the direct or indirect role of HSFA1 in histone dissociation from the HSP genes has not been shown in plants. Thus, the activation signal coming from the plasma membrane activates HSFA1 which binds HSEs and may order histone eviction and also recruit the RNA polymerase II to transcribe HSPs (Fig. 7).

IV.2) Histones and DNA modifications by epigenetic

Epigenetic includes histone and DNA modification, RNA interference, and prions that are used by organisms to survive adverse conditions leading to turn "on" or "off" gene expression without altering the DNA sequence (200,201). Histones are made of globular proteins whose N-terminal tails are exposed on the surface of nucleosome for chemical modification such as acetylation, methylation, sumoylation, ubiquitination, and phosphorylation (202). The expression of genes might be regulated also by DNA chemical modifications such as methylation. In plants, DNA methylation is mediated by the RNA-directed DNA methylation pathway where DNA methyltransferase can catalyze the methylation of CG, CHG, and CHH sequence context (H = A, C, or T) (203–205). In *A. thaliana*, a high global level of cytosine methylation is observed when exposed to HS as compared to unstressed plants. This observation is supported by a similar methylation profile describes in *Cork oak* that grew at 55°C and in *Brassica napus* when exposed at 45°C (206–208). These results suggest that DNA methylation may regulate positively or

negatively gene expression. Histone and DNA chemical modification are also described to regulate gene expression in several biotic and abiotic stresses (Singroha and Sharma 2019). The role of epigenetic DNA methylation and histone modifications are more detailed in chapter 4.

IV.3) Repressors of HSP genes at low temperatures in plants

Several protein partners have been identified in plants to repress HSPs. The class of HSFBs may bound HSE at rest and late HS resulting in the inhibition of HSPs in plants (175). In *A. thaliana*, the microarray data of *hsfb1/hsfb2* mutant shows a higher accumulation of HSFA2, HSFA7a, and several HSPs at 23°C. Following noxious HS, the double mutant has a better survivability rate than WT (210). Supporting these observations, the lack of expression of *hsbp1* in tomato increases the thermotolerance resulting in a higher level of HSP70-1 and HSP70-5 (211). In *A. thaliana*, the transcription factor vascular plant one zinc finger protein 1 (Voz) can repress the activation of DREB2c which is required for the accumulation of HSP20s and HSP70. The lack of expression of voz1 and voz2-2 improves resistance against noxious HS (212,213).

V) Ongoing questions

HS is perceived by the plasma membrane by the presence of embedded CNGCs which mediate a periplasmic Ca^{2+} entry within the cytosol. Yet, an unknown signal activates the inactive hypophosphorylated HSF1s. They become translocated in the nucleus and bind HSEs. A complementary signal leads to the dissociation of bound histones from HSP genes and HSF1s may recruit the RNA polymerase II for the accumulation of HSPs required for the onset of AT in plants (Fig. 7). Several questions remain unanswered in the heat shock signaling pathway and should be addressed:

- What are the intermediate partners which mediate the HS signal from the CNGCs at the plasma membrane to the activation of HSF1?

- Which CaMs interact with CNGCs sensors and do they mediate the heat signaling?

- What is the specific mechanism that dissociates bound histones from HSP genes?

- What are the protein repressors of the HSR at low temperature?

Therefore, this thesis aimed to identify new genes involved in the plant heat sensing and signaling pathway, and in the repression of the HSR at non-HS temperatures.

References

1. Wodniok S, Brinkmann H, Glöckner G, Heidel AJ, Philippe H, Melkonian M, et al. Origin of land plants: Do conjugating green algae hold the key? BMC Evol Biol. 2011;11(1).

2. Suzuki N, Rivero RM, Shulaev V, Blumwald E, Mittler R. Abiotic and biotic stress combinations. New Phytol. 2014;203(1):32–43.

3. Pnueli L, Hallak-Herr E, Rozenberg M, Cohen M, Goloubinoff P, Kaplan A, et al. Molecular and biochemical mechanisms associated with dormancy and drought tolerance in the desert legume Retama raetam. Plant J. 2002;31(3):319–30.

4. Moore TG. science & & society. 2008;9:1–5.

5. Bita CE, Gerats T. Plant tolerance to high temperature in a changing environment: Scientific fundamentals and production of heat stress-tolerant crops. Vol. 4, Frontiers in Plant Science. 2013. p. 1–18.

6. Hatfield JL, Prueger JH. Temperature extremes: Effect on plant growth and development. Weather Clim Extrem. 2015;10:4–10.

7. Angeles-Malaspina M, González-Cruz JE, Ramírez-Beltran N. Projections of Heat Waves Events in the Intra-Americas Region Using Multimodel Ensemble. Adv Meteorol. 2018;2018:18–21.

8. Venkataraman C. Climate Change Signals and Response [Internet]. Venkataraman C, Mishra T, Ghosh S, Karmakar S, editors. Singapore: Springer Singapore; 2019. Available from: http://link.springer.com/10.1007/978-981-13-0280-0

9. Perkins-Kirkpatrick SE, Lewis SC. Increasing trends in regional heatwaves. Nat Commun [Internet]. 2020;11(1):1–8. Available from: http://dx.doi.org/10.1038/s41467-020-16970-7

10. Zhao C, Liu B, Piao S, Wang X, Lobell DB, Huang Y, et al. Temperature increase reduces global yields of major crops in four independent estimates. Proc Natl Acad Sci U S A. 2017;114(35):9326–31.

11. Lutz W, Kc S. Dimensions of global population projections : what do we know about future population trends and structures ? 2010;2779–91.

12. Mittler R, Finka A, Goloubinoff P. How do plants feel the heat? Trends Biochem Sci [Internet]. 2012;37(3):118–25. Available from: http://dx.doi.org/10.1016/j.tibs.2011.11.007

13. Meinke DW, Cherry JM, Dean C, Rounsley SD, Koornneef M. Arabidopsis thaliana: A model plant for genome analysis. Science (80-). 1998;282(5389).

14. Bahadur B, Rajam MV, Sahijram L, Krishnamurthy K V. Plant biology and biotechnology: Volume II: Plant genomics and biotechnology. Plant Biol Biotechnol Vol II Plant Genomics Biotechnol. 2015;II:1–768.

15. Liu J, Feng L, Li J, He Z. Genetic and epigenetic control of plant heat responses. Front Plant Sci.

2015;6(APR):1–21.

16. Balasubramanian S, Sureshkumar S, Lempe J, Weigel D. Potent induction of Arabidopsis thaliana flowering by elevated growth temperature. PLoS Genet. 2006;2(7):0980–9.

17. Zaidi NW, Dar MH, Singh S, Singh US. Trichoderma Species as Abiotic Stress Relievers in Plants [Internet]. Biotechnology and Biology of Trichoderma. Elsevier; 2014. 515–525 p. Available from: http://dx.doi.org/10.1016/B978-0-444-59576-8.00038-2

18. Clarke SM, Mur LAJ, Wood JE, Scott IM. Salicylic acid dependent signaling promotes basal thermotolerance but is not essential for acquired thermotolerance in Arabidopsis thaliana. Plant J. 2004;38(3):432–47.

19. Lindquist S. THE HEAT-SHOCK RESPONSE. 1986;

20. Baeumlisberger M, Karas M, Brüggemann W, Ashoub A, Neupaertl M. Characterization of common and distinctive adjustments of wild barley leaf proteome under drought acclimation, heat stress and their combination. Plant Mol Biol. 2015;87(4–5):459–71.

21. Higashi Y, Okazaki Y, Myouga F, Shinozaki K, Saito K. Landscape of the lipidome and transcriptome under heat stress in Arabidopsis thaliana. Sci Rep [Internet]. 2015;5:1–7. Available from: http://dx.doi.org/10.1038/srep10533

22. Finka A, Mattoo RUH, Goloubinoff P. Meta-analysis of heat-and chemically upregulated chaperone genes in plant and human cells. Cell Stress Chaperones. 2011;16(1):15–31.

23. Daniell JW, Chappell WE, Couch HB. Effect of Sublethal and Lethal Temperature on Plant Cells. Plant Physiol. 2008;44(12):1684–9.

24. Wasternack C. A plant's balance of growth and defense - revisited. New Phytol. 2017;215(4):1291–4.

25. Finka A, Cuendet AFH, Maathuis FJM, Saidi Y, Goloubinoff P. Plasma Membrane Cyclic Nucleotide Gated Calcium Channels Control Land Plant Thermal Sensing and Acquired Thermotolerance. Plant Cell [Internet]. 2012;24(8):3333–48. Available from: http://www.plantcell.org/cgi/doi/10.1105/tpc.112.095844

26. Tyler P. References and Notes. Labour's Lost Lead. 2020;333(July):616–21.

27. CAO YY, DUAN H, YANG LN, WANG ZQ, ZHOU SC, YANG JC. Effect of Heat Stress During Meiosis on Grain Yield of Rice Cultivars Differing in Heat Tolerance and Its Physiological Mechanism. Acta Agron Sin [Internet]. 2008;34(12):2134–42. Available from: http://dx.doi.org/10.1016/S1875-2780(09)60022-5

28. Tan W, Meng Q wei, Brestic M, Olsovska K, Yang X. Photosynthesis is improved by exogenous calcium in heat-stressed tobacco plants. J Plant Physiol [Internet]. 2011;168(17):2063–71. Available from: http://dx.doi.org/10.1016/j.jplph.2011.06.009

29. Vollenweider P, Günthardt-Goerg MS. Diagnosis of abiotic and biotic stress factors using the visible

symptoms in foliage. Environ Pollut. 2005;137(3):455–65.

30. Hua J. From freezing to scorching, transcriptional responses to temperature variations in plants. Curr Opin Plant Biol. 2009;12(5):568–73.

31. Tian J, Belanger FC, Huang B. Identification of heat stress-responsive genes in heat-adapted thermal Agrostis scabra by suppression subtractive hybridization. J Plant Physiol. 2009;166(6):588–601.

32. Ashraf M, Hafeez M. Thermotolerance of pearl millet and maize at early growth stages: Growth and nutrient relations. Biol Plant. 2004;48(1):81–6.

33. Wahid A. Physiological implications of metabolite biosynthesis for net assimilation and heat-stress tolerance of sugarcane (Saccharum officinarum) sprouts. J Plant Res. 2007;120(2):219–28.

34. Pharm IJ, Res P, B HMP, A LP, Nandagopalan V, A LS. Effect of Heat Treatment on Germination , Seedling Growth and Some Biochemical Parameters of Dry Seeds of Black Gram. 2012;1(4):194–202.

35. Niu Y, Xiang Y. An Overview of Biomembrane Functions in Plant Responses to High-Temperature Stress. 2018;9(July):1–18.

36. Grams TEE, Lautner S, Felle HH, Matyssek R, Fromm J. Heat-induced electrical signals affect cytoplasmic and apoplastic pH as well as photosynthesis during propagation through the maize leaf. Plant, Cell Environ. 2009;32(4):319–26.

37. Smertenko A, Dráber P, Viklický V, Opatrný Z. Heat stress affects the organization of microtubules and cell division in Nicotiana tabacum cells. Plant, Cell Environ. 1997;20(12):1534–42.

38. Müller J, Menzel D, Šamaj J. Cell-type-specific disruption and recovery of the cytoskeleton in Arabidopsis thaliana epidermal root cells upon heat shock stress. Protoplasma. 2007;230(3–4):231–42.

39. Wahid A, Gelani S, Ashraf M, Foolad MR. Heat tolerance in plants: An overview. Environ Exp Bot. 2007;61(3):199–223.

40. Sharkey TD. Effects of moderate heat stress on photosynthesis : importance of thylakoid reactions , rubisco deactivation , reactive oxygen species , and thermotolerance provided by isoprene. 2005;269–77.

41. Salvucci ME, Crafts-Brandner SJ. Inhibition of photosynthesis by heat stress: The activation state of Rubisco as a limiting factor in photosynthesis. Physiol Plant. 2004;120(2):179–86.

42. Morales D, Rodríguez P, Dell'Amico J, Nicolás E, Torrecillas A, Sánchez-Blanco MJ. High-temperature preconditioning and thermal shock imposition affects water relations, gas exchange and root hydraulic conductivity in tomato. Vol. 47, Biologia Plantarum. 2003. p. 203–8.

43. Salvucci ME, Osteryoung KW, Crafts-Brandner SJ, Vierling E. Exceptional sensitivity of Rubisco activase to thermal denaturation in vitro and in vivo. Plant Physiol. 2001;127(3):1053–64.

44. Fedyaeva A V., Stepanov A V., Lyubushkina I V., Pobezhimova TP, Rikhvanov EG. Heat shock induces production of reactive oxygen species and increases inner mitochondrial membrane potential in winter wheat cells. Biochem. 2014;79(11):1202–10.

45. Apel K, Hirt H. REACTIVE OXYGEN SPECIES: Metabolism, Oxidative Stress, and Signal Transduction. Annu Rev Plant Biol. 2004;55(1):373–99.

46. Simon HU, Haj-Yehia A, Levi-Schaffer F. Role of reactive oxygen species (ROS) in apoptosis induction. Apoptosis. 2000;5(5):415–8.

47. Huang H, Ullah F, Zhou DX, Yi M, Zhao Y. Mechanisms of ROS regulation of plant development and stress responses. Front Plant Sci. 2019;10(June):1–10.

48. Suzuki N, Koussevitzky S, Mittler R, Miller G. ROS and redox signalling in the response of plants to abiotic stress. Plant, Cell Environ. 2012;35(2):259–70.

49. Pan R, Jones AD, Hu J. Cardiolipin-Mediated Mitochondrial Dynamics and Stress Response in Arabidopsis. 2014;26(January):391–409.

50. Paradies G, Ruggiero FM, Petrosillo G, Quagliariello E. Peroxidative damage to cardiac mitochondria : cytochrome oxidase and cardiolipin alterations. 1998;424:155–8.

51. Atkin OK, Tjoelker MG. Thermal acclimation and the dynamic response of plant respiration to temperature. Trends Plant Sci. 2003;8(7):343–51.

52. Sharma SK, De Los Rios P, Goloubinoff P. Probing the different chaperone activities of the bacterial HSP70-HSP40 system using a thermolabile luciferase substrate. Proteins Struct Funct Bioinforma. 2011;79(6):1991–8.

53. Xu G, Pattamatta A, Hildago R, Pace MC, Brown H, Borchelt DR. Vulnerability of newly synthesized proteins to proteostasis stress. J Cell Sci. 2016;129(9):1892–901.

54. Cherkasov V, Grousl T, Theer P, Vainshtein Y, Gläßer C, Mongis C, et al. Systemic control of protein synthesis through sequestration of translation and ribosome biogenesis factors during severe heat stress. FEBS Lett [Internet]. 2015;589(23):3654–64. Available from: http://dx.doi.org/10.1016/j.febslet.2015.10.010

55. Yángüez E, Castro-Sanz AB, Fernández-Bautista N, Oliveros JC, Castellano MM. Analysis of genome-wide changes in the translatome of Arabidopsis seedlings subjected to heat stress. PLoS One. 2013;8(8).

56. Kantidze OL, Velichko AK, Luzhin A V, Razin S V. Heat Stress-Induced DNA Damage. 2016;8(29):75–8.

57. Ly V, Hatherell A, Kim E, Chan A, Belmonte MF, Schroeder DF. Interactions between Arabidopsis DNA repair genes UVH6, DDB1A, and DDB2 during abiotic stress tolerance and floral development. Plant Sci [Internet]. 2013;213:88–97. Available from: http://dx.doi.org/10.1016/j.plantsci.2013.09.004

58. Serrano N, Ling Y, Bahieldin A, Mahfouz MM. Thermopriming reprograms metabolic homeostasis to confer heat tolerance. Sci Rep. 2019;9(1):1–14.

59. Song L, Jiang Y, Zhao H, Hou M. Acquired thermotolerance in plants. Plant Cell Tissue Organ Cult. 2012;111(3):265–76.

60. Qin D, Wu H, Peng H, Yao Y, Ni Z, Li Z, et al. Heat stress-responsive transcriptome analysis in heat susceptible and tolerant wheat (Triticum aestivum L.) by using Wheat Genome Array. BMC Genomics. 2008;9:1–19.

61. Xin C, Wang X, Cai J, Zhou Q, Liu F, Dai T, et al. Changes of transcriptome and proteome are associated with the enhanced post-anthesis high temperature tolerance induced by pre-anthesis heat priming in wheat. Plant Growth Regul. 2016;79(2):135–45.

62. Mangelsen E, Kilian J, Harter K, Jansson C, Wanke D, Sundberg E. Transcriptome analysis of high-temperature stress in developing barley caryopses: Early stress responses and effects on storage compound biosynthesis. Mol Plant [Internet]. 2011;4(1):97–115. Available from: http://dx.doi.org/10.1093/mp/ssq058

63. Koussevitzky S, Suzuki N, Huntington S, Armijo L, Sha W, Cortes D, et al. Ascorbate Peroxidase 1 Plays a Key Role in the Response of Arabidopsis thaliana to Stress Combination * □. 2008;283(49):34197–203.

64. Panchuk II, Volkov RA, Scho F. Heat Stress- and Heat Shock Transcription Factor- Dependent Expression and Activity of Ascorbate Peroxidase in Arabidopsis 1. 2002;

65. Wang W, Vinocur B, Shoseyov O, Altman A. Role of plant heat-shock proteins and molecular chaperones in the abiotic stress response. Trends Plant Sci. 2004;9(5):244–52.

66. Finka A, Sood V, Quadroni M, De Los Rios PDL, Goloubinoff P. Quantitative proteomics of heat-treated human cells show an across-the-board mild depletion of housekeeping proteins to massively accumulate few HSPs. Cell Stress Chaperones. 2015;20(4):605–20.

67. Guihur A, Fauvet B, Finka A, Quadroni M, Goloubinoff P. Quantitative proteomic analysis to capture the role of heat-accumulated proteins in moss plant acquired thermotolerance. Plant Cell Environ. 2020;(December):1–17.

68. Glatz A, Pilbat AM, Németh GL, Vince-Kontár K, Jósvay K, Hunya Á, et al. Involvement of small heat shock proteins, trehalose, and lipids in the thermal stress management in Schizosaccharomyces pombe. Cell Stress Chaperones. 2016;21(2):327–38.

69. Vigh L, Török Z, Crul T, Maresca B, Schütz GJ, Viana F, et al. Plasma membranes as heat stress sensors: From lipid-controlled molecular switches to therapeutic applications. Biochim Biophys Acta - Biomembr [Internet]. 2014;1838(6):1594–618. Available from: http://dx.doi.org/10.1016/j.bbamem.2013.12.015

70. Park CJ, Seo YS. Heat shock proteins: A review of the molecular chaperones for plant immunity.

Plant Pathol J. 2015;31(4):323–33.

71. Finka A, Sharma SK, Goloubinoff P. Multi-layered molecular mechanisms of polypeptide holding, unfolding and disaggregation by HSP70/HSP110 chaperones. Front Mol Biosci [Internet]. 2015;2(June):29. Available from: http://europepmc.org/articles/PMC4456865/?report=abstract

72. Sedaghatmehr M, Mueller-Roeber B, Balazadeh S. The plastid metalloprotease FtsH6 and small heat shock protein HSP21 jointly regulate thermomemory in Arabidopsis. Nat Commun. 2016;7.

73. Finka A, Cuendet AF, Maathuis FJ, Saidi Y, Goloubinoff P. Plasma membrane cyclic nucleotide gated calcium channels control land plant thermal sensing and acquired thermotolerance. Plant Cell [Internet]. 2012;24(8):3333–48. Available from: http://www.ncbi.nlm.nih.gov/pubmed/22904147

74. Mayer MP, Bukau B. Hsp70 chaperones: Cellular functions and molecular mechanism. Cell Mol Life Sci. 2005;62(6):670–84.

75. Kampinga HH, Craig EA. The HSP70 chaperone machinery: J proteins as drivers of functional specificity. Nat Rev Mol Cell Biol [Internet]. 2010;11(8):579–92. Available from: http://dx.doi.org/10.1038/nrm2941

76. Rosenzweig R, Nillegoda NB, Mayer MP, Bukau B. The Hsp70 chaperone network. Nat Rev Mol Cell Biol [Internet]. 2019;20(11):665–80. Available from: http://dx.doi.org/10.1038/s41580-019-0133-3

77. Diamant S, Goloubinoff P. Temperature-controlled activity of DnaK-DnaJ-GrpE chaperones: Protein-folding arrest and recovery during and after heat shock depends on the substrate protein and the GrpE concentration. Biochemistry. 1998;37(27):9688–94.

78. Finka A, Goloubinoff P. Proteomic data from human cell cultures refine mechanisms of chaperone-mediated protein homeostasis. Cell Stress Chaperones. 2013;18(5):591–605.

79. Lin BL, Wang JS, Liu HC, Chen RW, Meyer Y, Barakat A, et al. Genomic analysis of the Hsp70 superfamily in Arabidopsis thaliana. Cell Stress Chaperones. 2001;6(3):201–8.

80. Sung DY, Guy CL. Physiological and Molecular Assessment of Altered Expression of Hsc70-1 in Arabidopsis . Evidence for Pleiotropic Consequences 1. 2015;

81. Zhang J, Wang L, Pan Q, Wang Y, Zhan J, Huang W. Scientia Horticulturae Accumulation and subcellular localization of heat shock proteins in young grape leaves during cross-adaptation to temperature stresses. 2008;117:231–40.

82. Bösl B, Grimminger V, Walter S. The molecular chaperone Hsp104-A molecular machine for protein disaggregation. J Struct Biol. 2006;156(1):139–48.

83. Kim HJ, Hwang NR, Lee KJ. Heat shock responses for understanding diseases of protein denaturation. Mol Cells. 2007;23(2):123–31.

84. Lee U, Rioflorido I, Hong SW, Larkindale J, Waters ER, Vierling E. The Arabidopsis ClpB/Hsp100 family of proteins: Chaperones for stress and chloroplast development. Plant J. 2007;49(1):115–27.

85. Hong SW, Vierling E. Hsp101 is necessary for heat tolerance but dispensable for development and germination in the absence of stress. Plant J. 2001;27(1):25–35.

86. Hu C, Lin SY, Chi WT, Charng YY. Recent gene duplication and subfunctionalization produced a mitochondrial GrpE, the nucleotide exchange factor of the Hsp70 complex, specialized in thermotolerance to chronic heat stress in Arabidopsis. Plant Physiol. 2012;158(2):747–58.

87. Component K, Author P, Source WBG, Society A, Biologists P, Url S, et al. HSP101 : A Key Component for the Acquisition of Thermotolerance in Plants. 2016;12(4):457–60.

88. Johnson JL. Evolution and function of diverse Hsp90 homologs and cochaperone proteins. Biochim Biophys Acta - Mol Cell Res [Internet]. 2012;1823(3):607–13. Available from: http://dx.doi.org/10.1016/j.bbamcr.2011.09.020

89. Donnelly BF, Needham PG, Snyder AC, Roy A, Khadem S, Brodsky JL, et al. Hsp70 and Hsp90 multichaperone complexes sequentially regulate thiazide-sensitive cotransporter endoplasmic reticulum-associated degradation and biogenesis. J Biol Chem [Internet]. 2013;288(18):13124–35. Available from: http://dx.doi.org/10.1074/jbc.M113.455394

90. Pratt WB, Toft DO. Regulation of signaling protein function and trafficking by the hsp90/hsp70-based chaperone machinery. Exp Biol Med. 2003;228(2):111–33.

91. Krishna P, Gloor G. The Hsp90 family of proteins in arabidopsis thaliana. Cell Stress Chaperones. 2001;6(3):238–46.

92. Xu ZS, Li ZY, Chen Y, Chen M, Li LC, Ma YZ. Heat shock protein 90 in plants: Molecular mechanisms and roles in stress responses. Int J Mol Sci. 2012;13(12):15706–23.

93. Thao NP, Chen L, Nakashima A, Hara SI, Umemura K, Takahashi A, et al. RAR1 and HSP90 form a complex with Rac/Rop GTPase and function in innate-immune responses in rice. Plant Cell. 2007;19(12):4035–45.

94. Yamada K, Fukao Y, Hayashi M, Fukazawa M, Suzuki I, Nishimura M. Cytosolic HSP90 Regulates the Heat Shock Response That Is Responsible for Heat Acclimation in Arabidopsis thaliana * □. 2007;282(52):37794–804.

95. Morimoto RI. The Heat Shock Response : Systems Biology of Proteotoxic Stress in Aging and Disease. Cold Spring Harb Symp Quant Biol. 2012;76:91–9.

96. Westerheide SD, Kawahara TLA, Orton K, Morimoto RI. Triptolide, an inhibitor of the human heat shock response that enhances stress-induced cell death. J Biol Chem. 2006;281(14):9616–22.

97. Saidi Y, Finka A, Muriset M, Bromberg Z, Weiss YG, Maathuis FJM, et al. The Heat Shock Response in Moss Plants Is Regulated by Specific Calcium-Permeable Channels in the Plasma Membrane. Plant Cell Online [Internet]. 2009;21(9):2829–43. Available from: http://www.plantcell.org/cgi/doi/10.1105/tpc.108.065318

98. Kyle Hadden M, Lubbers D, J. Blagg B. Geldanamycin, Radicicol, and Chimeric Inhibitors of the Hsp90 Nterminal ATP Binding Site. Curr Top Med Chem. 2006;6(11):1173–82.

99. Queitsch C, Sangster TA, Lindquist S. 47781 618..624. Nature [Internet]. 2002;417(June):618–24. Available from: papers3://publication/uuid/5C99B3E4-9B5E-4341-B05A-6136A878AA69

100. Goloubinoff P, Gatenby AA, Lorimer GH. GroE heat-shock proteins promote assembly of foreign prokaryotic ribulose bisphosphate carboxylase oligomers in Escherichia coli. Vol. 337, Nature. 1989. p. 44–7.

101. Wang L, Hingorani SR, Tuveson DA. es Bio Do No t D ist r. 2004;(July):657–9.

102. Flores-Pérez Ú, Jarvis P. Molecular chaperone involvement in chloroplast protein import. Biochim Biophys Acta - Mol Cell Res [Internet]. 2013;1833(2):332–40. Available from: http://dx.doi.org/10.1016/j.bbamcr.2012.03.019

103. Prasad TK, Hack E, Hallberg RL. Function of the maize mitochondrial chaperonin hsp60: specific association between hsp60 and newly synthesized F1-ATPase alpha subunits. Mol Cell Biol. 1990;10(8):3979–86.

104. Ursic D, Sedbrook JC, Himmel KL, Culbertson MR. The Essential Yeast Tcpl Protein Affects Actin and Microtubules. 1994;5(October):1065–80.

105. Vinh DB, Drubin DG. A yeast TCP-1-like protein is required for actin function in vivo. 1994;91(September):9116–20.

106. Vierling E. The Roles of Heat Shock Proteins in Plants THE ROLES OF HEAT SHOCK PROTEINS IN PLANTS. 2014;(November 2003).

107. Waters ER, Lee GJ, Vierling E. Evolution, structure and function of the small heat shock proteins in plants. J Exp Bot [Internet]. 1996;47(3):325–38. Available from: https://academic.oup.com/jxb/article-lookup/doi/10.1093/jxb/47.3.325

108. AL-Quraan NA, Locy RD, Singh NK, Sun W, Montagu M Van, Verbruggen N. Small heat shock proteins and stress toler.pdf. Plant Physiol Biochem [Internet]. 2002;1577(8):1–9. Available from: http://dx.doi.org/10.1016/j.plaphy.2010.04.011

109. Haslbeck M, Franzmann T, Weinfurtner D, Buchner J. Some like it hot: The structure and function of small heat-shock proteins. Nat Struct Mol Biol. 2005;12(10):842–6.

110. Basha E, O'Neill H, Vierling E. Small heat shock proteins and α-crystallins: dynamic proteins with flexible functions. Trends Biochem Sci [Internet]. 2012 Mar;37(3):106–17. Available from: https://linkinghub.elsevier.com/retrieve/pii/S0968000411001903

111. Waters ER. Tansley review Plant small heat shock proteins – evolutionary and functional diversity. 2020;24–37.

112. Sun W, Montagu M Van, Verbruggen N. Small heat shock proteins and stress toler.pdf. 2002;1577:1–

9.

113. Waters ER, Vierling E. Plant small heat shock proteins – evolutionary and functional diversity. New Phytol. 2020;

114. Mogk A, Bukau B. Role of sHsps in organizing cytosolic protein aggregation and disaggregation. Cell Stress Chaperones. 2017;22(4):493–502.

115. Veinger L, Diamant S, Buchner J, Goloubinoff P. The small heat-shock protein IbpB from Escherichia coli stabilizes stress-denatured proteins for subsequent refolding by a multichaperone network. J Biol Chem. 1998;273(18):11032–7.

116. Mogk A, Schlieker C, Friedrich KL, Schönfeld HJ, Vierling E, Bukau B. Refolding of substrates bound to small Hsps relies on a disaggregation reaction mediated most efficiently by ClpB/DnaK. J Biol Chem. 2003;278(33):31033–42.

117. Swindell WR, Huebner M, Weber AP. Transcriptional profiling of Arabidopsis heat shock proteins and transcription factors reveals extensive overlap between heat and non-heat stress response pathways. BMC Genomics [Internet]. 2007;8(1):125. Available from: http://bmcgenomics.biomedcentral.com/articles/10.1186/1471-2164-8-125

118. Haslbeck M, Vierling E. A First Line of Stress Defense: Small Heat Shock Proteins and Their Function in Protein Homeostasis. J Mol Biol [Internet]. 2015 Apr;427(7):1537–48. Available from: https://linkinghub.elsevier.com/retrieve/pii/S0022283615000819

119. Mogk A, Kummer E, Bukau B. Cooperation of Hsp70 and Hsp100 chaperone machines in protein disaggregation. Front Mol Biosci. 2015;2(MAY):1–10.

120. Glover JR, Lindquist S. Hsp104, Hsp70, and Hsp40: A novel chaperone system that rescues previously aggregated proteins. Cell. 1998;94(1):73–82.

121. Goloubinoff P, Mogk A, Ben Zvi AP, Tomoyasu T, Bukau B. Sequential mechanism of solubilization and refolding of stable protein aggregates by a bichaperone network. Proc Natl Acad Sci U S A. 1999;96(24):13732–7.

122. Horváth I, Multhoff G, Sonnleitner A, Vígh L. Biochimica et Biophysica Acta Membrane-associated stress proteins : More than simply chaperones. 2008;1778:1653–64.

123. Yang R, Yu G, Li H, Li X, Mu C. Overexpression of Small Heat Shock Protein LimHSP16.45 in Arabidopsis hsp17.6II Mutant Enhances Tolerance to Abiotic Stresses. Russ J Plant Physiol. 2020;67(2):231–41.

124. McLoughlin F, Basha E, Fowler ME, Kim M, Bordowitz J, Katiyar-Agarwal S, et al. Class I and II small heat shock proteins together with HSP101 protect protein translation factors during heat stress. Plant Physiol. 2016;172(2):1221–36.

125. Song N, Ahn Y. DcHsp17 . 7 , a Small Heat Shock Protein from Carrot , Is Upregulated under Cold

Stress and Enhances Cold Tolerance by Functioning as a Molecular Chaperone. 2010;45(3):469–74.

126. Yang G, Wang Y, Zhang K. Expression analysis of nine small heat shock protein genes from Tamarix hispida in response to different abiotic stresses and abscisic acid treatment. 2014;1279–89.

127. Sarkar NK, Kim Y, Grover A. Rice sHsp genes : genomic organization and expression profiling under stress and development. 2009;18.

128. Volkov RA, Panchuk II, Scho F. Small heat shock proteins are differentially regulated during pollen development and following heat stress in tobacco. 2005;487–502.

129. Chauhan H, Khurana N, Nijhavan A, Khurana JP, Khurana P. The wheat chloroplastic small heat shock protein (sHSP26) is involved in seed maturation and germination and imparts tolerance to heat stress. Plant, Cell Environ. 2012;35(11):1912–31.

130. Simões-Araújo JL, Rumjanek NG, Margis-Pinheiro M. Small heat shock proteins genes are differentially expressed in distinct varieties of common bean. Brazilian J Plant Physiol. 2003;15(1):33–41.

131. Hernandez LD, Vierling E. Expression of low molecular weight heat-shock proteins under field conditions. Plant Physiol. 1993;101(4):1209–16.

132. Sun X, Sun C, Li Z, Hu Q, Han L, Luo H. AsHSP17 , a creeping bentgrass small heat shock protein modulates plant photosynthesis and ABA-dependent and independent signalling to attenuate plant response to abiotic stress. 2016;1320–37.

133. Song H, Zhao R, Fan P, Wang X, Chen X, Li Y. in Arabidopsis thaliana enhances plant sensitivity to salt and drought stresses. 2009;955–64.

134. Schwarzländer M, Finkemeier I. Mitochondrial Energy and Redox Signaling in Plants. Antioxid Redox Signal. 2012;18(16):2122–44.

135. Sun A-Z, Guo F-Q. Chloroplast Retrograde Regulation of Heat Stress Responses in Plants. Front Plant Sci [Internet]. 2016;7(March):1–16. Available from: http://journal.frontiersin.org/Article/10.3389/fpls.2016.00398/abstract

136. Franklin KA. Plant Chromatin Feels the Heat. Cell. 2010;140(1):26–8.

137. Bussell JD, Estavillo GM, Che P, Pogson BJ, Smith SM, Zhou W. Signaling from the Endoplasmic Reticulum Activates Brassinosteroid Signaling and Promotes Acclimation to Stress in Arabidopsis. Sci Signal. 2010;3(141):ra69–ra69.

138. Chang F, Ma H, Yang H, Song Z-T, Liu J-X, Ding L, et al. Tissue-Specific Transcriptomics Reveals an Important Role of the Unfolded Protein Response in Maintaining Fertility upon Heat Stress in Arabidopsis. Plant Cell. 2017;29(5):1007–23.

139. Lin KF, Tsai MY, Lu CA, Wu SJ, Yeh CH. The roles of Arabidopsis HSFA2, HSFA4a, and HSFA7a in the heat shock response and cytosolic protein response. Bot Stud [Internet]. 2018;59(1). Available

from: https://doi.org/10.1186/s40529-018-0231-0

140. Hentze N, Le Breton L, Wiesner J, Kempf G, Mayer MP. Molecular mechanism of thermosensory function of human heat shock transcription factor Hsf1. Elife. 2016;5(1):1–24.

141. Finka A, Goloubinoff P. The CNGCb and CNGCd genes from Physcomitrella patens moss encode for thermosensory calcium channels responding to fluidity changes in the plasma membrane. Cell Stress Chaperones. 2014;19(1):83–90.

142. Balogh G, Horváth I, Nagy E, Hoyk Z, Benkõ S, Bensaude O, et al. The hyperfluidization of mammalian cell membranes acts as a signal to initiate the heat shock protein response. FEBS J. 2005;272(23):6077–86.

143. Rütgers M, Muranaka LS, Schulz-Raffelt M, Thoms S, Schurig J, Willmund F, et al. Not changes in membrane fluidity but proteotoxic stress triggers heat shock protein expression in Chlamydomonas reinhardtii. Plant Cell Environ. 2017;40(12):2987–3001.

144. Sangwan V, Örvar BL, Beyerly J, Hirt H, Dhindsa Rajinder S. Opposite changes in membrane fluidity mimic cold and heat stress activation of distinct plant MAP kinase pathways. Plant J. 2002;31(5):629–38.

145. Fan W, Evans RM. Turning Up the Heat on Membrane Fluidity. Cell [Internet]. 2015;161(5):962–3. Available from: http://dx.doi.org/10.1016/j.cell.2015.04.046

146. Saidi Y, Peter M, Fink A, Cicekli C, Vigh L, Goloubinoff P. Membrane lipid composition affects plant heat sensing and modulates Ca2+-dependent heat shock response. Plant Signal Behav. 2010;5(12):1530–3.

147. Falcone DL, Ogas JP, Somerville CR. Regulation of membrane fatty acid composition by temperature in mutants of Arabidopsis with alterations in membrane lipid composition. BMC Plant Biol. 2004;4:1–45.

148. Kaplan B, Sherman T, Fromm H. Cyclic nucleotide-gated channels in plants. 2007;581:2237–46.

149. Jarratt-Barnham E, Wang L, Ning Y, Davies JM. The complex story of plant cyclic nucleotide-gated channels. Int J Mol Sci. 2021;22(2):1–26.

150. Gao F, Han X, Wu J, Zheng S, Shang Z, Sun D, et al. A heat-activated calcium-permeable channel - Arabidopsis cyclic nucleotide-gated ion channel 6 - Is involved in heat shock responses. Plant J. 2012;70(6):1056–69.

151. Clough SJ, Fengler KA, Yu IC, Lippok B, Smith RK, Bent AF. The Arabidopsis dnd1 “defense, no death” gene encodes a mutated cyclic nucleotide-gated ion channel. Proc Natl Acad Sci U S A. 2000;97(16):9323–8.

152. Tan Y-Q, Yang Y, Zhang A, Fei C-F, Gu L-L, Sun S-J, et al. Three CNGC Family Members, CNGC5, CNGC6, and CNGC9, Are Required for Constitutive Growth of Arabidopsis Root Hairs as Ca2+-

Permeable Channels. Plant Commun. 2020;1(1):100001.

153. Tunc-Ozdemir M, Tang C, Ishka MR, Brown E, Groves NR, Myers CT, et al. A cyclic nucleotide-gated channel (CNGC16) in pollen is critical for stress tolerance in pollen reproductive development. Plant Physiol. 2013;161(2):1010–20.

154. Cui Y, Lu S, Li Z, Cheng J, Hu P, Zhu T, et al. CYCLIC NUCLEOTIDE-GATED ION CHANNELs 14 and 16 Promote Tolerance to Heat and Chilling in Rice. Plant Physiol. 2020;183(4):1794–808.

155. Yan Q, Huang Q, Chen J, Li J, Liu Z, Yang Y, et al. SYTA has positive effects on the heat resistance of Arabidopsis. Plant Growth Regul. 2017;81(3):467–76.

156. Li ZG, Ye XY, Qiu XM. Glutamate signaling enhances the heat tolerance of maize seedlings by plant glutamate receptor-like channels-mediated calcium signaling. Protoplasma. 2019;256(4):1165–9.

157. Mccormack E, Tsai Y, Braam J. Handling calcium signaling : Arabidopsis CaMs and CMLs. 2005;10(8).

158. Virdi AS, Singh S, Singh P. Abiotic stress responses in plants: Roles of calmodulin-regulated proteins. Front Plant Sci. 2015;6(OCTOBER):1–19.

159. Rhoads AR, Friedberg F. Sequence motifs for calmodulin recognition. FASEB J. 1997;11(5):331–40.

160. Fischer C, Kugler A, Hoth S, Dietrich P. An IQ domain mediates the interaction with calmodulin in a plant cyclic nucleotide-gated channel. Plant Cell Physiol. 2013;54(4):573–84.

161. Vadassery J, Scholz SS, Mithöfer A. Multiple calmodulin-like proteins in Arabidopsis are induced by insect-derived (Spodoptera littoralis) oral secretion. Plant Signal Behav. 2012;7(10):1277–80.

162. Aldon D, Galaud J. Plant Calmodulins and Calmodulin-Related Proteins. 2006;(June):96–104.

163. Fischer C, Defalco TA, Karia P, Snedden WA, Moeder W, Yoshioka K, et al. Calmodulin as a Ca2+-Sensing Subunit of Arabidopsis Cyclic Nucleotide-Gated Channel Complexes. Plant Cell Physiol. 2017;58(7):1208–21.

164. Niu WT, Han XW, Wei SS, Shang ZL, Wang J, Yang DW, et al. Arabidopsis cyclic nucleotide-gated channel 6 is negatively modulated by multiple calmodulin isoforms during heat shock. J Exp Bot. 2020;71(1):90–114.

165. Zhang W, Zhou RG, Gao YJ, Zheng SZ, Xu P, Zhang SQ, et al. Molecular and genetic evidence for the key role of AtCaM3 in heat-shock signal transduction in arabidopsis1[W][OA]. Plant Physiol. 2009;149(4):1773–84.

166. Liu HT, Sun DY, Zhou RG. Ca2+ and AtCaM3 are involved in the expression of heat shock protein gene in Arabidopsis. Plant, Cell Environ. 2005;28(10):1276–84.

167. Liu HT, Gao F, Li GL, Han JL, Liu DL, Sun DY, et al. The calmodulin-binding protein kinase 3 is part of heat-shock signal transduction in Arabidopsis thaliana. Plant J. 2008;55(5):760–73.

168. Yip Delormel T, Boudsocq M. Properties and functions of calcium-dependent protein kinases and their relatives in Arabidopsis thaliana. New Phytol. 2019;224(2):585–604.

169. Wu HC, Jinn TL. Oscillation regulation of Ca2+/calmodulin and heat-stress related genes in response to heat stress in rice (Oryza sativa L.). Plant Signal Behav. 2012;7(9):1056–7.

170. Liu H, Li B, Shang Z, Li X, Mu R, Sun D, et al. Calmodulin Is Involved in Heat Shock Signal Transduction in Wheat 1. 2003;132(July):1186–95.

171. Guo M, Liu J-H, Ma X, Luo D-X, Gong Z-H, Lu M-H. The Plant Heat Stress Transcription Factors (HSFs): Structure, Regulation, and Function in Response to Abiotic Stresses. Front Plant Sci [Internet]. 2016;7(February). Available from: http://journal.frontiersin.org/Article/10.3389/fpls.2016.00114/abstract

172. Scharf KD, Berberich T, Ebersberger I, Nover L. The plant heat stress transcription factor (Hsf) family: Structure, function and evolution. Biochim Biophys Acta - Gene Regul Mech [Internet]. 2012;1819(2):104–19. Available from: http://dx.doi.org/10.1016/j.bbagrm.2011.10.002

173. Santoro N, Johansson N, Thiele DJ. Heat Shock Element Architecture Is an Important Determinant in the Temperature and Transactivation Domain Requirements for Heat Shock Transcription Factor. Mol Cell Biol. 1998;18(11):6340–52.

174. Liu HC, Charng YY. Acquired thermotolerance independent of heat shock factor A1 (HsfA1), the master regulator of the heat stress response. Plant Signal Behav. 2012;7(5):1–5.

175. Czarnecka-Verner E, Yuan CX, Nover L, Scharf KD, Englich G, Gurley WB. Plant heat shock transcription factors: Positive and negative aspects of regulation. Acta Physiol Plant. 1997;19(4):529–37.

176. Mitsuda N, Ohme-Takagi M. Functional analysis of transcription factors in arabidopsis. Plant Cell Physiol. 2009;50(7):1232–48.

177. Mishra SK, Tripp J, Winkelhaus S, Tschiersch B, Theres K, Nover L, et al. In the complex family of heat stress transcription factors, HsfA1 has a unique role as master regulator of thermotolerance in tomato. Genes Dev. 2002;16(12):1555–67.

178. Liu HC, Liao HT, Charng YY. The role of class A1 heat shock factors (HSFA1s) in response to heat and other stresses in Arabidopsis. Plant, Cell Environ. 2011;34(5):738–51.

179. Yoshida T, Ohama N, Nakajima J, Kidokoro S, Mizoi J, Nakashima K, et al. Arabidopsis HsfA1 transcription factors function as the main positive regulators in heat shock-responsive gene expression. Mol Genet Genomics. 2011;286(5–6):321–32.

180. Ohama N, Sato H, Shinozaki K, Yamaguchi-Shinozaki K. Transcriptional Regulatory Network of Plant Heat Stress Response. Trends Plant Sci [Internet]. 2017;22(1):53–65. Available from: http://dx.doi.org/10.1016/j.tplants.2016.08.015

181. Liu H chin, Charng Y yung. Common and distinct functions of Arabidopsis class A1 and A2 heat shock factors in diverse abiotic stress responses and development. Plant Physiol. 2013;163(1):276–90.

182. Roncarati D, Scarlato V. Regulation of heat-shock genes in bacteria: from signal sensing to gene expression output. FEMS Microbiol Rev. 2017;41(4):549–74.

183. Anckar J, Sistonen L. Regulation of H SF 1 Function in the Heat Stress Response: Implications in Aging and Disease . Annu Rev Biochem. 2011;80(1):1089–115.

184. Nicholls S, Leach MD, Priest CL, Brown AJP. Role of the heat shock transcription factor, Hsf1, in a major fungal pathogen that is obligately associated with warm-blooded animals. Mol Microbiol. 2009;74(4):844–61.

185. Gallo GJ, Prentice H, Kingston RE. Heat shock factor is required for growth at normal temperatures in the fission yeast Schizosaccharomyces pombe. Mol Cell Biol. 1993;13(2):749–61.

186. von Koskull-Doring P, Scharf KD, Nover L. The diversity of plant heat stress transcription factors. Trends Plant Sci [Internet]. 2007;12(10):452–7. Available from: http://www.ncbi.nlm.nih.gov/pubmed/17826296

187. Hahn A, Bublak D, Schleiff E, Scharf KD. Crosstalk between Hsp90 and Hsp70 chaperones and heat stress transcription factors in tomato. Plant Cell. 2011;23(2):741–55.

188. Zou J, Guo Y, Guettouche T, Smith DF, Voellmy R. Repression of heat shock transcription factor HSF1 activation by HSP90 (HSP90 complex) that forms a stress-sensitive complex with HSF1. Cell. 1998;94(4):471–80.

189. Kim B-H, Schöffl F. Interaction between Arabidopsis heat shock transcription factor 1 and 70 kDa heat shock proteins. J Exp Bot [Internet]. 2002;53(367):371–5. Available from: http://jxb.oxfordjournals.org/content/53/367/371.full%5Cnhttp://jxb.oxfordjournals.org/lookup/doi/10.1093/jexbot/53.367.371

190. Yamada K, Fukao Y, Hayashi M, Fukazawa M, Suzuki I, Nishimura M. Cytosolic HSP90 regulates the heat shock response that is responsible for heat acclimation in Arabidopsis thaliana. J Biol Chem. 2007;282(52):37794–804.

191. Tomás D, Brazão J, Viegas W, Silva M. Differential effects of high-temperature stress on nuclear topology and transcription of repetitive noncoding and coding rye sequences. Cytogenet Genome Res. 2013;139(2):119–27.

192. Santos AP, Ferreira L, Maroco J, Oliveira MM. Abiotic stress and induced DNA hypomethylation cause interphase chromatin structural changes in rice rDNA loci. Cytogenet Genome Res. 2011;132(4):297–303.

193. Probst A V., Mittelsten Scheid O. Stress-induced structural changes in plant chromatin. Curr Opin Plant Biol [Internet]. 2015;27:8–16. Available from: http://dx.doi.org/10.1016/j.pbi.2015.05.011

194. March-Díaz R, Reyes JC. The beauty of being a variant: H2A.Z and the SWR1 complex in plants. Mol Plant [Internet]. 2009;2(4):565–77. Available from: http://dx.doi.org/10.1093/mp/ssp019

195. Cortijo S, Charoensawan V, Brestovitsky A, Buning R, Ravarani C, Rhodes D, et al. Transcriptional Regulation of the Ambient Temperature Response by H2A.Z Nucleosomes and HSF1 Transcription Factors in Arabidopsis. Mol Plant [Internet]. 2017;10(10):1258–73. Available from: https://doi.org/10.1016/j.molp.2017.08.014

196. Kumar SV, Wigge PA. H2A.Z-Containing Nucleosomes Mediate the Thermosensory Response in Arabidopsis. Cell [Internet]. 2010;140(1):136–47. Available from: http://dx.doi.org/10.1016/j.cell.2009.11.006

197. Smith AP, Jain A, Deal RB, Nagarajan VK, Poling MD, Raghothama KG, et al. Histone H2A.Z regulates the expression of several classes of phosphate starvation response genes but not as a transcriptional activator. Plant Physiol. 2010;152(1):217–25.

198. Zahraeifard S, Foroozani M, Sepehri A, Oh DH, Wang G, Mangu V, et al. Rice H2A.Z negatively regulates genes responsive to nutrient starvation but promotes expression of key housekeeping genes. J Exp Bot. 2018;69(20):4907–19.

199. Berriri S, Gangappa SN, Kumar SV. SWR1 Chromatin-Remodeling Complex Subunits and H2A.Z Have Non-overlapping Functions in Immunity and Gene Regulation in Arabidopsis. Mol Plant [Internet]. 2016;9(7):1051–65. Available from: http://dx.doi.org/10.1016/j.molp.2016.04.003

200. Perspectives EH. EPIGENETIC S. 2006;114(3):160–7.

201. Halfmann R, Lindquist S. No Title. 2014;629(2010).

202. Kouzarides T. Review Chromatin Modifications and Their Function. 2007;693–705.

203. Moore LD, Le T, Fan G. DNA methylation and its basic function. Neuropsychopharmacology [Internet]. 2013;38(1):23–38. Available from: http://dx.doi.org/10.1038/npp.2012.112

204. Kim M, Costello J. DNA methylation: An epigenetic mark of cellular memory. Exp Mol Med. 2017;49(4).

205. Gallego-Bartolomé J. DNA methylation in plants: mechanisms and tools for targeted manipulation. New Phytol. 2020;

206. Gao G, Li J, Li H, Li F, Xu K, Yan G, et al. Comparison of the heat stress induced variations in DNA methylation between heat-tolerant and heat-sensitive rapeseed seedlings. Breed Sci. 2014;64(2):125–33.

207. Correia B, Valledor L, Meijón M, Rodriguez JL, Dias MC, Santos C, et al. Is the Interplay between Epigenetic Markers Related to the Acclimation of Cork Oak Plants to High Temperatures? PLoS One. 2013;8(1).

208. Boyko A, Blevins T, Yao Y, Golubov A, Bilichak A, Ilnytskyy Y, et al. Transgenerational adaptation of

Arabidopsis to stress requires DNA methylation and the function of dicer-like proteins. PLoS One. 2010;5(3).

209. Singroha G, Sharma P. Epigenetic Modifications in Plants under Abiotic Stress. :1–14.

210. Ikeda M, Mitsuda N, Ohme-Takagi M. Arabidopsis HsfB1 and HsfB2b Act as Repressors of the Expression of Heat-Inducible Hsfs But Positively Regulate the Acquired Thermotolerance. Plant Physiol. 2011;157(3):1243–54.

211. Marko D, El-Shershaby A, Carriero F, Summerer S, Petrozza A, Iannacone R, et al. Identification and characterization of a thermotolerant TILLING allele of heat shock binding protein 1 in tomato. Genes (Basel). 2019;10(7).

212. Chen H, Hwang JE, Lim CJ, Kim DY, Lee SY, Lim CO. Arabidopsis DREB2C functions as a transcriptional activator of HsfA3 during the heat stress response. Biochem Biophys Res Commun [Internet]. 2010;401(2):238–44. Available from: http://dx.doi.org/10.1016/j.bbrc.2010.09.038

213. Song C, Lee J, Kim T, Hong JC, Lim CO. VOZ1, a transcriptional repressor of DREB2C, mediates heat stress responses in Arabidopsis. Planta [Internet]. 2018;(0123456789). Available from: http://link.springer.com/10.1007/s00425-018-2879-9

Scope of the PhD thesis

The mechanisms by which plants sense and respond to heat are not completely clear. This thesis aims to answer the following questions:

- What are the components of the heat shock signaling pathway that lead to the accumulation of HSPs in plants, mainly from the primary heat sensor CNGC2 and CNGC4 and to the activation of HSFA1?

- What is the mechanism by which HSP expression is repressed at low temperature?

Both questions are central in this thesis and were mainly the research topic.

Additionally, two projects were generated. The first was the identification of two CaMs, CaM1 and CaM5, which were found to interact strongly with the C-terminal cytosolic part of CNGC2, identified by Dr. Anthony Guihur through a yeast two-hybrid screen. Thus, the question was raised to understand the role of both CaM1 and CaM5 in the heat signal transduction.

The second additional project was to address the role and effect of HSP20s overexpression at a non-heat inducible temperature. It is suggested that their unnecessary expression at low temperatures might cause deleterious effects in plants. Therefore, this question was studied by the generation of an *A. thaliana* transgenic line which was expected to express the cytosolic HSP17.6a under the control of chemical.

Chapter 2: Generation and characterization of an *A. thaliana* transgenic line for a forward genetic screen.

Abstract

Several mediators of the heat shock signaling pathway were identified such as CaM3 and CBK3 whose lack of expression leads to a defective accumulation of HSP in *A. thaliana*. New components remain to be found mainly between the primary CNGC sensors and the terminal HSFA1 activator of transcription. Here, an *A. thaliana* transgenic line was generated, called HEAT INDUCIBLE BIOLUMINESCENCE AND TOXICITY (HIBAT), in an attempt to conduct a forward genetic screen (FGS). Under HS, HIBAT conditionally expresses a toxic fusion protein, made of nano-luciferase (nLUC) and D-amino acid oxidase (DAO1), under the control of a heat-inducible promoter. The nLUC emits light in the presence of furimazine and the DAO1 is toxic only with the presence of D-valine. HIBAT was isolated and characterized as containing a single transgene copy located in a non-coding sequence of chromosome 1. The fusion protein was found to accumulates strictly following heat increment treatments and develop toxicity in the presence of the proper concentration of D-valine. The heat-shock promoter was specific to HS as oxidative, osmotic, salt, FLAGELLIN 22 (FLG22), chilling and, cold shock did not induce the accumulation of the fusion protein. Under HS, isolated mutants, during the FGS, are expected to not emit bioluminescence, survive in the presence of D-valine, and ultimately validated by a lack of HSP expression. The transgenic line HIBAT was then chosen to conduct an FGS for *A. thaliana* mutants affected in the HSR in order to identify new components of the plant heat sensing and signaling pathway.

Introduction

To initiate the FGS, it was necessary to generate HIBAT to directly isolate candidates in the loss of heat sensing and signaling. The promoter pGmHsp17.3b from *Glycine max* showed to control the expression of small HSPs (1). Previously adapted within our laboratory, a moss transgenic line in *Physcomitrella Patens* was generated with this promoter followed by the GUS reporter (2). Although merely 500 bp long, pGmHsp17.3b presented the remarkable property to be strongly repressed at room temperature and to become highly expressed at temperatures above 32°C and less than 40°C. Based on the same approach, HIBAT was expected to drive the expression of nLUC-DAO1 under similar conditions and strictly avoid a leakiness of the fusion protein at low temperatures which may lead to toxicity in the presence of D-valine. The nLUC (19.6 KDa) was chosen to present a longer half-life, did not require ATP, and provide 100 fold time more bioluminescence as compared to common Firefly and Renilla luciferase (3). To optimize the strategy for the FGS, the *DAO1* was linked to *nLUC* to be used as an additional protein reporter. The *DAO1* gene was described both as a positive and negative marker selection in plants that strictly depend on D-amino acids employed (4). For example, D-alanine and D-serine were found to be lethal for plants at high concentrations and need to be degraded by DAO1. In contrast, the D-valine is toxic only in the presence of DAO1 which catabolizes harmful molecules such as keto-acid-3-methyl-2 oxobutanoate, NH3, and H_2O_2 in plants (5–8). To increase the likelihood of detecting nLUC-DAO1, a FLAG DYKDDDDK was added (Bartoloni et al., 1988).

Here, the isolated HIBAT plant was found to fulfill the following criteria to conduct the FGS:

- The nLUC-DAO1 was highly accumulated strictly under HS and tightly repressed at low temperatures.

- HIBAT contains one copy of the transgene located in a non-coding area of the *A. thaliana* genome.

- The selected HIBAT showed a similar physiological phenotype in terms of growth and development as compared to Col-0.

- The nLUC provided a high amount of bioluminescence under HS.

- The DAO1 was toxic only in the presence of D-valine and strictly following HS.

- Under HS, the nLUC-DAO1 expression was correlated with the expression of sHSP17.7.

- The accumulation of nLUC-DAO1 was strongly specific to HS compared to the other biotic and abiotic stresses.

The ethyl methyl sulfonate (EMS) mutation located in heat sensing and signaling genes would render candidates deficient in bioluminescence emission and resistant to D-valine treatment under HS. The lack of HSP expression would ultimately validate the loss of HSR in *A. thaliana* mutants during the FGS.

Results

Generation and selection of a transgenic *A. thaliana* line pGmHsp17.3b: nLUC-DAO1

To generate several HIBAT lines, the transgene was designed as shown in Figure 1a. The plasmid was introduced into *Agrobacterium* and transformed into Col-0 plants. The transgene constitutively express the OLEOSIN1 fused to a red fluorescent protein (RFP) to ensure successfully transformed lines. At the T1 generation, seeds that presented red fluorescent emission were selected as transformants based on Shimada et al., 2010 (Fig. 1b). At the T2 generation, five individual HIBAT line were isolated to confirmed to have the transgene such as lines 40, 41, 43, 46, and 51 as the plasmid control (Fig. 2a and b). Thus, they were selected and further analyzed for heat-induced expression of nLUC-DAO1.

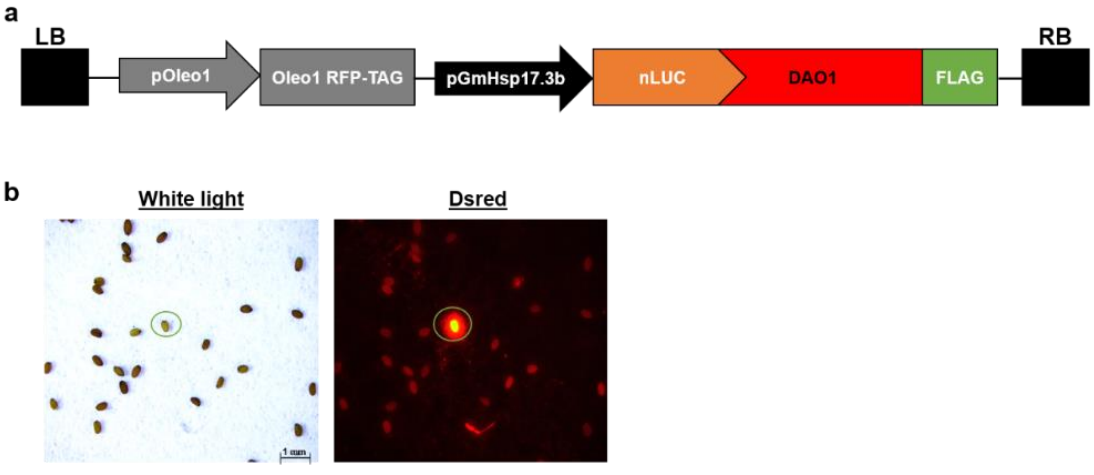

Figure 1: Transgene designed and selection of HIBAT lines at the T1 generation. (**a**) Generation of transgenic *A. thaliana* lines based on a fusion protein nano-luciferase, a conditional negative marker D-amino acid oxidase 1 (nLUC and DAO1) which both are driven by a heat-inducible promoter HSP17.3b from *Glycine max* (pGmHsp17.3b). The fusion protein is coupled with a protein marker DYKDDDDK (FLAG). The

selection of new transformants was facilitated by the constitutive expression of a red fluorescent TAG (RFP-TAG), coupled with OLEOSIN 1 (Oleo1 RFP-TAG) and driven by the promoter OLEOSIN 1 (pOleo1). LB; left border, RB; right border. (**b**) Selection of transformed seeds at the T1 generation using Dsred filter in Leica stereo microscopy. The Green circle represents a seed successfully transformed and expressing OLEOSIN 1 tagged with RFP (scale bar = 1mm).

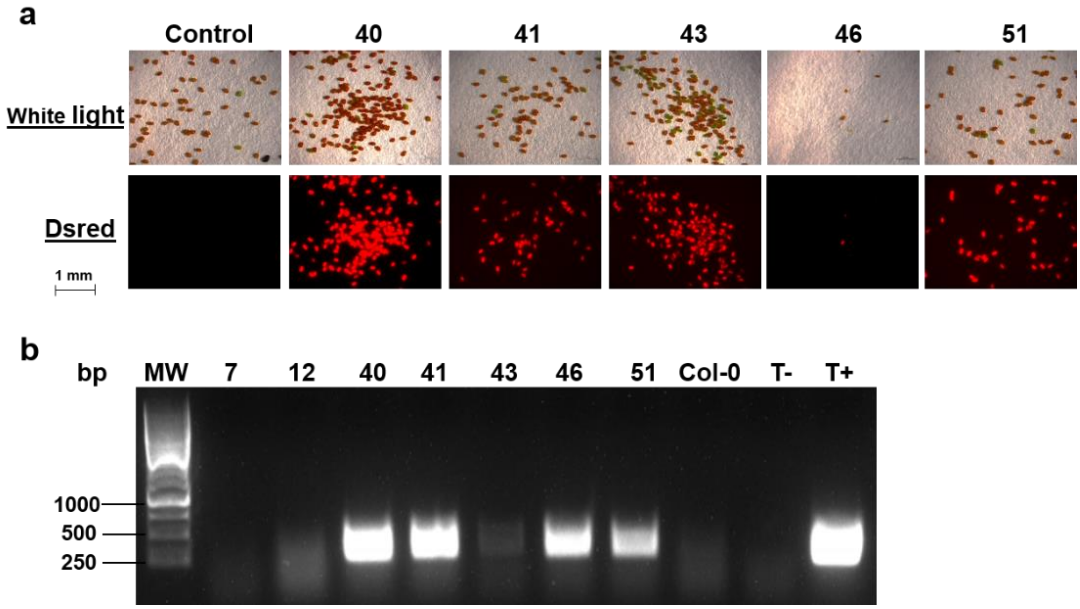

Figure 2: Selection of HIBAT lines containing the transgene at the T2 generation. (**a**) Selected HIBAT lines were analyzed at the T2 generation to express Oleo1-RFP at seeds stage (scale bar = 1mm). Names of each line are represented on top of pictures. (**b**) *DAO1* amplification in HIBAT lines by PCR. Genomic DNA extract from transformant plants was amplified by using primers overlapping the *DAO1* gene part (size expected 380 bp) and the plasmid containing the transgene as a positive control (T+). Negative controls did not contain DNA (T-) or contained the DNA from Col-0. Numbers represent the different HIBAT lines isolated on top of each lane of the agarose gel electrophoresis. Molecular weight (MW).

Selection of the proper HIBAT plant

Selected HIBAT lines were analyzed in their ability to express nLUC-DAO1 at low and high temperatures. The HIBAT-41 showed the lowest expression of nLUC-DAO1 compared to HIBAT-40 and HIBAT-43 at 22°C. The HIBAT lines 40, 43, and 51 were found to express a higher level of nLUC-DAO1 compared to the HIBAT-41 at 42°C (Fig. 3a and b). These lines could eventually cause toxicity due to a leakiness of nLUC-DAO1 expression, when in presence of D-valine at 22°C, or contained several transgene copies and they were then excluded and HIBAT-41 selected. Additionally, the fusion protein nLUC-DAO1 contained a FLAG at the N-terminal, which can be detected by Western blot. A calibration assay was performed through a pure protein extract containing BRASSINOSTEROID INSENSITIVE 1 (BRI1) coupled with the same FLAG. A concentration of 100 ng of BRI1 was found to produce a significant signal (Fig. 3c).

However, all HIBAT lines did not reveal the FLAG compared to BRI1 positive control when exposed to HS at 42°C for 1 hour (Fig 3d). Thus, the FLAG was unusable as a control for the accumulation of nLUC-DAO1, nevertheless the fusion protein was detectable by bioluminescence.

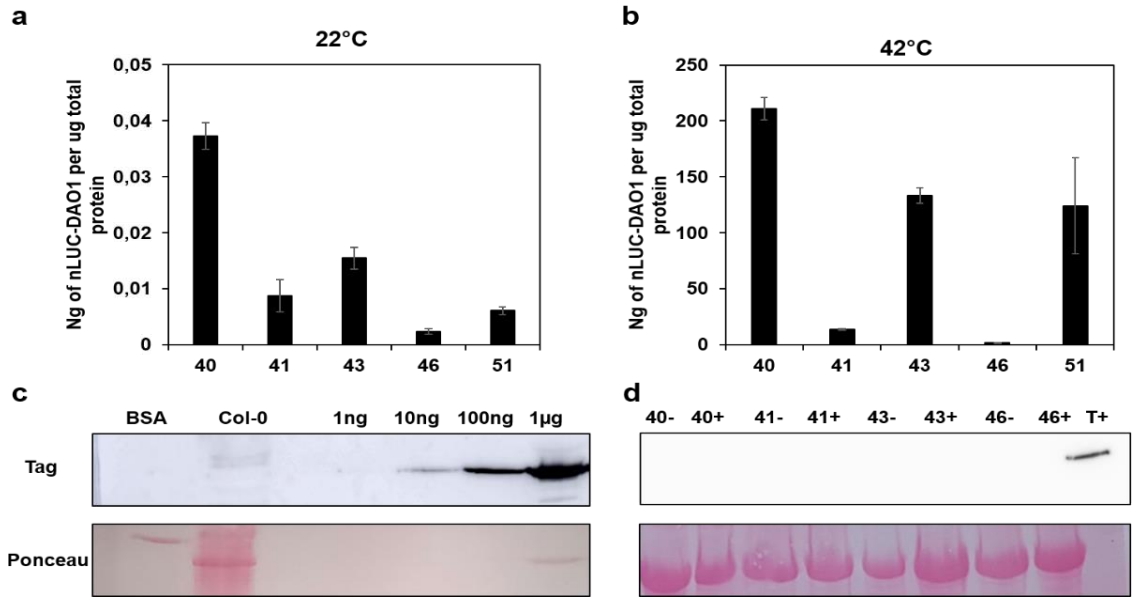

Figure 3: Accumulation of nLUC-DAO1 observed by bioluminescence and detection of the FLAG by Western blot in HIBAT lines at the T3 generation. (**a-b**) Accumulation of nLUC-DAO1 in the HIBAT lines at 22°C and 42°C. Two-week-old seedlings were exposed for 2 hours at 22°C or 42°C. The bioluminescence from the nLUC-DAO1 was normalized through a calibration curve assay from a pure nLUC extract synthesized in *E. Coli* (means ± S.D, n=5). (**c**) Calibration assay of BRASSINOSTEROID INSENSITIVE 1 (BRI1) coupled with the FLAG by Western blotting. BSA and the protein extract of Col-0 were used as negative controls. BRI1 extract was used at different concentrations respectively 1 ng, 10 ng, 100 ng, and 1 ug. (**d**) Flag detection assay in different HIBAT lines by Western blot. No heat stress (-), with heat stress (+), and T+ (BRI1 at 100ng). The numbers on top of the membrane represent the different HIBAT lines. The red ponceau represents the homogeneous loading between each sample through the expression of RUBISCO.

Because several transgene copies in different places of the genome would increase the selection of false-positive candidates during the FGS if the EMS induced mutation(s) in one of the transgenes, it was necessary to select a line with one copy number to minimize the EMS effect. Under microscopy, seeds that emitted red fluorescence were considered as transformants. Based on the Mendelian type of segregation, T2 lines that presented 25% of non-fluoresecent seeds were predicted to have a single copy, whereas a lower rate suggested multi-insertions (10). The HIBAT-41 line was found to contain one copy with 25% of non-fluoresecent seeds ratio compared to HIBAT lines 40, 43, and 51 expected to show multiple insertions. The HIBAT-46 line was not analyzed due to a lack of

seeds harvested (Table 1). To confirm the presence of a single copy in the HIBAT-41, the method of $2^{-\Delta\Delta CT}$ was applied adapted from Bubner and Baldwin, 2004. Based on the reference genes present in one copy in the *A. thaliana* genome such as *ACTIN* and *SAND*, the transgene expression was analyzed by qPCR in order to calculate the copy number. Two parts of the transgene, *nLUC*, and *DAO1* were amplified and compared with these reference genes. Results obtained indicated that HIBAT-41 contain a single copy, whereas line HIBAT-46 was hemizygous and line HIBAT-43 had two copies (Table 2). Thus, HIBAT-41 was chosen based on a weak nLUC-DAO1 expression at 22°C, presenting a high accumulation at 42°C and by the presence of a single transgene copy. The HIBAT-41 was then renamed simply HIBAT.

HIBAT transformant lines	40	41	43	46	51
One insertion	-	+	-	NA	-
Multi-insertion	+	-	+	NA	+

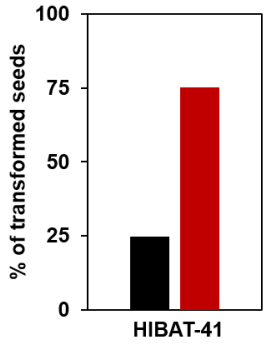

Table 1: Determination of the copy number through the segregation of seeds HIBAT lines at the T2 generation. The transgene copy number was determined by the segregation of transformant seeds giving an indication of one insertion or multi-insertion. Negative (-), positive (+), and no applicable (NA). The bar graph on the right of the table represents the percentage of transformed seeds (red) compared to not transformed seed (black) in the transformant *A. thaliana* HIBAT-41 line.

Hibat transformant lines	*nLUC/ACTIN*	*nLUC/SAND*	*DAO1/ACTIN*	*DAO1/SAND*	Mean	Copy number
HIBAT-41	0.520	0.980	0.850	1.690	0,78	1
HIBAT-43	1.78	1.93	1.890	1.99	1,89	2
HIBAT-46	0.100	0.220	0.110	0.200	0,157	0.5

Hemizygosis < 0.5
0.5 <1 copy < 1.5
1.5< 2 copies<2.5

Transgene / reference = (1+E)^ -ΔΔ Ct

E= Primers amplification efficiency (varying from 0 to 1)

Table 2: Determination of the copy number by using the $2^{-\Delta\Delta CT}$ method in HIBAT T2 lines. *SAND* and *ACTIN* were used as reference genes, whereas *nLUC* and *DAO1* were used as reference for the transgene. Means of each HIBAT line were obtained by using the formula (red) through results obtained by qPCR amplification from genes ratio (transgene/reference) and the primer efficiency. The range where the mean is located gave the exact copy number in each HIBAT line (black frame). The method applied was adapted from Bubner and Baldwin, 2004.

Transgene localization, physiology assays, and acquired thermotolerance in HIBAT

To ensure that the transgene localization did not disturb gene expression, the insertion was identified by the whole-genome DNA sequencing (WGDS) in HIBAT. The transgene DNA sequence was aligned against the genome of HIBAT. Reads overlapping the transgene borders and a part of the genome were obtained and blasted. A putative localization was identified and the genome of the HIBAT line was then aligned against the Col-0 reference. A gap was found at position 26180497 in chromosome 1, suggesting the presence of the transgene. Primers overlapping the transgene and the putative location in the HIBAT genome were designed. By PCR, a DNA product was obtained in HIBAT, whereas an absence of DNA amplification was observed in the negative control Col-0. *Sand* primers were used to confirm the gDNA extraction quality in both lines (Fig. 4). The transgene was found to be located between two genes. The first gene AT1G69590.1 encode for a putative DNA polymerase (according to TAIR) and our RNA sequencing of HIBAT did not reveal any expression at 22°C and 38°C. Therefore, it might be confirmed as a pseudogene and the transgene might not interfere. Interestingly, the second gene AT1G69600.1 encodes for a zinc finger homeodomain transcriptional factor family (ZFHD1) which may bind the promoter of the early response to dehydration stress 1 (ERD1). ZFHD1 was described to be induced by drought, high salinity and abscisic acid (12). Additionally, our transcriptome in HIBAT line reveals that at 38°C, ZFHD1 becomes up regulated (2 times more) as compared at low temperature which is also supported by the microarray data from BAR ePlant (http://bar.utoronto.ca/eplant/). Therefore, the insertion was confirmed in the HIBAT genome, predicted in a non-protein-coding region suggesting to minimally affect the expression of both distal genes.

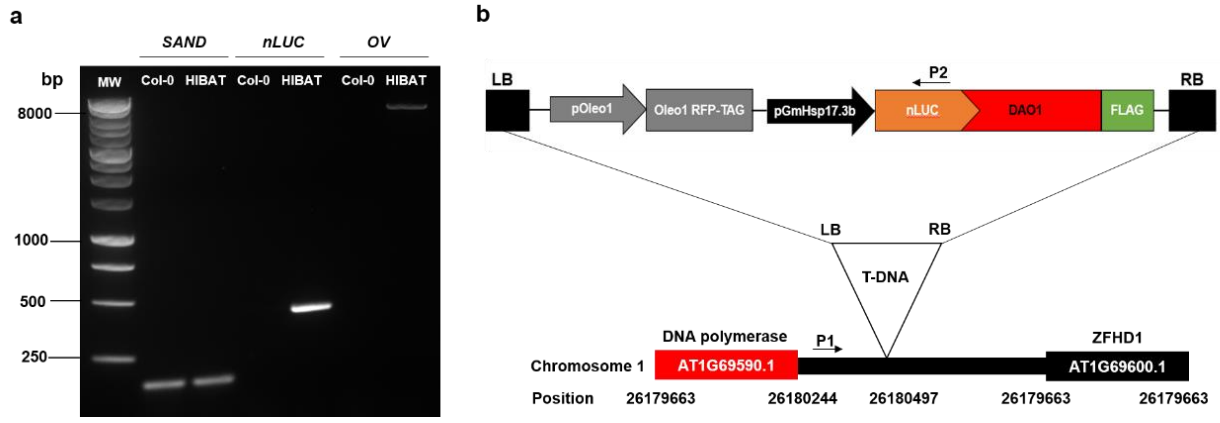

Figure 4: Transgene localization in HIBAT. (**a**) The transgene insertion in the HIBAT genome was confirmed by PCR. *SAND*, *nLUC*, a part of the transgene, and the genome of *A. thaliana* (OV), were amplified in both lines HIBAT and Col-0. The name of plants, molecular weight (MW), and primers used are

represented on the top of each lane of the agarose gel. (**b**) Schematic representation of the exact position of the T-DNA in the genome of HIBAT. RB: right border, LB: left border. P1 (nLUC Forward primer), and P2 (OV_Reverse primer) primers set were used to confirm the localization of the transgene in the genome of HIBAT. AT1G69590.1 is encoding for a putative (according to TAIR) DNA polymerase and ATG69600.1 for a Zinc Finger Homeodomain 1 (ZFHD1).

The HIBAT physiology compared to Col-0 was addressed by root length, biomass of shoot, and germination rate assays. At 5 and 10 days old, the line HIBAT did not showed significantly a delay in root length compared to Col-0 (Fig. 5a). At 9, 13, and 16 days old, the biomass assay in shoots revealed to be the same in both lines (Fig. 5b). The number of germinated seeds in the line HIBAT did not show a statistical difference at 5 and 10 days old compared to Col-0 (Fig. 5c). Thus, the HIBAT line was confirmed to present a sufficiently similar growth and development as Col-0 plants.

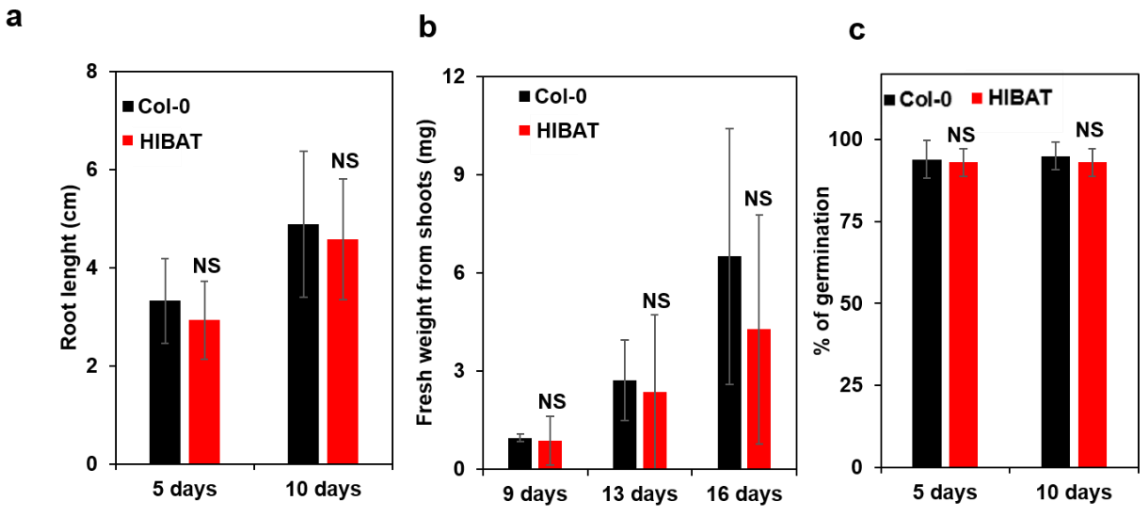

Figure 5: Physiology assays of HIBAT compared to Col-0. (**a**) Root length at 5 and 10 days old of both HIBAT and Col-0 plants (3 replicates containing 28 seedlings for each). (**b**) Fresh weight from shoots at 9, 13, and 16 days old of HIBAT and Col-0 lines (3 replicates containing 16 shoots seedlings for each). (**c**) Percentage of germination of the seed in HIBAT and Col-0 lines at 5 and 10 days old (2 replicates containing 50 seeds for each). Asterisks indicate statistically significant differences determined by student T.test (*, P<0.05, NS, No Significant).

The HIBAT and Col-0 lines were subjected to an AT test in order to address their response to HS. Both lines were subjected to a noxious HS for 1 hour at 45°C. Seven days later, HIBAT and Col-0 plants did not survive to the noxious HS as expected, presumably due to the non-establishment of suitable defenses in time. In contrast, HIBAT presented a slightly lower amount of survival when primed for 2 hours at 36°C and then subjected to the same noxious HS as compared to Col-0 (Fig. 6). These results indicate that the HIBAT is slightly more sensitive to extreme HS compared to Col-0. Despite this increase in thermosensitivity, HIBAT was still chosen for the FGS.

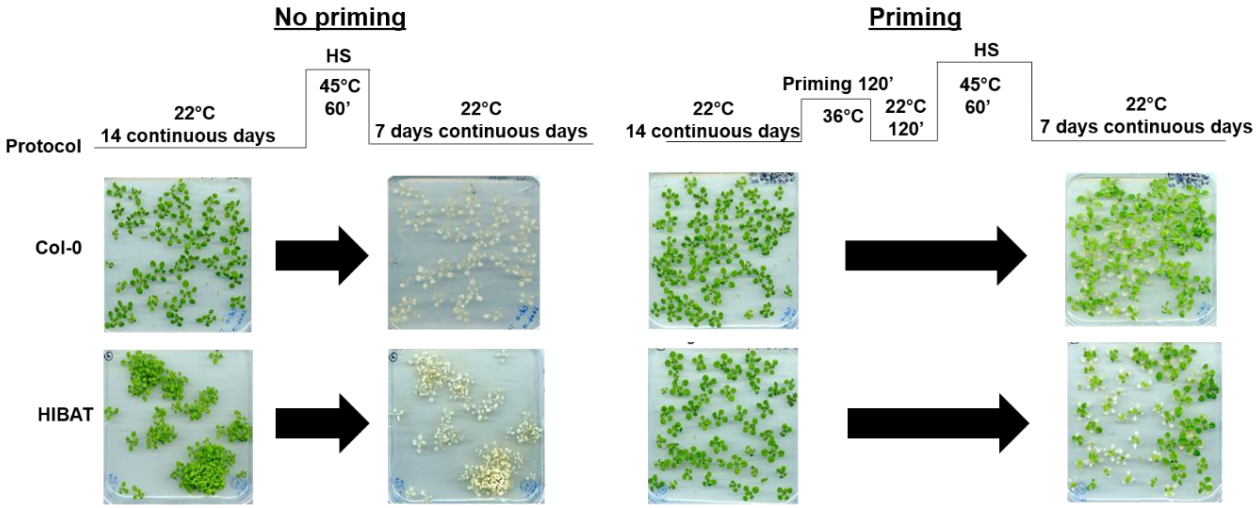

Figure 6: Acquired thermotolerance assay in the HIBAT and Col-0 lines. Left: no priming, right: with priming. Conditions applied for each plant are represented on top (protocol). Pictures were imaged at 14 and 21 days old.

Analysis of the bioluminescence *in vivo* and heat-inducible profile of HIBAT

The expression of nLUC-DAO1 *in vivo* and the sHSP17.7 accumulation was then analyzed in HIBAT. At 7 days and 5-weeks old, HIBAT and Col-0 lines were exposed at 22°C or 38°C for 2 hours followed by 2 hours at 22°C post-induction. As expected, only HIBAT subjected to HS emitted bioluminescence *in vivo* compared at 22°C and to Col-0 (Fig. 7a and b). These results confirm that HIBAT induces bioluminescence specifically depending on HS conditions. The Western blotting analysis was performed to compare the accumulation of the sHSP17.7 in both HIBAT and Col-0 lines. The quadruple *hsfa1* mutant in *A. thaliana* was used as a negative control since it was shown to have a defective HSP accumulation under HS and at establishing AT (13). 5 weeks old leaves from lines HIBAT, Col-0, and QK *hsfa1* mutant were exposed to 22°C, 34°C, or 38°C for 2 hours followed by 2 hours at 22°C post-induction. An absence of sHSP17.7 accumulation in the QK *hsfa1* was observed for all temperature conditions as well as Col-0 and HIBAT plants when exposed at 22°C (Fig. 7c). At 34°C and 38°C, sHSP17.7 accumulation was found to be similar in Col-0 and HIBAT lines. Thus, both lines did not present a difference of sHSP17.7 accumulation, and HIBAT was confirmed to be suitable for the FGS.

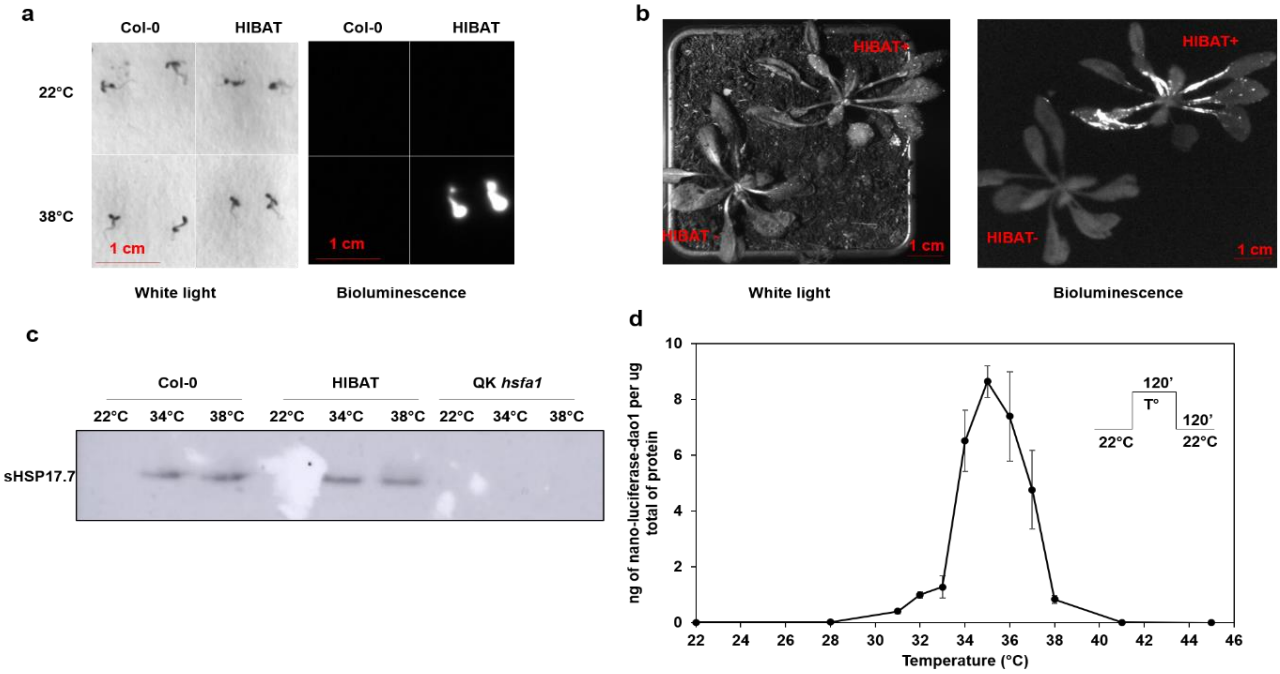

Figure 7: Expression *in vivo* of the heat-inducible nLUC-DAO1 and sHSP17.7 in HIBAT. (**a-b**) Bioluminescence emission of the HIBAT plants at 22°C and 38°C at 7 days and 5 weeks old. Col-0 plants were used as a negative control. Both lines were exposed to 22°C or 38°C for 2 hours and followed by 2 hours at 22°C post-induction. Plants were imaged by ImageQuant LAS 500. (**c**) Expression of sHSP17.7 in Col-0, HIBAT, and QK *hsfa1* mutant. Leaves were exposed at 22°C, 34°C, or 38°C for 2 hours and followed by 2 hours of post-induction at 22°C. QK *hsfa1* mutant was used as a negative control. Proteins extract loaded were homogeneous and their concentrations were determined by Bradford assay before the pre-loading in the gel. (**d**) Heat inducible nLUC-DAO1 expression profile in HIBAT. 14 days old seedlings were exposed at different temperatures for 2 hours and followed by 2 hours of post-induction at 22°C. The bioluminescence from the nLUC-DAO1 was normalized through a calibration curve assay from a pure nLUC extract synthesized in *E. Coli* (means ± S.D, n = 4).

The optimal temperature of nLUC-DAO1 induction was determined through a heat-inducible profile in HIBAT (Fig. 7d). 14 days old seedlings were exposed to different temperatures for 2 hours followed by 2 hours at 22°C post-induction. HIBAT was found to completely repressed the fusion protein between 22°C and up to 28°C, with less than 0.01 ng nLUC-DAO1 detectable per ug total of protein. At 35°C, it resulted in the maximal accumulation of 8.6 ng of nLUC-DAO1 per ug total of protein, whereas higher temperatures led to the loss of nLUC-DAO1 accumulation. At 45°C, the same low level of nLUC-DAO1 was observed compared to 22°C. Thus, HIBAT accumulated the maximal fusion protein level at 35°C and confirmed to be totally repressed at low temperatures.

Elucidating the proper D-valine concentration to induce toxicity in HIBAT under HS

HIBAT and Col-0 plants grew in a different range of D-valine concentrations. At 7 days old, both lines were submitted to recurrent heat treatments at 38°C for 2 hours followed by 2 hours at 22°C post-induction for 5 consecutive days. At 2 weeks old, a concentration of 25 mM was found to be lethal in HIBAT without affecting Col-0 under HS condition. In contrast, a lower D-valine concentration was not efficient to kill HIBAT plants, whereas 30 mM was excessive and induced toxicity in both lines under iterative HS (Fig. 8). Survival seedlings were then transferred to the soil at 14 days old for all conditions tested in order to validate their phenotype. As expected at 35 days, an absence of survival was observed in HIBAT with the presence of 25 mM of D-valine, whereas Col-0 plants successfully survived (Fig. 9). Thus, the concentration to induce a complete lethality in HIBAT, without affecting Col-0, was found to be optimal with 25 mM of D-valine under HS. The DAO1 approach was then selected to be used as a conditional negative marker in order to eliminate candidates which are not affected in the HSR during the FGS.

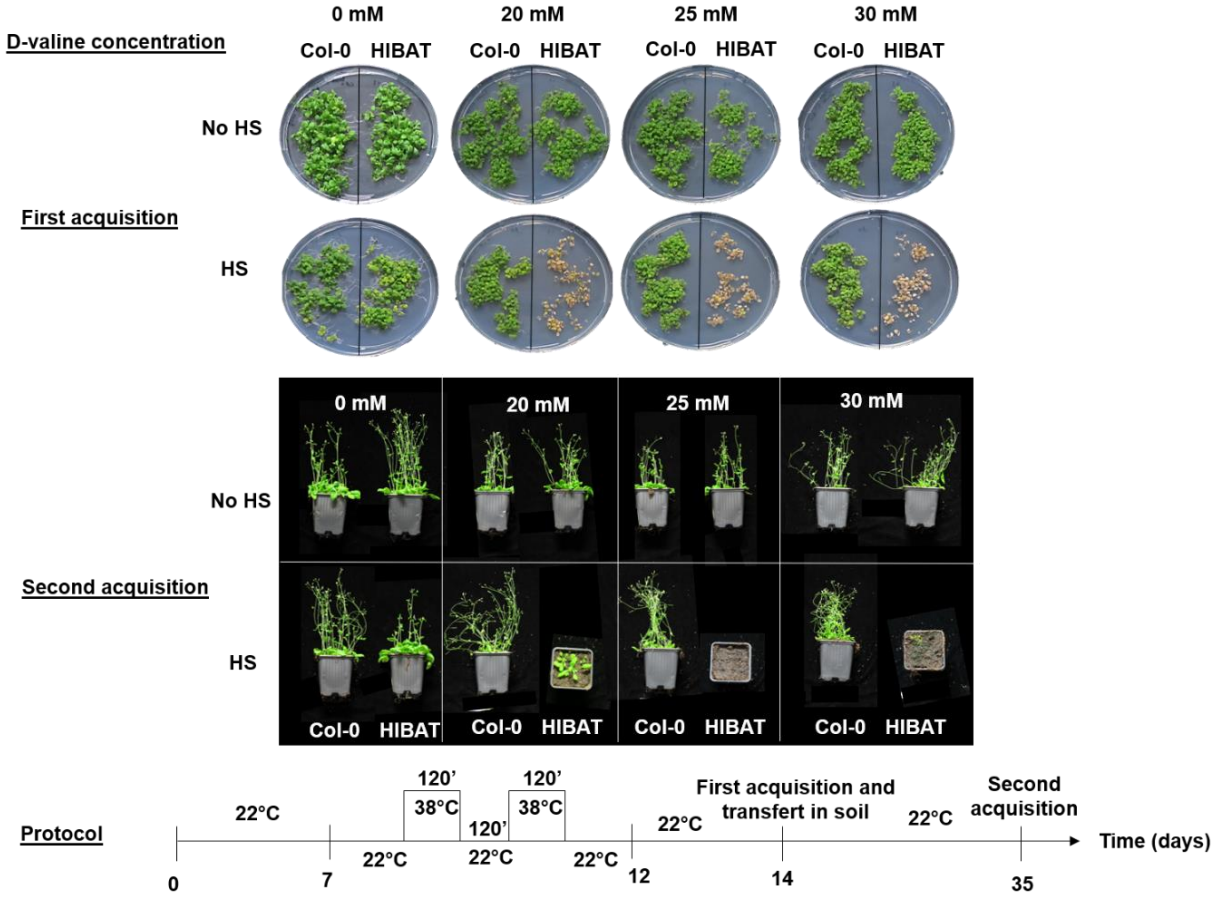

Figure 8: Iterative heat treatments and the presence of 25 mM of D-valine induced toxicity in HIBAT. D-valine range effect on Col-0 and the HIBAT lines under iterative heat shock (HS) or in the absence (No HS). (**Top**) Black lines in the middle of plates represent the separation between Col-0 (**left**) and HIBAT

(**Right**) plants. Pictures were imaged at 14 days old (first acquisition). D-valine concentrations applied are represented on top of each plate. (**Middle**) Col-0 and HIBAT seedlings survivals were transferred to the soil at 14 days old and pictures were imaged at 35 days (second acquisition. (**Bottom**) Plants followed the protocol that includes iterative heat treatment applied 2 times per day for 5 days.

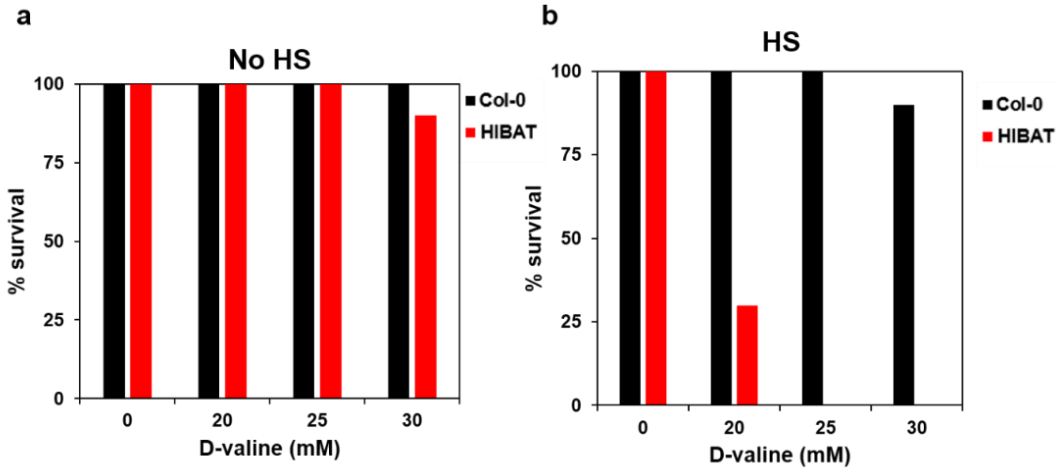

Figure 9: Percentage of survival after iterative heat exposures and D-valine treatments at 35 days. (**a-b**) Percentage of survival according to different concentrations of D-valine in Col-0 (black) and HIBAT lines (red). (**a**) Absence of iterative heat treatment (No HS) and (**b**) with recurrent heat shock (HS). The number of survivals was determined in a range of 50 to 70 seedlings for each condition. The survival rate was measured at 35 days old.

Effect of biotic and abiotic stresses on HIBAT

Here, the specificity of the HSR was addressed regarding different biotic and abiotic stresses assay. 12 days old HIBAT seedlings were exposed to H_2O_2, mannitol, NaCl, and FLG22 for 5 hours including 1 hour at 22°C followed by 2 hours at 22°C, 31°C (34°C for H_2O_2) , or 35°C (38°C for H_2O_2) and then submitted to 22°C for 2 hours post-induction. The effect of H_2O_2 revealed a low induction of nLUC-DAO1 at 22°C compared to untreated HIBAT plants, whereas no significant differences were observed at 34°C and 38°C in the presence and absence of H_2O_2 (Fig. 10a-c). The effect of mannitol did not show a difference of nLUC-DAO1 accumulation at 22°C and 31°C compared to untreated plants. A significantly nLUC-DAO1 expression was observed at 35°C compared to the absence of mannitol treatment (Fig. 10d-f). These results suggest that at high temperatures and in the presence of mannitol, the promoter is repressed by being affected excessively from both stresses. NaCl and FLG22 treatments did not show any significant difference in the expression nLUC-DAO1 at all temperature conditions compared to control (Fig. 11). Chilling and cold stresses were applied for 2 hours followed by 2 hours at 22°C post-induction in HIBAT seedlings and showed the same slight nLUC-DAO1 level

compared to plant control at 22°C (Fig. 12). These results are strong evidence that the promoter pGmHsp17.3b is highly specific to HS and is therefore optimal for an FGS.

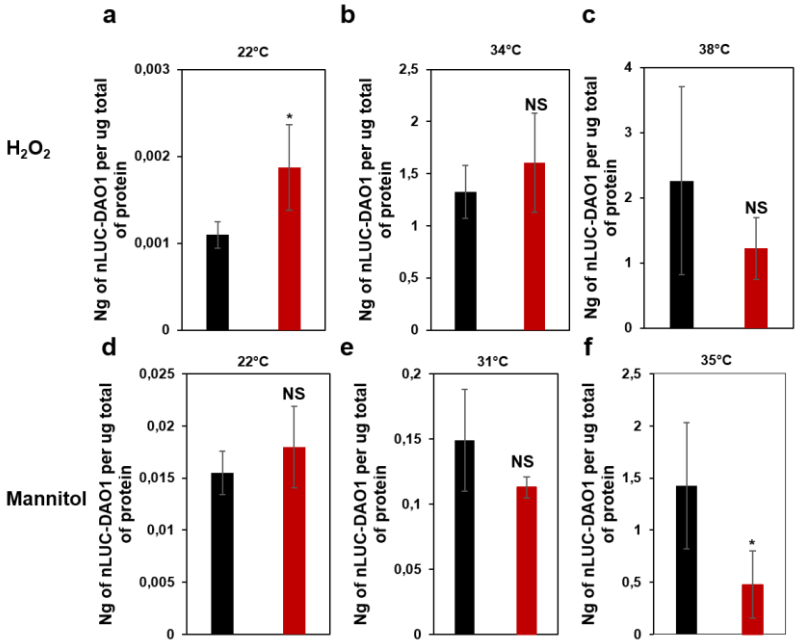

Figure 10: H_2O_2 and mannitol effect on the expression of nLUC-DAO1 in HIBAT at different temperature. (**a-c)** H_2O_2. (**d-f)** Mannitol. Seedlings on day 12 were exposed to 250 µM of H_2O_2 or 300 mM mannitol for 5 hours including 1 hour at 22°C, followed by 2 hours at different temperatures and then 2 hours of post-incubation at 22°C. Asterisks indicate statistically significant differences determined by student T.test (*, P<0.05, NS, No Significant). means ± S.D. (n = 4). Black: absence of mannitol or H_2O_2. Red; presence of mannitol or H_2O_2.

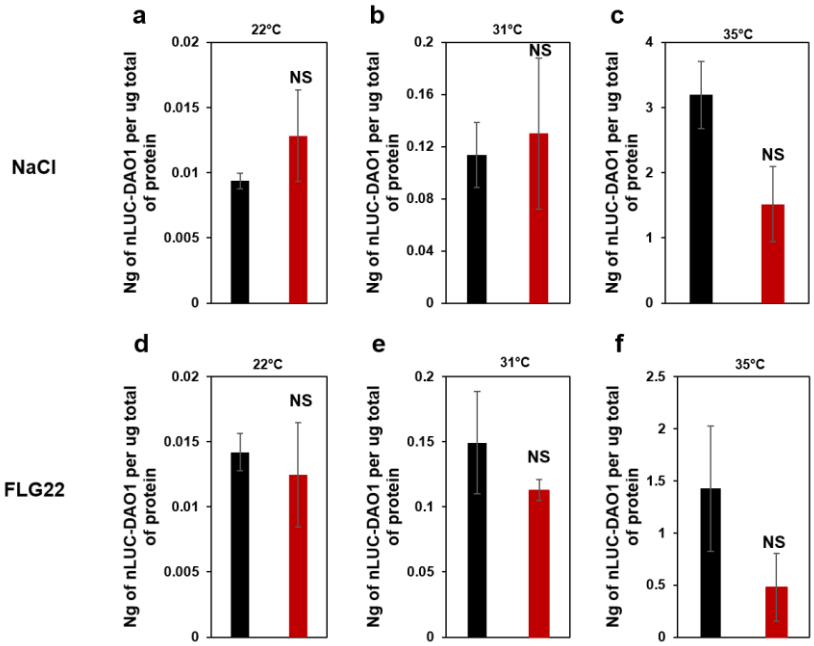

Figure 11: NaCl and FLG22 effect on the expression of nLUC-DAO1 in HIBAT at different temperature. (**a-c**) NaCl. (**d-f**) Flagellin 22. Seedlings on day 12 were exposed to 150 mM of NaCl or 1 mM of FLG22 for 5 hours including 1 hour at 22°C, followed by 2 hours at different temperatures and then 2 hours of post-incubation at 22°C. Asterisks indicate statistically significant differences determined by student T.test (*, P<0.05, NS, No Significant). means ± S.D. (n = 4). Black: absence of NaCl or flagellin. Red; presence of NaCl or FLG22.

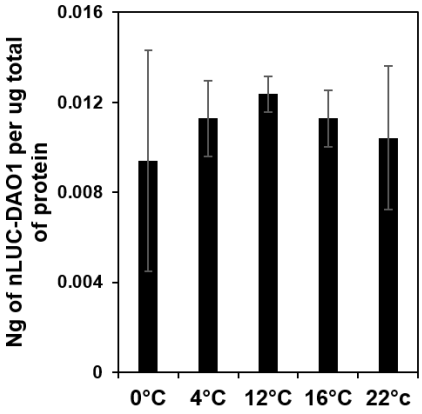

Figure 12: Chilling and cold shock effect on the expression of nLUC-DAO1 in HIBAT. Seedlings on day 12 were exposed to cold shock (0°C), chilling (4°C to 16°C) or at room temperature (22°C) for 2 hours and then followed by 2 hours of post-induction at 22°C. means ± S.D. (n = 4). An absence of significant difference was observed at 22°C compared to all other conditions and determined by student T.test.

Determination of the proper concentration of EMS for a FGS

EMS is a mutagen that causes irreversible damage to DNA that affect oxygen groups at position 6 on guanine and DNA phosphates. These chemical modifications result in a GC mutation to AT and would render several gene expression defective in plants (14). It was necessary to estimate the proper EMS concentration to avoid a high lethality in HIBAT during the FGS and to calculate the right amount of seeds to sow. Thus, 100 seeds from HIBAT were exposed to five different concentrations of EMS for 8 hours and the germination rate was calculated 7 days later (Fig. 13). Between 0.2% and 0.4% of EMS, the germination rate was approximately 80%, whereas 0.8% of EMS led to 40% germination loss. Therefore, an EMS concentration of 0.4% was acceptable and chosen which is supported by Martín et al., 2009 to conduct an FGS. Thus, the line HIBAT fulfills all the criteria to serve as a progenitor line to perform random EMS mutagenesis for the FGS.

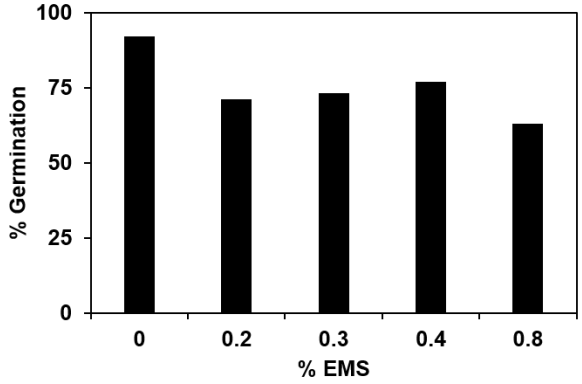

Figure 13: The effect of EMS on the germination of seeds in HIBAT. Seeds were mutagenized by EMS at different concentrations for 8 hours. 100 seeds were then sowed on soil and the germination rate was calculated 7 days later. The percentage of germination is represented according to the different EMS concentrations (v/v).

Discussion

Generation and characterization of HIBAT

Several HIBAT lines were initially selected to contain the transgene of interest. Contrary to the antibiotic segregation that renders longer the identification of positive transformants, HIBAT lines were identified due to the constitutive expression of RFP in seeds and then validated by PCR (Figs. 1 and 2). The HIBAT-41 was isolated among the others because it showed the weakest accumulation of nLUC-DAO1 at 22°C which was obligatorily required to avoid toxicity in the presence of D-valine. Under HS, HIBAT-41 accumulated a significantly a high level of nLUC-DAO1 (Fig. 3 and b). Although other HIBAT lines such as 40, 43, or 51 expressed a superior nLUC-DAO1 amount compared to HIBAT-41, they were excluded due to their higher basal levels at 22°C. Noticeably, the FLAG was not detectable in the HIBAT-41 but it revealed to not be essential for the FGS because the expression of nLUC-DAO1 expression can be analyzed by bioluminescence (Figs. 3c and 7a-b).

The isolated HIBAT was shown to present one copy of the transgene which was determined by the Mendelian type of segregation and the method $2^{-\Delta\Delta CT}$ (Tables 1 and 2) (16). The transgene was identified on chromosome 1, at position 26180497, ~500 nucleotides upstream of a putative pseudogene named AT1G69590.1 and ~800 nucleotides downstream of AT1G69600.1. According to TAIR10, AT1G69590.1 may encode for a putative DNA polymerase family member. Yet, microarrays and our own RNA

sequencing data from HIBAT showed an absence of AT1G69590.1 expression at low and high temperatures. Interestingly, the second gene AT1G69600.1 encodes for a zinc finger homeodomain transcriptional factor family (ZFHD1) which may bind the promoter of the early response to dehydration stress 1 (ERD1). ZFHD1 was described to be induced by drought, high salinity and abscisic acid (12). Additionally, our transcriptome in HIBAT line reveals that at 38°C, ZFHD1 becomes up-regulated (2 times more) as compared at low temperature which is also supported by the microarray data from BAR ePlant (http://bar.utoronto.ca/eplant/). Therefore, it cannot be excluded that the transgene might affect the expression of ZFHD1 resulting in a different phenotype since drought and heat stress can share common signaling pathway. Yet, the transgene insertion was then suggested to not affect any gene expression since its localization is in a non-coding area and should not render the FGS more difficult. Additionally, HIBAT was slightly more heat-sensitive in an AT assay compared to Col-0 and presented a delay in root length at 5 days old (Figs. 4, 5, and 6). Despite these slight differences, HIBAT was chosen to conduct the FGS. Under HS, the bioluminescence was detected successfully in HIBAT at the seedlings and rosettes stage. In contrast, an absence of bioluminescence emission was observed at 22°C (Fig. 7a-b). These results were supported by the heat-inducible profile curve and HIBAT was found to accumulate the maximal level of nLUC-DAO1 at 35°C (Fig. 7d). Additionally, the HIBAT heat inducibility behavior was confirmed to be similar to the transgenic line *Physcomitrella Patens* and supported the choice of using the promoter from *Glycine max* (2).

To select candidates during the FGS, two strategies were thought. The first was based on the nLUC bioluminescence emission and was similarly used in several FGS (17,18). To mimic the selection of mutants unable to respond to heat, which should present a defective bioluminescence emission under HS, HIBAT served as a negative and Col-0 as a positive candidate. The bioluminescence was distinguished between both lines and the strategy was presumably effective for the FGS (Supp Data 1). The second strategy consisted to use the toxic properties of DAO1. HIBAT plants revealed to be poisoned in the presence of 25 mM of D-valine and under iterative HS, whereas Col-0 successfully survived (Figs. 8 and 9). Thus, the DAO1 strategy was selected because it presented the advantage to screen rapidly a large number of EMS candidates unable at responding to HS. The bioluminescence approach was also chosen to validate the DAO1 strategy once the mutant selected. Under HS, HIBAT was found to provide approximately the same level

of sHSP17.7 as compared to Col-0 (Fig. 7c). EMS mutation(s) may occur within the transgene and could lead to the selection of false-positive candidates which become resistant to D-valine and do not emit bioluminescence under HS. Thus, it remains obligatorily to analyze the level of sHSP17.7 accumulation in EMS candidates by using the optimal temperature of induction at 35°C.

Different concentration of EMS was applied on HIBAT to test the germination of seeds. The EMS effect depends on its concentration and time of exposure and would induce different rates of nucleic acid substitutions (19). An EMS concentration of 0.4 mM for 8 hours was sufficient to not induce a high lethality on HIBAT seeds with an acceptable loss of 20% of germination (Fig. 13). This result was correlated with Martín et al., 2009 where the same loss of germination rate was observed in the *Landsberg erecta*. A DNA mutation is expected each 89 kb in the *Landsberg erecta* genome and 300 kb in Col-0 when both ecotypes are exposed to an EMS treatment for 17 hours at 0.20 mM (15). Because our concentration employed was higher on HIBAT, but the exposition time lower, an EMS treatment for 8 hours at 0.40 mM was chosen. This concentration is expected to cover the 30 000 protein-coding genes in *A. thaliana* by using 5 000 EMS seeds from HIBAT to initiate the FGS.

Effect of biotic and abiotic stresses on HIBAT

Crosstalk signaling exists between biotic and abiotic stresses. For example, drought and heat signaling have in common the same HSFA1 and DREB2A transcription factors that ultimately lead to the accumulation of HSPs (20). During the FGS, false-positive EMS candidates might be selected if the promoter chosen is not specific to heat. Thus, the line HIBAT was subjected to H_2O_2, mannitol, NaCl, and FLG22 treatments at 22°C, 31°C (34°C for H_2O_2), or 35°C (38°C for H_2O_2). H_2O_2 can activate HSFs which lead to the expression of sHSP17.6 and sHSP18.2 in Drosophila cells and *A. thaliana* (21,22). Here, an absence of synergism with HS in the nLUC-DAO1 accumulation was observed. However, a slight expression was detected at 22°C but not sufficient to activate a full HSR as observed at 38°C without H_2O_2 (Fig. 10a-c). These results confirm that H_2O_2 does not tend to activate the HSR at basal temperature and does not overexpress the HSR at high temperatures. Although H_2O_2 was demonstrated to be a secondary messenger of the heat signaling, a dose-response might provide a specific threshold which induces a large fraction of the HSR at low and high temperatures (23,24).

Mannitol and NaCl can induce damages in membranes that mediate several cytosolic signals (Belver and Travis, 1990). For example, it was shown that salt stress-induced an osmotic change within the cell resulting in the activation of HSFA6b and DREB2A which mediate the accumulation of HSPs in *A. thaliana* (25). Mannitol was described as a free radical scavenger which can draw fluid out of cells and induces toxicity in plants (26). Thereby, a combination of HS and mannitol or NaCl could negatively affect the HSR in plant cells. Tested concentrations did not influence the expression of nLUC-DAO1 and confirmed HIBAT to be specific to HS even though a slight repression of nLUC-DAO1 was observed at 35°C in the presence of mannitol. Additionally, the biotic elicitor FLG22 did not induce a significant effect in the HSR of HIBAT (Fig. 9d-f and Fig. 11a-c). Altogether, these results confirm that mannitol, NaCl, and FLG22 do not induce a significant difference at low and at high temperatures in HIBAT compared to untreated plants. The cold and chilling perception stresses are detected, as well as heat, by the plasma membrane fluidity. In contrast, cold and heat signals seem to be different within the cytosol (27). Chilling and cold stresses were found to not trigger the nLUC-DAO1 (Fig. 11d-f and Fig. 12). Thus, the promoter was found to be very specific to heat despite the existence of crosstalk in the heat signaling through and mainly shared by HSFs. However, all conditions were not tested including a dose-response of mannitol, H_2O_2, NaCl, and FLG22. Indeed, it cannot be excluded that these stresses might lead to the activation or repression of the promoter in HIBAT which a proper concentration and time of exposition might reach a critical threshold affecting the HSR. It remains also to study the effect of additional stresses such as drought and to analyze their impact on the HSR.

Conclusion

The aim of this chapter was to generate a progenitor line to be employed for an FGS and in an attempt to identify EMS mutants impaired in heat sensing and signaling. The HIBAT isolated line was found to fulfill all criteria previously mentioned in the introduction part. HIBAT seems to be an innovative strategy based on the new double reporter system. It remains relevant to consider the line HIBAT as a tool to study the impact of several stresses in the HSR due to the direct expression of nLUC-DAO1. Thereby, a paper is currently in preparation to address HIBAT properties to measure the HSR being correlated with the expression of HSPs.

Materials and methods

Transgene design and transformation of *A. thaliana* plants

DNA sequences of the promoter pGmHsp17.3b from *Glycin max*, nLUC, and DAO1 were obtained by the following references: Boute et al., 2016; Erikson et al., 2004; Saidi et al., 2005. They were synthesized by GenScript Biotech and cloned in a binary vector (https://www.genscript.com). The pGmHsp17.3b, *nLUC*, and *DAO1* genes were then cloned in the final pFR7m24GW vector which contained the OLEOSIN1 fused to the red fluorescent TAG and driven by the oleosin1 promoter. The vector pFR7m24GW were kindly obtained from the Niko Geldner group (University of Lausanne, unpublished). The vector pFR7m24GW which contained the transgene, was introduced into *A. thaliana* Col-0 plants via *Agrobacterium tumefaciens* (strain GV3101), by means of the floral-dip method adapted from Bechtold, 1998. Plant flowers of 6-8 weeks old were transformed in a solution containing 5% (v/v) of sucrose, 0.05% (v/v) Silwet L-77 (GE Specialty Materials), and the *Agrobacterium tumefaciens* containing the transgene for 1 min. Plants were horizontally lying and covered for 2 days and seeds were then harvested when mature.

The analysis of seeds segregation at the T1 and T2 generation of HIBAT lines

Seeds emitting red fluorescent (red TAG) were picked up with wet wooden toothpick at the T1 generation being viewed with epifluorescence Leica stereo microscopy (excitation wavelength 495 nm). The segregation analysis at the T2 generation, to determine the copy number, was performed by counting the ratio of black seed (non-transformed) and red seeds (transformed) under microscopy.

DNA genomic extraction

Leaves from plants were crushed and grinded by a plastic pestle in an Eppendorf tube of 1.5mL. Extracts were resuspended in 600 µl of STE-lysis buffer (100mM Tris-HCL (pH 7.5), 2% (w/v) SDS, and 10 mM of EDTA) and incubated at 65°C for 20 min minimum. DNA extractions were then cooled on ice (4°C) for 5 min and 200 µl of NH_4Ac (10M) were added, mixed, and centrifuged at 12 000g for 10 min. 650 µl of the supernatants were transferred in a new tube and 650 µl of isopropanol (100%) was added, mixed, and incubated for 5 min at room temperature and then centrifuged for 10 min at 12 000g. Supernatants were removed and pellets were washed with 1 mL of cold ethanol 70% and re-centrifuged for 10 min at 12 000g. This wash step was repeated 2 times. Ethanol was then removed, and tubes were let open until pellets became transparent and dry. DNA extracts were finally resuspended in 100 µl of EB buffer (10mM of Tris-HCL pH 8.0).

List of primers used

Genes name	Forward	Reverse
DAO1	TCAAGAAGTGGGTCGAGTTG	GGTAATTTGGCGTGATGTCC
nLUC	ACAGCCGGCTACAACCT	TCACTCCGTTGATGGTTACTC
Sand	AACTCTATGCAGCATTTGATCCACT	TGATTGCATATCTTTATCGCCATC
Actin	CGTTTCGCTTTCCTTACTGTTAGCT	AGCGAACGGATCTAGAGACTCACCTTG
Genome part (OV)	CAACAATCGGGAGATATTTGA	NA

Table 3: List of primers used for PCR and qPCR.

PCR amplification to validate the presence of the transgene in HIBAT plants

To validate the presence of the transgene in transformant plants, the *DAO1* gene was amplified by PCR using Arabidopsis genomic DNA and the corresponding primer set of *DAO1* (Table 3). PCR product was loaded in a gel (1% (w/v) of agarose, tris-base 40 mM, 20 mM acetic acid, 1mM EDTA, and gel red DNA marker diluted 1:20 000 (v/v) (BIOTIUM, ref 41001)) and migrated by electrophoresis at 80 Volt for 10 min follow by 120 V for 30 min.

Determination of the copy numbers by the method of $2^{-\Delta\Delta CT}$

RNA was extracted from seedlings using MACHEREY-NAGEL NucleoSpin RNA plant KIT (REF 740949.50). For cDNA synthesis, 500 ng of total RNA was reverse transcribed by using superscript II RNase A reverse transcriptase (Invitrogen, ref 18064-014) in a final volume of 15.25 µl. Each cDNA sample was generated in triplicate and diluted eightfold with water Quantitative real-time PCR analysis was performed in a final volume of 20 µl containing 2 µl of cDNA, 0.2 µM of each corresponding primer, 0.03 µM of reference dye and 10 µl of Brilliant III Ultra-Fast SYBR Green qPCR Master Mix (Agilent). Reactions were performed using an Mx3000P real-time PCR machine (Agilent) with the following program: 95°C for 3 min, then 40 cycles of 10 sec at 95°C and 20 sec at 60°C. Relative mRNA abundance of each *nLUC and DAO1* were normalized to the housekeeping genes *sand* and *actin.* Primers used are shown in Table 3. The efficiency of each primer was also determined by diluted cDNA samples at 1, 1/10, 1/100, 1/1 000 and 1/10 000 and submitted to qPCR analysis. A linear curve was performed for each dilution and the slope determined the efficiency of primers. Efficiency of primers found for each gene are the following: *nLUC*= 0.946; *Actin*= 0,9301; *Sand*= 0.935 and *Dao1*= 0.938 The method of $2^{-\Delta\Delta CT}$ was then applied and adapted from Bubner and Baldwin, 2004 method.

Transgene localization in the line HIBAT

The HIBAT was submitted to the whole genome DNA sequencing (see Materials and Methods Chapter 3). The transgene sequence was aligned against the HIBAT line genome using Galaxy 2.0 website tool (https://galaxyproject.org). Overlapping reads sequence between the transgene and HIBAT genome were then obtained by using Integrative Genomic Viewer software (IGV version 2.8.10). Reads were blasted to find their position in the *A. thaliana* genome (https://blast.ncbi.nlm.nih.gov/). A localization at 26180497 in chromosome 1 was obtained and confirmed by a gap found when the genome of HIBAT and Col-0 were aligned. The set of primer which contained OV and nLUC_Reverse (Table 3) were used to confirm the transgene localization in HIBAT by PCR.

Protein extraction and analysis

Seedlings or leaves from plants were grinded by a plastic pestle in an Eppendorf tube of 1.5mL and resuspended with a BAP buffer (50 mM Tris-HCL (pH 7.5), 100 mM NaCl, 250 mM mannitol, 5 mM EDTA, 10% (v/v) glycerol, and protease inhibitor cocktail diluted at 1:300 (v/v) (Sigma-Aldrich, ref P9599). Protein extracts were centrifuged for 10 min at 12 000g and at 4°C. Supernatants (soluble proteins) were transferred in a new Eppendorf tube of 1.5mL and protein concentrations were determined by BRADFORD assay (Sigma-Aldrich, ref 23238). The bioluminescence (nLUC-DAO1) was detected by using the Nano-Glo Luciferase Assay System Kit from Promega (ref 1110) and the HIDEX plate reader (version 5067). The bioluminescence was analyzed for 1 second giving count per second. The bioluminescence emission was converted in ng of nLUC-DAO1 per ug total of protein through a standard calibration curve of nano-luciferase purified from *E. Coli* system (Fig. 14).

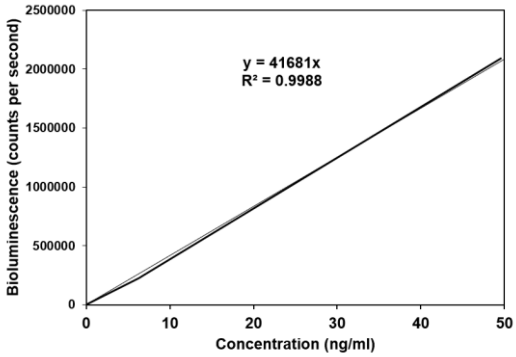

Figure 14: Calibration curve of the level of nano-luciferase relative to the bioluminescence emission. The concentration of nano-luciferase purified in an *E. Coli* system were determined by Bradford assay (0, 10,

20, 30, 40, and 50 ng/mL). The slope was then used to convert the bioluminescence detected in HIBAT plant and covert in ng of nano-luciferase per ug total of protein.

Western blot

Protein extract was homogenized in LBX buffer (Tris-HCL 0.5 M (pH 6.8), 20% glycerol (v/v), 20% SDS (w/v), 4% bromophenol blue (w/v), 5% 2-mercaptoethanol (v/v), and heated for 3 min at 90°C. Homogenates were loaded in Precast SDS PAGE gels 12% acrylamide (EXPEDON, ref Ab 119207). Electrophoresis was applied at 100 V for 15 min followed by 45 min at 130V (constant amperage) using the associated buffer of Precast SDS PAGE gels diluted at 1:50 (v/v). Precast SDS PAGE gels were transferred to nitrocellulose blotting membrane 0.2 µM (GE Healthcare Life Sciences, ref 10600001) by wet transfer using TRT buffer (20% (v/v) absolute Ethanol, and 5% (v/v) of the buffer associated with Precast SDS PAGE gels) for 50 min at 80 volts (amperage constant). Staining by PONCEAU S (Sigma-Aldrich, ref 09276) was applied on membranes for 5 min and the excess was washing with distilled water.

Membranes were blocked by using TRM buffer (5% milk powder (v/v), 50 mM Tris-HCL (pH 8), 150 mM NaCl) for 1 hour at room temperature. Primary antibody sHSP17.7 (from Abcam, ref Ab80171) was diluted at 1:2000 (v/v) in TRM buffer and the solution covered membranes for 2 hours at room temperature with gentle agitation. Membranes were washed 3 times for 10 min (gently agitation) with TRM buffer without milk and replace by 0.1% (v/v) Tween 20. A secondary peroxidase-conjugated goat antibody against rabbit IgG (from Biorad, ref 170-5046) was diluted at 1:2000 (v/v) in TRM buffer and the solution covered membranes for 1 hour at room temperature with gentle agitation. Membranes were still washed 3 times. The revelation was done by using the kit Clarity Western ECL substrate (Biorad, ref 102031318 and 102031316) and the acquisition was performed by using ImageQuant LAS 500 automatic exposition.

FLAG analysis

The peptide extract of BRASSINOSTEROID INSENSITIVE 1 (BRI1) coupled with FLAG was kindly provided by Julia Santiago group (University of Lausanne) and analyzed similarly in the section Materials and Methods “Western blotting analysis”. Briefly, HRSP-conjugated DYKDDDDK FLAG monoclonal antibody (Protein tech, ref HRP-66008) was diluted 1:1000 (v/v) in TRM buffer. A secondary peroxidase-conjugated goat antibody against mouse IgG (from Invitrogen, ref 62-6520) was applied and diluted at 1:2000. The revelation was done by using the kit Clarity Western ECL substrate (Biorad, ref 102031318

and 102031316) and the acquisition was performed by using ImageQuant LAS 500 automatic exposition.

Plant growth materials

Seeds of *A. thaliana* were surface sterilized with 70% ethanol and sowed on ½MS medium with 2.20 g/L of Murashige and Skoog media including MES buffer (Duchefa Biochimie, ref P14881.01), and 8 8 g/L of agar (pH 5.8). In all conditions mentioned in the Materials and Methods, seeds were always incubated at 4°C for 2 days to break the dormancy. The seeds were germinated and grown at 22°C under continuous light and then transferred to the soil at 22°C in long days conditions (16 hours light, 8 hours dark) for subsequent growth at 12-14 days old.

D-valine test

HIBAT and Col-0 plants were grown in the range of 0 mM, 20 mM, 25 mM, and 30mM of D-valine in plates containing $^{1/2}$MS medium. For 7 days, plants were placed in a phytotron and grown at 22°C in long days conditions (16 hours light, 8 hours dark). At 7 days, the phytotron program was set up to applied 2 HS at 38°C for 2 hours with an apart of 2 hours at 22°C of post-recovery for a total of 5 days. At 12 days old, the phytotron program was then set up at 22°C for 2 days, and plates were imaged. At 14 days old, plants were transferred in the soil in long days conditions (16 hours light, 8 hours dark) at 22°C, and at 35 days old, plates were imaged, and the survival rate calculated.

Acquired thermotolerance assays

HIBAT and Col-0 *A. thaliana* plants were grown in $^{1/2}$MS medium for 14 days in continuous days conditions and plates were imaged. At 14 days old, plants were submitted to priming at 36°C for 2 hours followed by 2 hours of post-recovery at 22°C and then exposed to a noxious heat shock at 45°C for 45 min. Unprimed plants were exposed to the same noxious HS. Plants were then grown for 7 days at 22°C and plates were imaged.

Bioluminescence in vivo of line HIBAT

HIBAT and Col-0 *A. thaliana* plants grew in $^{1/2}$MS medium for 7 days in continuous days conditions or in the soil for 5 weeks at 22°C in long days conditions (16 hours light, 8 hours dark). Heat treatment was applied in a phytotron for 2 hours at 38°C followed by 2 hours of post-recovery at 22°C. The substrate of the nano-luciferase (furimazine, Kit from Promega (ref 1110)) was spread in plates at 7 days old or on plants 5 weeks old (diluted 1:100 (v/v)). Plates were imaged by using ImageQuant LAS 500 automatic exposition.

Heat-inducible expression profile of nLUC-DAO1 in the line HIBAT

HIBAT seedlings (n= 10-15 for a total of 4 replicates) were grown on $^{1/2}$MS medium in continuous days conditions for 14 days. Seedlings were then transferred in an Eppendorf tube of 1.5 mL containing 1 mL of Evian water (adapted from Macherel et al., 2013) and heated in a thermoblock for 2 hours followed by 2 hours of post-recovery at 22°C. Proteins were then extracted following the same protocol in the section Materials and Methods “protein extraction and analysis” in order to analyze the amount of nLUC-DAO1.

Physiology assays

HIBAT and Col-0 plants were grown in continuous days conditions at 22°C. At 5 days and 10 days old, root length was measured using ImageJ software (version 1.53) among 3 replicates (n=28 for each). At 9, 13, or 16 days old, shoots from seedlings were dissociated from roots and weighted among 3 replicates (n=16 for each). Germination was calculated at 5 days and 10 days old among 2 replicates (n=50 for each).

Abiotic and biotic stresses assays

12 days old HIBAT seedlings (n= 10-15 per sample for a total of 4 replicates) were previously grown in continuous days conditions at 22°C. They were transferred in an Eppendorf tube of 1.5 mL containing 250 µM H_2O_2, 300 mM mannitol, 150 mM of NaCl, or 1 mM of Flagellin 22 in a final volume of 1 mL of Evian water. Seedlings were then exposed for 1 hour at 22°C followed by 2 hours at different temperatures (22°C, 31°C or 35°C except for H_2O_2 with 34°C and 38°C) followed by 2 hours of post-incubation at 22°C. Proteins were then extracted following the same protocol in the section Materials and Methods “protein extraction and analysis” in order to analyze the amount of nLUC-DAO1. Independently, the cold stress and chilling were applied on seedlings for 2 hours using a thermoblock (4°C, 12°C, 16°C, and 22°C) or ice (0°C) followed by 2 hours of post-induction at 22°C. All temperature conditions were controlled by a thermometer.

EMS treatment

1 g of HIBAT dry seeds were soaked in a 50 mL plastic tube with 40 mL of 100 mM K2HPO4 buffer (pH 7.5) at 4°C overnight. New fresh 40 mL K_2HPO_4 buffer (pH 7.5) was replaced in the 50 mL plastic tube and different concentration of EMS (Sigma-Aldrich, ref M0880) was added, respectively 0%, 0.2%, 0.3%, 0.4%, and 0.8% (v/v) for 8 hours with gently shaking. Seeds were then washed thoroughly 20 times with water (40mL) per wash. After EMS mutagenized, seeds were sowed in soil and grew for 7 days in long days

conditions (16 hours light, 8 hours dark). The survival rate for all concentrations applied was finally calculated.

Strategy to select mutants with a defective HSR by bioluminescence emission

Seedlings plants from HIBAT and Col-0 were grown for 7 days in continuous days in $^{1/2}$MS medium. At 7 days, plates were submitted to HS at 38°C for 1 hour, and the substrate of the nano-luciferase (furimazine, Kit from Promega (ref 1110)) was spread on plates (diluted 1.100). Plates were then imaged by using ImageQuant LAS 500 automatic exposition.

Statistical analysis

We assume a normal distribution of values and homogeneity of variance by using the Leven test for all replicates. The determination of statically differences between samples was evaluated by Student's T-test using the R software (version 4.0.3).

Contributions

The design of the transgene, the cloning in the final vector, and the transformation in *A. thaliana* plants were contributed by Dr. Anthony Guihur. The calibration curve assay to convert the bioluminescence emission in ng of nLUC-DAO1 per ug total of protein was performed by Dr. Anthony Guihur and the laboratory technician John Perrin. Physiology tests including root length, germination, and shoot weight assay were performed by Dr. Anthony Guihur and by the apprentice technician Gizem Demirkiran. The heat-inducible profile of the line HIBAT was contributed by the Ph.D. Alexandra Waskow.

References

1. Swindell WR, Huebner M, Weber AP. Transcriptional profiling of Arabidopsis heat shock proteins and transcription factors reveals extensive overlap between heat and non-heat stress response pathways. BMC Genomics [Internet]. 2007;8(1):125. Available from: http://bmcgenomics.biomedcentral.com/articles/10.1186/1471-2164-8-125
2. Saidi Y, Finka A, Chakhporanian M, Zrÿd JP, Schaefer DG, Goloubinoff P. Controlled expression of recombinant proteins in Physcomitrella patens by a conditional heat-shock promoter: A tool for plant research and biotechnology. Plant Mol Biol. 2005;59(5):697–711.
3. Boute N, Lowe P, Berger S, Malissard M, Robert A, Tesar M. NanoLuc Luciferase - A multifunctional tool for high throughput antibody screening. Front Pharmacol. 2016;7(FEB):1–11.
4. Erikson O, Hertzberg M, Näsholm T. A conditional marker gene allowing both positive and negative selection in plants. Nat Biotechnol [Internet]. 2004;22(4):455–8. Available from: http://www.nature.com/doifinder/10.1038/nbt946
5. Smirnoff N, Arnaud D. Hydrogen peroxide metabolism and functions in plants. New Phytol.

2019;221(3):1197–214.
6. van der Eerden LJM. Toxicity of ammonia to plants. Agric Environ. 1982;7(3–4):223–35.
7. Ogier De Baulny H, Saudubray JM. Branched-chain organic acidurias. Semin Neonatol. 2002;7(1):65–74.
8. Taylor NL, Heazlewood JL, Day DA, Millar AH. Lipoic Acid-Dependent Oxidative Catabolism of α-Keto Acids in Mitochondria Provides Evidence for Branched-Chain Amino Acid Catabolism in Arabidopsis. Plant Physiol. 2004;134(2):838–48.
9. Bartoloni, A., Pizza, M., Bigio, M., Nucci,D., Ashworth, L.A., Irons, L.I., Robinson, A., Burns, D., Manclark, C., Sato, H., and Rappuoli R. © 19 8 8 Nature Publishing Group http://www.nature.com/naturebiotechnology. Nat Biotechnol. 1988;6:709–12.
10. Shimada TL, Shimada T, Hara-Nishimura I. A rapid and non-destructive screenable marker, FAST, for identifying transformed seeds of Arabidopsis thaliana: TECHNICAL ADVANCE. Plant J. 2010;61(3):519–28.
11. Bubner B, Baldwin IT. Use of real-time PCR for determining copy number and zygosity in transgenic plants. Plant Cell Rep. 2004;23(5):263–71.
12. Tran LSP, Nakashima K, Sakuma Y, Osakabe Y, Qin F, Simpson SD, et al. Co-expression of the stress-inducible zinc finger homeodomain ZFHD1 and NAC transcription factors enhances expression of the ERD1 gene in Arabidopsis. Plant J. 2007;49(1):46–63.
13. Liu HC, Liao HT, Charng YY. The role of class A1 heat shock factors (HSFA1s) in response to heat and other stresses in Arabidopsis. Plant, Cell Environ. 2011;34(5):738–51.
14. Sega GA. A review of the genetic effects of ethyl methanesulfonate. Mutat Res Genet Toxicol. 1984;134(2–3):113–42.
15. Martín B, Ramiro M, Martínez-Zapater JM, Alonso-Blanco C. A high-density collection of EMS-induced mutations for TILLING in Landsberg erecta genetic background of Arabidopsis. BMC Plant Biol [Internet]. 2009;9(1):147. Available from: http://bmcplantbiol.biomedcentral.com/articles/10.1186/1471-2229-9-147
16. Ingham DJ, Money S. Quantitative Real-Time PCR Assay for Determining Transgene Copy Number in. 2001;31(1).
17. Franklin KA. Plant Chromatin Feels the Heat. Cell. 2010;140(1):26–8.
18. Chinnusamy V, Stevenson B, Lee B, Zhu J. Screening for gene regulation mutants by bioluminescence imaging. Sci STKE. 2002;2002(140):pl10.
19. Greene EA, Codomo CA, Taylor NE, Henikoff JG, Till BJ, Reynolds SH, et al. Spectrum of chemically induced mutations from a large-scale reverse-genetic screen in Arabidopsis. Genetics. 2003;164(2):731–40.
20. Yoshida T, Ohama N, Nakajima J, Kidokoro S, Mizoi J, Nakashima K, et al. Arabidopsis HsfA1 transcription factors function as the main positive regulators in heat shock-responsive gene expression. Mol Genet Genomics. 2011;286(5–6):321–32.
21. Volkov RA, Panchuk II, Mullineaux PM, Schöffl F. Heat stress-induced H2O2 is required for effective expression of heat shock genes in Arabidopsis. Plant Mol Biol. 2006;61(4–5):733–46.
22. Davletova S, Rizhsky L, Liang H, Shengqiang Z, Oliver DJ, Coutu J, et al. Cytosolic ascorbate

peroxidase 1 is a central component of the reactive oxygen gene network of Arabidopsis. Plant Cell. 2005;17(1):268–81.

23. Černý M, Habánová H, Berka M, Luklová M, Brzobohatý B. Hydrogen peroxide: Its role in plant biology and crosstalk with signalling networks. Int J Mol Sci. 2018;19(9).
24. Maruta T, Noshi M, Tanouchi A, Tamoi M, Yabuta Y, Yoshimura K, et al. H 2O 2-triggered retrograde signaling from chloroplasts to nucleus plays specific role in response to stress. J Biol Chem. 2012;287(15):11717–29.
25. Huang YC, Niu CY, Yang CR, Jinn TL. The heat stress factor HSFA6b connects ABA signaling and ABA-mediated heat responses. Plant Physiol. 2016;172(2):1182–99.
26. Nunnually ME. Book and Multimedia Reviews System : Physiology and Implications for the Treatment of Shock. 2009;108(2):2009.
27. Guo X, Liu D, Chong K. Cold signaling in plants: Insights into mechanisms and regulation. J Integr Plant Biol. 2018;60(9):745–56.
28. Bechtold N. In Planta Agrobacterium Mediated Transformation of Adult Arabidopsis thaliana Plants by Vacuum Infiltration. Methods. 1998;82:259.
29. Macherel D, Abdelilah B, Pierart A, Baecker V, Avelange-Macherel M-H, Rolland A, et al. Simple system using natural mineral water for high-throughput phenotyping of Arabidopsis thaliana seedlings in liquid culture. Int J High Throughput Screen. 2013;1.

Supplementary data

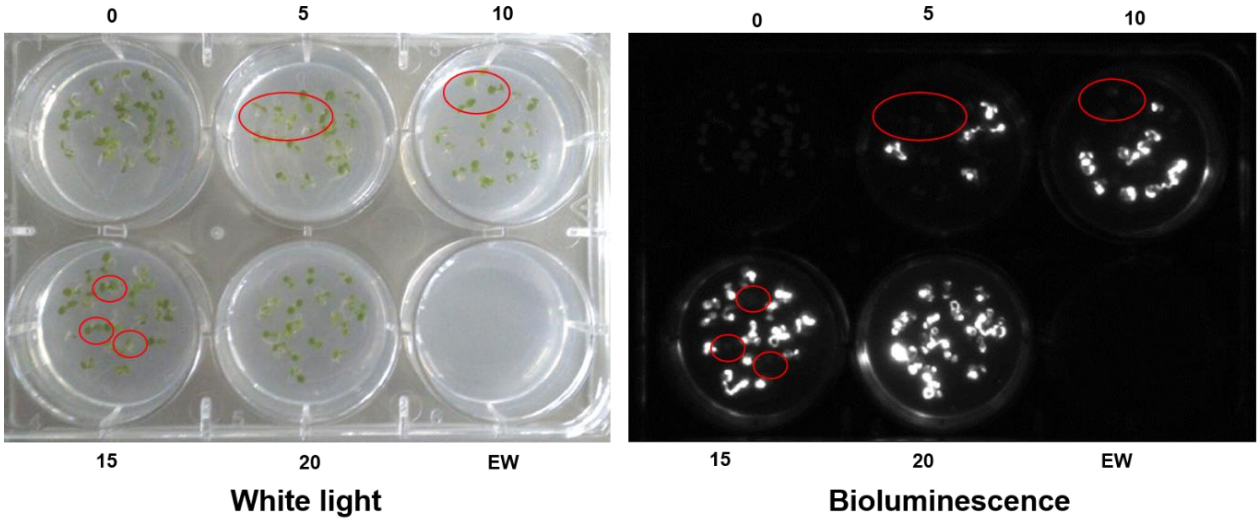

Supplementary data 1: FGS strategy to select EMS candidates with a defective bioluminescence emission using HIBAT and Col-0 plants under HS. Col-0 and HIBAT were mixed in the same wells. Total numbers of HIBAT seedlings are indicated on the top and bottom of each well. Total of seedlings per well= 20, EW (empty well). Seedlings at 7 days old were exposed to 38°C for 1 hour and nLUC furimazine substrate was spayed on plates. The red circle represents Col-0 seedlings that were unable to emit bioluminescence correlated with EMS candidates impaired in heat sensing and signaling pathway during FGS.

Chapter 3: A forward genetic screen in *A. thaliana* to search for new genes involved in plant heat sensing and signaling pathway.

Abstract

The characterized HIBAT was used through an FGS, in an attempt to isolate mutants which were unable to sense and respond to heat. After EMS mutagenesis, several candidates were found to be able to survive iterative heat treatments in the presence of D-valine. Under HS, survivals of HIBAT mutants were confirmed to be defective at emitting bioluminescence and to accumulate HSPs as compared to the parental line. At the F2 generation, seven candidates were segregated on D-valine and under heat treatments. The Offspring survivals, for each individual line, were pooled and submitted to the whole genome DNA sequencing (WGDS) in an attempt to identify single nucleotide polymorphisms (SNPs) in the causal gene(s). Near significant SNPs were found in different genes, presumably responsible for defective HSR and T-DNA insertion lines were analyzed. Yet, none of these lines were defective in the heat-induced accumulation of sHSP17.7. The sequencing data revealed heterogeneity of SNP repartitions over the genome of HIBAT mutants and suggested that all individual offspring were not homogenous for their heat-responsive phenotype. HIBAT mutants were then analyzed for their ability to accumulate nLUC-DAO1 and HSPs under HS in a large number of offspring but they were not following the expected ratio at the M3, M4, and F2 generations. Most of the offspring were found to had reverted to the parental phenotype, i.e. they accumulated nLUC-DAO1 and HSPs under HS. Thus, these observations suggested a transient and reversible epigenetic phenotype had repressed the expression of nLUC-DAO1 and/or HSPs, rather than from DNA mutations in the gene(s) responsible for heat-sensing and signaling.

Introduction

Different approaches can be used to identify genes involved in a biological process of interest. For example, transposable elements and T-DNA insertions, usually 5 to 25 kb in length, can act as a genomic marker in *A. thaliana* and disrupt genes expression leading to the study of their function (1,2). T-DNA insertions were shown to be physically more stable through multiple generations as compared to transposons (3,4). However, forward and reverse genetic screens present the advantage to provides objective information regarding a mutation's connection to a phenotype observed which does not require prior knowledge about the gene being studied (5). Mutation(s) in a gene of interest can produce consistent phenotypic changes which can be identified through reporter genes (6,7). To conduct an FGS, EMS is usually used which causes irreversible damages in DNA (8). EMS treatment causes GC to AT transition mutations and thereby induce SNPs over the genome. SNPs act as a genomic marker which can occur within or in a regulatory region near to the gene which can be responsible for a phenotype(s) (9). Isolated plant mutants are then submitted to the WGDS as compared to the progenitor line which is used as a reference genome. SNPs are mapped and indicate putative genes involved in the biological process of interest. This voluntary method has been described to be efficient at elucidating new genes through several FGS leading to bring additional knowledge in the plant field (10–13). Thus, the progenitor line HIBAT was used to perform an FGS approach in an attempt to isolate candidates impaired in the heat sensing and signaling pathway. The selected mutants should survive under iterative HS in the presence of D-valine and concomitantly defective for the accumulation of nLUC-DAO1 and HSPs.

Results

Identification and selection of EMS HIBAT mutants

To generate HIBAT mutants, an EMS treatment was performed on 5 000 seeds of the T4 HIBAT progenitor line. Most of the mutations induced by EMS are expected to be recessive at the M1 generation and plants must be selfed to dilute recessive traits. At the M2 generation, it should result in 25% of homozygous descendants with a recessive mutation of interest according to the Mendelian type of segregation. Owing to EMS toxicity, 3871 M1 individual lines were harvested from the initial 5 000 seeds sowed. At the M2 generation, pools were generated which each contained seeds from 25 individual HIBAT mutant lines (156 in totals). An additional general pool was made with seeds from all the 3871 harvested plants. Pools were next screened on D-valine and under iterative

HS to find survivals (Fig. 1). Several M2 HIBAT mutants were selected for being resistant to iterative heat treatments in the presence of D-valine at 11 days old. They were transferred to a new fresh D-valine media to ascertain their ability to survive under HS. This second round of heat treatments led to eliminate false positives candidates. Col-0 was used as a positive control being able to survive, whereas the progenitor HIBAT did not survive and confirmed the selection of M2 HIBAT mutants resistant to HS. In total, 200 survivals were isolated from pools at the M2 generation and the DAO1 properties had provided a rapid elimination of candidates that respond to HS.

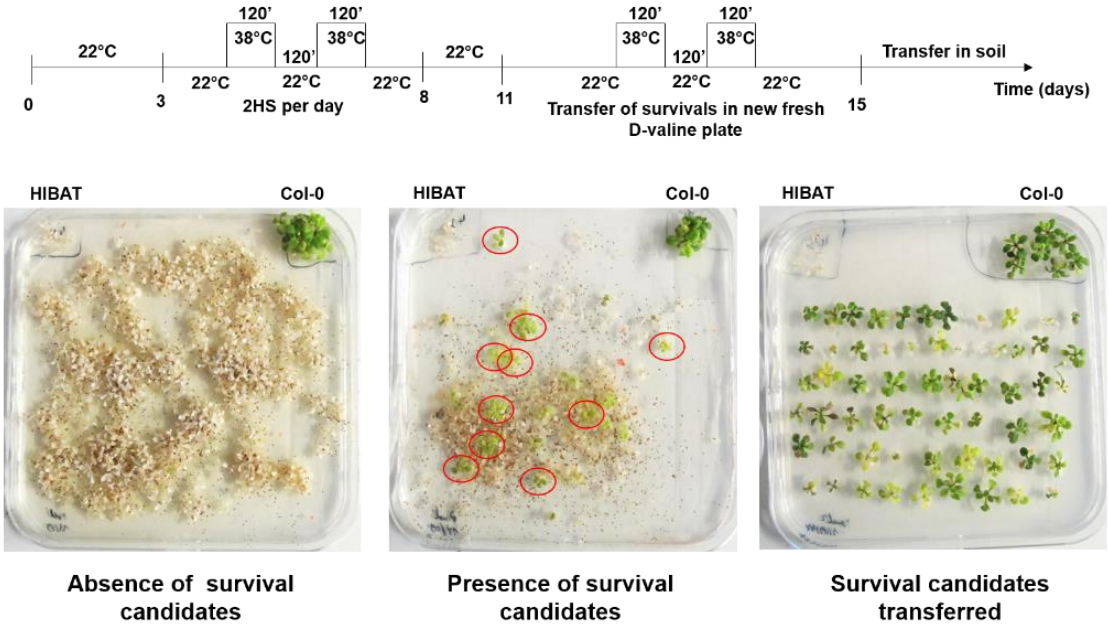

Figure 1: Selection of M2 HIBAT mutants on D-valine plate under iterative heat treatments. Each plate contains the progenitor HIBAT and Col-0 lines used as controls (top of plates, respectively left and right corner). (**Left plate**) Absence of HIBAT mutants able to survive in the presence of D-valine under iterative heat treatments (11 days). (**Middle plate**) Several candidates (red circle) were identified as being able to survive in the presence of 25 mM of D-valine under iterative heat treatments (11 days). (**Right plate**) Survival of HIBAT mutants were transferred to a new fresh D-valine plate and subjected to new iterative HS for 4 days and plants were transferred to soil at 15 days old. The selection of EMS HIBAT candidates followed the protocol represented on top.

Because this phenotype could result from a mutation in the *DAO1* gene, we focused on putative mutants that also were repressing sHSP17.7 expression which is encoded in a different chromosome (5). 5 to 8 weeks old leaves from selected HIBAT mutants were subjected to a single HS at 35°C for 2 hours followed by 2 hours at 22°C post-induction. The parental line HIBAT was used as a control. As expected at 22°C, the reference did not express both nLUC-DAO1 and sHSP17.7, and at 35°C a high expression was observed.

Among selected HIBAT candidates, different heat-responsive phenotypes were identified (Fig. 2a-d). For example, mutants that presented an accumulation of nLUC-DAO1 and sHSP17.7 at 35°C were not selected such as HIBAT-P94 which expressed 98% of nLUC-DAO1 and 134% of sHSP17.7 compared to HIBAT+. This result suggests that these plants were able to respond to heat although they previously survived in presence of D-valine under HS cycles (Fig. 2a). Other candidates such as HIBAT-P24 did not accumulate nLUC-DAO1 but expressed an optimal sHSP17.7 expression (120%) at 35°C compared to control. This result indicates that these mutants could have a mutation in the transgene, leading to survive in the presence of D-valine, and which validate ultimately the requirement to analyze the expression of HSPs (Fig. 2b). HIBAT mutants which showed a defective or an absence of both nLUC-DAO1 and sHSP17.7 accumulation were selected such as HIBAT-P81, HIBAT-P13, HIBAT-P87, and HIBAT-PA21 (Fig. 2a-d). Thus, 40 M2 HIBAT mutants from both pools were retained for their ability to survive on D-valine treatment under iterative HS and for being defective to accumulate nLUC-DAO1 and sHSP17.7.

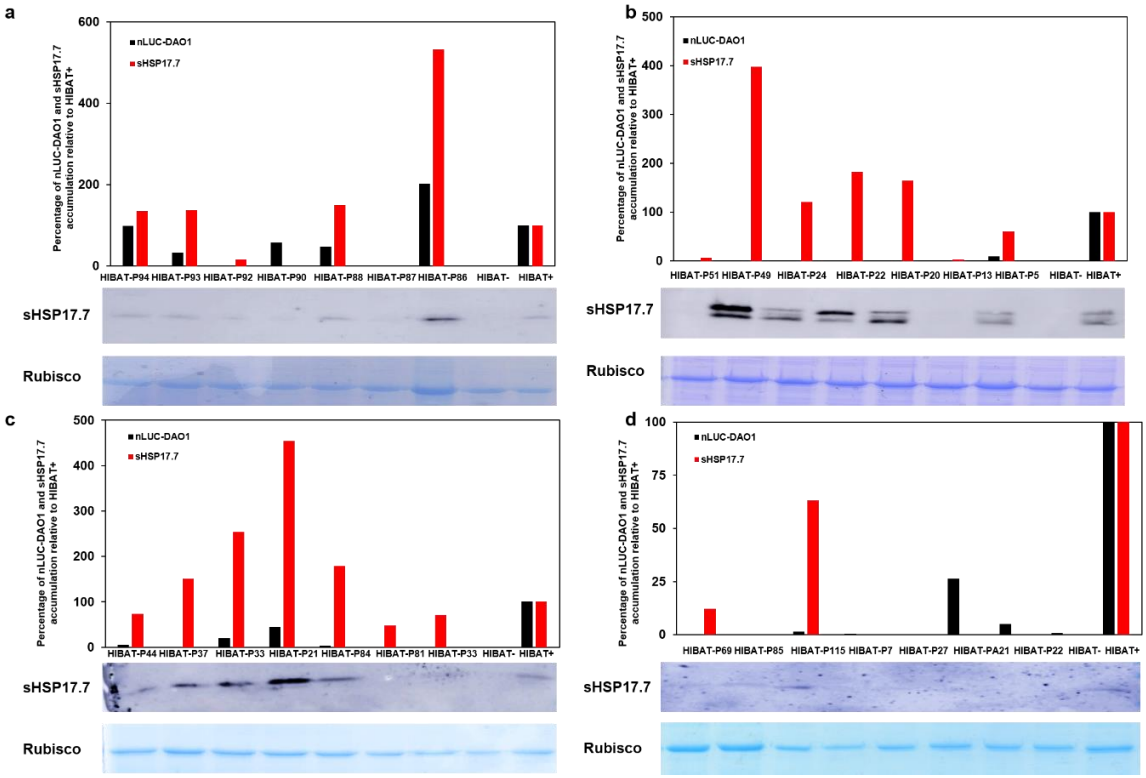

Figure 2: Accumulation of nLUC-DAO1 and sHSP17.7 of M2 HIBAT mutants under HS. (**a-d**) Leaves 5 to 8 weeks old from M2 HIBAT candidates were exposed at 35°C for 2 hours followed by 2 hours at 22°C of post-recovery. The progenitor HIBAT was used as a control in the absence of HS (HIBAT-) or with the same HS applied on M2 HIBAT mutants (HIBAT+). The Western blot below each graph represents the accumulation of sHSP17.7 observed in all HIBAT candidates and the parental line. The homogeneous

loading for each protein sample is represented by the accumulation of the RUBISCO which is shown by Coomassie blue staining. Because gels and membranes are semi-quantitative assays, the accumulation of sHSP17.7 were normalized against the HIBAT+ and using the expression of RUBISCO in graphs. The quantification was performed by ImageJ software. Total protein-loaded; a= 34 ug, b= 16 ug, c= 14 ug and d= 10 ug.

M2 HIBAT candidates previously selected were selfed and subjected similarly to the same selective assays at the M3 generation in order to validate their inability at responding to HS (Fig. 3a-d). Candidates HIBAT-P81B, HIBAT-P13A, HIBAT-P87B, and HIBAT-PA21b were confirmed to survive to D-valine under iterative treatments and were defective in the accumulation of nLUC-DAO1 and sHSP17.7 (Fig 3a-d). Unexpectedly, the offspring HIBAT-PA21a showed a higher expression of nLUC-DAO1 and sHSP17.7 under HS compared to HIBAT-PA21b which both came from the same parent line HIBAT-PA21. This result indicates that an apparent loss of mutations across generations occurred leading to dilute the heat-responsive phenotype which cannot be explained by a Mendelian type of segregation. The HIBAT-PA21b candidate was further selected (Fig. 3d). Additionally, the expression of HSP101 was addressed in isolated M3 HIBAT mutants (Fig. 4a and b). Under HS, HSP101 was described to be constitutively expressed at low-temperature levels and highly accumulated. HSP101 expression was found to be required for short-term and long-term thermotolerance in *A. thaliana* and HSP101 was thereby used as an additional marker of the HSR where the gene is located on chromosome 1 (14). All candidates, except HIBAT-P44 and HIBAT-P13a, were defective to accumulate a high level of HSP101 at 35°C compared to the parental line. This result confirmed a possible mutation(s) in the heat shock signaling pathway. Thus, 18 M3 HIBAT candidates were retained by presenting a defective accumulation in both nLUC-DAO1, sHSP17.7, and different levels of expression of HSP101 under HS.

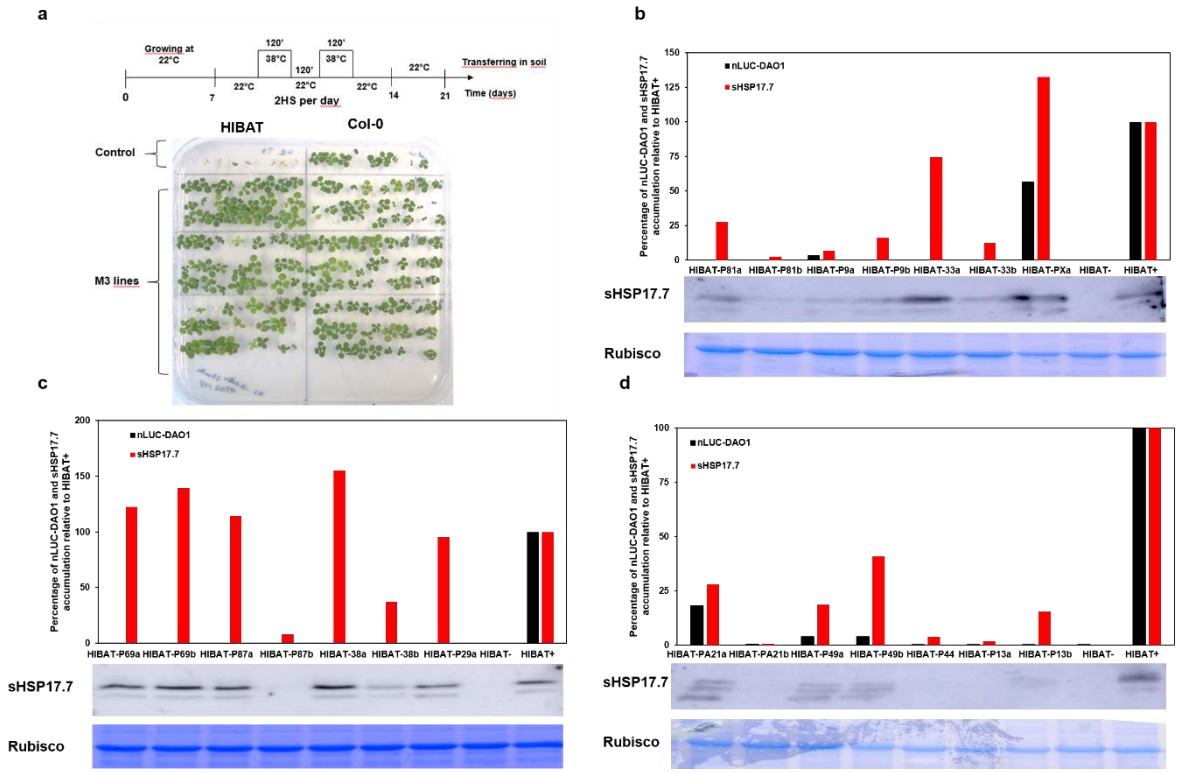

Figure 3: Segregation on D-valine treatment under iterative HS and accumulation of nLUC-DAO1 and sHSP17.7 of M3 HIBAT mutants. (**a**) Selected M3 HIBAT candidates were subjected to D-valine treatment under iterative HS. Around 20 offspring from each M3 HIBAT mutant lines were treated with D-valine and followed the heat protocol represented on top. Each plate contained the progenitor HIBAT and Col-0 lines used as controls (top of the plate, respectively left and right corners). M3 HIBAT candidates and control are delimitated by the black lines in plates. The picture was imaged at 21 days old before to transfer plant in soil. (**c-d**) Leaves 5 to 8 weeks old from M3 HIBAT candidates were exposed at 35°C for 2 hours followed by 2 hours at 22°C of post-recovery. The progenitor HIBAT was used as a control in the absence of HS (HIBAT-) or with the same HS applied on M3 HIBAT mutants (HIBAT+). The Western blot below each graph represents the accumulation of sHSP17.7 observed in all HIBAT candidates and the reference line. The homogeneous loading for each protein sample is represented by the accumulation of the RUBISCO which is shown by Coomassie blue staining. Because gels and membranes are semi-quantitative assays, the accumulation of sHSP17.7 were normalized against the HIBAT+ and using the expression of RUBISCO in graphs. The quantification was performed by ImageJ software Total protein-loaded; b= 17 ug, c= 20 ug, and d= 17 ug.

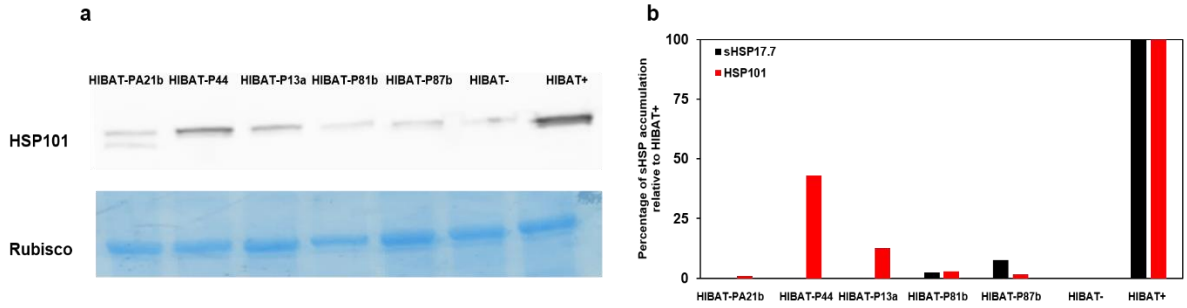

Figure 4: Sum up of the accumulation of sHSP17.7 and HSP101 in selected M3 HIBAT mutants under HS. (**a)** Leaves 5 to 8 weeks old from M3 HIBAT candidates were exposed at 35°C for 2 hours followed by 2 hours at 22°C of post-recovery. The progenitor HIBAT was used as a control in the absence of HS (HIBAT-) or with the same HS applied on M3 HIBAT mutants (HIBAT+). The Western blot represents the accumulation of HSP101 observed in all HIBAT candidates and the reference line. The homogeneous loading for each protein sample is represented by the accumulation of the RUBISCO which is shown by Coomassie blue staining (Total protein-loaded= 23 ug). (**b**) Representation of the accumulation of HSP in percentage observed by Western blot on M3 HIBAT candidates and normalized by the intensity of HSP detected in HIBAT+ line after HS. Because gels and membranes are semi-quantitative assays, the accumulation of HSPs were normalized against the HIBAT+ and using the expression of RUBISCO in graphs. The quantification was performed by ImageJ software.

EMS treatment led to induce mutations in genes which are not linked with the heat-responsive phenotype and the non-relevant SNPs must be diluted to simplify the mapping after the WGDS. M3 HIBAT mutants isolated were thereby crossed with the parental line. Because mutation(s) are suspected to be recessive at the F1 generation, offspring should be sensitive to D-valine treatment due to the gain of the allele of the parental line. Thus, at the F2 generation, seven mutants were segregated on D-valine treatment and under HS cycles in an attempt to select homozygous offspring affected by the loss of heat sensing and signaling. It should result in 25% of survival which was following a Mendelian type of segregation (Table 1). Offspring of HIBAT-P13 and HIBAT-P81 lines presented significantly 25% of survival, whereas other candidates did not respect the segregation even though close to 25%. Because these mutant lines were observed across generations to have lost their ability to accumulate HSPs under HS, they were selected for the WGDS. Between 30 to 60 survivals from each different F2 mutants were pooled to ensure the probability to find a true cluster of SNPs over the genome. The parental line HIBAT was also subjected to the sequencing and used as a reference genome for the SNPs mapping. A sum up of the defective accumulation of nLUC-DAO1 and HSP of M3 HIBAT candidates submitted to the WGDS is shown in Figure 5. An overview of the main steps followed during the FGS is summarized in Figure 6.

Mutant	Theorotical no survival	Theorotical survival	No survival observed	Survival observed	Segregation (%)	χ^2	P-value
HIBAT-P13 (n=338)	253	85	260	78	23.1	0.396	0.53
HIBAT-P42b (n=338)	253	85	281	57	16.9	6.989	0.008
HIBAT-P87 (n=291)	218	73	249	42	14.4	10.414	0.0013
HIBAT-P81 (n=156)	117	39	122	34	21.8	0.447	0.508
HIBAT-P66 (n =338)	253	85	287	51	15.1	10.64	0.001
HIBAT-P28 (n=338)	253	85	276	62	18.3	4.599	0.032
HIBAT-PXa (n=338)	253	85	276	62	18.3	4.599	0.032

Table 1: Segregation on D-valine and under iterative HS treatments of F2 HIBAT mutants. n represents the total number of offspring segregated in D-valine media for each individual F2 HIBAT line. Theoretical numbers of expected survival and real survival observed were based on a Mendelian type of segregation. The Chi-squared test (X^2) was then applied based to respect 25% of survivals. P-value > 0.05 is considered to follow a Mendelian type of segregation (1:4) showing no significant difference compared to theoretical numbers.

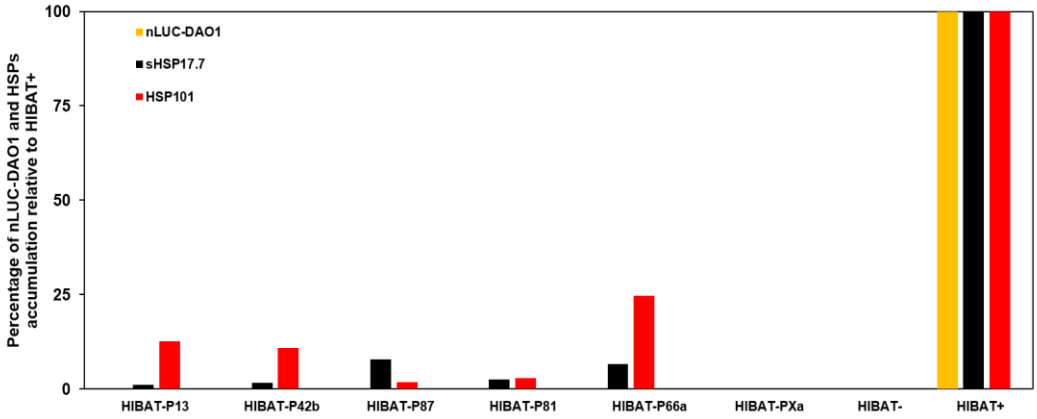

Figure 5: Sum up of the accumulation of nLUC-DAO1 and HSPs of M3 mutants that were sequenced at the F2 generation. The accumulation of nLUC-DAO1 and HSPs from M3 candidates were normalized by the intensity observed in the HIBAT+ line after HS. All HIBAT candidates were exposed at 35°C for 2 hours followed by 2 hours at 22°C of post-recovery. The progenitor HIBAT was used as a control in the absence of HS (HIBAT-) or with the same HS applied on M3 HIBAT mutants (HIBAT+). The candidate, HIBAT-P28 which was sequenced, is not represented because the accumulation of HSP101 was not performed. Because gels and membranes are semi-quantitative, the accumulation of HSPs were normalized against the HIBAT+ and using the expression of RUBISCO in graphs. The quantification was performed by ImageJ software.

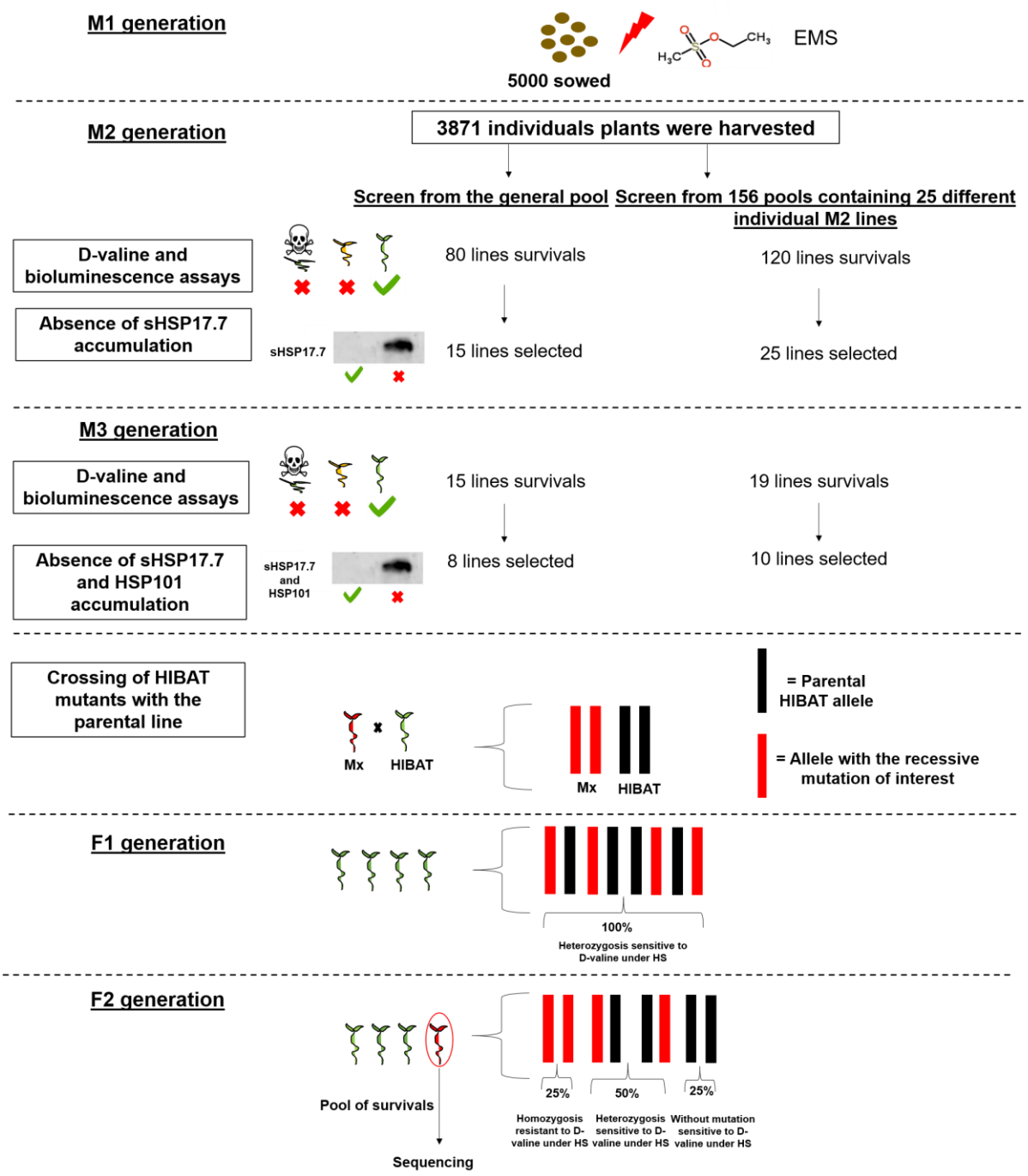

Figure 6: Overview of steps followed to select HIBAT mutants impaired in the heat sensing and signaling pathway during the FGS. The schematic representation starts from the mutagenesis of HIBAT seeds and ends for the selection of F2 HIBAT candidates that were ultimately sent to the whole-genome DNA sequencing. At each generation, HIBAT candidates were segregated on D-valine treatment and under iterative HS except at the F1 generation due to the gain of an allele of the parental line. The analysis of nLUC-DAO1 and HSP accumulation assays were tested at the M2 and M3 generation. The number of individual lines selected is represented for each generation. The Mendelian type of segregation at the F1 and F2 generation is theoretical and only true for a recessive mutation in one gene responsible for a defective heat sensing and signaling pathway.

The identification of SNPs and analysis of putative genes through T-DNA insertion lines

The WGDS revealed a large heterogeneity repartition of SNPs over the genome in sequenced mutants. This observation indicated that pooled offspring from the same HIBAT F2 candidate were mixed with offspring that have the phenotype of the parent line regarding HS. However, among the seven HIBAT candidates, four were showing near confident SNPs. Genes were investigated by seeking T-DNA homozygous insertion lines (Tables 2 and 3). T-DNA lines were screened for the potential defective accumulation of sHSP17.7 under HS, using the Col-0 mother line as a control (Fig. 7a-e). Lines N571207, N653041, and N876373 revealed a lower accumulation level of sHSP17.7 under HS as compared to Col-0 (Fig. 7b and c). Because Western blot is a semi-quantitative analysis, lines N571207 and N653041 were subjected to an additional assay. Both unexpectedly showed a similar level of sHSP17.7 accumulation at 35°C compared to Col-0 and they were then excluded (Fig. 7d and e).

Lines sequenced	Chromosome	Position	Reference allele	Detected allele	TAIR ID	Localization	STOP Codon
HIBAT-P42b	1	28062402	C	T (90% of 97)	AT1G74690	Promoter	-
	1	28166389	C	T (86% of 81)	AT1G75010	Exon	-
	1	27822092	G	A (90% of 96)	AT1G73980	Exon	-
	1	26000943	C	T (91% of 94)	AT1G69160	Exon	-
	3	20066178	C	T (53% of 105)	AT3G54200	Promoter	+
HIBAT-P66a	5	20654734	C	T (68% of 62)	AT5G50780	Intron	+
	1	26514093	G	A (70% of 102)	AT1G70370	Exon	-
	1	18264941	C	T (80% of 101)	AT1G64000	Exon	-
HIBAT-P28	4	14973597	G	A (68% of 111)	AT4G30720	Exon	-
	4	14739120	G	A (63% of 123)	AT4G30140	Intron	+
HIBAT-PXa	2	7725877	C	T (60% of 97)	AT2G17780	Intron	+
	2	7495190	C	T (58% of 95)	AT2G17230	Exon	-
	4	11692392	C	T (57% of 69)	AT4G22070	Exon	-
	2	9012701	C	T (67% of 82)	AT2G20980	Promoter	-
	2	15953022	G	A (60% of 85)	AT2G38110	Exon	-

Table 2: SNPs detection in four HIBAT mutants responsible putatively for a defective accumulation of nLUC-DAO1 and HSPs. The SNP localizations of F2 HIBAT mutants are represented and include their position in the genome and in the gene. The percentage of identical reads that ascertain the presence of true SNP is shown in the bracket on the total number of reads generated during the WGDS. Absence (-), presence (+).

Lines sequenced	TAIR ID	T-DNA Lines	Position of t-DNA	NASC Code	Coding protein identified according to TAIR
	AT1G74690	SALK_013815.54.75.x	Exon	N653041	Encodes a microtubule-associated protein
	AT1G75010	SALK_062123.33.90.x	Exon	N859859	Accumulation and replication of chloroplast 3
	AT1G73980	SALKseq_079237.0	Exon	N579237	Triphosphate tunnel metalloenzyme
	AT1G69160	SALKseq_071515.1	Promoter	N571515	Big grain like 1 (suppressor)
HIBAT-P42b	AT3G54200	SAIL_860_A02	Exon	N838557	Late embryogenesis abundant (LEA)
	AT5G50780	GABI_249F08	Exon	N745959	Microrchida (MORC4) DNA repair. Involved in RNA-directed DNA methylation
	AT5G50780	SALKseq_047719.1	Intron	N547719	Microrchida (MORC4) DNA repair. Involved in RNA-directed DNA methylation
	AT1G70370	SALKseq_071207.0	Exon	N571207	Polygalacturonase 2
HIBAT-P66a	AT1G64000	SAILseq_737_D01.0	Exon	N876373	ATWRKY56, transcription factor
	AT4G30720	SALKseq_059716.0	Exon	N559716	PDE327, pigment defective 327
HIBAT-P28	AT4G30140	SALK_014093.40.50.x	Exon	N685287	Cuticle destructing factor 1
	AT2G17780	SAIL 1292 E05	Exon	N861724	MCA2, Encodes a mechanosensitive channel candidate
	AT2G17230	SALKseq_11107.1	Exon	N883041	Exordium like 5, brassinosteroid-dependent regulation of growth and development
	AT2G17780	SALK_129208.47.75.x	Exon	N629208	MCA2, Encodes a mechanosensitive channel candidate
	AT4G22070	WiscDsLoxHs116_04F	Intron	N911070	ATWRKY 31, Transcription Factor
	AT2G20980	SAILseq_32_C11.1	Intron	N801554	Minichromosome maintenance 10, initiation of DNA replication
HIBAT-PXa	AT2G38110	SALK_146013	Exon	N646013	Glycerol-3-phosphate SN-2-acyltransferase 6, GPAT6, cutin biosynthetic process

Table 3: List of T-DNA insertion lines to investigate genes involved in the loss of heat sensing and signaling pathway. The localization of the foreign T-DNA of each gene is indicated as well as the coding protein identified according to TAIR10.

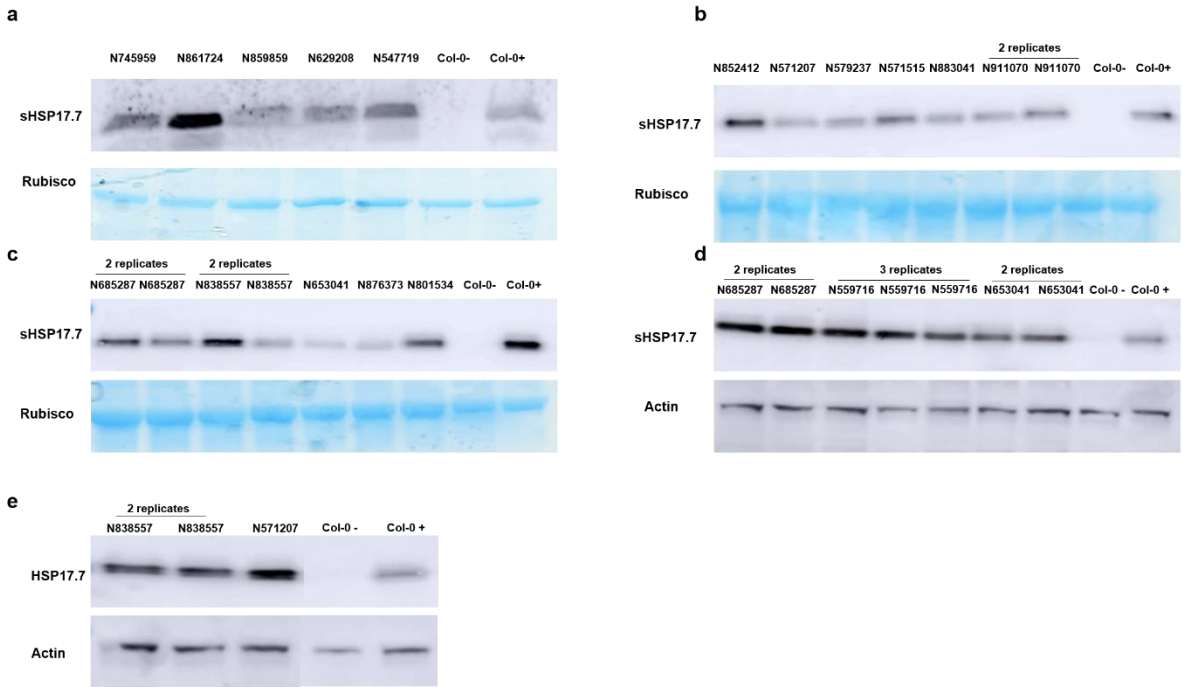

Figure 7: Analysis of the accumulation of sHSP17.7 in T-DNA insertion lines under HS. (**a-e**) 5 weeks old leaves of homozygous T-DNA insertion lines were exposed at 35°C for 2 hours followed by 2 hours of post-recovery at 22°C. Lines Col-0 was used as controls with an absence of HS (Col-0-) or with the same HS applied on the T-DNA insertion lines (Col-0+). The western blot represents the accumulation of sHSP17.7 observed in the T-DNA insertion line and Col-0 controls. The homogeneous loading for each protein sample

is represented by the presence of the RUBISCO which is shown by Coomassie blue staining or by the ACTIN detected with the corresponding antibody. Total protein-loaded; a= 22 ug, b= 30 ug, c= 31 ug, d= 35 ug and e= 15 ug.

One interesting SNP was detected in the HIBAT-P66a candidate and localized in the *WRKY56* exon gene (line N876373), known as a transcription factor. In *A. thaliana*, WRKY25, WRKY26, WKRY33, and WRKY39 were shown to mediate the heat signaling leading to the accumulation of HSPs and the onset of AT (15–17). Thus, WRKY56 might be a good potential candidate. The SNP was identified on chromosome 1, among a significant cluster of DNA mutations, and resulting in an amino acid substitution leucine to proline in the coding sequence of *WRKY56* (Fig. 8a and b). Two additional biological replicates from the T-DNA insertion line N876373 were subjected to 22°C, 33°C, or 35°C for 2 hours followed by 2 hours of post-recovery at 22°C. The same expression levels of sHSP17.7 were observed for all conditions as compared to Col-0 control and the *WRKY56* gene candidate was excluded (Fig. 8c). Similarly, an SNP was identified in a gene of the mutant HIBAT-PXa, encoding for *glycerol-3-phosphate SN-2-acyltransferase 6* (GPAT6) which is located on chromosome 2 and leading to amino acid substitution proline to leucine (Fig. 9a-c). However, the GPAT6 T-DNA insertion line did not show a difference in the accumulation of sHSP17.7 at 22°C, 33°C, and 35°C compared to Col-0 plants (Fig. 9c). Thus, all T-DNA insertion lines tested were not responsible for a defective sHSP17.7 accumulation, and the identification of the causal gene(s) remained to be elucidated.

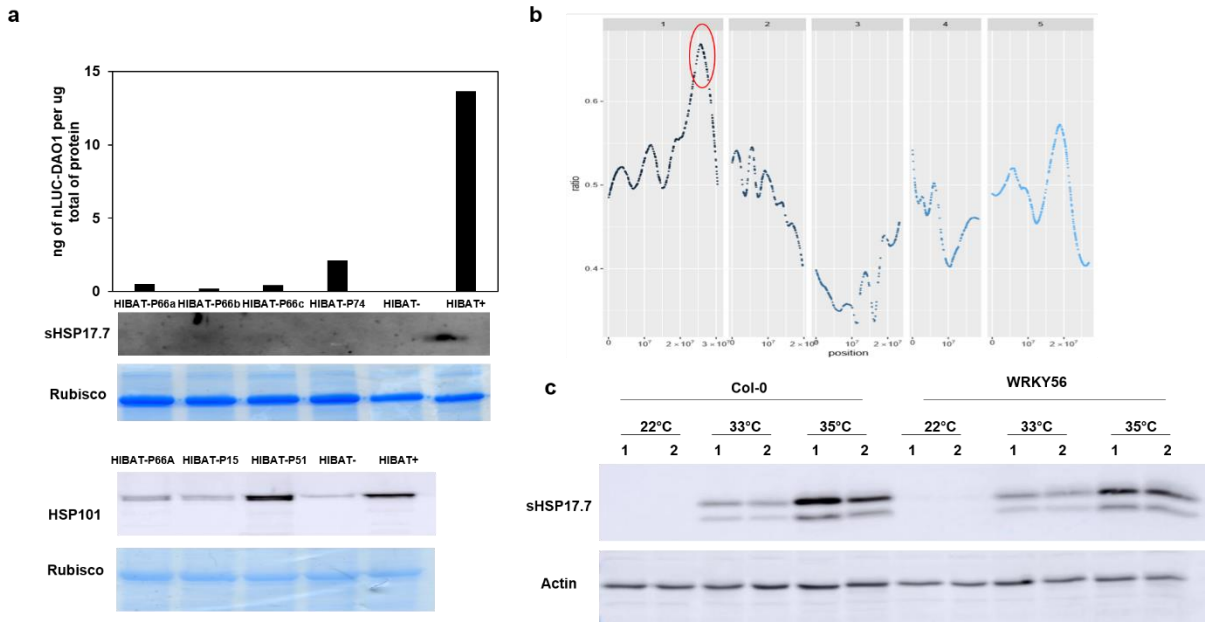

Figure 8: Accumulation of sHSP17.7 in the T-DNA insertion *WRKY56*. (**a**) 5 weeks old leaves from EMS M3 HIBAT candidates were exposed at 35°C for 2 hours followed by 2 hours at 22°C of post-recovery. The

progenitor HIBAT was used as a control in the absence of HS (HIBAT-) or with the same HS applied on M3 HIBAT mutants (HIBAT+). The Western blot below the graph represents the accumulation of sHSP17.7 observed in all HIBAT candidates and the reference line. The homogeneous loading for each protein sample is represented by the accumulation of the RUBISCO which is shown by Coomassie blue staining. Total protein-loaded = 20 ug. (**b**) Repartition of SNP cluster over chromosomes identified in the candidate HIBAT-P66a. The red circle represents the localization of a cluster where was identified the SNP in the gene WRKY56. X-axis, Chromosomal location; y-axis, ratio variable of SNP. (**c**) 5 weeks old leaves from the WRKY56 T-DNA line were exposed at 33°C or 35°C for 2 hours followed by 2 hours of post-recovery at 22°C. Line Col-0 was used as a control without heat treatment (Col-0 -) or with the same HS applied in the WRKY56 T-DNA insertion line (Col-0 +). The Western blot represents the accumulation of sHSP17.7 observed in lines *WRK56* and Col-0. The homogeneous loading for each protein sample is represented by the ACTIN, detected with the associated antibody. Temperatures exposition and lines are represented on top of the membrane. Numbers represent individual biological replicate. Total protein-loaded per sample; a= 28 ug (Top), 23 ug (bottom) and c= 50 ug.

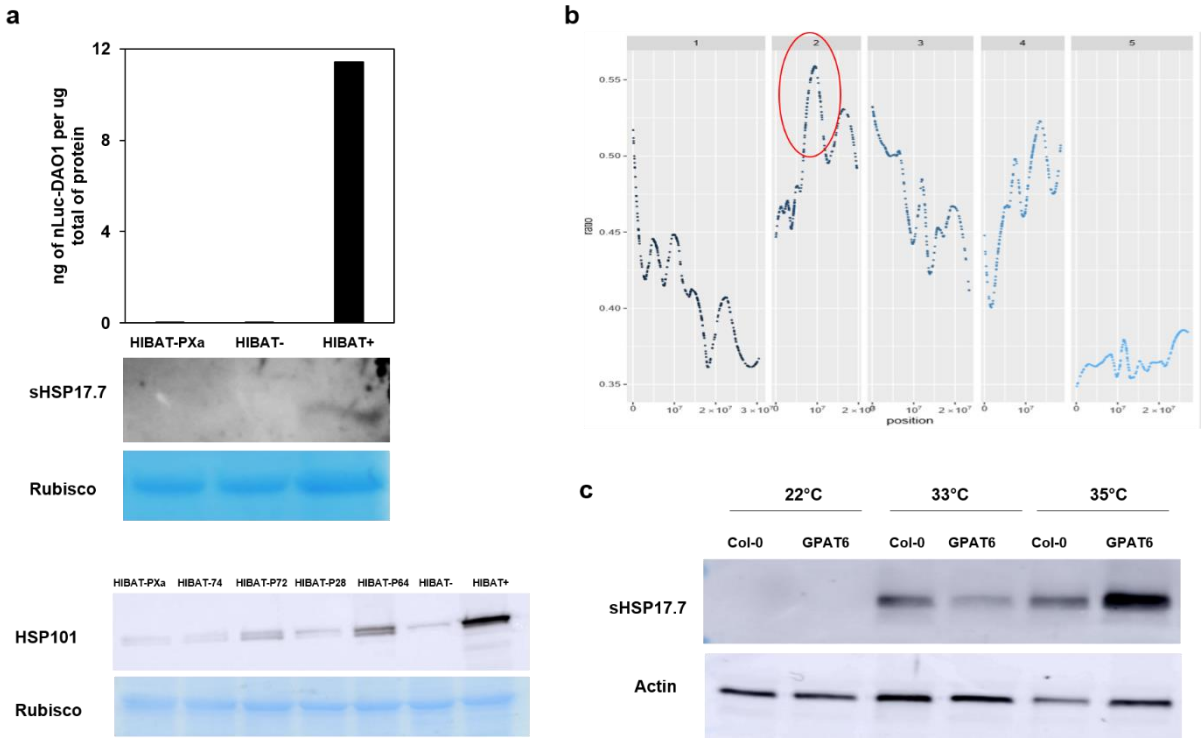

Figure 9: Accumulation of sHSP17.7 in the T-DNA insertion *GPAT6*. (**a**) 5 weeks old leaves from M3 HIBAT-PXa candidate was exposed at 35°C for 2 hours followed by 2 hours at 22°C of post-recovery. The progenitor HIBAT was used as a control in the absence of HS (HIBAT-) or with the same HS applied on M3 HIBAT-PXa mutant (HIBAT+). The Western blot below the graph represents the accumulation of sHSP17.7 observed in all HIBAT candidates and the reference line. The homogeneous loading for each protein sample is represented by the accumulation of the RUBISCO which is shown by Coomassie blue staining. Total protein-loaded = 15 ug. (**b**) Repartition of SNP cluster over chromosomes identified in the candidate HIBAT-PXa. The red circle represents the localization of a cluster where was identified the SNP in the gene WRKY56. X-axis, Chromosomal location; y-axis, ratio variable of SNP. (**c**) 5 weeks old leaves from the GPAT6 T-DNA line were exposed at 33°C or 35°C for 2 hours followed by 2 hours of post-recovery at 22°C.

Line Col-0 was used as a control without heat treatment (Col-0 -) or with the same HS applied in the GPAT6 T-DNA insertion line (Col-0 +). The Western blot represents the accumulation of sHSP17.7 observed in lines GPAT6 and Col-0. The homogeneous loading for each protein sample is represented by the ACTIN, detected with the associated antibody. Temperatures exposition and lines are represented on top of the membrane. Numbers represent individual biological replicate. Total protein-loaded per sample; a= 30 ug (Top), 23 ug (bottom) and c= 21 ug.

Analysis of HIBAT candidates at the M3 or M4 and F2 generation to follow a Mendelian type of segregation

Although additional T-DNA insertions remain to be analyzed and confirmed to be a true knock-out line, the high contamination observed in mutants sequenced led us to presume that offspring were not following a Mendelian type of segregation at each generation. One possibility is the loss of heat-sensitive phenotype was caused by the iterative heat treatments which triggered an epigenetic phenomenon. Thus, a large number of offsprings from HIBAT candidates sequenced were tested for following or not a Mendelian type of segregation at the M3 or M4 and F2 generations. Each individual offspring was analyzed for their ability to survive in the presence of D-valine under HS cycles. According to the Mendelian type of segregation, it was expected that 100% of offspring were homogenous for a loss of heat-responsive phenotype at the M3 and M4 generation and 25% at the F2 generation. Candidates M3-HIBAT-P13, M3-HIBAT-P81, and M3-HIBAT-P87 showed 100% of offspring resistant to D-valine under iterative HS. In contrast, other candidates presented different segregation such as M4-HIBAT-PXa (37%), M4-HIBAT-P42b (90.6%), and M4-HIBAT-P28 (0.8%). The mutant M3-HIBAT-P66 was not analyzed due to a lack of seed harvested (Table 4). Additionally, all offspring survivals were analyzed for their ability to express both nLUC-DAO1 and sHSP17.7 under HS. The expression level of nLUC-DAO1 and sHSP17.7 mutants were divided into three categories; a similar expression level (>75%), an intermediate expression level (25%-75%), and a low expression level (<25%) as compared to the parental line under HS. Unexpectedly, within the same generation from one HIBAT candidate line, different expression ratios were found. For example, 93,33% of M4-HIBAT-P42b offspring presented less than 25% of nLUC-DAO1 accumulation compared to the parental line under HS. Surprisingly, 66,66% of these same offspring accumulated more than 75% of sHSP17.7 and did not present the same expression level as nLUC-DAO1. Moreover, offspring that accumulated less than 25% of nLUC-DAO1 from M3-HIBAT-P13, M3-HIBAT-P81, and M3-HIBAT-P87 lines, showed different levels of sHPS17.7 expression (Table 5). Similar results were observed at the F2 generation for both nLUC-DAO1 and

sHSP17.7 accumulation in offspring of HIBAT mutants (Table 6). The candidate HIBAT-P42b is shown in Figure 10 and used as a detailed example for the ability of offspring to express both nLUC-DAO1 and sHPS17.7 at the M4 and F2 generation. Additionally, the transgene was sequenced for all HIBAT candidates at the M3 or M4 generation and did not reveal a mutation. Altogether, these results suggest that the transient phenotype resulted from a reversible epigenetic mechanism that could be established during the recurrent heat treatments. For example, the transgene and/or HSP genes, that are not located on the same chromosome, might be silenced by chemical modifications such as methylation or acetylation but it remained to be demonstrated.

EMS HIBAT candidates	Survival	No survival	Survivals segregation (%)
M3-HIBAT-P13 (n=135)	135	0	100
M3-HIBAT-P81 (n=137)	137	0	100
M4-HIBAT-PXa (n=127)	47	80	37
M4-HIBAT-P42b (n=138)	125	13	90.6
M3-HIBAT-P66	NA	NA	NA
M4-HIBAT-P28 (n=136)	11	126	0.8
M3-HIBAT-P87 (n=139)	139	0	100

Table 4: Segregation analysis on D-valine and under iterative heat treatments of sequenced HIBAT mutants at the M3 or M4 generation. n represents the total number of offspring tested on D-valine treatment and under HS cycles of each M3 and M4 HIBAT mutants. The segregation of survivals is represented in percentage.

EMS M3/M4 HIBAT candidates	nLUC-DAO1 intensity relative to HIBAT+			sHSP17.7 intensity relative to HIBAT+		
	<25%	**25%-75%**	**>75%**	**<25%**	**25%-75%**	**>75%**
M3-HIBAT-P13 (n=16)	16 (100%)	0 (0%)	0 (0%)	0 (0%)	7 (43,75%)	9 (56,25%)
M3-HIBAT-P81 (n=13)	13 (100%)	0 (0%)	0 (0%)	1 (7,69%)	0 (0%)	12 (92,30%)
M4-HIBAT-PXa (n=16)	2 (12,5%)	6 (37,5%)	8 (50%)	0 (0%)	0 (0%)	16 (100%)
M4-HIBAT-P42b (n=18)	15 (93,33%)	1 (5,55%)	0 (0%)	0 (0%)	6 (33,33%)	12 (66,66%)
M3-HIBAT-P66	NA	NA	NA	NA	NA	NA
M4-HIBAT-P28 (n=9)	2 (22,22%)	2 (22,22%)	5 (55,55%)	8 (88,88%)	1 (11,11%)	0 (0%)
M3-HIBAT-P87 (n=16)	16 (100%)	0 (0%)	0 (0%)	3 (18,75%)	6 (37,5%)	7 (43,75%)

Table 5: Analysis of the accumulation of nLUC-DAO1 and sHSP17.7 in HIBAT sequenced candidates at the M3 or M4 generation as compared to the parental line under HS. n represents the total number of offspring tested for the accumulation of nLUC-DAO1 and sHSP17.7 of each M3 or M4 HIBAT mutants. The accumulation of nLUC-DAO1 and sHSP17.7 in offspring were classified into 3 groups of intensity compared to HIBAT control under HS (HIBAT+), respectively, <25%, 25%-75%, or >75%. The segregation analysis for the line HIBAT-P66 was not applicable (NA).

EMS F2 HIBAT candidates	nLUC-DAO1 intensity relative to HIBAT+			sHSP17.7 intensity relative to HIBAT+		
	<25%	25%-75%	>75%	<25%	25%-75%	>75%
HIBAT-P13 (n=12)	11 (91,66%)	0 (0%)	1 (8,33%)	5 (41,66%)	2 (16,66%)	5 (41,66%)
HIBAT-P81 (n=14)	14 (100%)	0 (0%)	0 (0%)	5 (35,71%)	4 (28,57%)	5 (35,71%)
HIBAT-PXa (n=16)	2 (12,5%)	4 (25%)	10 (62,5%)	0 (0%)	0 (0%)	16 (100%)
HIBAT-P42b (n=15)	7 (46,66%)	4 (26,66%)	4 (26,66%)	1 (6,66%)	7 (46,66%)	7 (46,66%)
HIBAT-P66 (n=16)	12 (75%)	3 (18,75%)	1 (6,25%)	8 (50%)	4 (25%)	4 (25%)
HIBAT-P28 (n=11)	9 (81,81%)	2 (18,18%)	0 (0%)	0 (0%)	1 (9,09%)	11 (100%)
HIBAT-P87 (n=16)	14 (87,5%)	1 (6,25%)	1 (6,25%)	1 (6,25%)	9 (56,25%)	6 (37,5%)

Table 6: Analysis of the accumulation of nLUC-DAO1 and sHSP17.7 of HIBAT sequenced candidates at the F2 generation as compared to the parental line under HS. n represents the total number of offspring tested for the accumulation of nLUC-DAO1 and sHSP17.7 of each F2 HIBAT mutants. The accumulation of nLUC-DAO1 and sHSP17.7 in offspring were classified into 3 groups of intensity compared to HIBAT control under HS (HIBAT+), respectively, <25%, 25%-75%, or >75%.

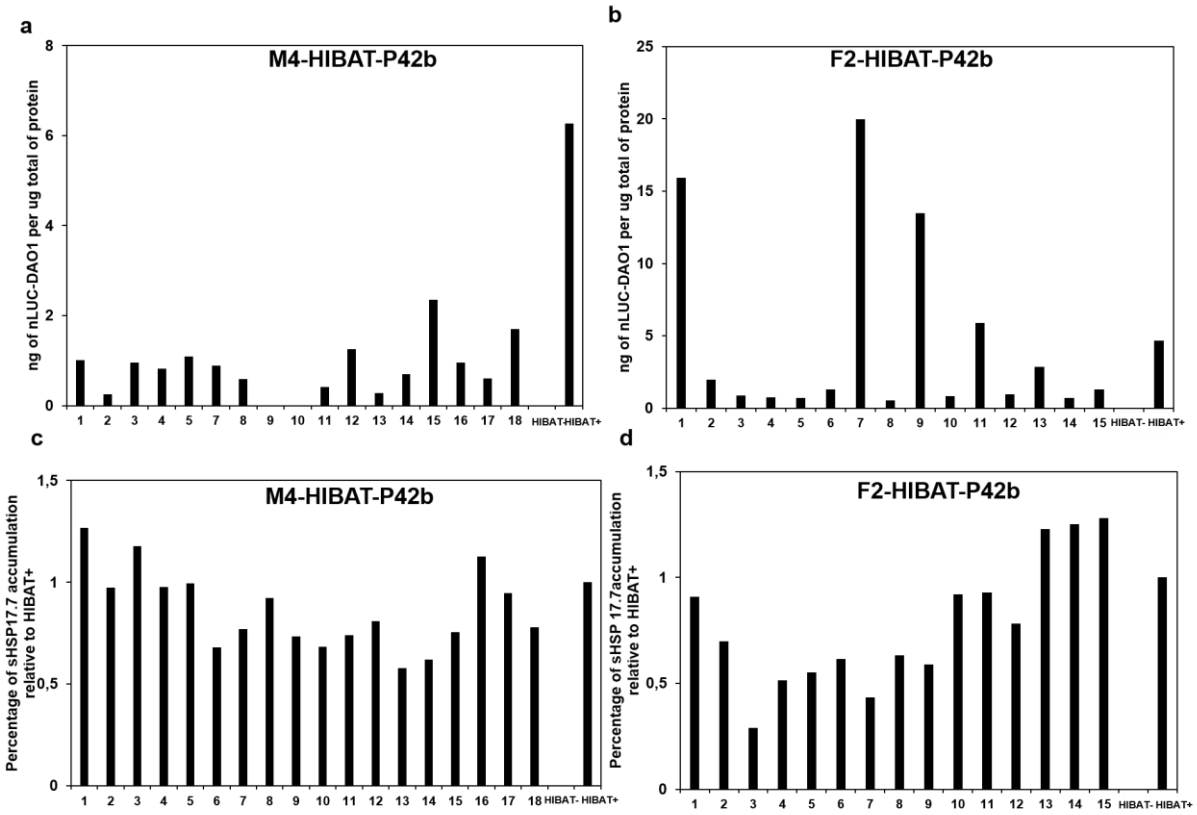

Figure 10: Analysis of the accumulation of nLUC-DAO1 and sHSP17.7 under HS of offspring from M4 and F2 in the HIBAT-P42b candidate. 5 to 8 weeks old leaves from offspring were exposed at 35°C for 2 hours followed by 2 hours of post-recovery at 22°C. The parental HIBAT was used as a control in the absence of HS (HIBAT-) or with the same HS applied on M3 HIBAT-P42b mutant (HIBAT+). (**a-b**) Accumulation of nLUC-DAO1 in offspring at the M4 (**a**) and F2 generation (**b**). (**c-d**) Accumulation of sHSP17.7 in offspring relative to HIBAT+ at the M4 (**c**) and F2 (**d**) generation. The expression of sHSP17.7 of offspring were normalized by the ACTIN level detected by western blot and by the expression level of sHSP17.7 from the parental line under HS, using the ImageJ software. Numbers represent one individual offspring from the HIBAT-P42b candidate.

The HIBAT mutants sequenced were submitted to an AT test at the M3 or M4 generation to validate or not a loss of heat sensing and signaling pathway. It was expected that mutants are unable to prime defenses caused by an absence of HSP expression and resulting in a defective AT. The parental line was used as a control and revealed to be sensitive when exposed to a noxious HS at 45°C for 1 hour, whereas a heat priming at 37°C and followed by the same noxious HS confer the AT in a large majority of plants (Fig. 11). In contrast, HIBAT-P81 and HIBAT-P87 lines were found to be defective in the onset of AT when subjected to a heat priming. These results suggest a loss of the capacity to sense HS and to establish suitable defenses. All other HIBAT mutants successfully established the AT after a heat priming such as HIBAT-PXa. One hypothesis is that mutants were transiently defective to respond to heat caused by HS cycles during their previous generation and the epigenetic phenomena might temporally repress the expression of HSPs. In the next generation and with the absence of iterative HS, mutants might have lost the epigenetic chemical modifications on HSP genes leading to their expression and ultimately to the AT.

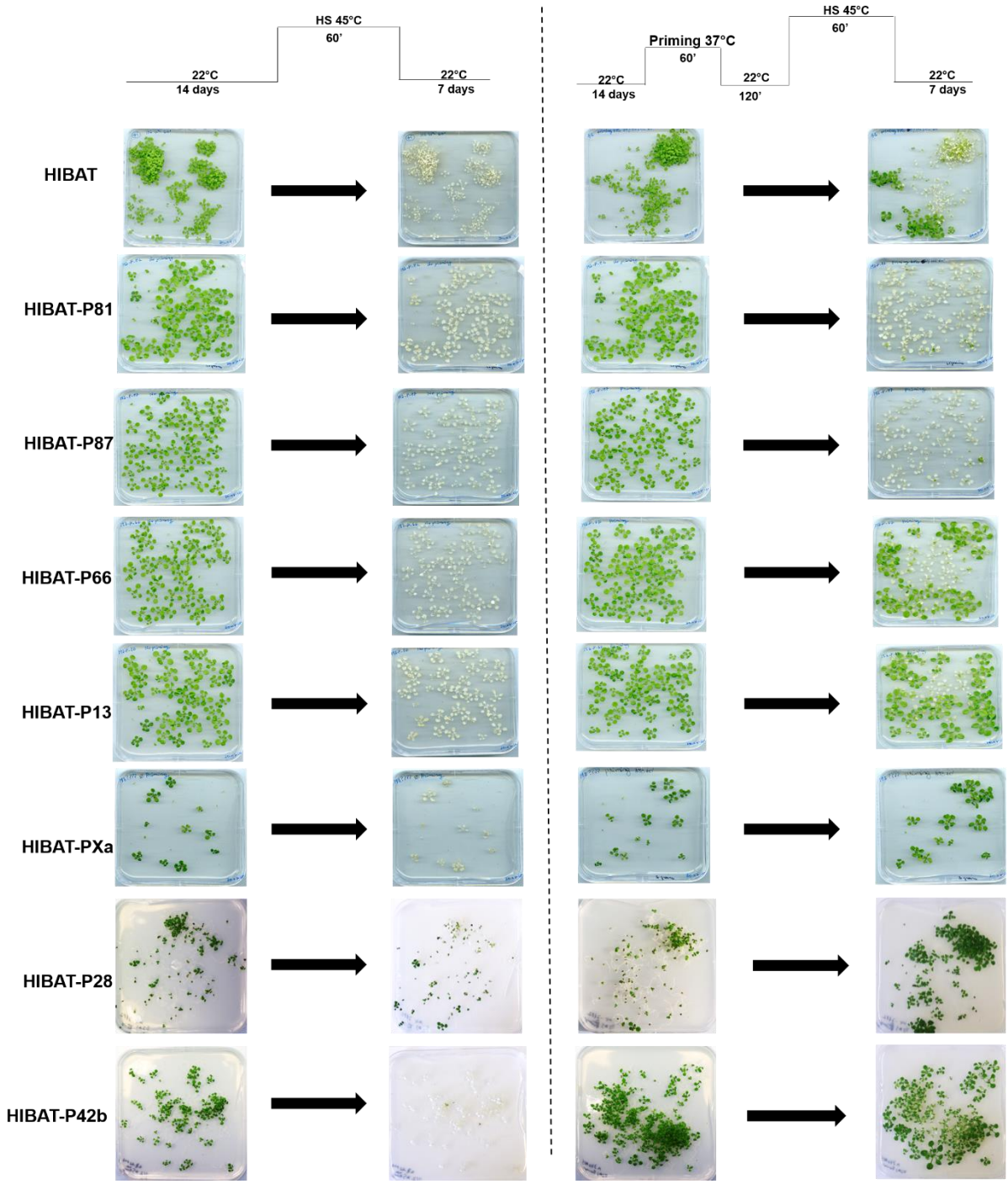

Figure 11: Acquired thermotolerance assay of HIBAT mutants at the M3 or M4 generation. Left; HS treatment without a heat priming, right; HS treatment with a heat priming. The parental line HIBAT was used as a positive control and pictures were imaged at 14 and 21 days old. The protocol applied is represented on top.

Discussion

Selection of candidates impaired in heat sensing and identification of causal genes through T-DNA insertion lines

The FGS was initiated by using the HIBAT line specifically generated to select mutants impaired in the heat sensing and signaling pathway in *A. thaliana*. Several candidates were isolated to be apparently defective to sense HS as they survived in the presence of D-valine and under iterative heat treatments (Fig. 1). The conditional toxic negative gene *DAO1* confirmed to be a good strategy to eliminate a large number of EMS HIBAT candidates responding to HS (18). Some mutants were confirmed to be defective to accumulate nLUC-DAO1 and concomitantly in sHSP17.7 expression which indicated that the phenotype did not result of a mutation in the transgene at the M2 and M3 generation (Figs. 2 and 3). Supporting these observations, candidates such as HIBAT-PXa were found to be defective in the accumulation of both HSP101 and sHSP17.7 under HS that suggested a possible mutation very upstream in the heat shock signaling pathway, close to the sensors. In contrast, other mutants such as HIBAT-P66 were able to accumulate HSP101 but unable to express sHSP17.7 which indicated a mutation at different levels of the heat shock signaling pathway (Figs. 4 and 5). M3 HIBAT candidates that presented ultimately a defective accumulation of HSPs were crossed with the HIBAT parental line. At the F2 generation, seven candidates were analyzed for following a Mendelian type of segregation for 25% offspring survivals in the presence of D-valine under HS (Table 1). Five candidates were not following such segregation by presenting less than 25% of survival that could be explained by the loss of mutation or by the presence of several genes affected in the heat sensing and signaling pathway. They were nevertheless chosen and subjected to the WGDS. Sequencing results revealed near significant SNPs in several genes among the four HIBAT mutants. The SNPs detection was focused mainly on exons and by the presence of a stop codon in promoters and introns genes (Table 2). Yet, none of T-DNA insertion line were defective to accumulate sHSP17.7 under HS and the identification of the causal genes remained nor elucidated (Table 3 and Figs. 7, 8, and 9)

Sequencing results also revealed that SNP repartitions over the genome were heterogenous for HIBAT mutants. Although some offspring survived in the presence of D-valine under HS cycles at the F2 generation, some of them may have lost temporally their ability to express both nLUC-DAO1 and/or sHSP17.7. It resulted in pooled of offspring that

some might be affected by a mutation in the gene(s) of the heat sensing and signaling pathway, whereas others might be chemically silenced in nLUC-DAO1 and/or sHSP17.7 genes caused by an epigenetic mechanisms which did not alter DNA sequences. This might explain the observation of heterogeneity of SNPs which was diluted in the mutants sequenced. Such an epigenetic mechanism might then occur, supposedly caused by HS cycles on mutants, and repressed the HSR which might be reversible and therefore lost in the following generations.

Analysis of HIBAT mutants sequenced for following a Mendelian type of segregation

To indicate for such an epigenetic phenomenon, the segregation of offspring for each HIBAT mutants sequenced were analyzed in their heat-responsive phenotype for following or not a Mendelian type of segregation at the M3 or M4 and F2 generation. Results showed that three HIBAT candidates resulted in 100% offspring survivability, whereas other mutants presented different ratios less than 100% (Table 4). Supporting these observations, all offspring HIBAT mutants showed different ratios which were less than 100% to accumulate nLUC-DAO1 and sHSP17.7 as compared to the parental line under HS. For example, the line HIBAT-P28 showed 22% of survivals emitting less than 25% of nLUC-DAO1, and 88% of the same offspring accumulated less than 25% of sHSP17.7 compared to the parental line under HS (Table 5). Similar results were found for all HIBAT candidates sequenced at the F2 generation (Table 6). These observations strongly indicated that among mutants sequenced, their offspring did not follow a Mendelian type of segregation. Additionally, it was expected that the number of offspring from the same HIBAT mutant would be defective in both nLUC-DAO1 and sHSP17.7 under HS if such an epigenetic mechanism occurred. This observation was not observed such as in the candidate M4-HIBAT-P28 and suggests that both genes were not affected obligatorily and homogenously by this mechanism (Tables 5 and 6). The transgene was sequenced in an attempt to reveal a mutation that could cause this abnormal segregation but did not show a mutation in the promoter or in the nLUC-DAO1 sequence for all HIBAT candidates. This result excludes the possibility of candidates to have survived or been defective to emit light caused by a mutation in the transgene. One hypothesis is that the abnormal segregation was associated with an epigenetic program caused by the iterative heat treatments leading to the nLUC-DAO1 and/or HSP gene(s) repression.

Conclusion

Although the FGS revealed several potential mutants impaired in the transduction of the heat signal, the identification of causal genes remains to be elucidated. Interestingly, the loss of heat-sensitive phenotype seems to be caused by an epigenetic mechanism. The silencing of nLUC-DAO1 and HSPs was not completely transfected from one generation to another expected in a Mendelian manner and could be caused by iterative heat treatments. Thus, the repression of both nLUC-DAO1 and HSP genes might be caused not due to a mutation in DNA but potentially by chemical modifications of the chromatin. It remains to elucidate how plants trigger the epigenetic program and which are the genes preferentially targeted leading to their transient and reversible repression. The identification of new partners of the heat shock signaling pathway might be reconsidered with a new FGS by using the HIBAT line. The selection of mutants could be based only on the defective expression of bioluminescence following a single HS and the iterative heat treatments which are necessary to induce DAO1 toxicity would be excluded. Thus, the isolated candidates would be then validated by a defective expression of HSPs, expecting to follow a Mendelian type of segregation, and submitted to the WGDS to identify new genes involved in the heat sensing and signaling pathway.

Materials and methods

EMS treatment

2.5 g of HIBAT dry seeds were soaked in a 50 mL plastic tube with 40 mL of 100 mM K2HPO4 buffer (pH 7.5) at 4°C overnight. New fresh 40 mL K_2HPO_4 buffer (pH 7.5) containing 0.4% of EMS (v/v) (Sigma-Aldrich, ref M0880) was replaced in the 50 mL plastic tube for 8 hours with gently shaking. Seeds were then washed thoroughly 20 times with water (40mL) per wash). After EMS mutagenized, M1 seeds were sowed in the soil to generate and harvest the M2 generation of HIBAT mutant lines in a greenhouse with long days conditions (16 hours of light, 8 hours of dark) at 22°C.

Selection of HIBAT mutant on D-valine and under iterative heat treatments

HIBAT and Col-0 *A. thaliana* plants were grown in the presence of 25 mM of D-valine in plates containing $^{1/2}$MS medium with 2.20 g/L of Murashige and Skoog media including MES buffer (Duchefa Biochimie, ref P14881.01), 8 8 g/L of agar (pH 5.8). Seeds were always incubated at 4°C for 2 days to break the dormancy. Plants were growing in a phytotron at 22°C for 3 days with long-day conditions (16 hours light, 8 hours dark). The phytotron program was set up to applied 2 HS at 38°C for 2 hours with an apart of 2 hours

at 22°C of post-recovery for a total of 5 days. The phytotron program was then set up at 22°C for 3 days more and survival plants were transferred to new D-valine fresh media. Plants were then submitted to a new round of heat treatments for 5 days, plates were imaged, and plant survivals were transferred to the soil at 15 days old for subsequent analysis. At the M3 and F2 generation, plants follow steps as described above and follow the protocol shown in Figure 3.

Protein extraction

5 to 8 weeks old leaves from plants were grinded by a plastic pestle in an Eppendorf tube of 1.5mL and resuspended with a BAP buffer (50 mM Tris-HCL (pH 7.5), 100 mM NaCl, 250 mM mannitol, 5 mM EDTA, 10% (v/v) glycerol, and protease inhibitor cocktail diluted at 1:300 (v/v) (Sigma-Aldrich, ref P9599). Protein extracts were centrifuged for 10 min at 12 000g and at 4°C. Supernatants (soluble proteins) were transferred in a new Eppendorf tube of 1.5mL and protein concentrations were determined by BRADFORD assay (Sigma-Aldrich, ref 23238). The bioluminescence (nLUC-DAO1) was detected by using the Nano-Glo Luciferase Assay System Kit from Promega (ref 1110) and the HIDEX plate reader (version 5067). The bioluminescence was analyzed for 1 second giving count per second. The bioluminescence emission was converted in ng of nLUC-DAO1 per ug total of protein through a standard calibration curve of nLUC shown in materials and method in chapter 1.

Heat shock treatment on plants before western blot analysis

5 to 8 weeks old leaves from HIBAT and T-DNA insertion lines were transferred in an Eppendorf tube of 1.5 mL containing 1 mL of Evian water (adapted from Macherel et al., 2013) and heated in a thermoblock at 22°C, 33°C or 35°C for 2 hours followed by 2 hours of post-recovery at 22°C. Proteins were then extracted following the same protocol in the section Materials and Methods “protein extraction and analysis” in order to analyze the amount of nLUC-DAO1 and used for the western blotting analysis to detect the accumulation of HSPs.

Western blot

Protein extract was homogenized in LBX buffer (Tris-HCL 0.5 M (pH 6.8), 20% glycerol (v/v), 20% SDS (w/v), 4% bromophenol blue (w/v), 5% 2-mercaptoethanol (v/v), and heated for 3 min at 90°C. Homogenates were loaded in Precast SDS PAGE gels 12% acrylamide (EXPEDON, ref Ab 119207). Electrophoresis was applied at 100 V for 15 min followed by 45 min at 130V (constant amperage) using the associated buffer of Precast

SDS PAGE gels diluted at 1:50 (v/v). Precast SDS PAGE gels were transferred to nitrocellulose blotting membrane 0.2 µM (GE Healthcare Life Sciences, ref 10600001) by wet transfer using TRT buffer (20% (v/v) absolute Ethanol, and 5% (v/v) of the buffer associated with Precast SDS PAGE gels) for 50 min at 80 volts (amperage constant). Coomassie blue staining was applied for 5 min using Instant Blue solution from Sigma-Aldrich (ref ISB1L).

Membranes were blocked by using TRM buffer (5% milk powder (v/v), 50 mM Tris-HCL (pH 8), 150 mM NaCl) for 1 hour at room temperature. Primaries antibody sHSP17.7 (Abcam, ref Ab80171, diluted 1:2000), HSP101 (Marq biosciences, ref SPC 305, diluted 1:2000), and ACTIN (Sigma Aldrich, ref A0480, diluted 1:2000) were added in TRM buffer and the solution covered membranes for 2 hours at room temperature with gentle agitation. Membranes were then washed 3 times for 10 min (gently agitation) with TRM buffer without milk and replace by 0.1% of Tween 20 (v/v). Secondary peroxidase-conjugated goat antibody against rabbit IgG (from Biorad, ref 170-5046) was diluted at 1:2000 (v/v) in TRM buffer and the solution covered membranes for 1 hour at room temperature with gentle agitation. Membranes were still washed 3 times. The revelation was done by using the kit Clarity Western ECL substrate (Biorad, ref 102031318 and 102031316) and the acquisition was performed by using ImageQuant LAS 500 automatic exposition.

Normalization of the accumulation of HSPs and nLUC-DAO1 in mutants with HIBAT+

Data obtained from nLUC-DAO1 and HSP accumulation in HIBAT mutants were normalized compared to the parental line HIBAT under HS. The background of nLUC-DAO1 and HSP expression from the mother line HIBAT without HS was removed for calculation. The normalization of HSP accumulation was done through the acquisition of images from ImageQuant LAS 500. Images showing the accumulation of HSPs were normalized in HIBAT candidates compared to the parental HIBAT under HS using the constitutive expression of actin or RUBISCO as a reference. Data were obtained using ImageJ software (version 1.53).

Extraction of genomic DNA from plants

Survival of offspring seedlings were crushed and grinded by a plastic pestle in an Eppendorf tube of 1.5mL. The Extracts were resuspended in 600 µl of STE-lysis buffer (100mM Tris-HCL (pH 7.5), 2% (w/v) SDS, and 10 mM of EDTA) and incubated at 65°C for 20 min minimum. Thereafter, DNA extractions were then cooled on ice (4°C) for 5 min

and 200 µl of NH_4Ac (10M) were added, mixed, and centrifuged at 12 000g for 10 min. 650 µl of the supernatants were transferred in a new tube and 650 µl of isopropanol (100%) was added, mixed, and incubated for 5 min at room temperature and then centrifuged for 10 min at 12 000g. Supernatants were removed and pellets were washed with 1 mL of cold ethanol at 70% and re-centrifuged for 10 min at 12 000g. This wash step was repeated 2 times. Ethanol was then removed, and tubes were let open until pellets became transparent and dry. DNA extracts were finally resuspended in 100 µl of EB buffer (10mM of Tris-HCL pH 8.0).

Whole DNA genome sequencing of HIBAT mutants

100 ng total of DNA from each HIBAT candidates and the mother line were sent to the Whole DNA genome sequencing at the Lausanne Genomic Technologies facility. The cDNA library used Nextera DNA Flex and the sequencing was applied with pairwise-ends, coverage of 100 by the Illumina new sequencing generation systems HISeq 4000 PE. Data generated from the sequencing were in Fastq files format. They were transformed in Bam files by removing potential PCR duplicate through Galaxy 2.0 website tool (https://galaxyproject.org). SNPs were then detected by using a pipeline and adapted from Wachsman et al., 2017. The ratios of read and the SNPs localization in the genome of HIBAT mutants were then obtained in Excel files. The function of genes where SNPs were identified was performed by using data from Salk institute genomic analysis laboratory (http://signal.salk.edu/cgi-bin/tdnaexpress).

Acquired thermotolerance assays

HIBAT mutants and the parental line were grown in $^{1/2}$MS medium for 14 days in continuous days conditions and plates were imaged. At 14 days old, plants were submitted to a heat priming at 37°C for 1 hour followed by 2 hours of post-recovery at 22°C and then exposed to a noxious heat shock at 45°C for 1 hour. In parallel, unprimed plants were only exposed to the same noxious HS. Plants were then grown for 7 days at 22°C and. Plates were imaged at 14 and 21 days old.

Analysis of the Mendelian segregation at the F2 generation in HIBAT mutants

At, the F2 generations, HIBAT mutants were segregated on D-valine treatment under HS cycles. At 21 days old, a Chi-squared test was applied based on a Mendelian type of segregation to respect 1:4 of survivors by using the R software (version 4.0.3).

T-DNA insertion lines ordered and genotyping

T-DNA insertion lines were obtained from NASC (http://arabidopsis.info/BasicForm). The Protein function reported were obtained from TAIR10 (https://www.arabidopsis.org). The GPAT6 mutant lines were kindly obtained from Christiane Nawrath group (University of Lausanne). The genotyping of the T-DNA insertion lines was done by following the protocol from Salk institute genomic analysis laboratory (http://signal.salk.edu). Primer used for BP salk lines: LBb1.3_Salk 5'-ATTTTGCCGATTTCGGAAC-3'. Sail lines: LB1_sail 5'-GCCTTTTCAGAAATGGATAAATAGCCTTGCTTCC-3'. GABI lines: GABI_LB 5'-GGGCTACACTGAATTGGTAGCTC-3'. WiscDsLoxHs lines: WiscDsLoxHs_LB 5'-AATAGCCTTTACTTGAGTTGGCGTAAAAG-3'.

TAIR ID	T-DNA Lines	LP primer	RP primer
AT1G74690	SALK_013815.54.75.x	ACTCAGCCTCGACTAAAAGCC	AAGTTGCAGAGACCAATACCG
AT1G75010	SALK_062123.33.90.x	ACCTCTTCTAGACGCTTTCGG	ATGGGTCTGACGAGTTCATTG
AT1G73980	SALKseq_079237.0	TTCTGCTCATGCTTTGATTTG	AGCAAGGGTGATTAATCTGGG
AT1G69160	SALKseq_071515.1	GAACTCGGTTGCTTGTGTCTC	TCGACAAACAGGTTTGGAATC
AT3G54200	SAIL_860_A02	GCTTCCAAGTTTCAATCAAAGG	AAGGTAGTGACGGAAAGAGCC
AT5G50780	GABI_249F08	TCAGGAAAGATTTCACGAATTG	ACCTGCAGAAACTTCCCAATC
AT5G50780	SALKseq_047719.1	CATGGAGACAGAAGCTTCTGC	TCTGTTACCACGCTGTTACCC
AT1G70370	SALKseq_071207.0	GACGTGTCCATGTGACAGATG	AACGGTCAATCATTCACAAGC
AT1G64000	SAILseq_737_D01.0	GCAACAACCAAACCATATTCG	TGACATGTACATGCATTTTTGG
AT4G30720	SALKseq_059716.0	CAGAAGGTTTGCTTCAAGCC	TTCCTAGATGAGGCTTTCCG
AT4G30140	SALK_014093.40.50.x	GTACTCAAGGTGCAGCTGGAG	TGAAGTAAACAAAACACGGGC
AT2G17780	SAIL 1292 E05	GGCATAGACGCTCTGAAACTG	TAACGAGAAAAGAAAGCGTGG
AT2G17230	SALKseq_11107.1	AAGCTTAGAGGTCGTCGGTTC	CTTCCTGAATCGTGAGACGAG
AT2G17780	SALK_129208.47.75.x	GGCATAGACGCTCTGAAACTG	TAACGAGAAAAGAAAGCGTGG
AT4G22070	WiscDsLoxHs116_04F	CTTCAGATGACACTTCGGCTC	ACTCCACTGAATGCTGTTTGG
AT2G20980	SAILseq_32_C11.1	CGAATAATAACATTGCTTTCTGATG	AGCTTTACCTAATGCGCAAGC
AT2G38110	SALK_146013	CAAAGTGCGATGTTAAGGACC	CACTTGAAAGGTTCCAACAAATC

Table 7: List of primers used for the genotyping of homozygous T-DNA insertion lines.

Contributions

The sowed of EMS M1 HIBAT seeds and plants harvesting was contributed by Dr. Anthony Guihur, Dr. Bruno Fauvet, Pr. Pierre Goloubinoff, Dr. Satyam Tiwari, the Ph.D. Mathieu Rebeaud, Evangeline Lhermenier, laboratory technicians John Perrin and Tatiana Fomekong. Acquired thermotolerance and the Western blot of M3 HIBAT candidates were contributed by the laboratory technician Tatiana Fomekong. The DNA sequencing analysis

of HIBAT candidates and the selection of T-DNA insertion lines were performed by Dr. Anthony Guihur.

References

1. Krysan PJ, Young JC, Sussman MR. T-DNA as an insertional mutagen in Arabidopsis. Plant Cell. 1999;11(12):2283–90.
2. Parinov S, Sevugan M, Ye D, Yang WC, Kumaran M, Sundaresan V. Analysis of flanking sequences from Dissociation insertion lines: A database for reverse genetics in Arabidopsis. Plant Cell. 1999;11(12):2263–70.
3. Miyoshi C, Kim SJ, Ezaki T, Ikkyu A, Hotta-Hirashima N, Kanno S, et al. Methodology and theoretical basis of forward genetic screening for sleep/wakefulness in mice. Proc Natl Acad Sci U S A. 2019;116(32):16062–7.
4. Martienssen RA. Functional genomics: Probing plant gene function and expression with transposons. Proc Natl Acad Sci U S A. 1998;95(5):2021–6.
5. Moresco EMY, Li X, Beutler B. Going forward with genetics: Recent technological advances and forward genetics in mice. Am J Pathol [Internet]. 2013;182(5):1462–73. Available from: http://dx.doi.org/10.1016/j.ajpath.2013.02.002
6. Fire A, Xu S, Montgomery MK, Kostas SA, Driver SE, Mello CC. 35888. Nature. 1998;391(February):806–11.
7. Kutscher LM, Shaham S. Forward and reverse mutagenesis in C. elegans. WormBook. 2014;(212):1–26.
8. Sega GA. A review of the genetic effects of ethyl methanesulfonate. Mutat Res Genet Toxicol. 1984;134(2–3):113–42.
9. Vignal A, Milan D, SanCristobal M, Eggen A. A review on SNPs and other types of molecular markers. Genet Sel Evol. 2008;40:241–64.
10. Page DR, Grossniklaus U. The art and design of genetic screens: Arabidopsis thaliana. Nat Rev Genet. 2002;3(2):124–36.
11. Stamatiou G, Vidaurre DP, Shim I, Tang X, Moeder W, Bonetta D, et al. Forward Genetic Screening for the Improved Production of Fermentable Sugars from Plant Biomass. PLoS One. 2013;8(1).
12. Zwiewka M, Friml J. Fluorescence imaging-based forward genetic screens to identify trafficking regulators in plants. Front Plant Sci. 2012;3(MAY):1–14.
13. Schreiber KJ, Austin RS, Gong Y, Zhang J, Fung P, Wang PW, et al. Forward chemical genetic screens in Arabidopsis identify genes that influence sensitivity to the phytotoxic compound sulfamethoxazole. BMC Plant Biol [Internet]. 2012;12(1):1. Available from: BMC Plant Biology
14. Hong SW, Vierling E. Hsp101 is necessary for heat tolerance but dispensable for development and germination in the absence of stress. Plant J. 2001;27(1):25–35.
15. Wu KL, Guo ZJ, Wang HH, Li J. The WRKY family of transcription factors in rice and arabidopsis and their origins. DNA Res. 2005;12(1):9–26.
16. Li S, Fu Q, Chen L, Huang W, Yu D. Arabidopsis thaliana WRKY25, WRKY26, and WRKY33 coordinate induction of plant thermotolerance. Planta. 2011;233(6):1237–52.

17. Li S, Zhou X, Chen L, Huang W, Yu D. Functional characterization of Arabidopsis thaliana WRKY39 in heat stress. Mol Cells. 2010;29(5):475–83.
18. Erikson O, Hertzberg M, Näsholm T. A conditional marker gene allowing both positive and negative selection in plants. Nat Biotechnol [Internet]. 2004;22(4):455–8. Available from: http://www.nature.com/doifinder/10.1038/nbt946
19. Macherel D, Abdelilah B, Pierart A, Baecker V, Avelange-Macherel M-H, Rolland A, et al. Simple system using natural mineral water for high-throughput phenotyping of Arabidopsis thaliana seedlings in liquid culture. Int J High Throughput Screen. 2013;1.
20. Wachsman G, Modliszewski JL, Valdes M, Benfey PN. A simple pipeline for mapping point mutations. Plant Physiol. 2017;174(3):1307–13.

Chapter 4: Investigation of a possible epigenetic program to reversibly repress the heat shock response in *A. thaliana*.

Abstract

The results from the FGS indicated a possible existence of an epigenetic mechanism that would be responsible for the loss of heat sensing and signaling phenotype in the HIBAT mutants. Epigenetic silencing might occur such as methylations on histones and DNA in response to the iterative HS. Additionally, such chemical modifications could have become lost or kept in the same or in the next generation. It would be relevant to demonstrate that plants have evolved mechanisms which can suppress transiently and reversibly the costly HSR under excessive recurrent HS. Here we address one possibility that epigenetic occurred by using a specific inhibitor of DNA methylation, zebularine. Without prior EMS treatment, 15 120 seeds of HIBAT were grown in the presence of D-valine and with or without zebularine for 31 days under iterative HS. A survival difference of 24-fold was found between both conditions. In particular, 312 seedlings were apparently able to survive in the presence of D-valine and without zebularine, whereas only 13 seedlings were isolated in the additional presence of the inhibitor. This result suggests that epigenetic methylation on the toxic nLUC-DAO1 reporter gene during the iterative HS was likely the reason for the resistance of the line HIBAT to D-valine. Survivals isolated from the condition without zebularine were then subjected to a single HS and more than 50% of the survivals had lost their initial phenotype and accumulated again both nLUC-DAO1 and sHSP17.7. Remarkably, 17% of survival were attenuated or defective in the expression of sHSP17.7. This observation would indicate that the epigenetic methylation does not target specifically the transgene located on chromosome 1 but also sHSP17.7 present on chromosome 5. Thus, the existence of an epigenetic program aiming at transiently silencing all parts of the plant HSR is highly considered. An RNA sequencing of the nLUC-DAO1 and sHSP17.7 on co-inhibited mutants and a methylome analysis would address and characterized the peculiarities of this possible HSR specific epigenetic program.

Introduction

Conrad Waddington was the first to observe an epigenetic landscape that represents the cellular process decision during cell development. He defined the epigenetic as “The branch of biology which studies the causal interactions between genes and their products which bring the phenotype into being” (1). The genetic evolution over the following years led to reconsider epigenetic as "The study of changes in gene function that are mitotically and/or meiotically heritable and that do not entail a change in DNA sequence" (2). Among epigenetic mechanisms, chemical DNA methylation can occur on the C5 position of the cytosine mediated by a family of DNA methyltransferases leading to the formation of 5-methylcytosine. Methylation markers can also be located in the CG, CHG, and CHH sequence context where H is A, C, or T nucleic acids (3,4). In plants, DNA methylation is mediated by the RNA-directed DNA methylation pathway where DNA methyltransferase can catalyze DNA methylation in all sequence contexts (5). A high global level of cytosine methylation was observed in *A. thaliana* when exposed in their previous generation to an HS as compared to unstressed plants. Supporting this observation, the same methylation profile was described in *Cork oak* that grew at 55°C and in *Brassica napus* when exposed at 45°C (6–8). These results suggest that DNA methylation plays a key role in gene expression under HS. Additionally, methylation can occur on histones which might wrap some HSP genes when *A. thaliana* plants were subjected at 37°C for 60 min followed by 90 min of post-recovery at 23°C and then to a high temperature at 44°C for 45 min. Heat-responsive loci such as sHSP18.2, sHSP21, and sHSP22 led to the accumulation of H3K4me2 and H3K4me3 that was retained at the recovery phase and further elevated upon two successive HS, leading to a better induction of responsive HSP loci in plants (9). This observation remains interesting in our case where several HSP genes wrapped by histones might be also targeted by methylation during the FGS. In unstressed plants, several genes were described to be repressed by methylation marks which can be alleviated to respond toward stresses. For example, the DNA fragment *ZmMI1* in maize was shown to be methylated under normal conditions and became demethylated during chilling. Supporting these observations, in tobacco cells, the methylated *NtGPDL* genomic loci was demethylated under salt and low-temperature stresses (10–12). These results suggest that the environmental response of plants mediates the methylation and demethylation at coding regions resulting in a chromatin alteration structure and leads to gene transcription or inhibition.

The FGS described the path to find several HIBAT mutants in a loss of HSP expression phenotype under HS. Isolated HIBAT candidates should follow a Mendelian type of segregation for a mutation in one recessive gene responsible for a loss of heat sensing and signaling pathway. It was expected to observe 100% of offspring unable to express nLUC-DAO1 and sHSP17.7 under HS at the M3 and the M4 generation and 25% at the F2 generation. Yet, HIBAT mutants did not follow such segregation and systematically fewer offspring were with the expected phenotype. For example, the candidate HIBAT-PXa showed 37% of offspring survivals in the presence of D-valine under HS cycles. Among them, 12,5% accumulated less than 25% of nLUC-DAO1, whereas 100% of them expressed the same level of sHSP17.7 as compared to the parental HIBAT line at the M4 generation. These observations suggest that the phenotype is not the result of a DNA mutation but from reversible modifications, such as environmentally elicited DNA methylations, RNAi, or transposable elements (TE). Here, this chapter focused on one possibility that the HSR in HIBAT mutants resulting from an epigenetic DNA methylation program. The zebularine was described to inhibit DNA methyltransferase activity (13). Thus, if methylation is important for the repression of the HSR, one prediction is that zebularine would reduce the frequency of false HS resistant phenotype in HIBAT plants.

Results

The effect of zebularine on HIBAT plants

To address the putative epigenetic DNA methylation mechanism, Col-0 and HIBAT lines were used as controls and showed to be able at surviving in presence of D-valine, zebularine, or both conditions without iterative HS (Supp data 1). These results also indicate that a concentration of 40 µM of zebularine and 25 mM of D-valine employed is not toxic for both lines at low temperatures. 15 120 HIBAT seeds were divided into three groups of 5 040 seeds and grew in the presence of D-valine and with (+) or without (-) zebularine under HS cycles such as similarly during the FGS (Fig. 1). Col-0 survived for all conditions, whereas a large majority of HIBAT plants did not survive when in presence of D-valine. At 22 days, survivals were transferred to new fresh media containing D-valine and +/- zebularine to ascertain that both compounds were not degraded or totally consumed by plants. Survivals were then subjected to new HS cycles. At 31 days old, additional plants were found to not survive, confirming the necessity to renew the media

and remaining survivals were transferred in soil. At 38 days old, the exact number of survivals was calculated (Fig. 2).

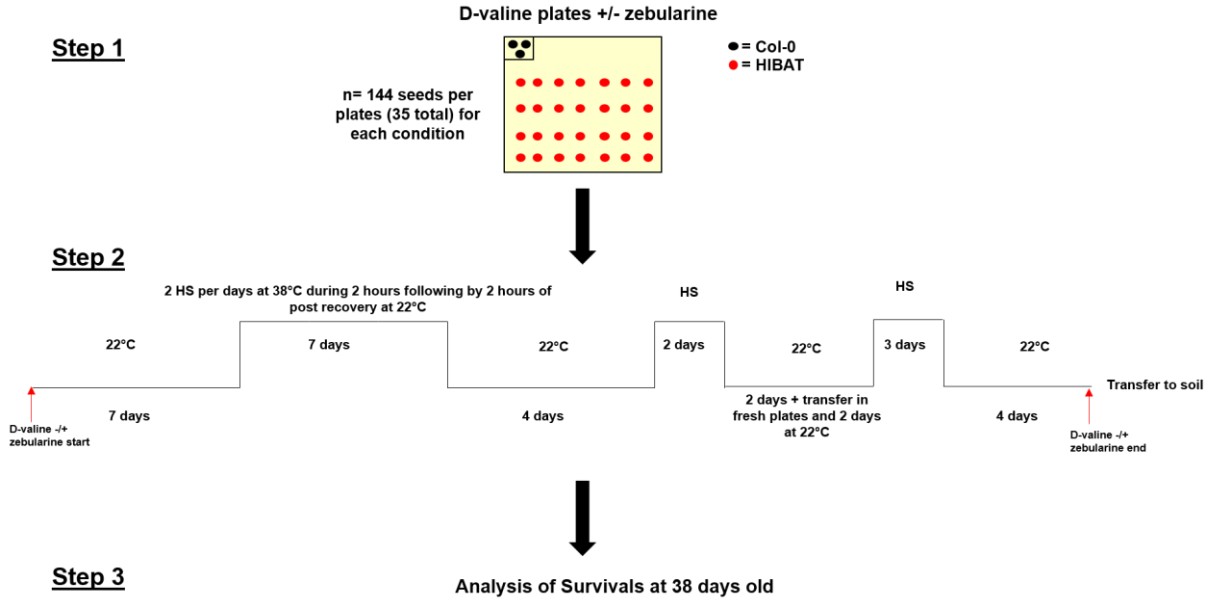

Figure 1: Overview of the survival selection from D-valine plates with or without of zebularine under iterative heat treatments. Step 1: 5 040 seeds (3 replicates) from the HIBAT line were sowed on D-valine plates with zebularine (+) or without (-) (n=3 replicates for each condition). Col-0 was used as control since its shown to resist for all conditions applied. **Step 2**: Plants, in the presence of D-valine and +/- zebularine, were subjected to the following protocol shown in the figure which included iterative heat treatments. At 22 days, survivals were transferred to a new fresh containing D-valine and +/- zebularine media and subjected to additional HS cycles. At 31 days, survivals were transferred in soil. **Step 3**: Survivals number was estimated from both conditions (-/+ zebularine) at 38 days old.

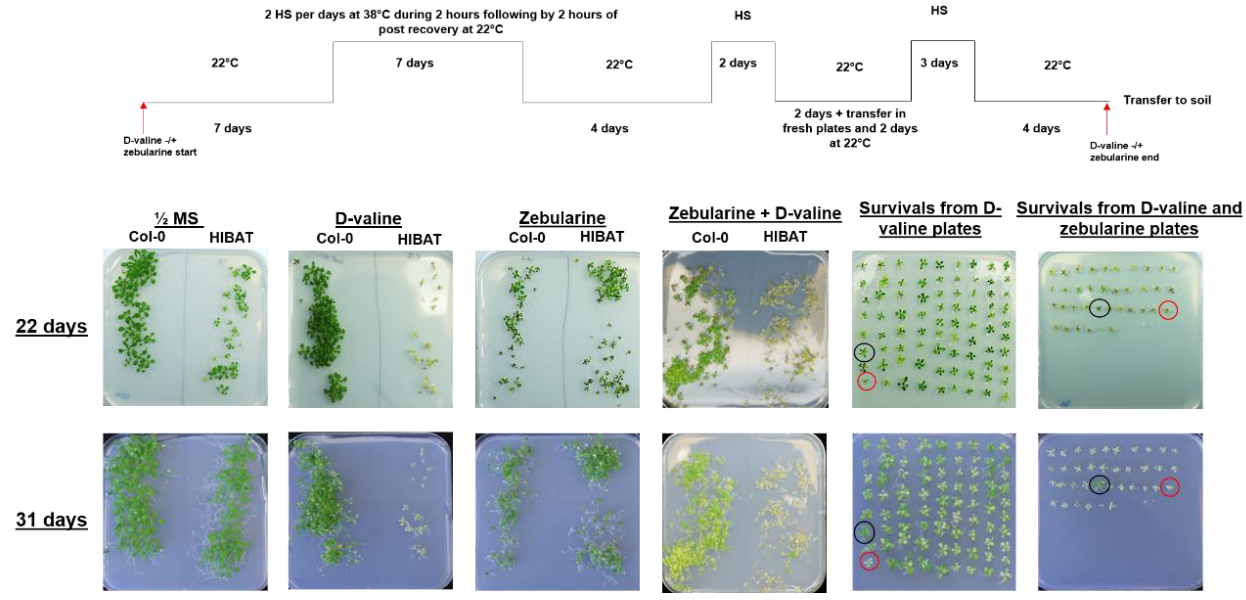

Figure 2: Selection of HIBAT survivals grew in the presence of D-valine, +/- zebularine and under iterative heat treatments. Plates ½ MS, D-valine, zebularine, or both compounds contained Col-0 and HIBAT lines. At 22 days, survivals of HIBAT plants from all conditions were selected and transferred to a

new fresh media containing the associated compounds, and pictures were imaged. At 31 days, controls plates and HIBAT survivals were imaged and transferred in soil. The black circle represents an example of a HIBAT plant survival, whereas the red circle shows a HIBAT plant which did not survive. Control plates without HS conditions are shown in supplementary data 1.

A concentration superior to 20 µM of zebularine was described to affect plant growth and development (13). Yet, 40 µM of zebularine was found to not affect the germination process as compared to untreated plants (Fig. 3a). The total number of survival from D-valine and +/- zebularine conditions was then calculated. Significantly, 2.12% of HIBAT plants survived in the absence of zebularine treatment as compared to 0.087% in the presence of zebularine, i.e. 24 times less (Table 1 and Fig. 3b). Because HIBAT plants were not treated with EMS as compared during the FGS, this result indicates that HS cycles were responsible for the inhibition of nLUC-DAO1. In contrast, the zebularine had apparently repressed the putative epigenetic methylation program which maintained the toxicity of nLUC-DAO1.

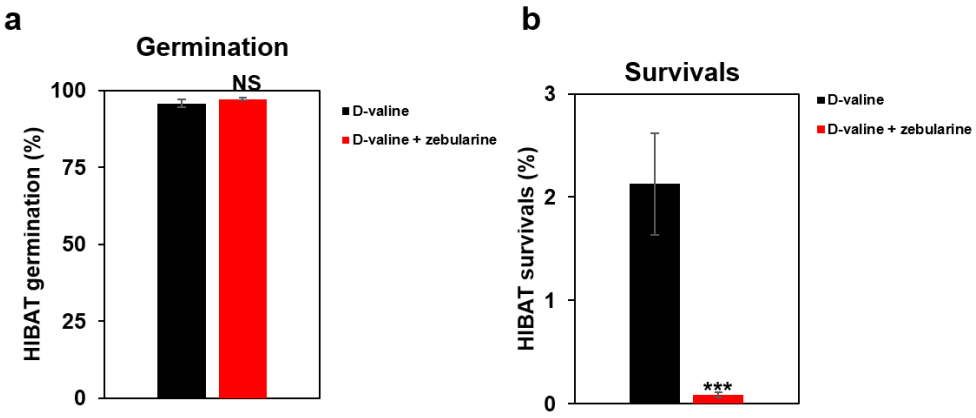

Figure 3: Germination of HIBAT seeds and survival in the presence of D-valine and +/- zebularine under HS cycles. (**a**) Percentage of seeds germination of HIBAT in the presence of D-valine and +/- zebularine. Between both conditions, the student T.test revealed no significant difference (NS) (*, P<0.05, NS, No Significant). (**b**) Percentage of HIBAT plants in the presence of D-valine and +/- zebularine at 38 days old (means ± S.D. (n = 3). A Chi-squared test was applied due to the large population observed and revealed a significant difference between both conditions (***<0.0005 p-value). Black bar : D-valine, red bar : D-valine + zebularine.

Conditions	Replicate 1	Replicate 2	Replicate 3	Mean replicates	Sd survival	Normalized mean replicates
Absence of zebularine	45/4663	79/4882	188/4945	104/4830	74,7	2,12%
Presence of zebularine	3/4867	2/4888	8/4963	4,3/4906	3,2	0,087%

Table 1: Numbers of HIBAT survivals observed in the presence of D-valine and +/- zebularine under HS cycles. In columns, the numbers of HIBAT survivals are represented on the total of dead plants in

presence of D-valine and with or without zebularine. The normalization was applied and convert in percentage to obtain the ratio of HIBAT survivals over the 3 replicates of both conditions.

Analysis of the accumulation of nLUC-DAO1 and sHSP17.7 of HIBAT survivals

6-8 weeks old leaves of HIBAT survivals were subjected to a single HS at 35°C in an attempt to analyze the accumulation of nLUC-DAO1 and sHSP17.7. An independent line HIBAT, that was not subjected to HS cycles and to D-valine -/+ zebularine, was used as a control. Expectedly, the reference showed an accumulation of nLUC-DAO1 and sHSP17.7 only under HS. Among the 79 HIBAT survivals found during the second replicate without zebularine, 52 of them were analyzed. The expression level of nLUC-DAO1 and sHSP17.7 HIBAT survival were divided into three categories; a similar expression level (>75%), an intermediate expression level (25%-75%), and a low expression level (<25%) as compared to control (HIBAT+) under HS. 51,9% of survival were able to express more than 75% of nLUC-DAO1, whereas 42,3% was observed for an intermediate defective expression and 5,7% did not accumulate nLUC-DAO1 compared to HIBAT+. Additionally, 82,7% were able to express more than 75% of sHSP17.7, 13,5% presented intermediate expression, and 3,84% a defective expression as compared to HIBAT+ (Table 2 and Fig. 4). These results indicate that a majority of plants have recovered their ability to sense HS and the nLUC-DAO1 and sHSP17.7 may temporarily be repressed during HS cycles and then alleviated. In contrast, plants defective in the expression of both genes could maintain epigenetic marks even after the end of HS cycles. The number of offspring that accumulated the same level of nLUC-DAO1 and sHSP17.7 was not identical. This would suggest that the DNA methylation mechanism on both genes is not obligatorily connected due to their localization on a different chromosome.

Conditions	nLUC-DAO1 intensity relative to HIBAT+			sHSP17.7 intensity relative to HIBAT+		
	<25%	25%-75%	>75%	<25%	25%-75%	>75%
D-valine (n=52)	3 (5,7%)	22 (42,3%)	27 (51,9%)	2 (3,84%)	7 (13,46%)	43 (82,69%)
Zebularine (n=2)	1 (50%)	1 (50%)	0	0	0	2 (100%)

Table 2: Analysis of the accumulation of nLUC-DAO1 and sHSP17.7 in HIBAT survival after a single heat shock. n represents the total number of survival tested for the accumulation of nLUC-DAO1 and sHSP17.7 from -/+ zebularine treatment. The accumulation of nLUC-DAO1 and sHSP17.7 in survival were classified into 3 groups of intensity compared to HIBAT control under HS (HIBAT+), respectively, <25%, 25%-75%, or >75%.

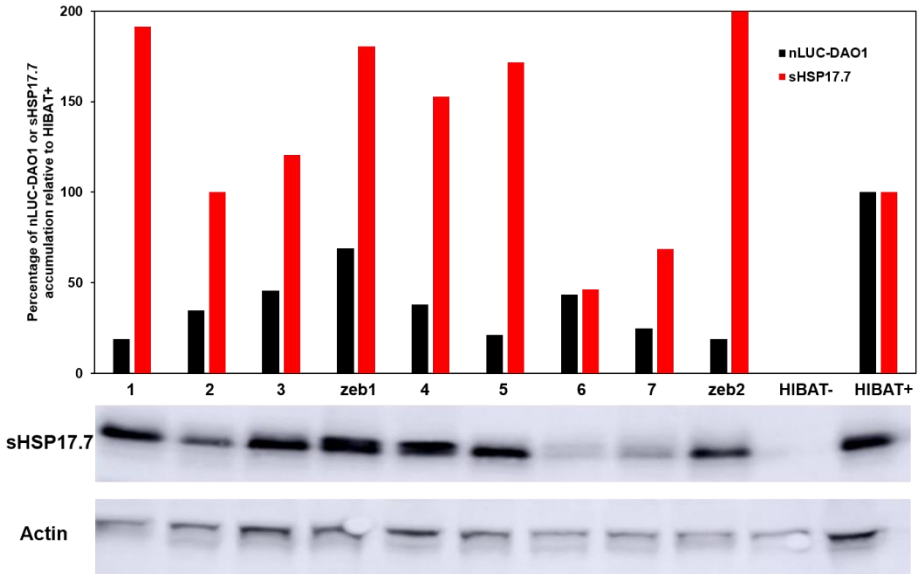

Figure 4: Example of the expression of nLUC-DAO1 and sHSP17.7 accumulation under an HS of HIBAT survivals after -/+ zebularine treatment. 6 to 8 weeks old leaves from survivals were exposed at 35°C for 2 hours followed by 2 hours of post-recovery at 22°C. The line HIBAT without prior treatment of -/+ zebularine was used as a control with HS (HIBAT-) and without HS (HIBAT+). The Western blot below of the graph represents the accumulation of sHSP17.7. The expression of sHSP17.7 in survivals were normalized by the level of ACTIN level detected by western blot and by the expression level of sHSP17.7 from the control under HS, using the ImageJ software. Total protein-loaded; 11 ug.

For the second replicate in the presence of D-valine and zebularine, only 2 HIBAT survivals were found to be resistant to HS cycles. They expressed significantly less nLUC-DAO1, whereas the level of sHSP17.7 was not reduced as compared to HIBAT+ under HS (Table 2 and Fig. 4). Because both survivals survived in the presence of zebularine treatment, this result might indicate that nLUC-DAO1 expression is repressed by a different mechanism rather than epigenetic methylation. In contrast, the expression sHSP17.7 was suggested to not be silenced.

Discussion

Interestingly, it was observed 24-fold less of HIBAT survivals in the presence of zebularine treatment and under HS cycles (Figs. 2, 3, and Table 1). This result indicates that transient methylation epigenetic mechanism was avoided by the presence of zebularine and HIBAT plants stand the toxicity of D-valine by being unable to accumulate nLUC-DAO1. As expected in the absence of zebularine and if an epigenetic DNA mechanism occurred, 51.9% of survivals accumulated nLUC-DAO1 and 82.7% of sHSP17.7 at the same level as the control under a single HS (Table 2). Firstly, this result

demonstrates that the link between these two genes is not tight and confirms the heterogeneity in the expression of both during the FGS in offspring HIBAT mutants that were sequenced. Secondly, the number of survivals that expresses nLUC-DAO1 under HS is not the same for sHSP17.7. This suggests that DNA methylations might occur preferentially on the toxic transgene rather than the sHSP17.7 gene. Thirdly, our results indicate that most survivals recovered the expression of both nLUC-DAO1 and sHSP17.7 under HS and might be repressed transiently during HS cycles and then alleviated 2 weeks later following the single HS.

Yet, less than 20% of HIBAT survival from the absence of zebularine treatment, were defective to accumulate both nLUC-DAO1 and sHPS17.7 under HS. It can be hypothesized that concurrent repression of the toxic reporter gene with other distally located HSP genes, lead plants to trigger an emergency program that can repress the HSR. It might result in the repression of HSP genes when their activation, if not toxic but at least excessive, can overburden plant cells with costly accumulated proteins. The possibility of such a general specific epigenetic program to repress the HSR is relevant and must be investigated. Thus, a methylome on survival plants from the absence of zebularine treatment and defective to express nLUC-DAO1 and sHSP17.7 under HS, might provide information on this mechanism and 3 different scenarios can be expected:

1) A majority of *A. thaliana* genes, including HSPs, were methylated. It would indicate that the methylation mechanism is not specific to heat-induced genes resulting in global epigenetic DNA methylation.

2) The DNA methylation pattern is specific to all HSR genes which would indicate that cells may preferentially silence heat-induced proteins.

3) Only a small fraction of HSP genes are methylated. For example, HSP20s are repressed as compared to HSP90 and HSP70, which would indicate that HSP20s are costly, if not deleterious for plants, and must be repressed transiently.

The methylome analysis would be completely new and inform of such epigenetic program which has evolved in plants to repress the HSR under recurrent HS conditions. In parallel, an RNA sequencing on the nLUC-DAO1 and sHSP17.7 co-inhibited survivals would address, if under HS, other genes that are likely up-regulated by heat become down-regulated. Both methylome and RNA sequencing analysis are complementary and would bring new knowledge in the plant field.

The study of the segregation of HIBAT plants, which have repressed nLUC-DAO1 and sHSP17.7 in the absence of zebularine treatment, in the next generations should be

investigated. It would indicate that epigenetic methylation marks can be transmitted and resulting from an adaptation of plants against recurrent heat exposures over one or several generations. For example, it was shown that epigenetic regulation of gene expression, induced by environmental exposure, can persist in the next sexual generation in stressed animals and plants (14–16). The transgenerational memory was described as epigenetic inheritance and refers to the transmittance of epigenetic states. Thus, a part of offspring can benefit of adaptive advantages or genomic flexibility for better fitness. Supporting this observation, it was demonstrated that HS, flagellin, or UV-C exposure exhibited transgenerational epigenetic inheritance in plants and resulted in better fitness advantages (14,17,18). In *A. thaliana*, changes in DNA methylation at the certain site of a silenced target gene were responsible for the transgenerational memory such as CG methylation playing a central role in epigenome stability (19). Additionally, transgenerational memory of heat responses was also suggested to potentially allow long-term adaptation and rapid evolution because chromatin modifications can be mitotically or meiotically heritable. In *A. thaliana*, HS induces transgenerational phenotypic changes over three generations resulting in early flowering. However, heritable effects disappeared after two generations without HS treatment (20). Yet, this study lacks a methylome analysis, and methylation marks have not been described to be stable up to 2 following generations in plants.

Results also showed that two HIBAT plants survived in the presence of zebularine treatment. Both were able to accumulate sHSP17.7, whereas nLUC-DAO1 was significantly repressed under HS (Table. 2 and Fig. 4). Because zebularine were supposed to avoid methylation marks, this observation indicates that the defective expression of nLUC-DAO1 would be caused by another epigenetic mechanism. Indeed, epigenetic also includes histone modification, RNA interference, and prions that are employed by organisms to survive to adverse conditions leading to turn "on" or "off" gene expression without altering the DNA sequence (21,22). Histones are made of globular proteins whose N-terminal tails are exposed on the surface of nucleosome for chemical modification such as acetylation, methylation, sumoylation, ubiquitination, and phosphorylation (23). In plants, RNA interference pathways were shown to be mediated by miRNA and siRNA. While prions were not considered as traditional epigenetic mechanisms but were rethink where the definition means “all mechanisms for the inheritance of biological traits that do not involve alterations to the DNA sequence” (24–26). Another possibility which would explain the survivability of these 2 HIBAT plants might be caused by TE, which are mobile

units of DNA, and might be inserted in the nLUC-DAO1. TE are known to comprise large genomic portions playing key roles in chromosome architecture and gene regulation in *A. thaliana* (27). For example, under HS, the retrotransposon ONSEN showed to generate a mutation in the abscisic acid (ABA) responsive gene. It resulted in an ABA-insensitive phenotype leading to stress tolerance (28). Altogether, these observations suggest that other mechanisms might occurred and silenced nLUC-DAO1 and sHSP17.7 during the FGS and in these two HIBAT survivals in the presence of zebularine. Additionally, it is also relevant to consider that DAO1 reaction in presence of D-valine release H_2O_2. As mention in chapter 1, ROS cause irreversible damage to proteins DNA, and lipids (29,30). The combination of HS cycles and DAO1 expression may lead to a transient repression of the transgene and/or HSPs in order to avoid ROS accumulation before reaching an irreversible threshold leading to cell death. Yet, ROS accumulation was not demonstrated and remains to be elucidated.

Conclusion

The FGS did not lead to identified new genes involved in the heat sensing and signaling pathway. Our results strongly suggested epigenetic methylation phenomena not caused by a single but several HS cycles. It is relevant to consider that plants can have the ability, during extreme conditions, to establish an emergency epigenetic program to avoid the expression preferentially of HSP genes in a general and reversible way. A methylome and an RNA sequencing analysis on co-inhibited nLUC-DAO1 and sHSP17.7 survivals would confirm such an epigenetic program.

Materials and Methods

Heat treatment applied on HIBAT line in the presence of D-valine and -/+ zebularine

HIBAT lines were grown in the presence of 25 mM of D-valine and/or 40 µM of zebularine (StressMarq biosciences, ref SIH-560) and containing ½MS medium with 2.20 g/L of Murashige and Skoog media including MES buffer (Duchefa Biochimie, ref P14881.01), 8 8 g/L of agar (pH 5.8). Seeds were incubated at 4°C for 2 days to break dormancy. Plants were growing in a phytotron at 22°C for 7 days with long-day conditions (22°C in a 16/8 hours light/dark cycle). The phytotron program was set up to applied 2 HS per day at 38°C for 2 hours with an apart of 2 hours at 22°C of post-recovery for a total of 7 days. The phytotron program was set up at 22°C for supplemental 4 days and plants were then submitted 2 days of HS cycles. The phytotron program was then set up at 22°C for 4 days and survivals were transferred on new fresh ½MS medium containing 25 mM D-

valine, 40 µM zebularine, or both. Plates were imaged at 22 days old. Plants were then submitted for 4 days of heat treatment cycles followed by 4 days at 22°C. Plates were imaged at 31 days old and survivals were transferred to soil in long-day conditions. The survival rate was calculated 38 days old. The same protocol was applied for control plates but without heat treatments (Supp data 1).

Protein extraction

5 to 8 weeks old leaves from plants were grinded by a plastic pestle in an Eppendorf tube of 1.5mL and resuspended with a BAP buffer (50 mM Tris-HCL (pH 7.5), 100 mM NaCl, 250 mM mannitol, 5 mM EDTA, 10% (v/v) glycerol, and protease inhibitor cocktail diluted at 1:300 (v/v) (Sigma-Aldrich, ref P9599). Protein extracts were centrifuged for 10 min at 12 000g and at 4°C. Supernatants (soluble proteins) were transferred in a new Eppendorf tube of 1.5mL and protein concentrations were determined by BRADFORD assay (Sigma-Aldrich, ref 23238). The bioluminescence (nLUC-DAO1) was detected by using the Nano-Glo Luciferase Assay System Kit from Promega (ref 1110) and the HIDEX plate reader (version 5067). The bioluminescence was analyzed for 1 second giving count per second. The bioluminescence emission was converted in ng of nLUC-DAO1 per ug total of protein through a standard calibration curve of nLUC as shown in Chapter 2.

Heat shock treatment on plants before Western blot

5 to 8 weeks old leaves from survival and HIBAT control lines transferred in an Eppendorf tube of 1.5 mL containing 1 mL of Evian water (adapted from Macherel et al., 2013) and heated in a thermoblock at 22°C or 35°C for 2 hours followed by 2 hours of post-recovery at 22°C. Proteins were then extracted following the same protocol in the section Materials and Methods “protein extraction and analysis” in order to analyze the amount of nLUC-DAO1 and used for the western blot to detect the accumulation of HSPs.

Western blot

Protein extract was homogenized in LBX buffer (Tris-HCL 0.5 M (pH 6.8), 20% glycerol (v/v), 20% SDS (w/v), 4% bromophenol blue (w/v), 5% 2-mercaptoethanol (v/v), and heated for 3 min at 90°C. Homogenates were loaded in Precast SDS PAGE gels 12% acrylamide (EXPEDON, ref Ab 119207). Electrophoresis was applied at 100 V for 15 min followed by 45 min at 130V (constant amperage) using the associated buffer of Precast SDS PAGE gels diluted at 1:50 (v/v). Precast SDS PAGE gels were transferred to nitrocellulose blotting membrane 0.2 µM (GE Healthcare Life Sciences, ref 10600001) by

wet transfer using TRT buffer (20% (v/v) absolute Ethanol, and 5% (v/v) of the buffer associated with Precast SDS PAGE gels) for 50 min at 80 volts (amperage constant).

Membranes were blocked by using TRM buffer (5% milk powder (v/v), 50 mM Tris-HCL (pH 8), 150 mM NaCl) for 1 hour at room temperature. Primaries antibody sHSP17.7 (Abcam, ref Ab80171, diluted 1:2000), and ACTIN (Sigma Aldrich, ref A0480, diluted 1:2000) were added in TRM buffer and the solution covered membranes for 2 hours at room temperature with gentle agitation. Membranes were then washed 3 times for 10 min (gently agitation) with TRM buffer without milk and replace by 0.1% (v/v) Tween 20. Secondary peroxidase-conjugated goat antibody against rabbit IgG (from Biorad, ref 170-5046) was diluted at 1:2000 (v/v) in TRM buffer and the solution covered membranes for 1 hour at room temperature with gentle agitation. Membranes were still washed 3 times. The revelation was done by using the kit Clarity Western ECL substrate (Biorad, ref 102031318 and 102031316) and the acquisition was performed by using ImageQuant LAS 500 automatic exposition.

Normalization of the accumulation of HSPs and nLUC-DAO1 compared to HIBAT+

Data obtained from nLUC-DAO1 and HSP accumulation in HIBAT mutants were normalized compared to HIBAT control under HS. The background of nLUC-DAO1 and sHSP17.7 expression from the mother line HIBAT without HS was removed for calculation. The normalization of HSP accumulation was done through the acquisition of images from ImageQuant LAS 500. Images showing the accumulation of HSPs were normalized in HIBAT candidates compared to the HIBAT control under HS using the constitutive expression of actin as a reference. Data were obtained using ImageJ software (version 1.53).

Statistical analysis

The determination of statically differences between samples were evaluated by Chi-squared or student T.test using the R software (version 4.0.3).

Contributions

The preparation of plates media that contained finally 30 240 seeds over the 3 replicates were contributed by Dr. Anthony Guihur, Dr. Bruno Fauvet, Dr. Satyam Tiwari, the Ph.D. student Mathieu Rebeaud, laboratory technicians John Perrin and the apprentice Gizem Demirkiran.

References

1. Mayer W V. Towards A Theoretical Biology C. H. Waddington. Am Biol Teach. 1969;31(8):537–8.
2. Wu CT, Morris JR. Genes, genetics, and epigenetics: A correspondence. Science (80-). 2001;293(5532):1103–5.
3. Moore LD, Le T, Fan G. DNA methylation and its basic function. Neuropsychopharmacology [Internet]. 2013;38(1):23–38. Available from: http://dx.doi.org/10.1038/npp.2012.112
4. Kim M, Costello J. DNA methylation: An epigenetic mark of cellular memory. Exp Mol Med. 2017;49(4).
5. Gallego-Bartolomé J. DNA methylation in plants: mechanisms and tools for targeted manipulation. New Phytol. 2020;
6. Gao G, Li J, Li H, Li F, Xu K, Yan G, et al. Comparison of the heat stress induced variations in DNA methylation between heat-tolerant and heat-sensitive rapeseed seedlings. Breed Sci. 2014;64(2):125–33.
7. Correia B, Valledor L, Meijón M, Rodriguez JL, Dias MC, Santos C, et al. Is the Interplay between Epigenetic Markers Related to the Acclimation of Cork Oak Plants to High Temperatures? PLoS One. 2013;8(1).
8. Boyko A, Blevins T, Yao Y, Golubov A, Bilichak A, Ilnytskyy Y, et al. Transgenerational adaptation of Arabidopsis to stress requires DNA methylation and the function of dicer-like proteins. PLoS One. 2010;5(3).
9. Lämke J, Brzezinka K, Altmann S, Bäurle I. A hit-and-run heat shock factor governs sustained histone methylation and transcriptional stress memory. EMBO J. 2016;35(2):162–75.
10. Choi CS, Sano H. Abiotic-stress induces demethylation and transcriptional activation of a gene encoding a glycerophosphodiesterase-like protein in tobacco plants. Mol Genet Genomics. 2007;277(5):589–600.
11. Popova O V., Dinh HQ, Aufsatz W, Jonak C. The RdDM pathway is required for basal heat tolerance in arabidopsis. Mol Plant [Internet]. 2013;6(2):396–410. Available from: http://dx.doi.org/10.1093/mp/sst023
12. Steward N, Ito M, Yamaguchi Y, Koizumi N, Sano H. Periodic DNA methylation in maize nucleosomes and demethylation by environmental stress. J Biol Chem. 2002;277(40):37741–6.
13. Baubec T, Pecinka A, Rozhon W, Scheid OM. Effective , homogeneous and transient interference with cytosine methylation in plant genomic DNA by zebularine. 2009;542–54.
14. Molinier J, Ries G, Zipfel C, Hohn B. Transgeneration memory of stress in plants. Nature. 2006;442(7106):1046–9.
15. Koturbash I, Baker M, Loree J, Kutanzi K, Hudson D, Pogribny I, et al. Epigenetic dysregulation underlies radiation-induced transgenerational genome instability in vivo. Int J Radiat Oncol Biol Phys. 2006;66(2):327–30.
16. Williams BP, Gehring M. Stable transgenerational epigenetic inheritance requires a DNA methylation-sensing circuit. Nat Commun [Internet]. 2017;8(1). Available from: http://dx.doi.org/10.1038/s41467-017-02219-3
17. Zhonga SH, Liu JZ, Jin H, Lin L, Li Q, Chen Y, et al. Warm temperatures induce transgenerational

epigenetic release of RNA silencing by inhibiting siRNA biogenesis in Arabidopsis. Proc Natl Acad Sci U S A. 2013;110(22):9171–6.

18. Lang-Mladek C, Popova O, Kiok K, Berlinger M, Rakic B, Aufsatz W, et al. Transgenerational inheritance and resetting of stress-induced loss of epigenetic gene silencing in arabidopsis. Mol Plant. 2010;3(3):594–602.
19. Mathieu O, Reinders J, Čaikovski M, Smathajitt C, Paszkowski J. Transgenerational Stability of the Arabidopsis Epigenome Is Coordinated by CG Methylation. Cell. 2007;130(5):851–62.
20. Suter L, Widmer A. Environmental Heat and Salt Stress Induce Transgenerational Phenotypic Changes in Arabidopsis thaliana. PLoS One. 2013;8(4).
21. Perspectives EH. EPIGENETIC S. 2006;114(3):160–7.
22. Halfmann R, Lindquist S. No Title. 2014;629(2010).
23. Kouzarides T. Review Chromatin Modifications and Their Function. 2007;693–705.
24. Holoch D, Moazed D. RNA-mediated epigenetic regulation of gene expression. Nat Publ Gr [Internet]. 2015;16(2):71–84. Available from: http://dx.doi.org/10.1038/nrg3863
25. Xie M, Yu B. siRNA-directed DNA Methylation in Plants. 2015;(Pol V):23–31.
26. Special section. 2010;330(October):629–33.
27. Sigman MJ, Slotkin RK. The first rule of plant transposable element silencing: Location, location, location. Plant Cell. 2015;28(2):304–13.
28. Ito H, Kim JM, Matsunaga W, Saze H, Matsui A, Endo TA, et al. A Stress-Activated Transposon in Arabidopsis Induces Transgenerational Abscisic Acid Insensitivity. Sci Rep. 2016;6(March):1–12.
29. Fedyaeva A V., Stepanov A V., Lyubushkina I V., Pobezhimova TP, Rikhvanov EG. Heat shock induces production of reactive oxygen species and increases inner mitochondrial membrane potential in winter wheat cells. Biochem. 2014;79(11):1202–10.
30. Apel K, Hirt H. REACTIVE OXYGEN SPECIES: Metabolism, Oxidative Stress, and Signal Transduction. Annu Rev Plant Biol. 2004;55(1):373–99.
31. Macherel D, Abdelilah B, Pierart A, Baecker V, Avelange-Macherel M-H, Rolland A, et al. Simple system using natural mineral water for high-throughput phenotyping of Arabidopsis thaliana seedlings in liquid culture. Int J High Throughput Screen. 2013;1.

Supplementary data

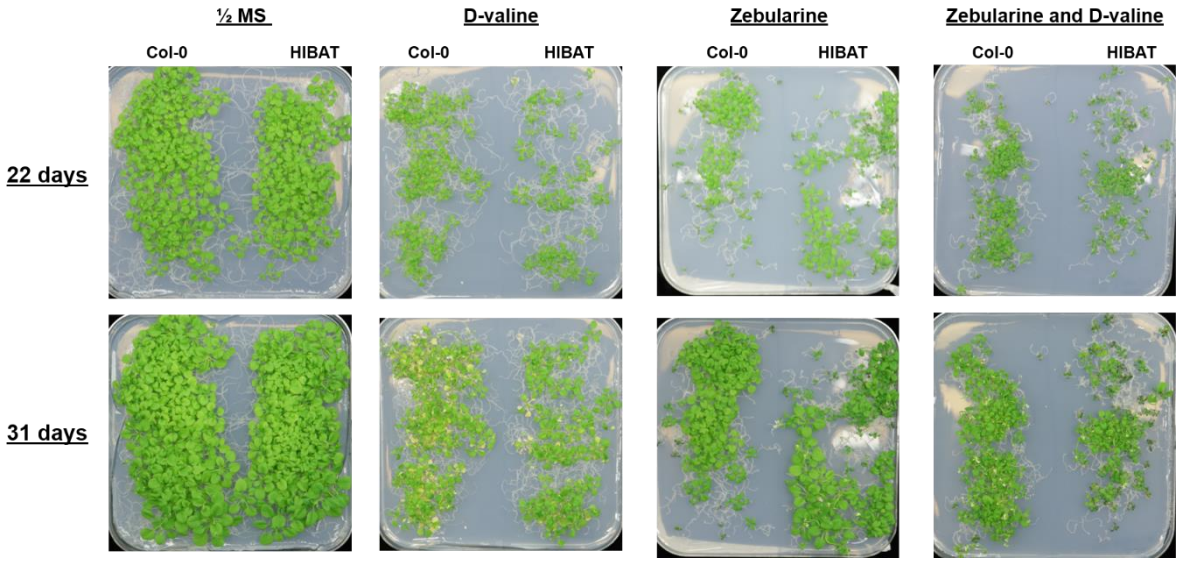

Supplementary data 1: Control of HIBAT and Col-0 lines in the presence of D-valine and -/+ zebularine at 22°C. Plates contained both Col-0 (right) and HIBAT (left) lines that grew in the absence (½ MS) or in the presence of D-valine and -/+zebularine for 31 days at 22°C. This temperature condition served as control compared to the iterative heat treatments applied in figure 2 in an attempt to show that compound concentrations used were not toxic for both Col-0 and HIBAT lines.

Chapter 5: A forward genetic screen in *A. thaliana* to search for repressors of the heat shock response at low temperatures.

Abstract

H2.AZ has been shown to repress the transcription of HSP70 at non-HS temperatures in *A. thaliana* (1). Yet, all repressors of HSP genes at basal temperatures remain unclear in plants. Here, the HIBAT line was used as a progenitor for an FGS. In contrast with the first approach described in chapter 3 in which we aimed to isolate loss of heat shock signaling activation under HS, the second FGS aimed to isolate loss of heat shock signaling repression at 22°C. The general pool used during the first FGS, which contained 3 871 individual EMS M2 plants, were grown without D-valine and screened for increased bioluminescence at 22°C. One viable mutant, called light 5 (L5), expressed higher levels of nLUC-DAO1, sHSP17.7, and HSP101 compared to the HIBAT parental line at 22°C and 31°C, whereas their level revealed to be the same at 35°C. At the M3 generation, 9 offspring from the L5 line followed a Mendelian type of segregation by expressing significantly more nLUC-DAO1 and sHSP17.7 compared to the HIBAT progenitor at 31°C. Offspring were pooled and submitted to the WGDS in an attempt to identify SNPs responsible for the dis-inhibited HSR phenotype at 22°C and 31°C. 232 SNPs were found and among them, 16 causing stop codons in exons. The corresponding T-DNA insertion lines were ordered and remain to identify whose have the same deregulated HSP expression at 31°C as in the mutant L5. Because a large number of SNPs were observed, the M3 L5 mutant was crossed with the parental HIBAT line. Future research would evolve the sequencing of offspring with the same phenotype in the background that was diluted by the crossing.

Introduction

The induction of the HSR results from two complementary mechanisms. The first is the eviction of histones and the second is HSFA1 bound HSE which recruits the RNA polymerase II for the transcription of HSP genes. A mutation in the *ARP6* gene, which is involved in the chromatin remodeling complex of H2A.Z, has been shown to be causing overexpression of HSP70 at chilling, low, and mild temperatures (1–3). This suggests that H2A.Z acts as a repressor of the HSP70 expression. Yet, H2A.Z is associated with many types of genes including those which are not induced by heat such as genes involved in phosphate starvation (4,5). Therefore, the removal of H2A.Z from HSP genes cannot be considered as a specific mechanism allowing the activation of the HSR. Moreover, the mechanism that mediates the dissociation of histones from HSP genes is not elucidated. Apparent additional proteins involved in the HSR mechanism at low temperature and late HS in *A. thaliana* have been described. The lack of HSFb, the heat shock binding protein 1 (HSBP1), and the VASCULAR PLANT ONE-ZINC-FINGER 1 (VOZ1) expression resulted in an overaccumulation of HSP at non-HS temperature (6–9). These proteins seem to be involved in the repression of the HSR, but it remains to identify all repressors in plants. This chapter described a similar approach of Kumar and Wigge but which was improved in two ways: Firstly, we used the promoter pGmHsp17.3b which is more tightly repressed as compared to HSP70 at low temperatures. Secondly, we used a more powerful reporter which is the nano-luciferase as compared to the luciferase. Thus, we aimed to isolate de-regulated mutants of the HSR which express a higher accumulation of nLUC-DAO1 and HSPs at low temperature.

Results

Isolation of the L5 candidate

A pool of 3 871 individual EMS M2 HIBAT lines was grown at 22°C without D-valine. They were screened for increased nLUC-DAO1 and sHSP17.7. 12 days old seedlings were sprayed with furimazine (substrate of nLUC), in order to observe excessive bioluminescence at 22°C. A no EMS HIBAT line was used as a control and was exposed previously at 35°C for 1 hour followed by 2 hours of post-incubation at 22°C. Two candidates were found, among them L5, to emit abnormal bioluminescence at 22°C compared to the HIBAT control (Fig. 1a). Thereafter, 5 weeks old leaves from the L5 candidate and HIBAT line were subjected to 22°C, 31°C, or 35°C exposure for 2 hours followed by 2 hours of post-incubation at 22°C. Whereas it showed more nLUC-DAO1 and

HSPs at 22°C and even more at 31°C, the same accumulation level at 35°C was observed as compared to the parental HIBAT line (Fig. 1b and c). These results suggest that an HSR repression gene(s) is affected by a mutation in the L5 mutant. The same level of nLUC-DAO1 and HSPs at 35°C indicate the selection of a candidate, which is deregulated in the HSR at low and mild temperature, but not at high temperature. The L5 mutant showed a higher number and bigger purple leaves including a delay in flowering compared to the HIBAT line at 5 weeks old (Fig. 1d). This phenotype might be caused by the HSR derepression that overproduced several heat-inducible proteins, which are normally repressed, and affect plant growth and development. Thus, the L5 candidate was chosen as a putative mutant in the repression of the HSR.

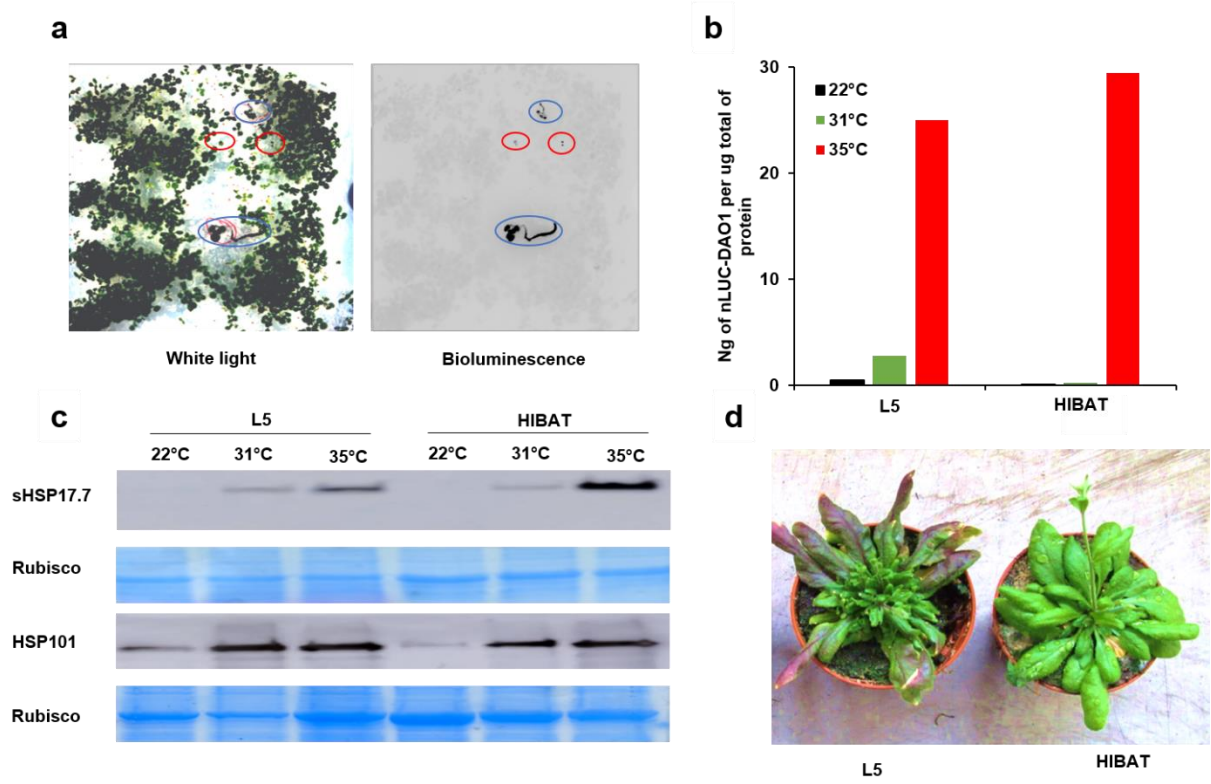

Figure 1: Abnormal expression of the HSR in the L5 mutant. (**a**) Searching for putative EMS M2 HIBAT mutants which express abnormal bioluminescence at 22°C at 12 days old. Left, white light, right, bioluminescence. The parental HIBAT line was used as a control and subjected to an HS at 35°C for 1 hour followed by 2 hours of post-induction at 22°C and then added on the plates (blue circle). HIBAT mutants with abnormal bioluminescence are represented by a red circle. The furimazine (substrate of nLUC) was sprayed on plate and were imaged by ImageQuant LAS 500 automatic exposition. (**b-c**) 5 weeks old leaves from the parental HIBAT line and L5 candidate were exposed to 22°C, 31°C or 35°C, for 2 hours followed by 2 hours at 22°C of post-recovery. The expression of nLUC-DAO1, sHSP17.7, and HSP101 were then analyzed. The homogeneous loading for each protein sample is represented RUBISCO which by Coomassie blue. Total protein loaded= 27 ug. (**d**) Phenotypes observed in the parental HIBAT line and L5 candidate at 5 weeks old.

At the M3 generation, the L5 candidate followed a Mendelian type of segregation suggesting a mutation in one gene recessive responsible for a high accumulation of nLUC-DAO1 and HSPs at 31°C. 13 offspring were screened and subjected to a mild temperature at 31°C for 2 hours followed by 2 hours of post-induction at 22°C. 11 offspring expressed the expected higher level of nLUC-DAO1 and sHSP17.7 compared to the parental HIBAT line. For example, offspring number 2 accumulated a level of 1.5-fold nLUC-DAO1 and 1.3-fold sHSP17.7 more compared to the HIBAT line control at 31°C (Figs. 2 and 3). Because all individual offspring presented a different ratio in the expression of both genes compared to the parental HIBAT line, two groups were generated in order to submit them to the WGDS. The first group, called “full”, contained 9 candidate offspring that accumulated at least 1.20 fold more of sHSP17.7, whereas a second group called “pool” contained 5 offspring that showed at least 1.8 fold more of sHSP17.7 compared to the HIBAT line at 31°C (Fig. 3). All offspring L5 candidates chosen for the sequencing showed identical phenotypes such as purple leaves and a delay in flowering compared to the HIBAT line (Fig. 4).

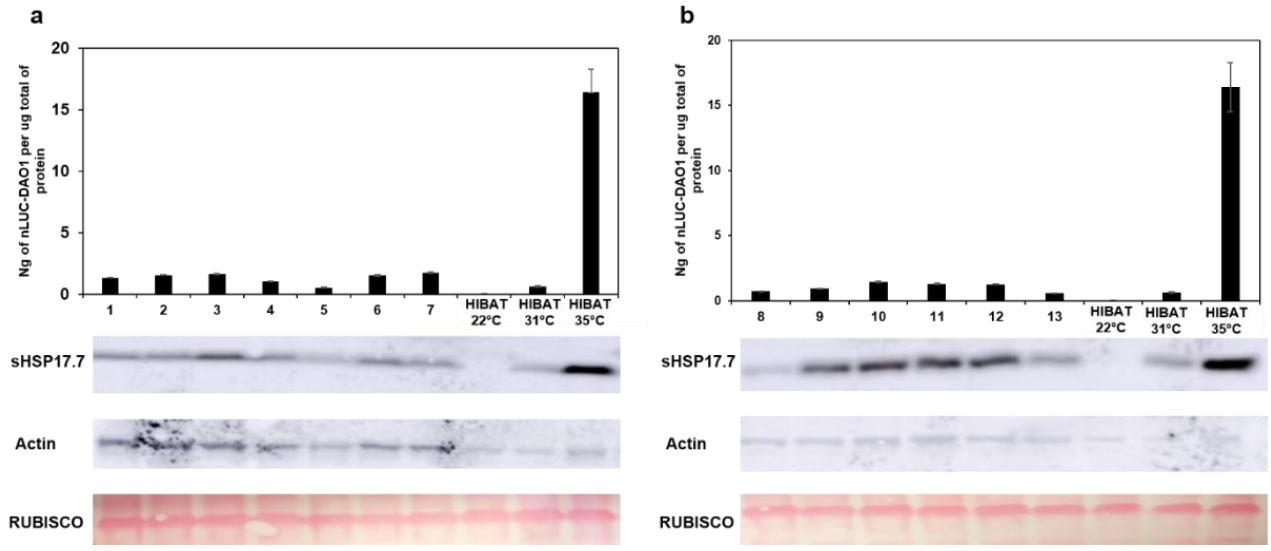

Figure 2: Accumulation of the nLUC-DAO1 and sHSP17.7 at 31°C of the M3 L5. (**a-b**) Leaves 5 weeks old of the L5 mutant were exposed at 31°C for 2 hours followed by 2 hours at 22°C of post-recovery. The parental HIBAT was used as a control in the absence of HS (HIBAT 22°C), with the same HS applied on L5 mutant (HIBAT 31°C) or at 35°C (HIBAT 35°C). The western blot below each graph represents the accumulation of sHSP17.7 observed in all offspring of HIBAT L5 candidate and HIBAT line control. The homogeneous loading for each sample is represented by the Actin and the accumulation of RUBISCO stained by PONCEAU S. Total protein-loaded; a= 24 ug and b= 27 ug. Numbers represent individual offspring of the mutant L5.

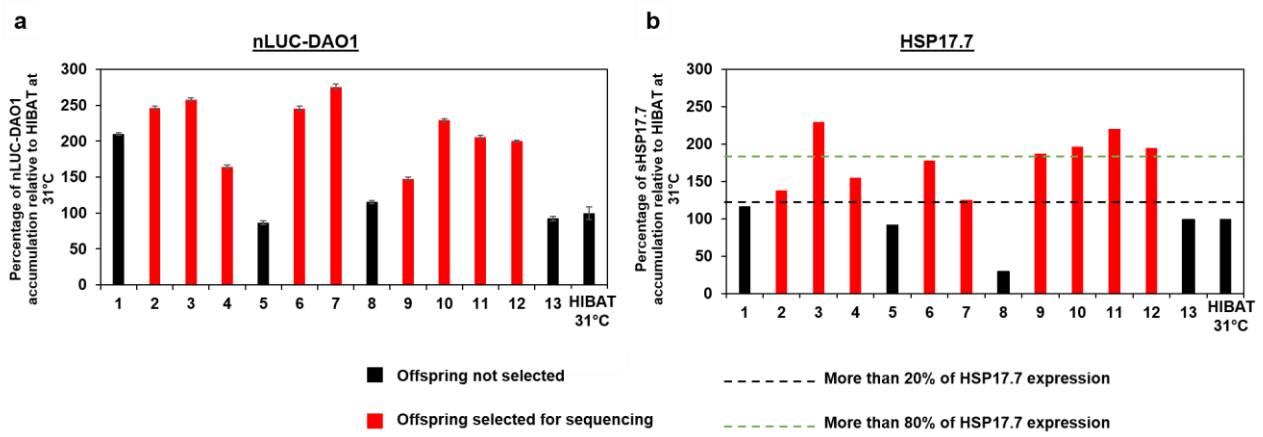

Figure 3: Percentage of the accumulation of nLUC-DAO1 and HSP17.7 at 31°C compared to the parental line HIBAT. Leaves 5 weeks old of L5 HIBAT mutants were exposed at 31°C for 2 hours followed by 2 hours at 22°C of post-recovery. The parental HIBAT was used as a control with the same mild HS applied of the L5 mutant. (**a**) Percentage of nLUC-DAO1 observed in offspring candidates L5 relative to HIBAT control at 31°C, means ± S.D. (n = 7). (**b**) Percentage of the accumulation of sHSP17.7 of offspring from the L5 mutant relative to HIBAT at 31°C. Numbers represent individual offspring of the L5 mutant. The bars in red represents individual offspring that showed significantly 20% more in the accumulation of nLUC-DAO1 and sHSP17.7 compared to HIBAT control and were then submitted to the WGDS. The accumulation of nLUC-DAO1 and sHSP17.7 of L5 offspring mutant were normalized against the reference HIBAT at 31°C.

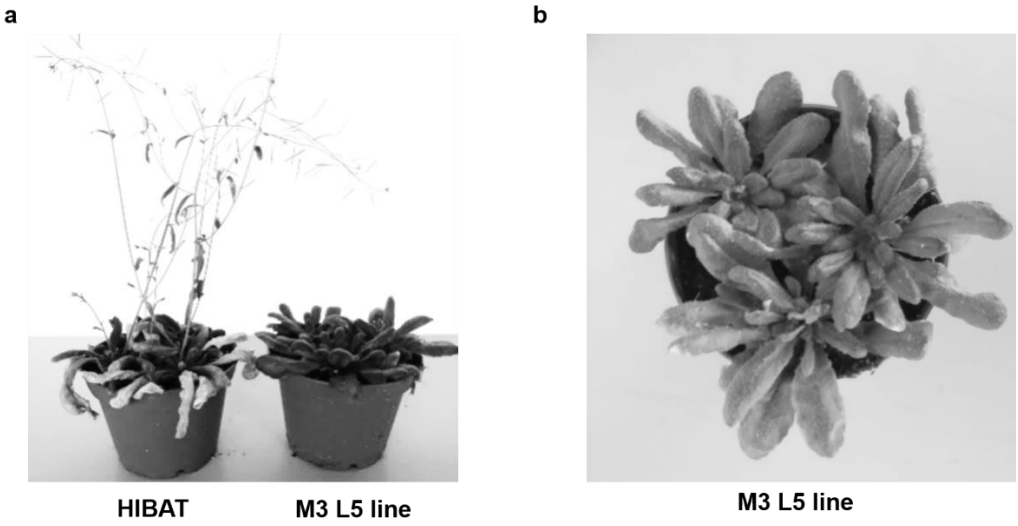

Figure 4: Delay of growth observed in the M3 L5 mutant compared to the parental line at 10 weeks old. (a) View from the front. (b) Top view of the L5 mutant. Pictures were imaged in a LED growth chamber (purple light) and could not be taken out to avoid contamination. Thus, pictures were adapted in black and white colors.

Identification of putative gene candidates

The sequencing from the two groups presented the same confident 232 SNPs. Among them, 16 caused a stop codon in genes putatively responsible for an HSR derepression phenotype. Therefore, the 16 corresponding T-DNA insertion lines were

ordered (Table 1). A stop codon at the beginning and in the middle of a gene was expected to have a higher impact on the mRNA transcription and protein translation becoming inactive or not synthesized. In contrast, a stop codon localized at the end of the gene may minimize their effect. For example, *BSK9*, *ASIL2*, and, *NAT10* showed a stop codon at the beginning of the gene, whereas *NDPK1* and *SSL13* genes were located at the end of their DNA sequence. Both *NDPK1* and *SSL13* genes could produce potentially a functional protein. Additionally, the HSR derepression phenotype can be caused not by a stop codon but by an amino acid substitution leading to affect protein function or by a SNP localized in the promoter. Thus, 232 SNPs were identified, and their excessive number led us to decrease the genetic noise induce by the EMS by crossing the L5 candidate with the parental line. At the F2 generation, offspring with the expected phenotype would be sequenced in order to reduce the list of SNPs identified.

Chromosome	Position	Reference allele	Detected allele	Position of the stop codon in the gene	Gene name	TAIR ID	Amino acids affected	Tair function
3	2837189	C	T	Start	BSK9	AT3G09240	Leu345	Kinase with tetratricopeptide repeat domain-containing protein
3	4151157	C	T	Middle	HAC5	AT3G12980	Gln1050	Encodes an enzyme with histone acetyltransferase activity that can use both H3 and H4 histones as substrates
1	26785935	G	A	Middle	FAB1C	AT1G71010	Trp867	Encodes a protein that is predicted to act as a phosphatidylinositol-3P 5-kinase
3	8647294	G	A	Middle	AT3G23930	AT3G23930	Trp89	Troponin T, skeletal protein
4	7917663	G	A	Middle	MET3	AT4G13610	Trp525	MEE57 DNA (cytosine-5-)-methyltransferase
1	20727253	G	A	Start	TBP2	AT1G55520	Gln46	TATA-box binding protein
5	1777056	C	T	Middle	AT5G05910	AT5G05910	Gln67	RING/U-BOX superfamily protein
3	21007355	G	A	Start	SIB1	AT3G56710	Gln52	SIGMA FACTOR BINDING PROTEIN 1
3	4708370	C	T	Start	ASIL2	AT3G14180	Trp84	6B-INTERACTING PROTEIN 1-LIKE 2, ASIL2 sequence-specific DNA binding transcription factor
3	21994948	G	A	End	SSL13	AT3G59530	Trp332	Calcium-dependent phosphotriesterase superfamily protein
1	24370270	G	A	Start	NAT10	AT1G65550	Arg100	Xanthine/uracil permease family
3	6502941	G	A	Start	AT3G18860	AT3G18860	Trp138	Transducin family protein / WD-40 repeat family protein
4	5924330	G	A	End	NDPK1	AT4G09320	Trp158	NDPK1, NUCLEOSIDE DIPHOSPHATE KINASE 1
3	16729191	G	A	End	AT3G45577	AT3G45577	Trp94	tRNA-intron endonuclease
1	12235295	G	A	Middle	TPS22	AT1G33750	Trp306	TERPENE SYNTHASE 22, TPS22
3	16370856	G	A	Middle	PDAT2	AT3G44830	Trp329	Lecithin: cholesterol acyltransferase family protein

Table 1: SNP candidates identified in the L5 mutants which lead to a stop codon. The table describes the exact position of the SNPs detected in the genome of the L5 mutant including the reference allele and the new detected allele caused by the SNP. The TAIR ID is also mentioned as well as a description of the coding protein according to TAIR10. The localization of the SNP is mentioned to be at the beginning, middle or at the end of the gene.

Discussion

Several protein partners of the HSR repression at non-HS temperature were identified in plants. The class of HSFbs was described to bind HSE of HSP genes in tomato and in *A. thaliana*. It results in the inhibition of the transcription of HSPs at late HS leading ultimately to the repression of the HSR (6). HSFb1 and HSF2b showed to repress the heat inducible HSFA2, HSFA7a, and several HSP genes transcriptions in *A. thaliana*. The microarray data of *hsfb1/hsfb2* mutant described a higher accumulation of HSP genes

compared to Col-0 at 23°C. When the double mutant was exposed to a noxious HS at 42°C for 70 or 80 min, plant mutants showed a higher rate of survivability as compared to plant control. This result indicates that *HSFB1* and *HSFB2* genes are involved in the HSR repression at low temperatures and their lack of expression enhances the resistance of plants to noxious HS caused by the excessive derepression of HSPs (10). In tomato, HSBP1 was identified as a main negative regulator of the HSR at late HS. The *hsbp1* mutant increased the thermotolerance which resulted in a higher level of HSP70-1 and HSP70-5 under HS compared to plant control. However, this phenotype was not observed at low temperatures but nevertheless confirms HSBP1 in the negative regulation of the HSR in tomato at late HS (7). Additionally, DREB2C was described as the positive regulator of the HSR that mediated HSFA3 activation under HS. Overexpression *dreb2c* lines accumulated significantly more HSP20s and HSP70 compared to Col-0 at non-HS temperature and enhanced plant survivability to noxious HS in *A. thaliana* (11). However, VOZ1 acts as a repressor of DREB2C, and *voz1* and *voz2-2* mutants were shown to improve the resistance against noxious HS. In unstressed plants, VOZ1 attached DREB2c, whereas under HS, DREB2c became unleash from VOZ1 leading to the expression of HSPs (8). These observations demonstrate that VOZ1 acts as a repressor of the HSR by inhibiting the activity of DREB2C which is involved in the accumulation of HSP in *A. thaliana*. Thus, several proteins were found to repress the HSR at low temperatures and at late HS, but it remains to find additional partners in plants.

The candidate L5 was isolated to express significantly a higher level of nLUC-DAO1 and HSPs at 22°C and 31°C compared to the HIBAT at the M2 and M3 generation (Fig. 1, 2 and 3). This phenotype reminded the heat-inducible profile of the *cngc2* channel mutant being thermosensitive in *A. thaliana* (12). Yet, it has to be demonstrated that the L5 candidate shows the same thermosensitivity at all temperatures tested in the *cngc2* mutant in order to validate the same HSR profile. At the M3 generation, L5 mutant was sequenced and 232 were significant SNPs were identified which among them 16 led to a stop codon (Table 1). Therefore, the 16 corresponding T-DNA insertion lines were ordered and remained to be analyzed for a defective repression of the HSR at low and mild temperatures.

Two identified genes seem to be relevant such as *HAC5* and *PDAT2*. *HAC5* encodes for a histone acetyltransferase. It was shown to interact with both H3 and H4 histones as a substrate which evocated the result from Kumar and Wigge, 2010. Interestingly, under HS, the complex HAC1/CBP was found to be a coregulator of HSFA1

and HSFB1 in *A. thaliana* (13). This result suggests that HAC5, if having the same function as its homologs HAC1, may regulate also HSFB1 activity (9). The lack of expression of HAC5 would result in the overexpression of sHSP17.7 at a low temperature in the L5 candidate. Additionally, the *PDTA2* gene encodes for a lecithin which belongs to the cholesterol acyltransferase family. The *pdta1* mutant was shown to be required for the fatty acid synthesis of triacylglycerols (TAGs) in the cytosol. PDTA1 lack of expression led to a defective accumulation of TAGs which are the major fatty acid donor in *A. thaliana* (14). This observation might indicate that PDTA2 could perform a similar function as its homolog PDTA1. It may result in a lack of TAGs production which leads to hypo saturated lipids contents at the plasma membrane and resulting in a higher level of the HSPs at low temperatures in the L5 candidate. A lipidomic analysis would indicate that the L5 mutant contains a lack of saturated lipids due to the defective expression of PDTA2. Yet, it remains to demonstrate the role of PDTA2 in the HSR in plants. All T-DNA insertion lines would be analyzed in their ability to express sHSP17.7 at 31°C compared to the reference line Col-0. If the phenotype observed does not result from the T-DNA insertions lines analysis, offspring of the L5 candidates, which have been crossed with the parental line HIBAT, would be sequenced at the F2 generation, in an attempt to reduce the excessive number of SNPs.

Conclusion

It is important to emphasize that the transcription of HSP genes result from the alleviation of the inhibitory transcription repression mechanism and the transcription activation mechanism. Histones wrapped on HSP genes may avoid the RNA polymerase recruitment by HSFA1 but also the presence of HSFBs bound on HSE inhibit HSP transcription at low and late HS. Two complementary mechanisms must take place in the HSR. The first is the alleviation of HSP gene repression and the second is the recruitment of the RNA polymerase by HSFA1 for the active transcription of HSPs. Thus, the first FGS aimed to address the activation part of the heat shock signaling pathway, whereas the second FGS addressed the protein partners that repressed the HSR.

Materials and Methods

Plant growth materials and isolation of the L5 candidate

A general pool of EMS M2 containing 3871 individual HIBAT lines (see Chapter 3, section “Material and Methods”) was used and sowed on ½MS medium with 2.20 g/L of

Murashige and Skoog media including MES buffer (Duchefa Biochimie, ref P14881.01), 8 8 g/L of agar (pH 5.8). Plants were grown in continuous light conditions at 22°C for 12 days old. The substrate of the nano-luciferase, from Nano-Glo Luciferase Assay System Kit from Promega (ref 1110), was sprayed to plates (dilution 1:100). Additionally, a no EMS seedlings HIBAT line was subjected to HS in an Eppendorf tube of 1.5mL in presence of Evian water (adapted from Macherel et al., 2013) at 35°C for 1 hour followed by 2 hours of post-induction at 22°C and then added in plates. The detection of the bioluminescence was performed by ImageQuant LAS 500 automatic exposition.

Protein extraction

5 to 8 weeks old leaves from plants were grinded by a plastic pestle in an Eppendorf tube of 1.5mL and resuspended with a BAP buffer (50 mM Tris-HCL (pH 7.5), 100 mM NaCl, 250 mM mannitol, 5 mM EDTA, 10% (v/v) glycerol, and protease inhibitor cocktail diluted at 1:300 (v/v) (Sigma-Aldrich, ref P9599). Protein extracts were centrifuged for 10 min at 12 000g and at 4°C. Supernatants (soluble proteins) were transferred in a new Eppendorf tube of 1.5mL and protein concentrations were determined by BRADFORD assay (Sigma-Aldrich, ref 23238). The bioluminescence (nLUC-DAO1) was detected by using the Nano-Glo Luciferase Assay System Kit from Promega (ref 1110) and the HIDEX plate reader (version 5067). The bioluminescence was analyzed for 1 second giving count per second. The bioluminescence emission was converted in ng of nLUC-DAO1 per ug total of protein through a standard calibration curve of nLUC as shown in Chapter 2.

Western blot

Protein extract was homogenized in LBX buffer (Tris-HCL 0.5 M (pH 6.8), 20% glycerol (v/v), 20% SDS (w/v), 4% bromophenol blue (w/v), 5% 2-mercaptoethanol (v/v), and heated for 3 min at 90°C. Homogenates were loaded in Precast SDS PAGE gels 12% acrylamide (EXPEDON, ref Ab 119207). Electrophoresis was applied at 100 V for 15 min and then 45 min at 130V (constant amperage) using the associated buffer of Precast SDS PAGE gels diluted at 1:50 (v/v). Coomassie blue staining was applied for 5 min using Instant Blue solution from Sigma-Aldrich (ref ISB1L). Precast SDS PAGE gels were transferred to nitrocellulose blotting membrane 0.2 µM (GE Healthcare Life Sciences, ref 10600001) by wet transfer using TRT buffer (20% (v/v) absolute Ethanol, and 5% (v/v) of the buffer associated with Precast SDS PAGE gels) for 50 min at 80 volts (amperage constant). Staining by PONCEAU S (Sigma-Aldrich, ref 09276) was applied on membranes for 5 min and the excess was washing with distilled water.

Membranes were blocked by using TRM buffer (5% milk powder (v/v), 50 mM Tris-HCL (pH 8), 150 mM NaCl) for 1 hour at room temperature. Primaries antibody sHSP17.7 (Abcam, ref Ab80171, diluted 1:2000), HSP101 (Marq biosciences, ref SPC 305, diluted 1:2000), and ACTIN (Sigma Aldrich, ref A0480, diluted 1:2000) were added in TRM buffer and the solution covered membranes for 2 hours at room temperature with gentle agitation. Membranes were then washed 3 times for 10 min (gently agitation) with TRM buffer without milk and replace by 0.1% (v/v) of Tween 20. Secondary peroxidase-conjugated goat antibody against rabbit IgG (from Biorad, ref 170-5046) was diluted at 1:2000 (v/v) in TRM buffer and the solution covered membranes for 1 hour at room temperature with gentle agitation. Membranes were still washed 3 times. The revelation was done by using the kit Clarity Western ECL substrate (Biorad, ref 102031318 and 102031316) and the acquisition was performed by using ImageQuant LAS 500 automatic exposition.

Heat shock treatments

5 to 8 weeks old leaves from L5 and HIBAT mother line lines were transferred in an Eppendorf tube of 1.5 mL containing 1 mL of Evian water (adapted from Macherel et al., 2013) and heated in a thermoblock at 22°C, 31°C or 35°C for 2 hours followed by 2 hours of post-recovery at 22°C. Proteins were then extracted following the same protocol in the section Materials and Methods “protein extraction and analysis” in order to analyze the amount of nLUC-DAO1 and used for the western blotting analysis of HSPs.

Normalization of the accumulation of HSPs and nLUC-DAO1 compared to HIBAT+

Data obtained from the accumulation of nLUC-DAO1 and HSPs of offspring from L5 mutant were normalized compared to HIBAT control under HS. The background of nLUC-DAO1 and sHSP17.7 expression from the mother line HIBAT without HS was removed for calculation. The accumulation of HSP was observed due to the acquisition of images from ImageQuant LAS 500. Images showing the accumulation of HSPs were normalized in the offspring of the L5 mutant compared to the HIBAT control under HS using the constitutive expression of actin as a reference. Data were obtained using ImageJ software (version 1.53).

Extraction of genomic DNA

The offspring of L5 mutant were crushed and grinded by a plastic pestle in an Eppendorf tube of 1.5mL. Extracts were resuspended in 600 µl of STE-lysis buffer (100mM Tris-HCL (pH 7.5), 2% (w/v) SDS, and 10 mM of EDTA) and incubated at 65°C for 20 min minimum. Thereafter, DNA extractions were cooled on ice (4°C) for 5 min and

200 µl of NH_4Ac (10M) were added, mixed, and centrifuged at 12 000g for 10 min. 650 µl of the supernatants were transferred in a new tube and 650 µl of isopropanol (100%) was added, mixed, and incubated for 5 min at room temperature and then centrifuged for 10 min at 12 000g. Supernatants were removed and pellets were washed with 1 mL of cold ethanol 70% and re-centrifuged for 10 min at 12 000g. This wash step was repeated 2 times. Ethanol was then removed from tubes let open until that pellets became transparent and dry. DNA extracts were finally resuspended in 100 µl of EB buffer (10mM of Tris-HCL pH 8.0).

Whole DNA genome sequencing of HIBAT candidates

100 ng total of DNA from L5 offspring candidate were sent to the Whole DNA genome sequencing at the Lausanne Genomic Technologies facility. The cDNA library used Nextera DNA Flex and the sequencing was applied with pairwise-ends, coverage of 150 by the Illumina new sequencing generation systems HISeq 4000 PE. Data generated from the sequencing were in Fastq files format and were transformed in Bam files by removing potential PCR duplicate through Galaxy 2.0 website tool (https://galaxyproject.org). SNPs were then detected by using a pipeline and adapted from Wachsman et al., 2017. The ratios of read and the SNPs localization in the genome of HIBAT mutants were then obtained in Excel files. The function of genes where SNPs were identified was performed by using data from Salk institute genomic analysis laboratory (http://signal.salk.edu/cgi-bin/tdnaexpress).

T-DNA insertion lines analysis

The Protein function reported were obtained from TAIR (https://www.arabidopsis.org). T-DNA insertions were obtained from NASC (http://arabidopsis.info/BasicForm).

Contributions

The DNA extraction from of offspring of L5 mutant was performed by Dr. Anthony Guihur and the apprentice laboratory technician Gizem Demirkiran. The localization of SNPs was contributed by Dr. Anthony Guihur.

References

1. Kumar SV, Wigge PA. H2A.Z-Containing Nucleosomes Mediate the Thermosensory Response in Arabidopsis. Cell [Internet]. 2010;140(1):136–47. Available from:

http://dx.doi.org/10.1016/j.cell.2009.11.006
2. March-Díaz R, Reyes JC. The beauty of being a variant: H2A.Z and the SWR1 complex in plants. Mol Plant [Internet]. 2009;2(4):565–77. Available from: http://dx.doi.org/10.1093/mp/ssp019
3. Franklin KA. Plant Chromatin Feels the Heat. Cell. 2010;140(1):26–8.
4. Smith AP, Jain A, Deal RB, Nagarajan VK, Poling MD, Raghothama KG, et al. Histone H2A.Z regulates the expression of several classes of phosphate starvation response genes but not as a transcriptional activator. Plant Physiol. 2010;152(1):217–25.
5. Zahraeifard S, Foroozani M, Sepehri A, Oh DH, Wang G, Mangu V, et al. Rice H2A.Z negatively regulates genes responsive to nutrient starvation but promotes expression of key housekeeping genes. J Exp Bot. 2018;69(20):4907–19.
6. Czarnecka-Verner E, Yuan CX, Nover L, Scharf KD, Englich G, Gurley WB. Plant heat shock transcription factors: Positive and negative aspects of regulation. Acta Physiol Plant. 1997;19(4):529–37.
7. Marko D, El-Shershaby A, Carriero F, Summerer S, Petrozza A, Iannacone R, et al. Identification and characterization of a thermotolerant TILLING allele of heat shock binding protein 1 in tomato. Genes (Basel). 2019;10(7).
8. Song C, Lee J, Kim T, Hong JC, Lim CO. VOZ1, a transcriptional repressor of DREB2C, mediates heat stress responses in Arabidopsis. Planta [Internet]. 2018;(0123456789). Available from: http://link.springer.com/10.1007/s00425-018-2879-9
9. Ikeda M, Mitsuda N, Ohme-Takagi M. Arabidopsis HsfB1 and HsfB2b act as repressors of the expression of heat-inducible Hsfs but positively regulate the acquired thermotolerance. Plant Physiol. 2011;157(3):1243–54.
10. Ikeda M, Mitsuda N, Ohme-Takagi M. Arabidopsis HsfB1 and HsfB2b Act as Repressors of the Expression of Heat-Inducible Hsfs But Positively Regulate the Acquired Thermotolerance. Plant Physiol. 2011;157(3):1243–54.
11. Chen H, Hwang JE, Lim CJ, Kim DY, Lee SY, Lim CO. Arabidopsis DREB2C functions as a transcriptional activator of HsfA3 during the heat stress response. Biochem Biophys Res Commun [Internet]. 2010;401(2):238–44. Available from: http://dx.doi.org/10.1016/j.bbrc.2010.09.038
12. Finka A, Cuendet AFH, Maathuis FJM, Saidi Y, Goloubinoff P. Plasma Membrane Cyclic Nucleotide Gated Calcium Channels Control Land Plant Thermal Sensing and Acquired Thermotolerance. Plant Cell [Internet]. 2012;24(8):3333–48. Available from: http://www.plantcell.org/cgi/doi/10.1105/tpc.112.095844
13. Anguli ARG, Otak SAK, Ishra SHKUM, Over LUTZN, Ort MAP, Charf KLIS, et al. Heat stress response in plants : a complex game with chaperones and more than twenty heat stress transcription factors. 2004;29(December):471–87.
14. Mueller SP, Unger M, Guender L, Fekete A, Mueller MJ. Phospholipid : Diacylglycerol Acyltransferase-Mediated Triacylglyerol Synthesis Augments Basal Thermotolerance 1. 2017;175(September):486–97.
15. Macherel D, Abdelilah B, Pierart A, Baecker V, Avelange-Macherel M-H, Rolland A, et al. Simple system using natural mineral water for high-throughput phenotyping of Arabidopsis thaliana seedlings

in liquid culture. Int J High Throughput Screen. 2013;1.

16. Wachsman G, Modliszewski JL, Valdes M, Benfey PN. A simple pipeline for mapping point mutations. Plant Physiol. 2017;174(3):1307–13.

Chapter 6: Generation of *cam1* and *cam5* Arabidopsis mutants by CRISPR methodology and T-DNA insertion lines.

Abstract

The primary thermosensors in *A. thaliana* cells, CNGC2 and CNGC4 located at the plasma membrane, were identified by Finka et al., 2012,. Both CNGCs expose to the cytosol a predicted calmodulin-binding site. Yet, the precise identity and the Ca^{2+} entry dependent mechanism of these heat-responsive channels, which mediate the specific transduction of a heat priming signal to accumulate HSPs, is unclear. In a yeast two-hybrid screen, using the cytosolic C-terminal domain of the CNGC2 as bait against a cDNA library *A. thaliana* gene, Dr. Anthony Guihur identified two CaMs, CaM1 and CaM5. Their role in the mediation of the heat signaling is then strongly suggested. Supporting putatively the involvement of these CaMs, two specific CaM inhibitors, W5 and W7, were found to repress the HSR at 34°C in the HIBAT line. Thus, a single and double *cam1/cam5* mutant line were generated by CRISPR and by the T-DNA approaches in an attempt to address their possible role in the heat signaling. Under HS, the T-DNA single homozygous line of both CaMs did not affect the HSR and accumulate optimally the same expression level of sHSP17.7 compared to Col-0 control. The question rises if CaM1 and CaM5 are only artifacts from the yeast two-hybrid assay or if both genes need to be mutated to significantly affect negatively the HSR. A double *cam1/cam5* mutant from T-DNA insertion lines was isolated. The lack of expression of CaM1 and CaM5 remains to be elucidated to ascertain the generation of a true knockout double mutant line. Once validated, the accumulation level of HSPs under HS and an AT assay would indicate if both CaM1 and CaM5 are involved in the heat shock signaling pathway.

Introduction

In *A. thaliana*, AtCaM3 was the only CaMs to be found at mediating the heat shock signaling but it has not been shown to interact with CNGCs sensors (2,3). Thus, additional CaMs remains to be identified to interact with CNGCs and to show those which are involved or not in the mediation of the heat signal. All CaMs have a sequence identity up to 80% except for CaM8 and CaM9 with 50% to 60% in *A. thaliana* (Supp data 1). Interestingly, CaM1 has the particularity to contain a fragment of 17 amino acids at the N-terminal, whereas CaM5 shows a fragment of 33 amino acids at the C-terminal. Both parts of the protein sequences are not common with other CaMs in *A. thaliana* (Fig. 1). This observation suggests that CaM1 and CaM5 do not share obligatorily identical functions in cells. Under HS, the partners of the CNGCs sensors leading to the accumulation of HSPs remained unknown (1,4). Bioinformatically identified CaMBD was used as a bait against a normalized cDNA library of 20 000 *A. thaliana* genes in a yeast two-hybrid screen which was carried out by Dr. Anthony Guihur (unpublished data). Among positive interactors candidates, CaM1 and CaM5 were found to strongly interact with CNGC2. Therefore, their role in the mediation of the heat shock signaling pathway is suggested.

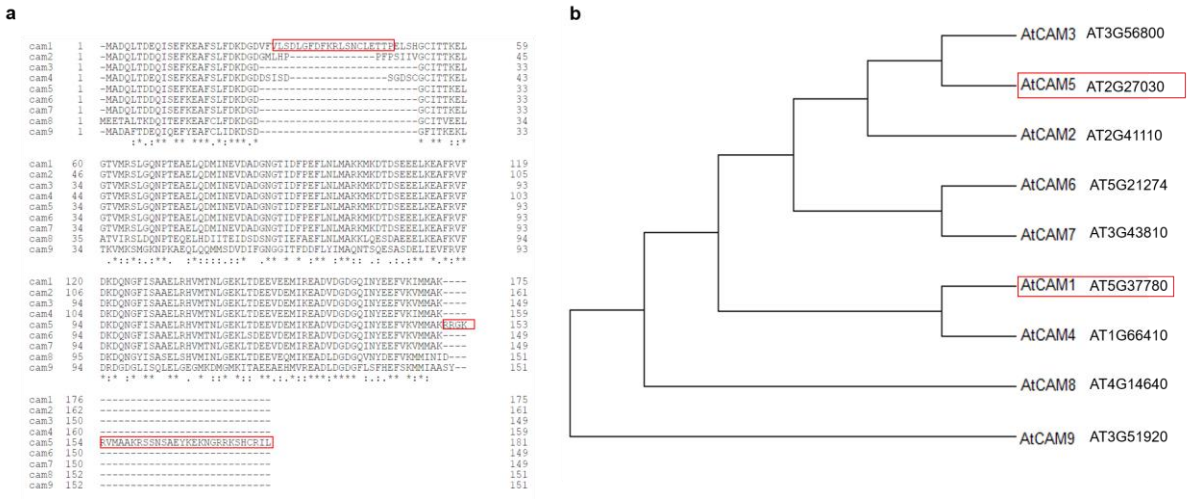

Figure 1: Alignment of protein sequences and molecular phylogenetic analysis of calmodulins in *A. thaliana*. Alignment of the CaM protein sequences (**a**) and phylogenetic tree (**b**) of the 9 calmodulins in *A. thaliana*. The evolutionary history was inferred by using the Maximum Likelihood method based on the JTT matrix-based model. The initial tree for the heuristic search was obtained automatically by applying Neighbor-Join and BioNJ algorithms to a matrix of pairwise distances estimated using a JTT model and then selecting the topology with superior log likelihood value. The analysis involved 9 amino acid sequences from the calmodulins. All positions containing gaps and missing data were eliminated. There was a total of 149 positions in the final dataset of *A. thaliana*. Evolutionary analyses were conducted in MEGA7 software (version 7.0).

In *A. thaliana*, a T-DNA insertion line does not create obligatorily a true knockout mutant depending on the insertion position in the gene. It can result in a low mRNA expression leading to the translation of the protein which might maintain or decrease its function(s) in the cellular process. For example, the T-DNA insertion line of CaM1 (SALK_107507), which is in the 3'UTR, was shown to accumulate a weak amount of mRNA transcript in root and shoot. In contrast, the T-DNA insertion line of CaM5 (SALK_027181), which is located in exon II, did not present an expression of mRNA, being a true knockout line (5). This result suggests that the CaM1 might assume a residual activity and function in cells. Therefore, the CRISPR/Cas9 approach was chosen in an attempt to create a true knockout single and double mutant of *cam1* and *cam5* by targeting specifically their exons. In parallel and to ascertain to create a double knockout or at least knockdown lines, the same CaM5 T-DNA insertion line (SALK_027181) and a new T-DNA insertion line CaM1 (SALK_202076C), located in exon, were studied and also crossed to generate a double mutant in *A. thaliana*.

Results

The W5 and W7 inhibitors of calmodulin affect the heat shock response

One way to address the possible involvements of CAMs in the heat shock signaling pathway is to use inhibitors such as N-(6-Aminohexyl)-1-naphtalensulfonamide (W5) and N-(6Aminohexyl)-5-chloro-1-naphtalenesulfonamide hydrochloride (W7). Both W5 and W7 were described, by small-angle X-ray scattering and nuclear magnetic resonance spectroscopy, to induce an inter-domain compaction of Ca^{2+}/CaM leading to inactivate CaMs activity (6). 12 days old HIBAT seedlings were treated with 100 µM of W5, W7, or both and submitted to 22°C for 1 hour followed by 2 hours at 22°C or 34°C and then followed by 2 hours of post-recovery at 22°C. The HSR was slightly induced in the presence of both W5 and W7 at 22°C compared to untreated plants, whereas the treatment with only one of the inhibitors did not affect significantly the HSR (Fig. 2a). At 34°C, a reduction of the HSR was found in the presence of both inhibitors compared to plant control (Fig. 2b). These results suggest that CaMs might be involved in the repression of the HSR at a low temperature. Yet, both inhibitors do not overexpress the same level of nLUC-DAO1 at 22°C compared to untreated plants at 34°C. In contrast, the inhibition of CaMs at 34°C leads to a clear reduction of the HSR and indicates their putative role in the heat signal.

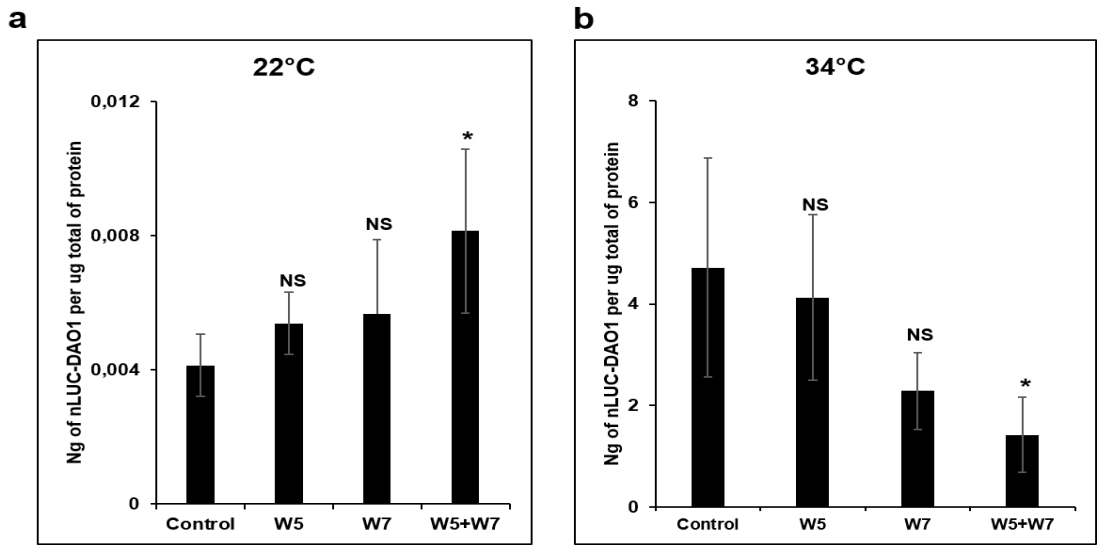

Figure 2: Effect of W5 and W7 inhibitors on the HSR of the HIBAT line at 22°C and 34°C. The accumulation of nLUC-DAO1 in the transgenic HIBAT line at 22°C (**a**) and 34°C (**b**). 12 days old seedlings were treated in the absence or in presence of 100 uM of W5, W7, or both. Seedlings were then submitted to 22°C for 1 hour followed by 2 hours at 22°C or 34°C and then exposed to 22°C for 2 hours of post-incubation. The bioluminescence in each sample was then analyzed. Asterisks indicate statistically significant differences compared to HIBAT control without W5 and W7 treatments (n=4) determined by student T.test (*, P<0.05, NS, No Significant).

Selection of single and double CRISPR mutant of *cam1* and *cam5*

In an attempt to generate a single and double mutant line of *cam1* and *cam5* by CRISPR/Cas9, gRNAs were created to target their exons. We expected to cause a significant deletion in both genes to inactivate their transcription. For example, the single mutant lines C1.1 (CaM1) and C5.1 (CaM5), which are both targeted by 2 gRNAs, are expected to present a deletion of 213 bp and 226 bp. At the T1 generation, 11 offspring from both lines were screened by PCR for deletion(s). The offspring 6 of C1.1 line, showed a deletion of 213 bp compared to Col-0 control (Fig. 4a). This result suggests that the *CaM1* gene is targeted by Cas9 which recognized the gRNAs designed. Among the 9 offspring of C5.1 line, plants 7 and 10 showed deletions and a normal size amplification of the CaM5 gene which suggests they are heterozygous (Fig. 4b). Offspring 7 presented a deletion of 226 bp as expected if the 2 gRNAs were recognized by Cas9, whereas offspring 10 showed a longer deletion size. Thus, offspring 6 of C1.1 and 7, 10 of C5.1 were chosen as a potential single mutant for *CaM1* and *CaM5*.

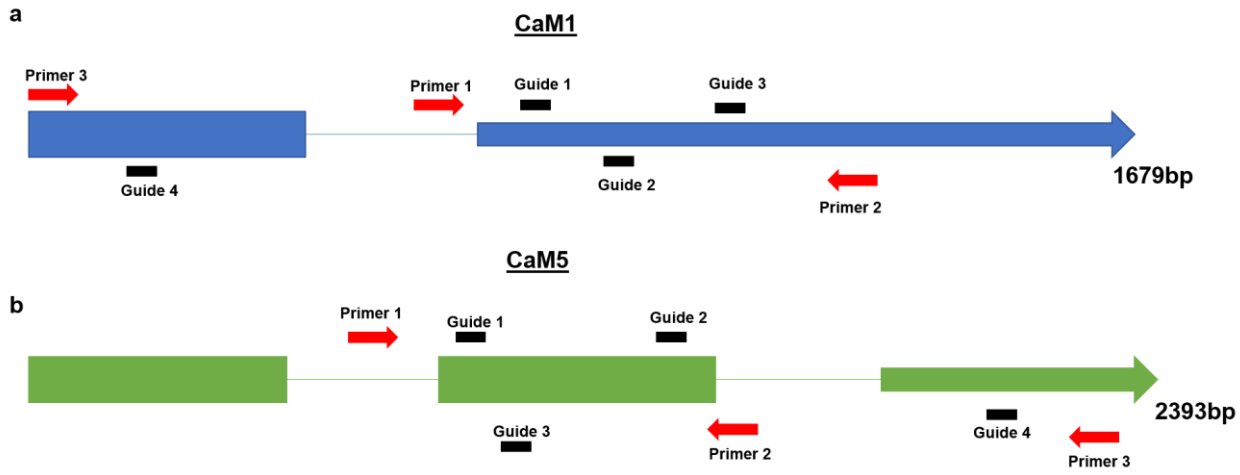

Figure 3: Localization of primers and gRNAs on *CaM1* and *CaM5*. (**a-b**) Four gRNAs were designed per calmodulins and 3 primers were generated to check the eventual deletion(s) induced by CRISPR/Cas9. Each cylinder represents the exons in the *CaMs* respectively, two for *CaM1* and three for *CaM5*. The length of each gene is represented at the end of the arrow.

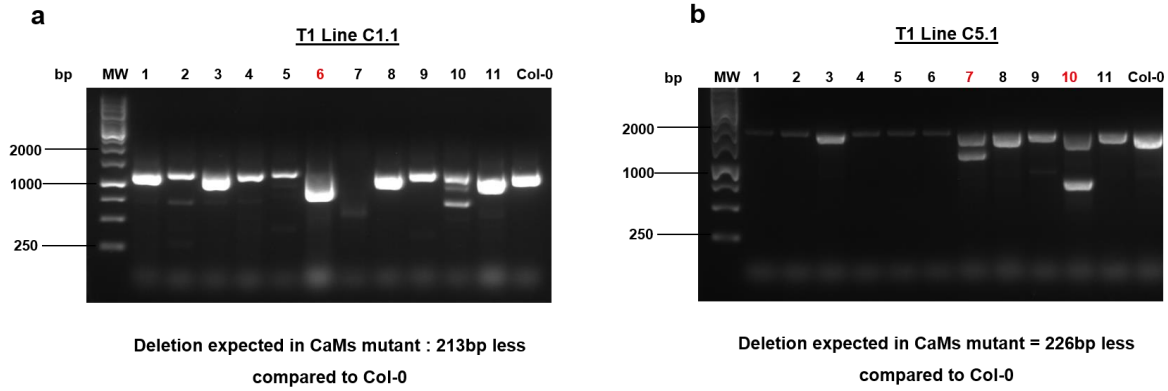

Figure 4: Genotyping of C1.1 and C5.1 single mutant line at the T1 generation. Genotyping of lines C1.1 (**a**) and C5.1 (**b**). *CaM1* and *CaM5* were amplified by using the respecting set of primers 1 and 2 (Fig. 3). Col-0 was used as a control for the length of *CaMs* amplification. The names of each CaM lines and the molecular weight (MW) are represented on top of each lane of the gel. Offspring (red number) were selected to present a deletion in *CaMs*.

At the T2 generation, seeds that did not emit red fluorescence (loss of CRISPR/Cas9 insertion) were selected to avoid the constitutive expression of Cas9 that could target random regions in the *A. thaliana* genome. The DNA was extracted from 3 weeks old leaves of offspring from lines C1.1 (6), C5.1 (7), and C5.1 (10), and confirmed by PCR and sequencing for a deletion or at least a frameshift in *CaM1* and *CaM5*. Offspring of the T2 line C1.1 (6) did not show the same deletion observed at the T1 generation but presented a short deletion of 35 bp located in exon 2 of *CaM1* (Fig. 5a). Offspring of the T2 line C5.1 (7) showed the same deletion as observed at the T1 generation (Fig. 5b). The line C5.1 (10) displayed to be heterozygous for offspring 2, 3, 4,

and 5 which all of them present both deletion and normal amplification of *CaM5* compared to Col-0 control (Fig. 5c). However, offspring 1 of T2 C5.1 (10) did not present a deletion but the sequencing result revealed a frameshift starting in the exon 2 of *CaM5* at the position 1 097 and was then selected. Thus, 1 CRISPR line single *cam1* mutant and two for *cam5* were generated successfully.

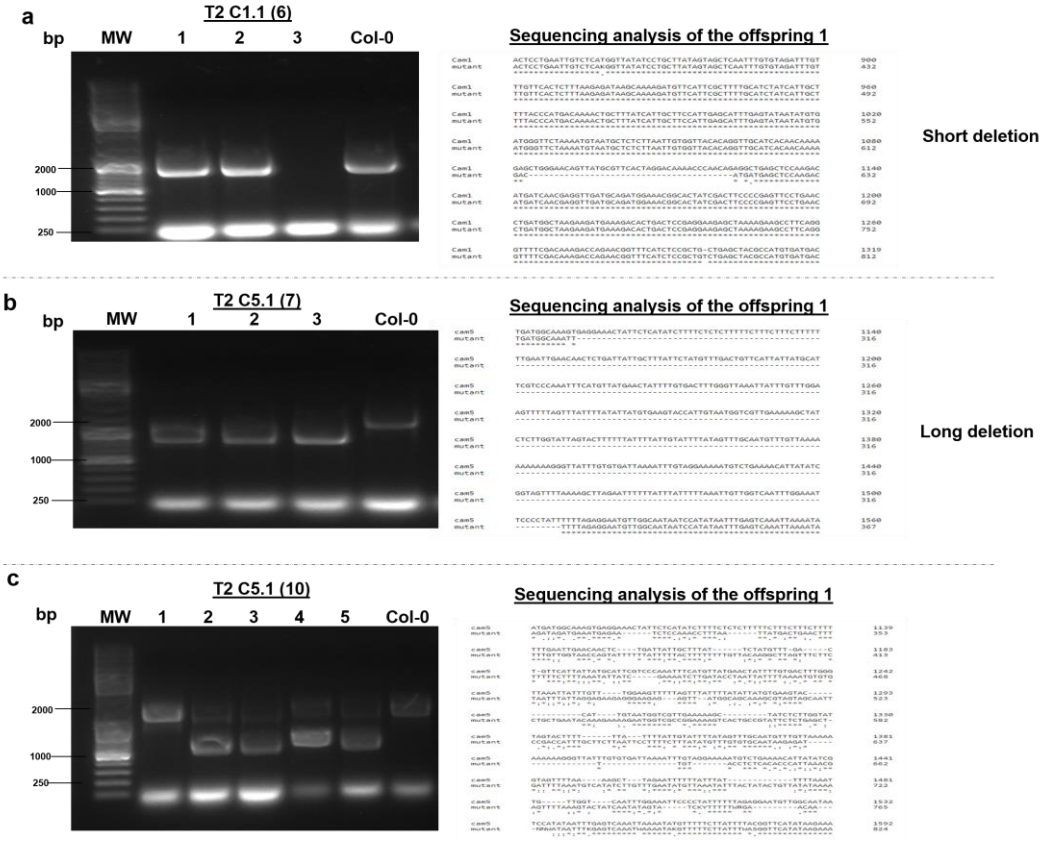

Figure 5: Genotyping of C1.1 and C5.1 single mutant line at the T2 generation. (**a-c**) Genotyping of the line C1.1(6) (**a**) and 2 lines C5.1 (7 and 10) (**b-c**). *CaM1* and *CaM5* were amplified by using the set of primers 1 and 2 (Fig. 3). Col-0 was used as a control for the length of *CaMs* amplification. The names of CaMs lines and the molecular weight (MW) are represented on top of each lane of the gel. The sequencing result of the corresponding *CaM* amplified by PCR is represented on the right of each PCR gel. The alignments were performed by Clustal Omega.

In order to optimize the chances to generate a double *cam1/cam5* mutant, two different lines were generated. The first, called C1.5', contained 4 gRNAs targeting exon 2 of *CaM1* and the 2 remaining, exon 2 and 3 of *CaM5*. The second, called C5.1' was also targeted by 4 gRNAs in exons 1 and 2 of *CaM1* and the 2 remaining in exon 2 of *CaM5*. At the T1 generation, among the 8 offspring from C1.5', only progeny number 8 showed a deletion in *CaM1* as well as a normal amplification compared to the Col-0 line which is suggested to be heterozygous (Fig. 6a). However, all offspring did not show deletion in the *CaM5* gene (Fig. 6b). Additionally, 9 offspring from C5,1' line did not present a deletion for

the *CaM1* compared to Col-0, whereas 3 offspring were observed (2, 6, and 9) to be homozygous for *CaM5* (Fig. 6c and d). An absence of frameshift was observed for all offspring which presented a least a deletion in one of both genes for C5.1' and C1.5' lines. The generation of a double *cam1/cam5* mutant was not successful and the individual homozygous CRISPR lines of CaM1 and CaM5, isolated at the T2 generation, were crossed. It remains also to screen additional lines of *cam1/cam5* mutant.

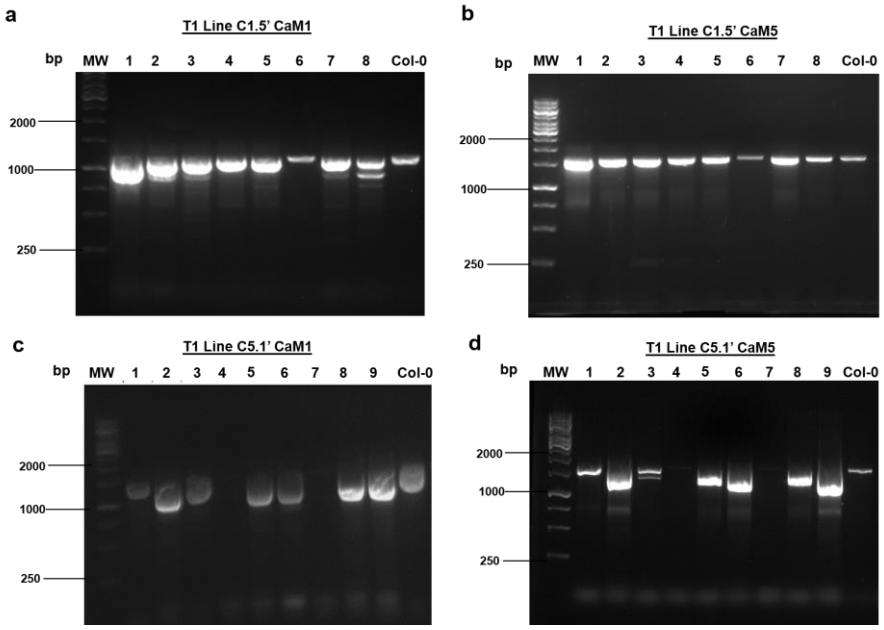

Figure 6: Genotyping of the double mutant *cam1* and *cam5* at the T1 generation. Several offspring from C1.5' (**a-b**) and C5.1' (**c-d**) lines were analyzed for a search of deletion in *CaM1* and *CaM5*. Primers set 1 and 2 were used for *CaM1* amplification in lines C1.5' and primers 2 and 3 for line C5.1'. Primers 2 and 3 were used for *CaM5* amplification in line C1.5' and primers 2 and 3 for line C5.1'. The Col-0 line was used as a control for the length of CaMs amplification. The Names of CaM lines and the molecular weight (MW) are represented on top of each lane of the gel.

Selection of homozygous single T-DNA insertion line of CaM1 and CaM5

In order to ascertain the generation of a knockout or at least a knockdown single and double *cam1* and *cam5* mutant, a T-DNA approach was initiated. The CaM1 T-DNA insertion line (SALK_202076C) which contained a T-DNA in exon III and the CaM5 T-DNA insertion line (SALK_027181) located in exon II, were chosen. Both lines were firstly genotyped to select homozygous candidates. Progenies 1, 2, 3, 5, and 6 of CaM1 and offspring number 2 of CaM5 were found to be homozygous (Fig. 7a and b). Because T-DNA were described to be located in exons, it was suggested that the mRNA of both CaM1 and CaM5 T-DNA lines was defective. Yet, a qPCR analysis remains to be performed to confirm their lack of transcript expression.

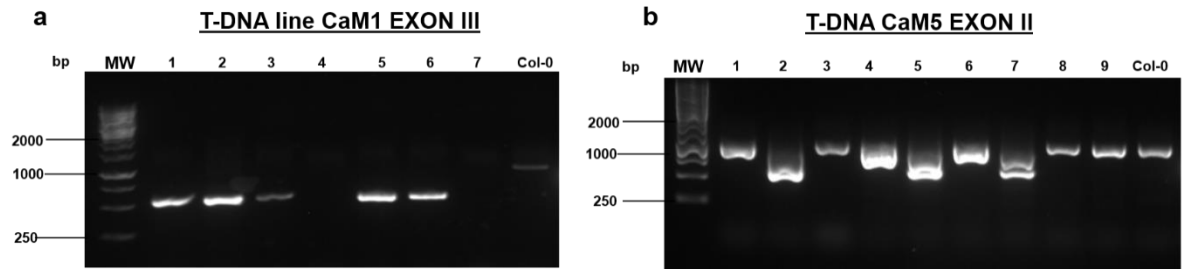

Figure 7: Genotyping of the T-DNA insertion lines of *CaM1* and *CaM5*. (**a-b**) Genotyping of T-DNA insertion lines *CaM1* (**a**) and *CaM5* (**b**). The set of primer LP+RP and BP+RP, (sequence obtained from the SALK institute) were used for the genotyping. Two individual PCR reactions were performed for each plant, and DNA products obtained were mixed and loaded in gels. Col-0 was used as a control for the length of CaMs amplification. Numbers represent individual offspring of each T-DNA insertion lines of CaM1 and CaM5 on top of each lane of the gel.

Analysis of the expression of sHSP17.7 in the single T-DNA insertion line of CaM1 and CaM5

The accumulation of sHPS17.7 under HS was addressed in an attempt to analyze the role of both CaMs in the heat signaling. 5 weeks old leaves from homozygous T-DNA insertions lines of both CaMs and Col-0 plants were subjected at 22°C or at 35°C for 2 hours followed by 2 hours of post-recovery at 22°C. At 35°C, the same level of sHSP17.7 was observed in the T-DNA CaM1 line compared to the Col-0 control. Different accumulations within the same replicates were found in the T-DNA CaM5 and more experiment is needed to validate these observations (Fig. 8a and b). Yet, these primary results might indicate that the T-DNA insertion line of CaM1 and CaM5 do not affect the HSR.

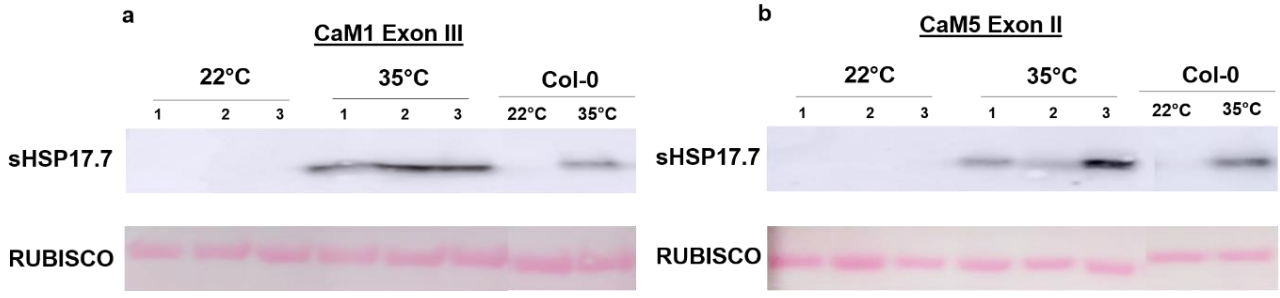

Figure 8: Accumulation of sHSP17.7 in the single T-DNA insertion lines CaM1 and CaM5 under HS. Accumulation of sHSP17.7 in T-DNA insertion lines CaM1 (**a**) and CaM5 (**b**) by Western blot. 5 weeks old leaves from the homozygous T-DNA insertion line were exposed at 35°C for 2 hours followed by 2 hours of post-recovery at 22°C. Col-0 was used as control with an absence of heat treatment (Col-0 22°C) or with the same HS applied on the T-DNA insertion line (Col-0 35°C). The homogeneous loading for each protein sample is represented by the presence of the RUBISCO which was stained by a solution of PONCEAU S. Total protein-loaded; a= 5 ug and b= 6 ug.

Selection of a homozygous T-DNA insertion line double mutant of *cam1/cam5*

T-DNA homozygous insertion lines CaM1 and CaM5 were crossed to generate a double *cam1/cam5* homozygous mutant. Both T-DNA insertion lines CaM1 and CaM5 were used as mother and father progenitor during the crossing. At the F1 generation, all offspring were expected to be heterozygous for both genes and 10 F1 progeny lines were genotyped and isolated (Fig. 9a and b). At the F2 generation, it should result in 1/16 (6.25%) of a double homozygous *cam1/cam5* mutant according to the Mendelian type of segregation. Thus, 36 offspring from the 10 individual F2 lines were segregated on hygromycin plates in order to eliminate non transformed lines. Survivals were then submitted to genotyping and the offspring number 1 was found to be homozygous for both genes *CaM1* and *CaM5*. Whereas other progenies were heterozygous for CaM1 and not for CaM5 such as lines 2, 3, 4, and 5 (Figs. 10a and b). Thus, one homozygous line for CaM1 and CaM5 was generated successfully and would be ascertained at the next generation by a new genotyping.

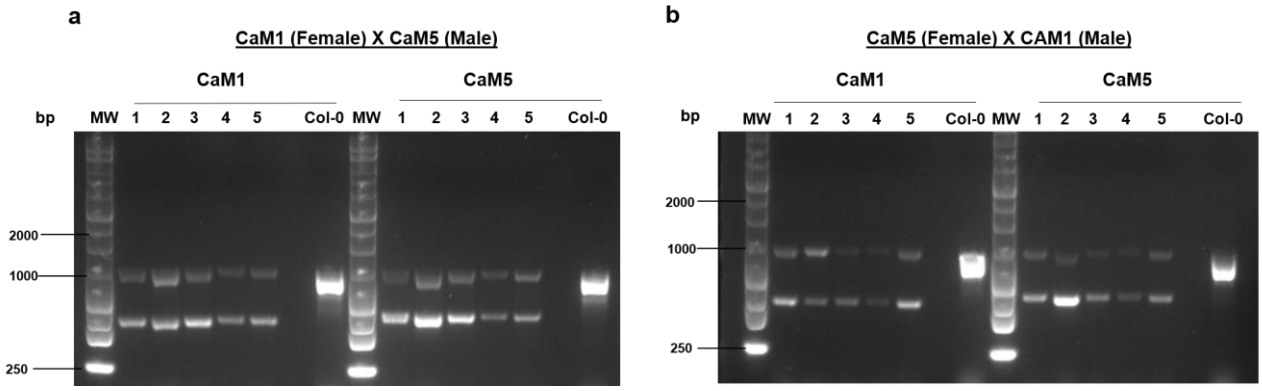

Figure 9: Genotyping of the double T-DNA insertion lines of CaM1 and CaM5 at the F1 generation. (**a-b**) Genotyping of the double mutant of CaM1 (Female) X CaM5 (male) (**a**) and CaM5 (female) X CaM1 (male) (**b**). The set of primer LP+RP and BP+RP, (sequence obtained from the SALK institute) were using for the genotyping. Two individual PCR reactions were performed for each plant, and DNA products obtained were mixed and loaded in gels. Col-0 was used as a control for the length of *CaMs* amplification. Numbers represent individual offspring of each F1 T-DNA insertion lines of CaM1 and CaM5 on top of each lane of the gel.

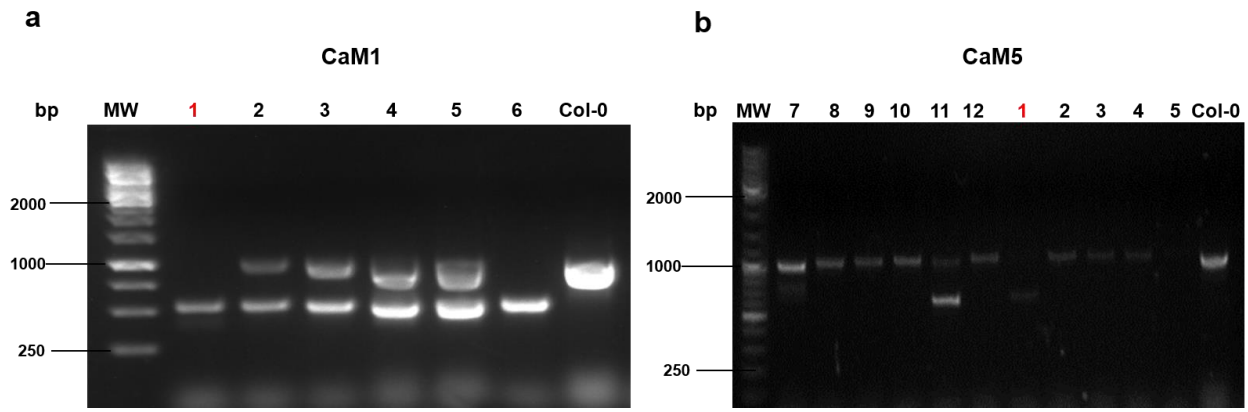

Figure 10: Isolation of a double homozygous T-DNA *cam1/cam5* mutant at the F2 generation. (**a-b**) Genotyping of the double mutant at the F2 generation for *CaM1* (**a**) and *CaM5* (**b**). The set of primer LP+RP and BP+RP, (sequence obtained from the SALK institute) were using for the genotyping. Two individual PCR reactions were performed for each plant, and DNA products obtained were mixed and loaded in gels. Col-0 was used as a control for the length of CaM amplification. Numbers represent individual offspring of each F2 T-DNA insertion lines of CaM1 and CaM5 on top of each lane of the agarose gel.

Discussion

The role of CaM1 and CaM5 in the heat signal and their impact on the HSR is unclear. At 22°C, W5 and W7 inhibitors showed a slight activation of nLUC-DAO1 suggesting that some CAMs may are involved in the repression of the HSR at non-HS temperature. In contrast, at 34°C, both inhibitors reduced significantly, at least 3 times, the HSR compared to untreated plants (Fig. 2). This result suggests that CaMs mediate the heat signaling during HS such as AtCaM3 (2,3). CaMs may have also an inhibitor effect at a low temperature, where their lack of activity leads to a slight HSR in the HIBAT line. Noticeably, CaMs could possibly ensure a dual role of being activator and inhibitor of the HSR.

Two single mutants were successfully isolated by CRISPR/Cas9 at the T2 generation for *CaM1* and *CaM5* genes. Both genes showed a deletion or a frameshift in their respective coding sequence (Figs. 4 and 5). In contrast, a double mutant of *cam1* and *cam5* was not generated (Fig. 6). It was shown that Cas9 did not obligatory recognize all gRNAs designed and can induce "off-target" positions in the genome at chromosomal locations that were not intended but nevertheless cut in cells (7,8). These observations might indicate that the Cas9 enzyme did not recognize all gRNAs and resulted in the absence of a deletion or a frameshift in *CaM1* or *CaM5*. Thus, the generation of a double mutant was focused on the T-DNA approach. The SALK_027181 T-DNA insertion line is defective to accumulate CaM5 mRNA, whereas further evidence is required for the SALK_202076C line even though the insertion is located in the exon II of CaM1 (9). Single

homozygous T-DNA insertion lines apparently showed an optimal accumulation of sHPS17.7 under HS compared to Col-0 (Fig. 8). It remains to perform an additional experiment for the CaM5 line to validate the phenotype. If an absence of sHSP17.7 is observed, it would indicate that both genes are not involved in the transmission of the heat signal. However, in *A. thaliana*, the plasma membrane Ca^{2+} ATPase (PMCA) have 2 CaMBD on its cytosolic part. The activity of PMCA depends of the number of AtCaM7 bound. A moderate activity was observed when one of the CaMBD of PMCA was attached by AtCaM7, whereas two bound AtCaM7 on the CaMBD are needed to fully activate of PMCA (10). These observations would indicate putatively that CNGC2 has to be bound by CaM1 and CaM5 to mediate the HSR. Therefore, the isolation of the double T-DNA *cam1/cam5* mutant obtained would serve to address this question (Fig. 10).

Although CaM1 and CaM5 were found to interact with CNGC2, it is also important to emphasize that these CaMs may not obligatorily be linked with the heat shock signaling pathway where they have been described in several responses in cells. For example, in *A. thaliana*, AtCaM1 positively regulates the production of ROS, leaf senescence, and ABA response (11). In soybean, CaM1 was also described to negatively regulate MYB2 which is involved in the salt and dehydration stresses response. In tobacco cells, CaM5 was described to mediate the plant disease signaling resistance (12–14). Additionally, CNGC2 was not only found to mediate the heat signaling but also to activate responses against the infection of pathogens (15). Altogether, these observations suggest that CaM1 and CaM5 may not be involved in the heat signaling and mediate other cellular signals when bound to CNGC2. Therefore, the double yeast hybrid, which leads to identify these two CaMs, might result from an artifact and remained to be further analyzed.

Conclusion

A double *cam1/cam5* mutant seems to be generated and the role of both genes in the heat shock signaling pathway might be addressed. To render these lines of research publishable, the lack of transcript expression of CaM1 and CaM5 by qPCR must be validated to ascertain the generation of a true-knockout line. Thereafter, the defective expression of HSPs under HS and a lack of ability of the double mutant to establish the AT would indicate the possible role of these two genes in the HSR. An RNA sequencing on the double mutant would show if several heat-inducible genes are found to be downregulated under HS. Additionally, at low and high temperatures, a pull-down assay and a quantitative mass spectrometry could possibly indicate if both proteins are bound to

CNGC2 and at which concentration level. The localization of CaM1 and CaM5 in vivo bound to CNGC2, by using fluorescent protein reporters, would ultimately validate their interaction at low and high temperatures and to confirm the yeast two-hybrid assay.

Materials and methods

Sequence alignment of calmodulins

Proteins sequences of CaMs from *A. thaliana* were obtained on TAIR (https://www.arabidopsis.org/). CaMs were then aligned in MEGA7 (version 7.0) Protein sequences comparative alignment between calmodulins, percentage of identity, and phylogenetic tree were obtained. The evolutionary history was inferred by using the Maximum Likelihood method based on the JTT matrix-based model. The initial tree for the heuristic search was obtained automatically by applying Neighbor-Join and BioNJ algorithms to a matrix of pairwise distances estimated using a JTT model and then selecting the topology with superior log likelihood value. The analysis involved 9 amino acid sequences from the calmodulins. All positions containing gaps and missing data were eliminated. There was a total of 149 positions in the final dataset of *A. thaliana*.

Protein extraction

5 to 8 weeks old leaves from plants were grinded by a plastic pestle in an Eppendorf tube of 1.5mL and resuspended with a BAP buffer (50 mM Tris-HCL (pH 7.5), 100 mM NaCl, 250 mM mannitol, 5 mM EDTA, 10% (v/v) glycerol, and protease inhibitor cocktail diluted at 1:300 (v/v) (Sigma-Aldrich, ref P9599). Protein extracts were centrifuged for 10 min at 12 000g and at 4°C. Supernatants (soluble proteins) were transferred in a new Eppendorf tube of 1.5mL and protein concentrations were determined by BRADFORD assay (Sigma-Aldrich, ref 23238). The bioluminescence (nLUC-DAO1) was detected by using the Nano-Glo Luciferase Assay System Kit from Promega (ref 1110) and the HIDEX plate reader (version 5067). The bioluminescence was analyzed for 1 second giving count per second. The bioluminescence emission was converted in ng of nLUC-DAO1 per ug total of protein through a standard calibration curve of nLCU as shown in Chapter 2.

Western blot

Protein extract was homogenized in LBX buffer (Tris-HCL 0.5 M (pH 6.8), 20% glycerol (v/v), 20% SDS (w/v), 4% bromophenol blue (w/v), 5% 2-mercaptoethanol (v/v), and heated for 3 min at 90°C. Homogenates were loaded in Precast SDS PAGE gels 12% acrylamide (EXPEDON, ref Ab 119207). Electrophoresis was applied at 100 V for 15 min

and then 45 min at 130 V (constant amperage) using the associated buffer of Precast SDS PAGE gels diluted at 1:50 (v/v). Precast SDS PAGE gels were transferred to nitrocellulose blotting membrane 0.2 µM (GE Healthcare Life Sciences, ref 10600001) by wet transfer using TRT buffer (20% (v/v) absolute Ethanol, and 5% (v/v) of the buffer associated with Precast SDS PAGE gels) for 50 min at 80 volts (amperage constant). Staining by PONCEAU S (Sigma-Aldrich, ref 09276) was applied on membranes for 5 min and the excess was washing with distilled water.

Membranes were blocked by using TRM buffer (5% milk powder (v/v), 50 mM Tris-HCL (pH 8), 150 mM NaCl) for 1 hour at room temperature. Primary antibody sHSP17.7 (from Abcam, ref Ab80171) was diluted at 1:2000 (v/v) in TRM buffer and the solution covered membranes for 2 hours at room temperature with gentle agitation. Membranes were then washed 3 times for 10 min (gently agitation) with TRM buffer without milk and replace by 0.1% (v/v) Tween 20. Secondary peroxidase-conjugated goat antibody against rabbit IgG (from Biorad, ref 170-5046) was diluted at 1:2000 (v/v) in TRM buffer and the solution covered membranes for 1 hour at room temperature with gentle agitation. Membranes were still washed 3 times. The revelation was done by using the kit Clarity Western ECL substrate (Biorad, ref 102031318 and 102031316) and the acquisition was performed by using ImageQuant LAS 500 automatic exposition.

W5 and W7 inhibitors assays

HIBAT line plants were grown in plates containing ½MS medium with 2.20 g/L of Murashige and Skoog media including MES buffer (Duchefa Biochimie, ref P14881.01), 8 8 g/L of agar (pH 5.8) in continuous day condition (22°C). Seeds were always incubated at 4°C for 2 days to break dormancy. At 12 days old, seedlings (n= 10-15, 4 replicates) were added in an Eppendorf tube and with 1 mL of Evian water and with the additional presence of 100 µM of W5 (Hello bio, ref HB0649) and/or 100 µM W7 (TOCRIS, ref 0369). Seedlings were then subjected to 22°C or 34°C for 2 hours followed by 2 hours of post-induction at 22°C. Proteins were then extracted following the same protocol in the section Materials and Methods “protein extraction and analysis” in order to analyze the amount of nLUC-DAO1.

Statistical analysis

We assume a normal distribution of values and homogeneity of variance by using the Leven test for all replicates. The determination of statically differences between samples was evaluated by Student’s T.test using the R software (version 4.0.3).

Extraction of genomic DNA and PCR

5 weeks old leaves from each individual plant were crushed and grinded by a plastic pestle in an Eppendorf tube of 1.5mL. Extracts were resuspended in 600 µl of STE-lysis buffer (100mM Tris-HCL (pH 7.5), 2% (w/v) SDS, and 10 mM of EDTA) and incubated at 65°C for 20 min minimum. Thereafter, DNA extractions were cooled on ice (4°C) for 5 min and 200 µl of NH_4Ac (10M) were added, mixed, and centrifuged at 12 000g for 10 min. 650 µl of the supernatants were transferred in a new tube and 650 µl of isopropanol (100%) was added, mixed, and incubated for 5 min at room temperature and then centrifuged for 10 min at 12 000g. Supernatants were removed and pellets were washed with 1 mL of cold ethanol 70% and re-centrifuged for 10 min at 12 000g. This wash step was repeated 2 times. Ethanol was then removed from tubes let open until that pellets became transparent and dry. DNA extracts were finally resuspended in 100 µl of EB buffer (10mM of Tris-HCL pH 8.0). DNA was amplified by using the corresponding set of primers for each plant. PCR product was loaded in a gel (1% (w/v) of agarose, tris-base 40 mM, 20 mM acetic acid, 1mM EDTA, and gel red DNA marker diluted 1:20 000 (v/v) (BIOTIUM, ref 41001)) and migrated by electrophoresis at 80 Volt for 10 min follow by 120 V for 30 min.

T1 and T2 segregation analysis of transformant CRISPR CaMs lines by microscopy

Seeds emitting red fluorescent (red TAG) were picked up with wet wooden toothpick at the T1 generation being viewed with epifluorescence microscopy (excitation wavelength 495 nm). At the T2 generation, seeds that were not emitted red fluorescence were pick up to not having the constitutive expression of Cas9 protein.

T-DNA insertion lines and generation of the double mutants

SALK_202076C (CAM1) and SALK_027181 (CAM5) were obtained from NASC (http://arabidopsis.info/BasicForm). The genotyping of both T-DNA insertion lines was done by following the protocol from the Salk institute genomic analysis laboratory (http://signal.salk.edu). Primer set for SALK_202076C: CAM1_LB 5'-TTTCAGCGACCTCTGTTTGTC-3' and CAM1_RP 5'- ATGTTCATTCGCTTTTGCATC-3. Primer set for SALK_027181: CAM5_LB 5'-TCCATTTTTGATTTTATTCCCC-3' and CAM1_RP 5'- AAGAAGCTTTCAGGGTTTTCG -3'. The primer used for BP Salk lines: LBb1.3_Salk 5'-ATTTTGCCGATTTCGGAAC-3'. Both Homozygous lines were then crossed between them to generate the double mutant CAM1 and CAM5. 10 individual lines were harvested at the F1 generation. At the F2 generation they were segregated on

hygromycin (30 mg/mL) plates ½MS medium in short days conditions (22°C in an 8/16 hours light/dark cycle) for 3 weeks. Survivals were then genotyped for both genes using the same set primers previously described.

Methodology of the generation of single and double mutant lines of *cam1* and *cam5* by CRISPR engineering

In an attempt to create single and double mutant lines of *cam1* and *cam5* by CRISPR/Cas9, 8 gRNAs were designed in the exons expecting to induce a large deletion and inactivate the transcription of both genes. 4 gRNA were designed to target the two exons of CaM1, and 4 other gRNA were designed to target exons 2 and 3 of CAM5 (Fig. 11). The exact position of gRNAs and primers on both genes is mentioned in Table 1. gRNAs were firstly designed on CRISP v2.0 website (http://crispr.hzau.edu.cn/cgi-bin/CRISPR2/CRISPR) by focusing mainly on the low number of mismatch sequences and on the high level of the ON-score for *CaM1* or *CaM5* in their exons. Thereafter, oligonucleotides guides ordered were annealed and ligated individually in entry vectors which all contained a ubiquitin promoter to express constitutively the gRNA. The 2 or 4 gRNAs were transferred in an intermediate vector, depending on the number of gRNAs (2 or 4), by golden gate assembly. Next, the intermediate vector, that contained all gRNAs designed, was cloned in a final vector by gateway reaction that contained the enzyme Cas9 and the constitutive expression of oleosin fused to a red TAG which was employed, after infection by *A. tumefaciens*, to detect transformant seeds (Fig. 11). Thus, a total of 6 different CRISPR lines were created by using 2 or 4 gRNAs in an attempt to generate single and double mutant of *cam1* and *cam5* (Table 2). All vectors were kindly provided by Niko Geldner group (University of Lausanne, unpublished). Transformation to Col-0 *A. thaliana* plants was performed as same in the section Material and Methods of chapter 2 included the red seeds transformant lines. All lines were growing in a growth chamber in long day conditions (22°C in a 16/8 hours light/dark cycle). DNA amplification of *CaM1* and *CaM5* obtained by PCR were then sequenced by Microsynth company. Gap or frameshift sequences were analyzed by Benching website (https://benchling.com) and aligned against the reference genes of *CaM1* and *CaM5* using Clustal Omega website (https://www.ebi.ac.uk/Tools/msa/clustalo/).

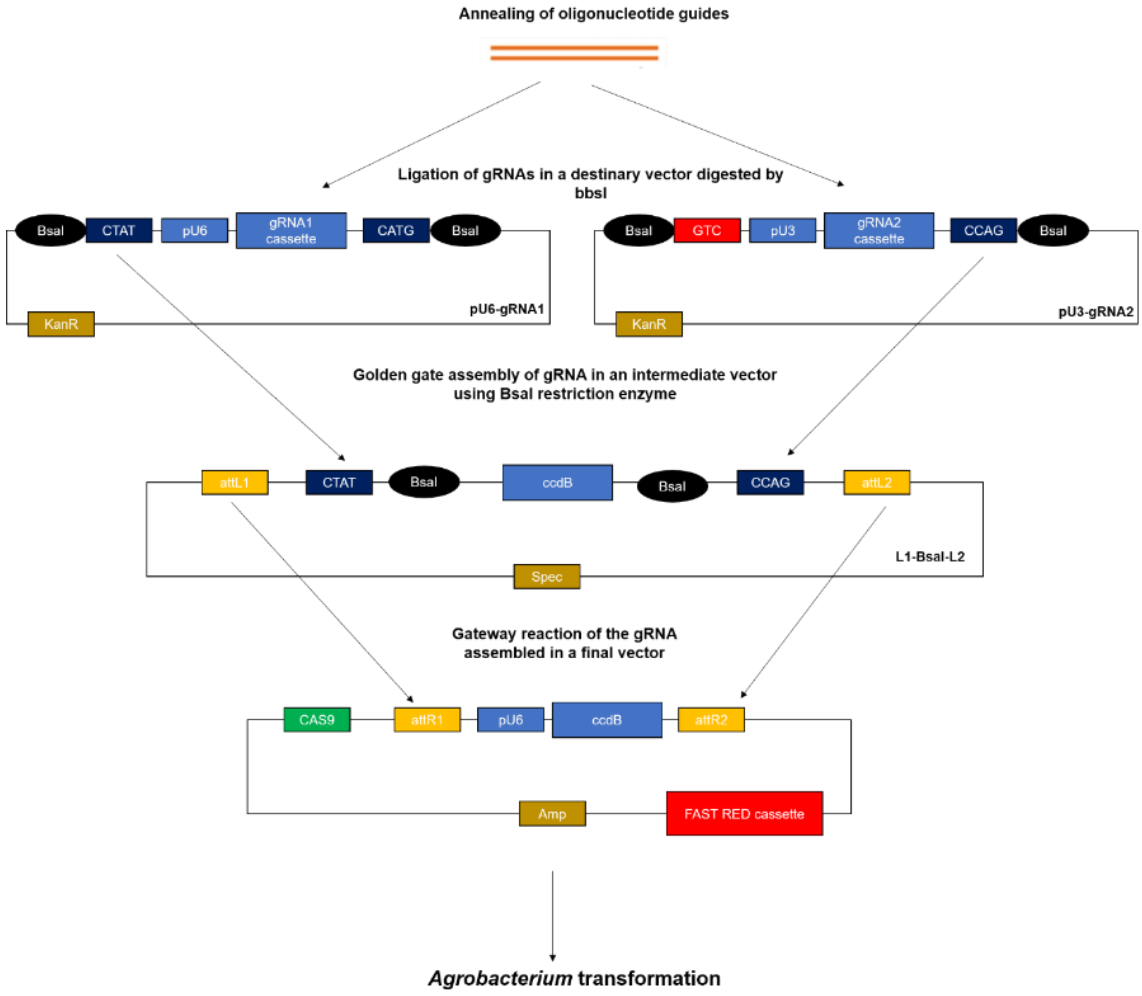

Figure 11: Schematic representation of the cloning steps of 2 and 4 gRNAs in a final vector for the transformation in Col-0 plant to generate *cam1* and *cam5* single mutant and double mutants. Oligonucleotide guides were firstly annealed and ligated in an entry vector (pU6-gRNA) which was previously digested by the BbsI restriction enzyme. Each vector contained a ubiquitin promoter (pU6 or pU3) to express constitutively the guide RNA and a cassette of kanamycin resistance (KanR). Guides RNA was then assembled in an intermediate vector (L1-BsaI-L2) by Golden Gate assembly targeting the replacement of the DNA gyrase poison gene (*ccdB*). The intermediate vector contained a spectinomycin cassette resistance for selection. Finally, gRNAs, that were assembled in the same vector, were then cloned in the final vector by Gateway reaction (attR1, attR2, attL1, and attL2) to replace the *ccdB* gene. The final vector contained the constitutive expression of Oleosin fused to red tag (Fast red cassette) which was used to select positive transformants in *A. thaliana* and resistance against ampicillin (Amp). Once the final vector that contained gRNAs, it was then cloned in *Agrobacterium tumefaciens* (strain GV3101) to infect and generate *cams* mutants**.**

CaMs	Name of gRNAs and Primers	Sequence	Position of gRNAs and primers on the gene	Expecting amplification according to primers used by PCR
CaM1 (1679bp)	Guide 1	GTTGCATCACAACAAAAGAGCT	1064	Primer 1+Primer 2=1193bp Primer 2+Primer 3= 1520bp
	Guide 2	ATCACATGGCGTAGCTCAGCAG	1295	
	Guide 3	TGATGGCTAAGTGATTTGATAA	1430	
	Guide 4	AGGCTAAAAGCTTCCTTGAATT	122	
	Primer 1	GCTTGTTGTCCTGTTTCGTTGA	425	
	Primer 2	ACCCATCGGTTTCAATCCAACT	1608	
	Primer 3	ATACCGCCTAGTTGAGTGACTG	88	
CaM5 (2393bp)	Guide 1	TGAGTTTCTGAACCTAATGGCT	845	Primer 1+Primer 2=596bp Primer 1+Primer 3=1642bp
	Guide 2	TCAAAGTTATGATGGCAAAGTG	1071	
	Guide 3	TAGCCATTAGGTTCAGAAACTC	844	
	Guide 4	AAATCCGTTTAATGGGTGTGAG	2274	
	Primer 1	GCATCACAACGAAAGAGCTAGG	725	
	Primer 2	AAAAAAGTACTAATACCAAGAG	1321	
	Primer 3	GCCTAAATGAACTTACTATATTGAT	2367	

Table 1: Localization and expected DNA length amplification for each gRNAs and primers designed for *CaM1* and *CaM5*. The position of gRNAs and primers are mentioned in the third column for each gene. The fourth column represents the expected amplification according to the set of primers used.

CRISPR lines generated	Guides designed in CaM1	Guides designed in CaM5	Expecting size by PCR amplification if all guides were targeted by CRISPR	Reference size if not targeted by CRISPR
C1.1	Guide 1 and 2	/	Primer 1+ Primer 2= 962bp	1193bp
C1.4	All 4 guides	/	Primer 2 + Primer 3=578bp	1520bp
C5.1	/	Guide 1 and 2	Primer 1 + Primer 2= 370bp	596bp
C5.4	/	All 4 guides	Primer 2+ Primer 3= 213bp	1642bp
C1.5'	Guides 1 and 2	Guides 3 and 4	CAM1 with Primer 1 + Primer 2= 962bp CAM5 with Primer 2 + Primer 3= 213bp	CAM1= 1193bp CAM5= 1642bp
C5.1'	Guides 3 and 4	Guides 1 and 2	CAM1 with Primer 2+ Primer 3= 578bp CAM5 with Primer 1+ Primer 2= 370bp	CAM1= 1520bp CAM5= 596bp

Table 2: Generation of 6 individual lines by CRISPR/Cas9 engineering of *cam1* and *cam5* single and double mutants. Two single mutants of *CaM1* called C1.1 and C1.4 contained 2 or 4 gRNAs. The same approached was performed for the *CaM5* gene respectively C5.1 and C5.4. Two lines were also generated for a double mutant *cam1* and *cam5*, C1.5' and C5.1', based on the same gRNAs used to generate the single mutant lines. Expecting size by PCR, for each mutant line generated which present a deletion in genes, are mentioned in the fourth column compared to the length of the reference genes (fifth column).

Contributions

Help was provided, for CRISPR strategy and gRNAs designed, by Dr. Robertas Ursache, Dr. Ines Barbosa, Dr. Anthony Guihur, and the laboratory technician Caroline Darimont-Nicolau. The yeast two-hybrid assay were performed by Dr. Anthony Guihur and the laboratory technician John Perrin. The percentage of CaMs homology and identity was contributed by the Ph.D. student Mathieu Rebeaud. The selection of the double

cam1/cam5 mutant on hygromycin media was contributed by the apprentice laboratory technician Gizem Demirkiran.

References

1. Finka A, Cuendet AFH, Maathuis FJM, Saidi Y, Goloubinoff P. Plasma Membrane Cyclic Nucleotide Gated Calcium Channels Control Land Plant Thermal Sensing and Acquired Thermotolerance. Plant Cell [Internet]. 2012;24(8):3333–48. Available from: http://www.plantcell.org/cgi/doi/10.1105/tpc.112.095844

2. Liu HT, Sun DY, Zhou RG. Ca2+ and AtCaM3 are involved in the expression of heat shock protein gene in Arabidopsis. Plant, Cell Environ. 2005;28(10):1276–84.

3. Zhang W, Zhou RG, Gao YJ, Zheng SZ, Xu P, Zhang SQ, et al. Molecular and genetic evidence for the key role of AtCaM3 in heat-shock signal transduction in arabidopsis1[W][OA]. Plant Physiol. 2009;149(4):1773–84.

4. Mittler R, Finka A, Goloubinoff P. How do plants feel the heat? Trends Biochem Sci [Internet]. 2012;37(3):118–25. Available from: http://dx.doi.org/10.1016/j.tibs.2011.11.007

5. AL-Quraan NA, Locy RD, Singh NK. Expression of calmodulin genes in wild type and calmodulin mutants of Arabidopsis thaliana under heat stress. Plant Physiol Biochem [Internet]. 2010;48(8):697–702. Available from: http://dx.doi.org/10.1016/j.plaphy.2010.04.011

6. Osawa M, Kuwamoto S, Izumi Y, Yap KL, Ikura M, Shibanuma T, et al. Evidence for calmodulin inter-domain compaction in solution induced by W-7 binding. FEBS Lett. 1999;442(2–3):173–7.

7. Haeussler M. CRISPR off-targets : a question of context. 2020;5–9.

8. Zischewski J, Fischer R, Bortesi L. Detection of on-target and off-target mutations generated by CRISPR / Cas9 and other sequence-speci fi c nucleases. Biotechnol Adv [Internet]. 2017;35(1):95–104. Available from: http://dx.doi.org/10.1016/j.biotechadv.2016.12.003

9. Al-quraan NA, Locy RD, Singh NK. Plant Physiology and Biochemistry Expression of calmodulin genes in wild type and calmodulin mutants of Arabidopsis thaliana under heat stress. Plant Physiol Biochem [Internet]. 2010;48(8):697–702. Available from: http://dx.doi.org/10.1016/j.plaphy.2010.04.011

10. Tidow H, Nissen P. Structural diversity of calmodulin binding to its target sites. FEBS J. 2013;280(21):5551–65.

11. Dai C, Lee Y, Lee IC, Nam HG, Kwak JM. Calmodulin 1 regulates senescence and ABA response in Arabidopsis. Front Plant Sci. 2018;9(July):1–13.

12. Heo W Do, Lee SH, Kim MC, Kim JC, Chung WS, Chun HJ, et al. Involvement of specific calmodulin isoforms in salicylic acid-independent activation of plant disease resistance responses. Proc Natl Acad Sci U S A. 1999;96(2):766–71.

13. Aldon D, Galaud J. Plant Calmodulins and Calmodulin-Related Proteins. 2006;(June):96–104.

14. Jae HY, Chan YP, Jong CK, Won DH, Mi SC, Hyeong CP, et al. Direct interaction of a divergent CaM isoform and the transcription factor, MYB2, enhances salt tolerance in Arabidopsis. J Biol Chem. 2005;280(5):3697–706.

15. Clough SJ, Fengler KA, Yu IC, Lippok B, Smith RK, Bent AF. The Arabidopsis dnd1 “defense, no death” gene encodes a mutated cyclic nucleotide-gated ion channel. Proc Natl Acad Sci U S A. 2000;97(16):9323–8.

Supplementary Data

	CaM1	CaM2	CaM3	CaM4	CaM5	CaM6	CaM7	CaM8
CaM1	/	/	/	/	/	/	/	/
CaM2	82.29/85.14	/	/	/	/	/	/	/
CaM3	82.29/85.14	100/100	/	/	/	/	/	/
CaM4	85.71/86.86	90.57/93.71	90.57/93.71	/	/	/	/	/
CaM5	82.29/85.14	100/100	100/100	90.57/93.71	/	/	/	/
CaM6	82.29/85.14	98.66/100.00	98.66/100.00	90.57/93.71	98.66/100.00	/	/	/
CaM7	82.86/85.14	99.33/100	99.33/100	91.19/93.71	99.33/100	99.33/100	/	/
CaM8	61.02/68.93	71.52/80.79	71.52/80.79	67.08/75.78	71.52/80.79	70.20/80.79	70.86/80.79	/
CaM9	43.50/55.37	49.01/64.90	49.01/64.90	47.83/60.87	49.01/64.90	49.01/64.90	49.67/64.90	46.05/62.50

Supp data 1: Percentage of identity and similarity of the 9 calmodulins in *A. thaliana*. The first number represents the percentage of identity and the second the similarity between calmodulins. Sequences were aligned and calculated in MEGA7 software (version 7.0).

Chapter 7: Generation of an *A. thaliana* transgenic line to analyze the effect of sHSP17.6a at low temperatures.

Abstract

Under HS, members of the HSP20 family are among the most dramatically induced HSPs in plants. In contrast to other HSPs, such as HSP70 and HSP90 which all have rather basal levels of accumulation at low temperatures, HSP20s are virtually not expressed at all. This observation raises the possibility that HSP20s may have a deleterious effect on plant fitness if they become expressed during unnecessary conditions. Here, we designed a cassette with a chemically inducible promoter which is expected, when transformed in *A. thaliana*, to accumulate different levels of sHSP17.6a in an attempt to address the role of HSP20 at low temperatures.

Introduction

The appropriate accumulation of HSP20s during a heat priming is correlated with the successful onset of AT in plants. Western and Northern blots analysis showed that some HSP20s, such as sHSP17.6a, are virtually absent from the cytosol of plants at 20°C (1–3). These results contrast with the other HSP molecular chaperone families which can present a constitutive expression. For example, both HSP90s and HSP70s have orthologs which are constitutively expressed and some which are heat-inducible (3). The transcriptome of HIBAT seedlings revealed that the members of the HSP20 family accumulated less transcript at 22°C compared to several classes of HSP70 and HSP90 (Fig. 1a). When seedlings were exposed at 38°C for 45 min, several HSP20s were found to accumulate 4 to 20-fold more of transcripts as compared to HSP70s and HSP90s (Fig 1b-d). These results confirm that members of HSP20 are the most repressed at 22°C and the most heat-inducible at 38°C compared to all HSP molecular chaperone families. Additionally, some members of HSP20, such as HSP15.4 and HSP14.7, are found to be repressed in both conditions. Whereas some HSP20s are more accumulated at 22°C compared to the other classes of HSP20s such as HSP18.5. These observations suggest that all HSP20s are not obligatorily heat-inducible and may participate in other functions in plant cells at low temperatures such as plant growth and development. The phylogenic tree seems to indicate that members of HSP20 slightly accumulated under both conditions (green frames) did not evolve separately from other HSP20s members (Fig. 2). The HSP20s family could be classified into two categories: The 1st group of HSP20s has members which are strongly repressed at 22°C and highly expressed at 38°C. The 2nd group contains members of HSP20s which are slightly expressed under both temperature conditions but not at a high level. It remains to understand the roles and functions of all members of HSP20s at low and high temperature in plant cells.

Both groups of HSP20s suggest that they might become problematic to plant physiology if they are highly expressed at low temperatures. To address this question, a recombinant *A. thaliana* line was generated which contain a chemical inducible promoter that can induce different quantity of sHSP17.6a only with the presence of imethoxfenozid (4,5). We expect that the accumulation of sHSP17.6a might reveal why this protein is so strongly repressed at low temperatures.

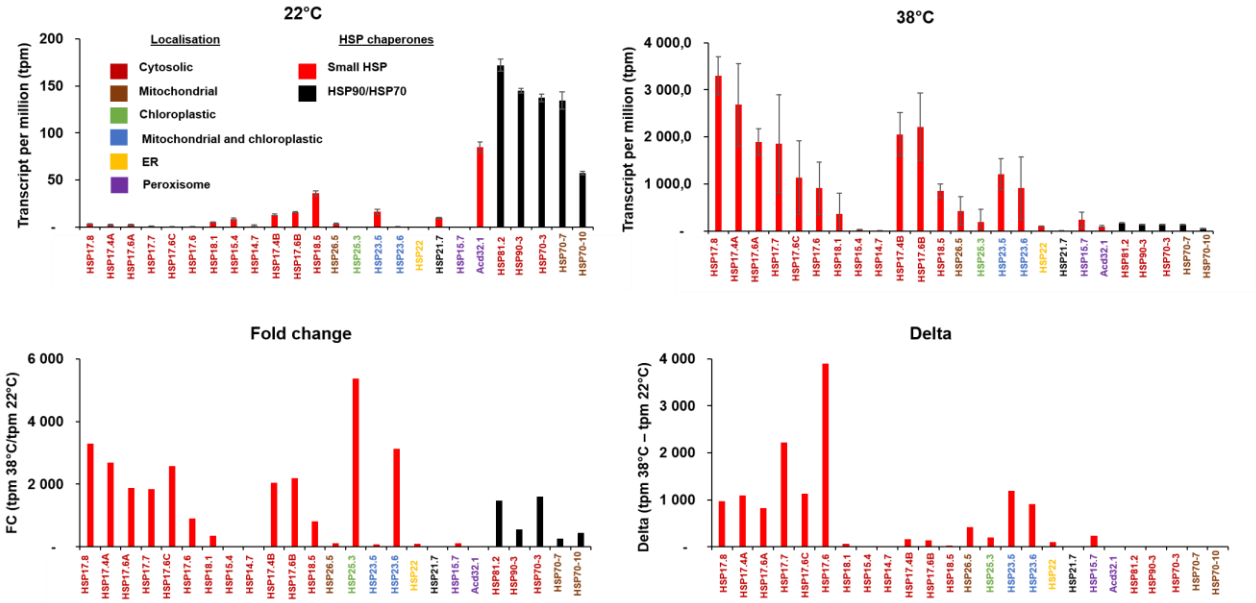

Figure 1: RNA sequencing data of HSP20 members at 22°C and 38°C in *A. thaliana*. (**a-b**) Accumulation of RNA transcript of HSP20s at 22°C (**a**) and 38°C (**b**). (**c**) Fold change obtained by the division of tpm at 38°C of HSPs by the tpm at 22°C. (**d**) Delta obtained by the subtraction of division of tpm at 38°C of HSPs by the tpm at 22°C. 2 weeks old seedlings were exposed at 22°C or 38°C for 40 min. RNA was extracted from both conditions, submitted to RNA sequencing facilities and the accumulation of transcript was obtained. The members of HSP20 are indicated in red, whereas some members of HSP90 and HSP70 are in black. The cellular localization of all HSP are indicated in the figure legend.

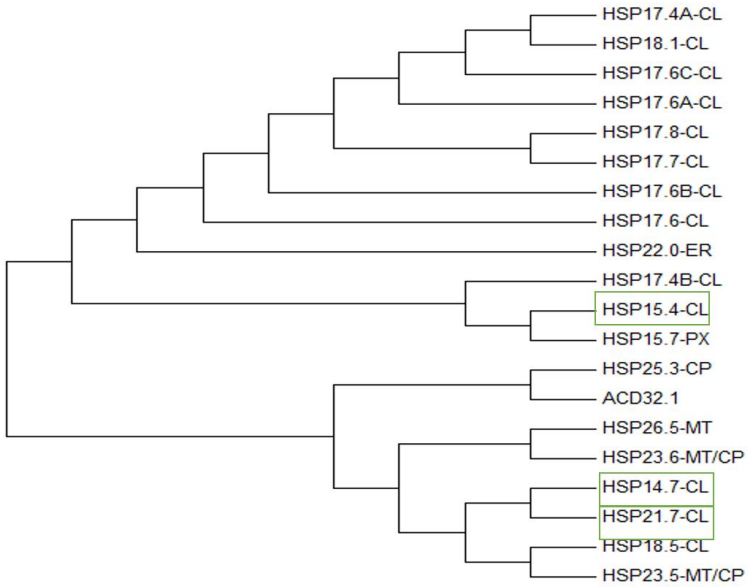

Figure 2: Phylogenetic tree analysis of protein sequences of HSP20s in *A. thaliana*. Phylogenetic tree of 17 HSP20s. The green frame underlines the members of HSP20 which are not highly expressed at low and high temperatures. The evolutionary history was inferred by using the Maximum Likelihood method based on the JTT matrix-based model. The initial tree for the heuristic search was obtained automatically by applying Neighbor-Join and BioNJ algorithms to a matrix of pairwise distances estimated using a JTT model

and then selecting the topology with superior log likelihood value. The analysis involved 20 amino acid sequences from the small HSPs. All positions containing gaps and missing data were eliminated. All ambiguous positions were removed for each sequence pair (pairwise deletion option). There was a total of 133 positions in the final dataset. Evolutionary analyses were conducted in MEGA7 software (version 7.0). CL= Cytosolic, MT= Mitochondrial, CP= Chloroplast, ER= Reticulum endoplasmic, PX= Peroxisome, ACD= Alpha crystallin domain.

Results

The *A. thaliana* transgenic line generated is called “CHEMICAL INDUCTION HEAT SHOCK PROTEIN” (CIHSP). It contains a transgene based of two systems of expression that lead ultimately to the production of sHSP17.7a (Fig. 3). The first system consists of a constitutive promoter from *cassava vein mosaic virus* (CsVM) that drives the expression of a fusion monomeric protein, called AGE. It is made of a the bZIP sequence from rice (RFA2), the DNA-binding domain of yeast (GAL4), and the ecdysone-binding region from the spruce budworm *C. fumiferana* (6–8). In the presence of the ligand imethoxfenozide, AGE becomes activated by dimerization and binds the inducible promoter 5XUAS which lead to the transcription of sHSP17.6a (9). Therefore, CIHSP lines are expected to express the sHSP17.6a at low temperatures by chemical induction.

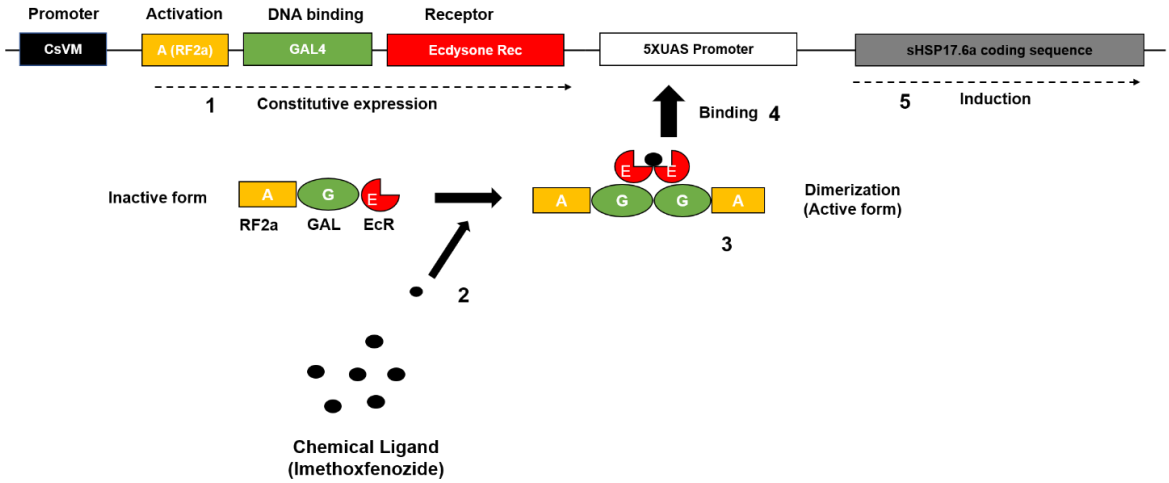

Figure 3: System of sHSP17.6a expression by chemical induction. The system contains a constitutive *cassava vein mosaic virus* (CsVM, black). It results in AGE protein expression made of bZIP protein from rice (RF2a, yellow), a DNA-binding domain from yeast (GAL4, green), and the ecdysone-binding region from the spruce budworm *C. fumiferana* (E, red). AGE protein is expressed constitutively in an inactive form (**1**). In the presence of the ligand imethxfenozide (**2**), AGE becomes in an active form by dimerization (**3**). AGE binds the 5XUAS (white) promoter (**4**) leading to the induction of sHSP17.6a under non-induced temperatures (grey) (**5**).

Col-0 plants were transformed, with the construct shown in Figure 2, by Agrobacterium to generate several T1 CIHSP lines. The segregation of transformant

plants was performed on hygromycin media and 8 CIHSP lines were selected to be resistant. At the T2 generation, isolated lines were re-segregated on hygromycin media to address the number of transgene copy (Fig. 4a). We aimed to select lines with a single copy that several copies would increase the chance to affect coding regions. 6 CIHSP lines showed 75% of offspring survival which suggests the presence of a single copy such as CIHSP-2. The presence of the transgene was validated by PCR (Supp data. 1). The other lines which presented more than 75% of offspring survival were excluded which indicated multi-insertion such as T2-CIHSP-1 (91%) (Fig. 4b). Thus, 6 lines which contained a single copy of the transgene were isolated and chosen (Table 1).

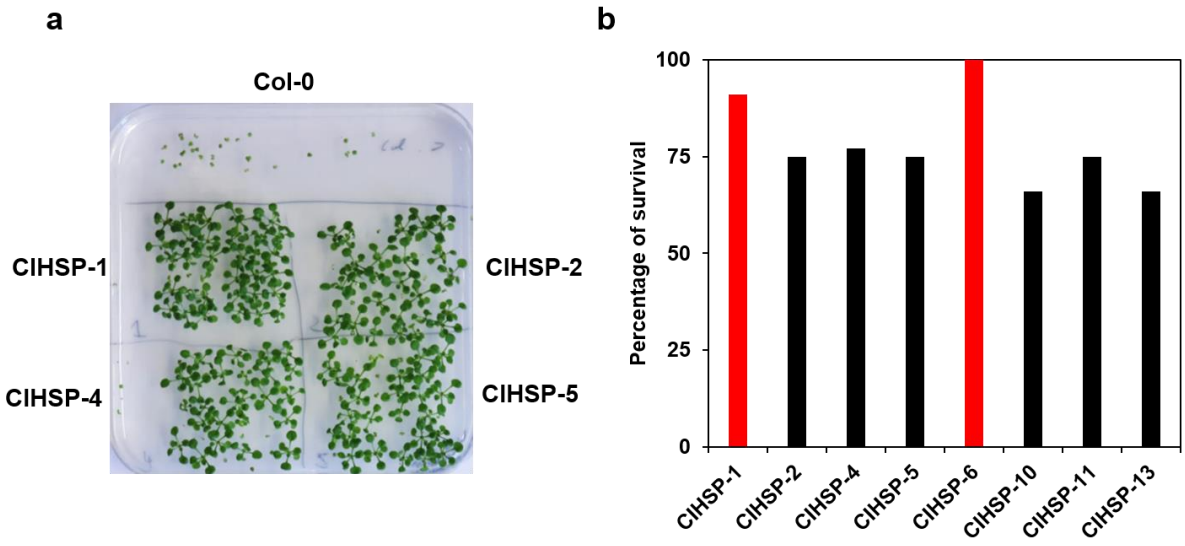

Figure 4: Segregation of the T2 CIHSP on hygromycin media and prediction of the transgene copy number. (**a**) Selection of the CIHSP T2 survivals on hygromycin media at 21 days. Col-0 was used as a negative control and was unable to survive (Top of the plate). (**b**) Percentage of the survival of the T2-CIHSP lines found to predict the number of transgene copy. A ratio of survival higher than 75% is predicted to have multi-insertion (black bars), whereas a ratio close to 75% (red bars) indicates the presence of a single copy (n=36 offspring per T2-CIHSP line).

Lines T2	Number of survival after segregation on hygromycin plates (n= 36)	Prediction of copy number	Name of individual offspring after segregation	Total of individual line selected
CIHSP-1	33 (91%)	Multicopy	CIHSP-1-36	1
CIHSP-2	27 (75%)	Single copy	CIHSP-2-30 and CIHSP-2-33	2
CIHSP-4	28 (77%)	Single copy	CIHSP-4-25 and CIHSP-4-26	2
CIHSP-5	27 (75%)	Single copy	CIHSP-5-19 and CIHSP-5-20	2
CIHSP-6	36 (100%)	Multicopy	CIHSP-6-10, CIHSP-6-11, and CIHSP-6-12	3
CIHSP-10	24 (66%)	Single copy	CIHSP-10-2, CIHSP-10-4, CIHSP-10-5, CIHSP-10-6, and CIHSP-10-8	5
CIHSP-11	27 (75%)	Single copy	CIHSP-11-56, CIHSP-11-58, CIHSP-11-59, CIHSP-11-60, and CIHSP-11-62	5
CIHSP-13	24 (66%)	Single copy	CIHSP-13-42, CIHSP-13-44, and CIHSP-13-46	3

Table 1: Prediction of the copy number of the transgene in the CIHSP lines at the T2 generation. 36 offspring from 8 individual T2 CIHSP plants were segregated on hygromycin media. The number of survivals was calculated at 3 weeks old (column 2). It resulted in 75% survival for one transgene copy, whereas a higher ratio indicated multi-insertion according to the Mendelian type of segregation. Several individual offspring were then selected at the T2 generation to have one transgene copy and analyzed at the T3 generation for their genotype (columns 4 and 5).

At the T3 generation, progenies CIHSP-2, CIHSP-4, CIHSP-5, and CIHSP-11 lines were submitted to another round of hygromycin selection in order to isolate homozygous T3 lines for the transgene insertion (Fig. 5a). It should result in 100% survival for a homozygous phenotype, whereas a lower rate indicates a mix in the population which might contain non-transformant (25%), heterozygous (50%), and homozygous (25%) offspring according to the Mendelian type of segregation. The line T3-CIHSP-11-56 showed 100% of offspring survival and was suggested to be homozygous (Fig. 5b). In contrast, other lines, such as CIHSP-2-33, showed a lower rate than 100% of offspring survival which indicated a heterozygous phenotype. Although those plants are heterozygous, they were selected to be screened at the next generation to isolate additional homozygous candidates (Table 2). Thus, it remains to analyze the CIHSP-11-56 line with the proper concentration of imethoxfenozide in order to induce the sHPS17.6a at low temperatures.

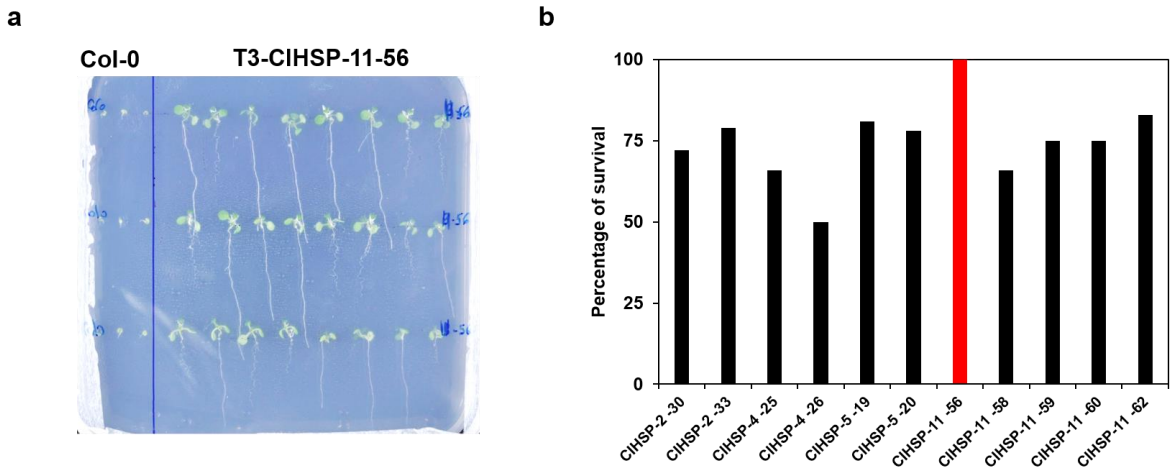

Figure 5: Segregation of T3-CIHSP single copy line on hygromycin media and isolation of the homozygous T3-CIHSP-11-56. (**a**) Segregation of T3-CIHSP-11-56 homozygous plant on hygromycin media at 21 days. Col-0 was used as a negative control and was unable to survive (Top of the plate). (**b**) Percentage of survival of T3-CIHSP single-copy lines to predict heterozygous or homozygous lines. It should result in 100% survival for the homozygous line (red bar), whereas a ratio lower than 100% of survival indicated homozygous lines (black bars) according to the Mendelian type of segregation (n=24 to 26 offspring per individual T3-CIHSP lines).

	CIHSP-2 -30	CIHSP-2 -33	CIHSP-4 -25	CIHSP-4 -26	CIHSP-5 -19	CIHSP-5 -20	CIHSP-11 -56	CIHSP-11 -58	CIHSP-11 -59	CIHSP-11 -60	CIHSP-11 -62
Number of Seeds sowed	26	25	24	24	24	24	24	24	24	24	24
Total seeds germinated	25	25	24	23	22	23	24	21	24	24	24
Number of survival	18 (72%)	19 (79%)	16 (66%)	12 (50%)	18 (81%)	18 (78%)	24 (100%)	14 (66%)	18 (75%)	18 (75%)	20 (83%)
Prediction	HZ	HZ	?	?	HZ	HZ	HM	/	HZ	HZ	HZ

Table 2: Segregation number of offspring survival of the T3-CIHSP lines. A total of 11 individual T3-CIHSP lines were segregated on hygromycin media and the number of survivals was calculated to predict heterozygous and homozygous lines. It results in 100% of survival for homozygous lines, whereas a ratio lower than 100% indicated heterozygous lines according to the Mendelian type of segregation (n=24 to 26 offspring per individual T3-CIHSP lines).

Discussion

The overexpression of sHSP17 *Agrostis stolonifera* in *A. thaliana* shows a reduction of leaf chlorophyll content leading to a clear reduction of photosynthesis activity at low and high temperatures (10). This observation suggests that some members of HSP20s are not beneficial for plant fitness. Here, several new transgenic lines were generated expecting to express the sHSP17.6a by chemical induction. We hypothesized that the constitutive expression of sHSP17.6a might induce a deleterious effect on plant fitness and would

indicate why plants need to repress several members of HSP20s at low temperatures. The advantage of the chemical promoter, in the CIHSP lines, is to control the expression of the sHSP17.6a by a dose-response which is not possible with a constitutive promoter. The positive candidate called CIHSP-11-56 was isolated to contain a single copy of the transgene and being homozygous at the T3 generation (Figs. 4 and 5). Because the transgene insertion cannot be predicted during the *A. thaliana* transformation, we aim at selecting several homozygous single copy CIHSP lines.

Thus, it remains to localize the insertion of the transgene in the genome of CIHSP-11-56 to ensure that it does not lead to affect the coding regions. A dose-response in the presence of imethoxfenozide must be performed in order to induce the higher level of sHSP17.6a at low temperatures which can be validated by qPCR and Western blot. Once the concentration of ligand identified, several assays can be investigated to demonstrate a putative deleterious effect. Physiological analysis of the plants which overexpressed sHSP17.6a at low temperatures would be visually observed to indicate disadvantage effects such as a delay in growth and development. Additionally, the abnormal production of ROS and the expression of genes involved in the cell death program, such as by RNA sequencing, would indicate if the unnecessary production of sHSP17.6a affects negatively plant cells. Yet, if an absence of disadvantage effect on plant is observed, the CIHSP line might serve to test the proper concentration of sHSP17.6a which is required for plants at surviving under HS.

Conclusion

The isolated line CIHSP-11-56 is expected to bring new knowledge about the role of sHSP17.6a and its impact at low temperatures in *A. thaliana*. The transcriptome analysis of HIBAT line suggests that members of HSP20s can be divided into 2 categories according to their expression level at low and high temperatures. Therefore, it is important to mention that only one class of HSP20s was chosen in our approach and its overexpression would not obligatorily induce a deleterious phenotype. If an absence of disadvantage effect is observed in CIHSP lines, it remains interesting to analyze the other members of HSP20s, if not all, at low temperatures.

Materials and methods

Sequence alignments of HSP20s

Proteins sequences of HSPs from *A. thaliana* were obtained on TAIR (https://www.arabidopsis.org/). HSPs were then aligned in MEGA7 (version 7.0) Protein sequences comparative alignment between HSPs and phylogenetic tree were generated. The evolutionary history was inferred by using the Maximum Likelihood method based on the JTT matrix-based model. The initial tree for the heuristic search was obtained automatically by applying Neighbor-Join and BioNJ algorithms to a matrix of pairwise distances estimated using a JTT model and then selecting the topology with superior log likelihood value. The analysis involved 20 amino acid sequences of HSPs. All positions containing gaps and missing data were eliminated. The TAIR ID used for the Figure 1 and 2 are the following: AT1G07400: HSP17.8; AT3G46230: HSP17.4A; AT1G59860: HSP17.6A; AT5G12030: HSP17.7; AT1G53540: HSP17.6C; AT5G12020: HSP17.6;AT5G59720: HSP18.1; AT4G21870: HSP15.4; AT5G47600: HSP14.7; AT1G54050: HSP17.4B; AT2G29500: HSP17.6B; AT2G19310: HSP18.5; AT2G19310: HSP18.5; At1g52560: HSP26.5; At4g27670: HSP25.3; At5g51440: HSP23.5; At4g25200: HSP23.6; At4g10250: HSP22.0; At5g54660: HSP21.7; At5g37670: HSP15.7; AT1G06460: ACD32.1; AT5G56030: HSP81-2; AT5G56010: HSP90-3; AT3G09440: HSP70-3; AT5G49910: HSP70-7; AT5G09590: HSP70-10.

Transformation of Arabidopsis plants and selection of CIHSP candidates

12 days old *A. thaliana* seedlings were submitted to 35°C for 40 min and the RNA was extracted from plants using MACHEREY-NAGEL NucleoSpin RNA plant KIT (REF 740949.50). cDNAs were obtained by using superscript II RNase A reverse transcriptase (Invitrogen, ref 18064-014). The coding sequence of sHSP17.6A was then amplified by PCR with a part of the cDNA sequence using the following set of primers: HSP17.6A_F 5'-CACCGAAACAATCGCTCTCTCT-3', HSP17.6A_F 5'-GAGGAATGACCATTCGCTGTC-3'. By GIBSON assembly (BioLabs, ref E5510S), the purified fragment obtained by PCR were then cloned in the digested vector pAGE5XGM35s (Martínez-Andújar et al., 2011) by using the following primers set: GHSP17.6a_F 5'-CGCTCGACCACCGAAACAATCGCTCTCTCTAC-3' and GHSP17.6a_R 5'-CGCCCGGGGAGGAATGACCATTCGGTGTCTT-3'. The insertion of the sHSP17.6a coding sequence was checked by PCR using the primers set HSP17.6A_F and M13_R 5'-TGTAAAACGGCCAGT-3'. The DNA product was sequenced to validate the absence of

mutations. The transformation vectors were introduced into *A. tumefaciens* strain GV3101 by electroporation and the resulting strains were used to transform *A. thaliana* Col-0 plants by the floral dip method (See chapter 2). Transformant plants at the T1, T2 and T3 generation were segregated on hygromycin (30 mg/mL) plates ½MS medium in short days conditions (22°C in an 8/16 hours light/dark cycle) for 3 weeks They were transferred in soil with long day conditions (22°C in an 16/8 hours light/dark cycle).

Extraction of genomic DNA and PCR analysis

5 weeks old leaves from each individual plant were crushed and grinded by a plastic pestle in an Eppendorf tube of 1.5mL. Extracts were resuspended in 600 µl of STE-lysis buffer (100mM Tris-HCL (pH 7.5), 2% (w/v) SDS, and 10 mM of EDTA) and incubated at 65°C for 20 min minimum. Thereafter, DNA extractions were cooled on ice (4°C) for 5 min and 200 µl of NH_4Ac (10M) were added, mixed, and centrifuged at 12 000g for 10 min. 650 µl of the supernatants were transferred in a new tube and 650 µl of isopropanol (100%) was added, mixed, and incubated for 5 min at room temperature and then centrifuged for 10 min at 12 000g. Supernatants were removed and pellets were washed with 1 mL of cold ethanol 70% and re-centrifuged for 10 min at 12 000g. This wash step was repeated 2 times. Ethanol was then removed from tubes let open until that pellets became transparent and dry. DNA extracts were finally resuspended in 100 µl of EB buffer (10mM of Tris-HCL pH 8.0). To validate the presence of the transgene at T2 generation, DNA of plants were amplified by using the set of primer GHSP17.6a_F and M13_R as mentioned above. PCR product was loaded in a gel (1% (w/v) of agarose, tris-base 40 mM, 20 mM acetic acid, 1mM EDTA, and gel red DNA marker diluted 1:20 000 (v/v) (BIOTIUM, ref 41001)) and migrated by electrophoresis at 80 Volt for 10 min follow by 120 V for 30 min.

Preparation of HIBAT sample for the RNA-seq

HIBAT line was grown in 1/2MS medium in continuous days conditions at 22°C. At 2 weeks old, seedlings were exposed to 22°C or 38°C for 40 min. RNA was extracted from plants using MACHEREY-NAGEL NucleoSpin RNA plant KIT (REF 740949.50). Three biological replicates (10-15 seedlings in each replicate) for each condition were sent for RNA sequencing with a total of 1ug of RNA (cDNA library used = Tuseq Stranded RNA, illumine sequencing = HISeq 2500).

RNA-SEQ processing

Purity-filtered reads were adapters and quality trimmed with Cutadapt (v. 1.8, Martin 2011). Reads matching to ribosomal RNA sequences were removed with fastq_screen (v. 0.11.1). Remaining reads were further filtered for low complexity with reaper (v. 15-065,11). Reads were aligned against *A. thaliana*. TAIR10.39 genome using STAR (v. 2.5.3a, 12). The number of read counts per gene locus was summarized with htseq-count (v. 0.9.1,13) using *A. thaliana*. TAIR10.39 gene annotation. Quality of the RNA-seq data alignment was assessed using RSeQC (v. 2.3.7,14). Reads were also aligned to the *A. thaliana*. TAIR10.39 transcriptome using STAR (v. 2.5.3a, 12) and the estimation of the isoforms abundance was computed using RSEM (v. 1.2.31,15). Data from both count estimation methods (htseq and RSEM) are provided. For the statistical data analysis described below, htseq count data was used.

Statistic RNA-SEQ

Normalization and Data Transformation:

Statistical analysis was performed for genes independently in R (R version 3.4.4). Genes with low counts were filtered out according to the rule of 1 count(s) per million (cpm) in at least 1 sample. Library sizes were scaled using TMM normalization. Subsequently, the normalized counts were transformed to cpm values, and a log2 transformation was applied, by means of the function cpm with the parameter setting prior.counts = 1 (EdgeR v 3.20.9; 16). TPM (Transcripts per million reads) data from the RSEM data processing pipeline were included.

Quality Control (Normalized Data):

Quality control on normalized data was performed through density profiles as well as hierarchical clustering by Ward's method and sample PCA.

Differential expression:

Sample names were corrected (switched) before the statistical analysis. Differential expression was computed with the Bioconductor package limma (limma v 3.34.9; 17) by fitting data to a linear model. The approach limma-trend was used. Fold changes were computed, and a moderated t-test was applied to compare the two experimental groups. P-values were adjusted by the Benjamini-Hochberg (BH) method, controlling for the false discovery rate (FDR).

Contributions

The cloning by Gibson assembly was contributed by Dr. Anthony Guihur. The phylogenetic tree of HSPs was contributed by the Ph.D. Mathieu Rebeaud. The RNA extraction and the data set from the RNA sequencing were performed by Dr. Anthony Guihur. The selection CIHSP lines on hygromycin media was contributed by the apprentice laboratory technician Gizem Demirkiran.

References

1. Simões-Araújo JL, Rumjanek NG, Margis-Pinheiro M. Small heat shock proteins genes are differentially expressed in distinct varieties of common bean. Brazilian J Plant Physiol. 2003;15(1):33–41.

2. Hernandez LD, Vierling E. Expression of low molecular weight heat-shock proteins under field conditions. Plant Physiol. 1993;101(4):1209–16.

3. Finka A, Cuendet AFH, Maathuis FJM, Saidi Y, Goloubinoff P. Plasma Membrane Cyclic Nucleotide Gated Calcium Channels Control Land Plant Thermal Sensing and Acquired Thermotolerance. Plant Cell [Internet]. 2012;24(8):3333–48. Available from: http://www.plantcell.org/cgi/doi/10.1105/tpc.112.095844

4. Martínez-Andújar C, Ordiz MI, Huang Z, Nonogaki M, Beachy RN, Nonogaki H. Induction of 9-cis-epoxycarotenoid dioxygenase in Arabidopsis thaliana seeds enhances seed dormancy. Proc Natl Acad Sci U S A. 2011;108(41):17225–9.

5. Hewa-kapuge S, Dougall SMC. Effects of Methoxyfenozide , Indoxacarb , and Other Insecticides on the Beneficial Egg Parasitoid Trichogramma nr . brassicae (Hymenoptera : Trichogrammatidae) Under Laboratory and Field Conditions. 2003;1083–90.

6. Dai S, Petruccelli S, Isabel M, Zhang Z, Chen S, Beachy RN. Functional Analysis of RF2a , a Rice Transcription Factor Functional Analysis of RF2a , a Rice Transcription Factor *. 2003;(January 2014).

7. Perera SC, Sundaram M, Krell PJ, Retnakaran A, Dhadialla TS, Palli SR. An Analysis Of Ecdysone Receptor Domains Required for Heterodimerization With Ultraspiracle. 1999;70(July 1998):61–70.

8. Laughont A, Gesteland RF. Primary Structure of the Saccharomyces cerevisiae GAL4 Gene. 1984;4(2):260–7.

9. Padidam M, Gore M, Lu DL, Smirnova O. Chemical-inducible , ecdysone receptor-based gene expression system for plants Chemical-inducible , ecdysone receptor-based gene expression system for plants. 2014;(March 2003).

10. Sun X, Sun C, Li Z, Hu Q, Han L, Luo H. AsHSP17 , a creeping bentgrass small heat shock protein modulates plant photosynthesis and ABA-dependent and independent signalling to attenuate plant response to abiotic stress. 2016;1320–37.

11 Davis MPA, van Dongen S, Abreu-Goodger C, Bartonicek N & Enright AJ. (2013). Kraken: A set of tools for quality control and analysis of high-throughput sequence data. Methods 63(1), 41-49. doi: 10.1016/j.ymeth.2013.06.027. PMID: 23816787

12 Dobin A, Davis CA, Schlesinger F, Drenkow J, Zaleski C, Jha S, Batut P, Chaisson M, Gingeras TR. (2013). STAR: ultrafast universal RNA-seq aligner. Bioinformatics 29(1):15-21. doi: 10.1093/bioinformatics/bts635. PMID: 23104886.

13 Anders S, Pyl PT, Huber W. (2015). HTSeq a Python framework to work with high-throughput sequencing data. Bioinformatics 31(2). Advance online publication. doi: 10.1093/bioinformatics/btu638. PMID: 25260700.

14 Wang L, Wang S, Li W. (2012). RSeQC: quality control of RNA-seq experiments. Bioinformatics 28(16):2184-5. doi: 10.1093/bioinformatics/bts356. PMID: 22743226.

15 Li B, Dewey CN**.** (2011). RSEM: accurate transcript quantification from RNA-Seq data with or without a reference genome. BMC Bioinformatics 12:323. doi: 10.1186/1471-2105-12-323. PMID: 21816040.

16 Robinson, MD, McCarthy, DJ, Smyth, GK (2010). edgeR: a Bioconductor package for differential expression analysis of digital gene expression data. Bioinformatics 26:139-140.

17 Ritchie ME, Phipson B, Wu D, Hu Y, Law CW, Shi W, Smyth GK. (2015). limma powers differential expression analyses for RNA-sequencing and microarray studies. Nucleic Acids Res. 43(7):e47. PMID: 25605792

Supplementary data

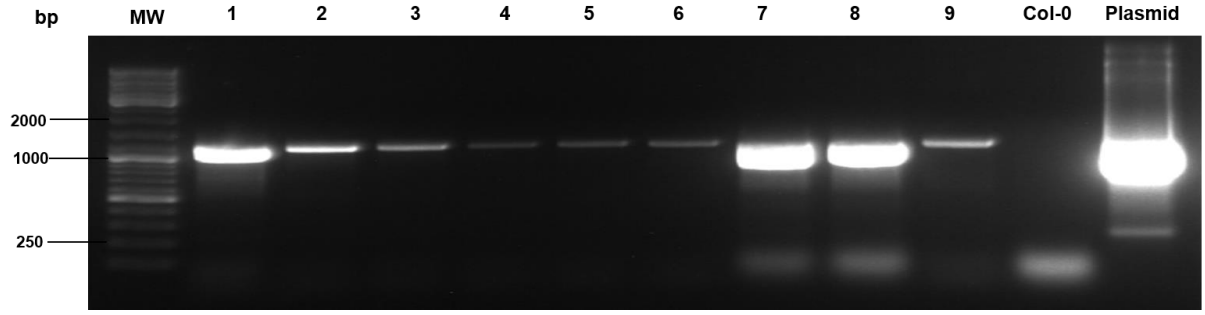

Supplementary data 1: Example of PCR analysis to validate the transgene of the T2 CIHISP in offspring survival. The plasmid was used as a positive control to validate the presence of the transgene in

the offspring survival from the different CIHSP lines. Col-0 was used as negative control which does not contain the transgene. On top of each lane of the agarose gel, numbers represent individual offspring survival from different CIHSP T2 lines.

General discussion

Crop plants are facing extreme variations in temperatures due to global warming and heat waves are predicted to be more frequent and intense (1). It is essential to increase our understanding of how plants can timely sense an upcoming drastic temperature increase and signal the nucleus to establish an appropriate molecular response, in order to withstand heat shock (HS) and heat-damages. To understand the activatory mechanisms of plant heat shock response (HSR) it is also necessary to elucidate the repressory mechanisms by which HSP genes are prevented from being expressed at non-heat-shock temperature. Increased knowledge about these two complementary aspects of the HSR is expected to provide means to engineer valuable crops capable to feed future generations. Therefore, the primary aim of this thesis was to identify genes involved in the activation and the repression of the heat shock signaling pathway in the model higher plant *A. thaliana*.

Generation of a transgenic *A. thaliana* line: HIBAT

Chapter 2 described the generation of an *A. thaliana* line (HIBAT) in order to analyze the HSR and aiming to perform a forward genetic screen (FGS) in search for new genes involved in the heat-sensing and signaling pathway. Here, we found that the nLUC-DAO1 was strictly repressed at low temperatures, with a very slight leakiness that did not induce major toxicity in the presence of D-valine. Under HS, nLUC-DAO1 was highly accumulated which produced a significant bioluminescence signal and was toxic for plants only in the presence of D-valine (Figs. 7, 8, and 9, chapter 2). Therefore, the promoter of the conditionally toxic reporter gene presented the expected behavior of being tightly repressed at low temperatures and strongly expressed at high temperature (2–4), which met our interest to analyze the HSR by a forward mutagenesis approach.

To conduct a FGS, it was necessary that HIBAT contained a single copy of the transgene (to avoid the selection of false mutant) located in a non-coding area and did not present any significant deleterious phenotype compared to the WT Col-0. At the seedlings stage, HIBAT did not show any difference in terms of root length, the biomass of shoot, and seeds germination as compared to Col-0. Yet, a slightly higher thermosensitivity was observed in HIBAT through an acquired thermotolerance (AT) assay (Figs. 5 and 6, chapter 2). The transgene was found to be a single copy which was located in a non-coding region, albeit between two genes (Fig. 4 chapter 2). The upstream AT1G69590.1 might encode for RNA-directed DNA polymerase (TAIR10). Yet, our transcriptomic data

showed no expression of this gene at low and high temperatures, suggesting to be a pseudogene. The downstream gene, AT1G69600, encodes for a zinc finger homeodomain 1 (ZFHD1) and might be required for the activation of early response to dehydration (5). The transcriptomic data showed that ZFHD1 is expressed at low temperature and becomes 2-fold time more accumulated under HS, also supported by the microarray data from BAR ePlant (http://bar.utoronto.ca/eplant/). The slightly higher thermosensitivity observed in HIBAT might not be obligatorily linked with ZFHD1 expression and could be attributed to the leakiness of nLUC-DAO1 at low temperatures. Thus, the transgene localization was not a reason to exclude HIBAT for conducting the FGS.

Because crosstalk signaling exists between abiotic and biotic stresses, it was necessary to address the specificity of the reporter promoter in HIBAT for heat and not for other stresses. For example, drought and heat signaling have in common the same HSFA1 and DREB2A transcription factors that ultimately lead to the accumulation of HSPs in *A. thaliana* (6). Additionally, salt stress can induce an osmotic change within the cell resulting in the activation of HSFA6b and DREB2A which mediate the accumulation of HSPs (7). This was demonstrated by exposing HIBAT to H_2O_2, mannitol, NaCl, cold, chilling, of FLG22, which did not cause over-accumulation nLUC-DAO1, at low or at high temperatures (Figs. 10, 11, and 12, chapter 2). Yet, we did not test all conditions including a dose-response of these stresses which might affect negatively or positively the activation of the promoter where a proper concentration and time of exposition might reach a critical threshold affecting the HSR (8). It remains to study the effect of additional stresses such as drought or light since their signaling pathway may share common transcription factors such as HSFs. The characterization of the HIBAT line nevertheless met the criteria to be used as a progenitor line to perform an FGS.

Identification of new genes involved in the heat sensing and signaling pathway using the characterized HIBAT line

Several mediators of the heat shock signaling pathway have been previously identified, such as CaM3 and CBK3 whose their lack of expression lead to a defective accumulation of HSP in *A. thaliana* (9,10). So far, new components remained to be found, mainly between the primary CNGC sensors at the plasma membrane and the transcription factor HSFA1 (11). Using HIBAT, a FGS was conducted to isolate mutants impaired in the accumulation of small HSPs, which are considered as the first line of defense against HS (12). Chapter 3 described several HIBAT mutants that were able to survive in the

presence of D-valine and defective to accumulate nLUC-DAO1 and HSPs under HS (Figs. 1, 2, and 3, chapter 3). Yet, this phenotype was lost or unexpected diluted in several progenies at the next generations (Tables 4, 5, and 6, chapter 3). The nLUC-DAO1 DNA sequence did not show mutations that could have been caused by the EMS treatment. Alongside the inhibition of nLUC-DAO1, some offspring mutants showed a down-regulated accumulation of sHSP17.7, whose genes are located on a different chromosome (Fig. 10, chapter 3). Therefore, the initial aim of the FGS, to find genes involved in the HS signaling pathway was not met. However, the concurrent down-regulation of distally located sHSP17.7 suggested the existence of an epigenetic program capable to reversibly repress the HSR when the over-expression of HSPs becomes excessive or toxic to the plant.

Investigation of a possible emergency epigenetic methylation program resulting from iterative heat treatments

The observation during the FGS suggested that the non-Mendelian allelic segregation of isolated mutants was not the result of a DNA mutation but from reversible modifications, such as environmentally elicited DNA methylations, RNAi, or transposable elements. Chapter 4 focused on one possibility that the HSR in HIBAT mutant phenotypes resulted from an epigenetic DNA methylation program caused by stressful HS cycles. This was addressed by applying zebularine, an inhibitor of DNA methyltransferase, which can avoid DNA methylation in humans cells and seems to not alter histone methylation (13,14). In presence of zebularine and D-valine, 24-fold less HIBAT seedlings survived iterative HS treatments than without zebularine, strongly indicating that DNA methylation was responsible for the transient silencing phenotype that we observed in the HSR in plants (Fig. 3, chapter 4). Several days after the end of the HS cycles, most survivals had recovered their ability to produce both nLUC-DAO1 and sHSP17.7 under a single HS, whereas few survivals were able to repress them (Tables 1 and 2, chapter 4). These findings suggest iterative heat-shocks plants can establish an emergency DNA methylation program to reversibly avoid an unnecessary excessive accumulation of costly HSPs.

Supporting our findings, DNA methylation levels are found to increase in several species, such as in *A .thaliana*, *Quercus Suber*, and *Brassica napus* under extreme heat conditions, leading to the regulation of genes involved in the plant HSR (15–17). The DNA methylation may not be specific to heat since it has been also described in the case of cold or salt stress (18–20). The environmental response of plants could be mediated by

the methylation and demethylation at coding regions, resulting in the alteration of the chromatin structure, and leading to the inhibition of gene transcription. The DNA methylation is regulated by the RNA-directed DNA methylation pathway, which is required for basal thermotolerance in *A. thaliana*. Interestingly, the lack of expression of nuclear RNA polymerase D2, dicer-like 3, RNA-dependent RNA polymerase 2, and argonaute 4, which are involved in the RdDM pathway, lead to a hypersensitive phenotype to HS in *A. thaliana* (19). In contrast, the lack of expression of chromomethylase 2, responsible for CHH methylation, improves the tolerance toward HS, strongly suggesting that the alleviation of methylation is required for plant response (21). Thus, under iterative HS, our results indicated that nLUC-DAO1 and HSP genes may have been negatively regulated by DNA methylation, leading to their reversible repression.

It cannot be excluded that the promoter HSP17 from soybean, driving the expression of nLUC-DAO1, might lead to a trans-activation of other HSP genes due to a strong homology of their promoters. The expression of one trans-activator gene may activate in trans multiple genes that have the same specific promoter region. In somatic cells of tobacco, a GUS gene (without enhancer) on one allele is activated in trans by an enhancer on the second allele resulting in a GUS activity (22). The inhibition of the transgene by DNA methylation could also result in the repression of HSP genes. In tobacco plants, silencing can occur between two homologous promoters. Two independent mechanisms might result from this observation such heavy methylation of both promoters or by a post-transcriptional gene silencing in which degradation of the mRNA occurred when transgenes or endogenous genes have been recognized by the cells (23). Yet, the epigenetic mechanism is highly complex and is not well understood.

Our results indicated that few survivors might constitutively repress nLUC-DAO1 and sHSP17.7 under HS, two weeks following the end of iterative HS (Table 2, chapter 4). The methylation marks may persist within the same generation and leading to the repression of the HSR. Methylation can also occur on histones, which can wrap several HSP genes, leading to their future up or down-regulation. For example, heat-responsive loci such as sHSP18.2, sHSP21, and sHSP22 lead to the accumulation of H3K4me2 and H3K4me3 that is retained at the recovery phase and further elevated upon two successive HS, leading to a better induction of responsive HSP loci in *A. thaliana* (24). This result indicates that if histones can be targeted by methylation after two HS, a similar mechanism could occur on DNA, leading to the methylation of HSP genes at the promoters or coding

regions. To confirm and further study this putative epigenetic DNA methylation program on the HSR, a methylome analysis should be performed. It would expectedly provide precious information, not only on methylated HSPs genes and nLUC-DAO1 but on all possibly other categories of methylated genes following iterative HS. A transcriptomic analysis would further identify the expression profile of genes that have been affected by such methylation. Additionally, it might be relevant to work with *A. thaliana* mutants impaired in DNA methylation. In *ddm1* mutant, the methylation level of 5-methylcytosine is reduced by 70% and exhibits normal plant growth and development (25). Mutants involved in the RDM pathway, such as DICER-LIKE mutants can be considered since they participate in the siRNA biogenesis which mediates DNA methylation (26,27). Therefore, it would be relevant to generate a new line by crossing HIBAT with DDM1. This could confirm our reduced number of survivals observed in presence of D-valine and zebularine in HIBAT since the new line would be expected to provide a similar result without zebularine.

The heritability of the repression of the HSR in offspring survivals would show if the phenotype can be transmitted across generations and more interestingly, at which frequency. The epigenetic regulation of gene expression, induced by environmental exposure, can persist in the next sexual generation in stressed animals and plants (28–30). Transgenerational memory is described as epigenetic inheritance and refers to the transmittance of epigenetic states. Thus, a part of the offspring can benefit from adaptive advantages or genomic flexibility for better fitness. Supporting this observation, it is demonstrated that HS, flagellin, or UV-C exposure can exhibit transgenerational epigenetic inheritance in plants and resulting in better fitness advantages (28,31,32). In *A. thaliana*, changes in DNA methylation at specific sites of a silenced target gene are responsible for the transgenerational memory, such as CG methylation, playing a central role in epigenome stability. The transgenerational memory of heat responses is suggested to potentially allow long-term adaptation and rapid evolution because chromatin modifications can be mitotically or meiotically heritable (33). Therefore, in our study, the transmission of the methylation marks across the generation, although not entirely new, would indicate at which frequency the phenotype can be inherited and if it is stable over several generations.

Searching for repressors of the heat shock response at low temperatures

Several repressors of the HSR have been discovered, such as ARP6, HSFb1, HSF2b, and VOZ1 in whose their lack of expression leads to an over-accumulation of HSP at a low temperature (34–36). It remains to find new repressors of HSP genes at basal temperatures plants. In chapter 5, mutated HIBAT seedlings were used in a different FGS, performed without HS cycles and D-valine. This permitted the identification of genes whose loss of function mutation would derepress the expression small HSPs at low temperatures. A candidate mutant called L5 was found to express significantly more nLUC-DAO1 and HSPs at 22°C and 31°C than the parental line HIBAT (Figs 1 and 2, chapter 5). L5 was then sequenced, and a list of 232 SNPs was obtained (Table 2, chapter 5). We firstly focused on 16 SNPs that caused stop codon in exon genes and their functions remain to be addressed through T-DNA insertion lines.

Two candidate genes might be relevant, such as *HAC5* (AT3G12980) and *PDAT2* (AT3G44830). *HAC5* encodes for a histone acetyltransferase and could interact with both H3 and H4 histones as a substrate which evocates the result from Kumar and Wigge, 2010. Interestingly, under HS, the complex HAC1/CBP can be a coregulator of HSFA1 and HSFB1 in *A. thaliana* (37), suggesting that if HAC5 is carrying a similar function as its homologs HAC1, it may inhibit HSFB1 activity (35). The lack of expression of HAC5 could be responsible for the higher expression of sHSP17.7 non inducing low temperature in L5.

PDTA2 encodes for lecithin, which belongs to the cholesterol acyltransferase family and shares high sequence homology with *PDTA1*. The pdta1 mutant is shown to accumulate a lower level of TAGs in the cytosol at a low and high temperature which suggests a role in the fatty acid synthesis (38). This suggests that PDTA2 might perform a similar function as its homolog PDTA1. Since the HSR depends in part on the fluidity of the plasma membrane, a lack of TAGs production could lead to less saturated lipids and hyperfluidity of the membrane (39,40). It would result in a higher expression of HSPs at low temperatures in the L5 candidate. This could be addressed by performing a lipidomic analysis. T-DNA heterozygous lines of HAC5 and PDTA2 were isolated and need to be segregated to obtain homozygous lines in order to analyze if a higher expression of HSP is observed at low and mild temperatures, as compared to the mother plant Col-0.

The possible role of CaM1 and CaM5 in the heat shock signaling pathway

Both thermosensors, CNGC2 and CNGC4, expose to the cytosol a predicted calmodulin-binding site (41,42). Yet, the precise identity and the Ca^{2+} entry-dependent mechanism of these heat-responsive channels, which mediate the specific transduction of a heat priming signal to accumulate HSPs, is unclear. Using a yeast two-hybrid screen, Dr. Anthony Guihur identified CaM1 and CaM5 as strong interactors of CNGC2. Chapter 6 showed a CRISPR approach which led to isolate single mutants, whereas a double mutant was isolated through T-DNA insertion lines (Figs. 6 and 10, chapter 6).

In *A. thaliana*, AtCaM3 mediates the heat shock signaling. A lack of AtCaM3 expression leads to a defective accumulation of HSP (30% less) under HS, but it has not been shown to interact with CNGC sensors (9,43). Thus, additional CaMs remain to be identified as potential interactors with the CNGCs and to show those that are involved in the specific mediation of the heat signal. Although the single mutant of CaM1 and CaM5 seem to accumulate optimally HSP17.7 under HS, it remains to analyze if the lack of expression of both genes affects the HSR (Fig. 8, chapter 6). Direct regulation HSPs by CaM1 and CaM5 has not been described. However, CaM1 can positively regulate ABA response, which slightly improves the thermotolerance of *A. thaliana* seedlings (44,45). CaM5 was found to mediate resistance of germinating seeds to heat and cold stresses (AL-Quraan et al., 2012). The HSR is mainly characterized by the accumulation of HSP chaperones but also includes other protein partners such as APX1. Therefore, it may be possible that both CaMs are needed to activate an efficient HSR but would not obligatorily regulate the accumulation of HSP chaperones. Interestingly in *A. thaliana*, the thermosensor CNGC6 is shown to be negatively regulated by CaM2/3/5 and CaM7 under HS by interacting with the IQ6 motif leading to the regulation of the channel (46). CaM1 and CaM5 could perform similar functions with CNGC2 and CNGC4 and mediate the heat shock signaling pathway at specific temperatures.

It remains to elucidate if the double CaM1 and CaM5 mutant does not accumulate HSPs under HS and analyze its ability to develop AT. If the HSR is negatively affected, it would be a strong indication that CaM1 and CaM5 are central players in the transduction of the heat signal in plants. A total transcriptomic analysis would address this hypothesis and indicate abnormally unexpressed genes that are normally upregulated under HS. Additionally, it remains to find if in the double *cam1/cam5* mutant the CNGC2 activity and

the calcium entry are affected under HS. A pleiotropic effect is possible as CaM1 and CaM5 can involve in various biotic and abiotic stresses such as salt resistance (47,48).

The effect of sHSP17.6a at low temperatures in *A. thaliana*

The proper and timely accumulation of HSP20s during heat priming is correlated with the successful onset of AT in plants. Western and Northern blots and proteomic analysis show that at 20°C some HSP20s, such as sHSP17.6a, are virtually absent from the cytosol of plants (49–52). This was confirmed with our transcriptome analysis of HIBAT which showed that members of HSP20 are the most repressed at 22°C and the most heat-inducible at 38°C, as compared to HSPs that are molecular chaperones (Fig. 1, chapter 7). The HSP20s could be classified into two categories:

- The 1st group of HSP20s has members which are strongly repressed at 22°C and highly expressed at 38°C.

-The 2nd group contains members of HSP20s which are slightly expressed under both temperature conditions but not at a high level.

It remains to understand the particular roles of the different members of the HSP20s at low and high temperatures in plant cells (53).

In Chapter 7, we generated an *A. thaliana* line (CIHSP), to study the effect of artificially expressing sHSP17.6a at a low temperature, by the imethoxfenozide (Fig. 3, chapter 7) (54). Given the strong repression of HSP17.6a expression at low temperature, we hypothesized that the artificial unduly over-expression of HSP17.6a expression at low temperature would have deleterious effects on the plant. Indeed, the overexpression of sHSP17 from *Agrostis stolonifera* in *A. thaliana* shows a reduction of leaf chlorophyll content leading to a clear reduction of the photosynthesis activity at low and high temperatures (55), suggesting that unnecessary expressed members of HSP20s may be detrimental for plant fitness. We isolated a homozygous line, containing a single copy of the transgene (Figs. 4 and 5, chapter 7). To test our hypothesis, it remains to assess the effect of different doses of the chemical to expressed sHSP17.6a at low temperatures, expecting a possible disadvantage phenotype in terms of growth and development. In case an increased amount of sHSP17.6a would cause such phenotype, a transcriptomic analysis would likely reveal unbiased information about the genes that may vary owing to the expression of sHSP17.6a at low temperature. In the absence of disadvantage effect,

the CIHSP line might still serve to test the proper concentration of sHSP17.6a, which is required for plants to surviving under HS.

Conclusion and perspectives

The HIBAT line was found as a new tool to analyze, through the direct expression of nLUC-DAO1, the heat shock signaling pathway, and the HSR. It remains to study the impact of additional stresses since crosstalk signaling exists between abiotic and biotic stresses. The unique properties of the HIBAT line are a matter for writing publication to be submitted in peer-review Journal.

The main results of this thesis strongly indicate that plants may have developed the ability to establish an emergency DNA methylation program during extreme heat conditions in nature, in order possibly to avoid the unnecessary costly massive expression of defensive HSP genes. A methylome and transcriptomic analysis on mutant co-inhibited on nLUC-DAO1 and HSPs remains to be performed to address the possibility that the over-expression of some HSPs might be deleterious to plants and must be tightly and rapidly regulated. This could generate a publication about a possible epigenetic program in higher plants in which the deleterious excessive expression of HSP genes would become reversibly silenced. Although the indications for the onset of an epigenetic silencing program, the identification of genes involved in the heat shock signaling pathway may still be considered with HIBAT treated only with a single HS rather than with iterative heat treatments.

We performed second FGS aiming to identify at low temperatures loss-of-function repressors of the heat shock signaling pathway. We are currently analyzing SNPs identified in exon genes leading to a stop codon. It cannot be excluded that other relevant SNP localized such in promoter might be responsible for the L5 phenotype. Yet, too many SNPs were identified and the F2 generation has been obtained. It remains to isolate offspring presenting a deregulated HSR to potentially perform a second DNA sequencing to facilitate the analysis of the causal gene(s) by future collaborators and researchers.

The potential involvement of CaM1 and CaM5 in the heat shock signaling remains to be analyzed. As discussed previously, an AT assay, transcriptomic analysis, and the deregulation of CNGC2 under HS by a lack of expression of both CaM have to be analyzed.

Annex: Perspective of publication

A mini review is currently in preparation with Dr. Anthony Guihur in Frontiers Plant Science. The following abstract have been submitted in the Journal.

“During summer days, land plants must anticipate upcoming harmful temperatures, to timely accumulate protective heat-shock proteins (HSPs) conferring acquired thermotolerance (AT). All organisms synthetize HSPs, many of which are members of the conserved chaperones families HSP100s, HSP90s, HSP70s, HSP60s, HSP40s and HSP20s. Plants can detect incremental changes from ambient temperatures through cyclic nucleotide-gated channels, which act as thermosensors in the plasma membrane. This review describes recent advances in temperature sensing and responses in plants and is mainly focused on the pathway from heat-sensing by the plasma membrane to the activation of the heat shock transcription factors (HSFs). An unclear cellular signal, likely involving calmodulins and kinases, triggers the activation of HSFs which act as positive regulators. HSF1 binds to specific DNA motifs in promoters of HSP genes, mediates the dissociation of bound histones, leading to their transcription. Although plants can alter the activities of enzymes that affect lipid composition and certain osmolytes to protect the cellular machinery, HSP chaperones can prevent, use, and revert the formation of misfolded proteins thereby avoiding heat-induced cell death. Remarkably, some HSPs are tightly repressed at low temperatures suggesting that costly mechanisms may become detrimental under unnecessary conditions and affect plant fitness. Here, the possible role of HSP20s in response to HS and their putative deleterious effect expression at non-HS temperature, will be discussed.”

Reference

1. Venkataraman C. Climate Change Signals and Response [Internet]. Venkataraman C, Mishra T, Ghosh S, Karmakar S, editors. Singapore: Springer Singapore; 2019. Available from: http://link.springer.com/10.1007/978-981-13-0280-0

2. Schöffl F, Raschke E, Nagao RT. The DNA sequence analysis of soybean heat-shock genes and identification of possible regulatory promoter elements. EMBO J. 1984;3(11):2491–7.

3. Nishal B, Tantikanjana T, Sundaresan V. An inducible targeted tagging system for localized saturation mutagenesis in Arabidopsis. Plant Physiol. 2005;137(1):3–12.

4. Saidi Y, Finka A, Chakhporanian M, Zrÿd JP, Schaefer DG, Goloubinoff P. Controlled expression of recombinant proteins in Physcomitrella patens by a conditional heat-shock promoter: A tool for plant research and biotechnology. Plant Mol Biol. 2005;59(5):697–711.

5. Tran LSP, Nakashima K, Sakuma Y, Osakabe Y, Qin F, Simpson SD, et al. Co-expression of the stress-inducible zinc finger homeodomain ZFHD1 and NAC transcription factors enhances expression of the ERD1 gene in Arabidopsis. Plant J. 2007;49(1):46–63.

6. Yoshida T, Ohama N, Nakajima J, Kidokoro S, Mizoi J, Nakashima K, et al. Arabidopsis HsfA1 transcription factors function as the main positive regulators in heat shock-responsive gene expression. Mol Genet Genomics. 2011;286(5–6):321–32.

7. Huang YC, Niu CY, Yang CR, Jinn TL. The heat stress factor HSFA6b connects ABA signaling and ABA-mediated heat responses. Plant Physiol. 2016;172(2):1182–99.

8. Zhang Q, Andersen ME. Dose Response Relationship in Anti-Stress Gene Regulatory Networks. 2007;3(3).

9. Zhang W, Zhou RG, Gao YJ, Zheng SZ, Xu P, Zhang SQ, et al. Molecular and genetic evidence for the key role of AtCaM3 in heat-shock signal transduction in arabidopsis1[W][OA]. Plant Physiol. 2009;149(4):1773–84.

10. Liu HT, Gao F, Li GL, Han JL, Liu DL, Sun DY, et al. The calmodulin-binding protein kinase 3 is part of heat-shock signal transduction in Arabidopsis thaliana. Plant J. 2008;55(5):760–73.

11. Mittler R, Finka A, Goloubinoff P. How do plants feel the heat? Trends Biochem Sci [Internet]. 2012;37(3):118–25. Available from: http://dx.doi.org/10.1016/j.tibs.2011.11.007

12. Haslbeck M, Vierling E. A First Line of Stress Defense: Small Heat Shock Proteins and Their Function in Protein Homeostasis. J Mol Biol [Internet]. 2015 Apr;427(7):1537–48. Available from: https://linkinghub.elsevier.com/retrieve/pii/S0022283615000819

13. Baubec T, Pecinka A, Rozhon W, Scheid OM. Effective , homogeneous and transient interference with cytosine methylation in plant genomic DNA by zebularine. 2009;542–54.

14. Billam M, Sobolewski MD, Davidson NE. Effects of a novel DNA methyltransferase inhibitor zebularine on human breast cancer cells. Breast Cancer Res Treat. 2010;120(3):581–92.

15. Boyko A, Blevins T, Yao Y, Golubov A, Bilichak A, Ilnytskyy Y, et al. Transgenerational adaptation of Arabidopsis to stress requires DNA methylation and the function of dicer-like proteins. PLoS One. 2010;5(3).

16. Correia B, Valledor L, Meijón M, Rodriguez JL, Dias MC, Santos C, et al. Is the Interplay between Epigenetic Markers Related to the Acclimation of Cork Oak Plants to High Temperatures? PLoS One. 2013;8(1).

17. Gao G, Li J, Li H, Li F, Xu K, Yan G, et al. Comparison of the heat stress induced variations in DNA methylation between heat-tolerant and heat-sensitive rapeseed seedlings. Breed Sci. 2014;64(2):125–33.

18. Choi CS, Sano H. Abiotic-stress induces demethylation and transcriptional activation of a gene

encoding a glycerophosphodiesterase-like protein in tobacco plants. Mol Genet Genomics. 2007;277(5):589–600.

19. Popova O V., Dinh HQ, Aufsatz W, Jonak C. The RdDM pathway is required for basal heat tolerance in arabidopsis. Mol Plant [Internet]. 2013;6(2):396–410. Available from: http://dx.doi.org/10.1093/mp/sst023

20. Steward N, Ito M, Yamaguchi Y, Koizumi N, Sano H. Periodic DNA methylation in maize nucleosomes and demethylation by environmental stress. J Biol Chem. 2002;277(40):37741–6.

21. Shen X, De Jonge J, Forsberg SKG, Pettersson ME, Sheng Z, Hennig L, et al. Natural CMT2 Variation Is Associated With Genome-Wide Methylation Changes and Temperature Seasonality. PLoS Genet. 2014;10(12).

22. Matzke M, Mette MF, Jakowitsch J, Kanno T, Moscone EA, Winden J Van Der, et al. A Test for Transvection in Plants : DNA Pairing May Lead to trans -Activation or Silencing of Complex Heteroalleles in Tobacco. 2001;

23. Rajeevkumar S, Anunanthini P, Sathishkumar R. Epigenetic silencing in transgenic plants. Front Plant Sci. 2015;6(September):1–8.

24. Lämke J, Brzezinka K, Altmann S, Bäurle I. A hit-and-run heat shock factor governs sustained histone methylation and transcriptional stress memory. EMBO J. 2016;35(2):162–75.

25. Vongs A, Kakutani T, Martienssen RA. Arabidopsis thaliana DNA Methylation Mutants. 2000;260(June 1993):1926–8.

26. Act DR. DICER-LIKE 1 and DICER-LIKE 3 Redundantly Act to Promote Flowering via Repression of FLOWERING LOCUS C in Arabidopsis thaliana. 2007;4(June):1359–62.

27. Yao Y, Bilichak A, Golubov A, Kovalchuk I. Arabidopsis thaliana siRNA biogenesis mutants have the lower frequency of homologous recombination. Plant Signal Behav [Internet]. 2016;11(7):1–11. Available from: http://dx.doi.org/10.1080/15592324.2016.1151599

28. Molinier J, Ries G, Zipfel C, Hohn B. Transgeneration memory of stress in plants. Nature. 2006;442(7106):1046–9.

29. Koturbash I, Baker M, Loree J, Kutanzi K, Hudson D, Pogribny I, et al. Epigenetic dysregulation underlies radiation-induced transgenerational genome instability in vivo. Int J Radiat Oncol Biol Phys. 2006;66(2):327–30.

30. Williams BP, Gehring M. Stable transgenerational epigenetic inheritance requires a DNA methylation-sensing circuit. Nat Commun [Internet]. 2017;8(1). Available from: http://dx.doi.org/10.1038/s41467-017-02219-3

31. Zhonga SH, Liu JZ, Jin H, Lin L, Li Q, Chen Y, et al. Warm temperatures induce transgenerational epigenetic release of RNA silencing by inhibiting siRNA biogenesis in Arabidopsis. Proc Natl Acad

Sci U S A. 2013;110(22):9171–6.

32. Lang-Mladek C, Popova O, Kiok K, Berlinger M, Rakic B, Aufsatz W, et al. Transgenerational inheritance and resetting of stress-induced loss of epigenetic gene silencing in arabidopsis. Mol Plant. 2010;3(3):594–602.

33. Mathieu O, Reinders J, Čaikovski M, Smathajitt C, Paszkowski J. Transgenerational Stability of the Arabidopsis Epigenome Is Coordinated by CG Methylation. Cell. 2007;130(5):851–62.

34. Franklin KA. Plant Chromatin Feels the Heat. Cell. 2010;140(1):26–8.

35. Ikeda M, Mitsuda N, Ohme-Takagi M. Arabidopsis HsfB1 and HsfB2b act as repressors of the expression of heat-inducible Hsfs but positively regulate the acquired thermotolerance. Plant Physiol. 2011;157(3):1243–54.

36. Song C, Lee J, Kim T, Hong JC, Lim CO. VOZ1, a transcriptional repressor of DREB2C, mediates heat stress responses in Arabidopsis. Planta [Internet]. 2018;(0123456789). Available from: http://link.springer.com/10.1007/s00425-018-2879-9

37. Anguli ARG, Otak SAK, Ishra SHKUM, Over LUTZN, Ort MAP, Charf KLIS, et al. Heat stress response in plants : a complex game with chaperones and more than twenty heat stress transcription factors. 2004;29(December):471–87.

38. Mueller SP, Unger M, Guender L, Fekete A, Mueller MJ. Phospholipid : Diacylglycerol Acyltransferase-Mediated Triacylglyerol Synthesis Augments Basal Thermotolerance 1. 2017;175(September):486–97.

39. Finka A, Goloubinoff P. The CNGCb and CNGCd genes from Physcomitrella patens moss encode for thermosensory calcium channels responding to fluidity changes in the plasma membrane. Cell Stress Chaperones. 2014;19(1):83–90.

40. Balogh G, Horváth I, Nagy E, Hoyk Z, Benkõ S, Bensaude O, et al. The hyperfluidization of mammalian cell membranes acts as a signal to initiate the heat shock protein response. FEBS J. 2005;272(23):6077–86.

41. Kaplan B, Sherman T, Fromm H. Cyclic nucleotide-gated channels in plants. 2007;581:2237–46.

42. Finka A, Cuendet AF, Maathuis FJ, Saidi Y, Goloubinoff P. Plasma membrane cyclic nucleotide gated calcium channels control land plant thermal sensing and acquired thermotolerance. Plant Cell [Internet]. 2012;24(8):3333–48. Available from: http://www.ncbi.nlm.nih.gov/pubmed/22904147

43. Liu HT, Sun DY, Zhou RG. Ca2+ and AtCaM3 are involved in the expression of heat shock protein gene in Arabidopsis. Plant, Cell Environ. 2005;28(10):1276–84.

44. Dai C, Lee Y, Lee IC, Nam HG, Kwak JM. Calmodulin 1 regulates senescence and ABA response in Arabidopsis. Front Plant Sci. 2018;9(July):1–13.

45. Larkindale J, Knight MR. Protection against heat stress-induced oxidative damage in Arabidopsis

involves calcium, abscisic acid, ethylene, and salicylic acid. Plant Physiol. 2002;128(2):682–95.

46. Niu WT, Han XW, Wei SS, Shang ZL, Wang J, Yang DW, et al. Arabidopsis cyclic nucleotide-gated channel 6 is negatively modulated by multiple calmodulin isoforms during heat shock. J Exp Bot. 2020;71(1):90–114.

47. Virdi AS, Singh S, Singh P. Abiotic stress responses in plants: Roles of calmodulin-regulated proteins. Front Plant Sci. 2015;6(OCTOBER):1–19.

48. Zhou S, Jia L, Chu H, Wu D, Peng X, Liu X, et al. Arabidopsis CaM1 and CaM4 Promote Nitric Oxide Production and Salt Resistance by Inhibiting S-Nitrosoglutathione Reductase via Direct Binding. PLoS Genet. 2016;12(9):1–28.

49. Simões-Araújo JL, Rumjanek NG, Margis-Pinheiro M. Small heat shock proteins genes are differentially expressed in distinct varieties of common bean. Brazilian J Plant Physiol. 2003;15(1):33–41.

50. Hernandez LD, Vierling E. Expression of low molecular weight heat-shock proteins under field conditions. Plant Physiol. 1993;101(4):1209–16.

51. Finka A, Cuendet AFH, Maathuis FJM, Saidi Y, Goloubinoff P. Plasma Membrane Cyclic Nucleotide Gated Calcium Channels Control Land Plant Thermal Sensing and Acquired Thermotolerance. Plant Cell [Internet]. 2012;24(8):3333–48. Available from: http://www.plantcell.org/cgi/doi/10.1105/tpc.112.095844

52. Guihur A, Fauvet B, Finka A, Quadroni M, Goloubinoff P. Quantitative proteomic analysis to capture the role of heat-accumulated proteins in moss plant acquired thermotolerance. Plant Cell Environ. 2020;(December):1–17.

53. Waters ER, Vierling E. Plant small heat shock proteins – evolutionary and functional diversity. New Phytol. 2020;

54. Martínez-Andújar C, Ordiz MI, Huang Z, Nonogaki M, Beachy RN, Nonogaki H. Induction of 9-cis-epoxycarotenoid dioxygenase in Arabidopsis thaliana seeds enhances seed dormancy. Proc Natl Acad Sci U S A. 2011;108(41):17225–9.

55. Sun X, Sun C, Li Z, Hu Q, Han L, Luo H. AsHSP17 , a creeping bentgrass small heat shock protein modulates plant photosynthesis and ABA-dependent and independent signalling to attenuate plant response to abiotic stress. 2016;1320–37.